U. S. Department of Energy
1000 Independence Avenue, S.W.
Washington, D.C. 20585

Fiscal Year 2018: Fourth Quarter

Progress Reports:
Advanced Battery Materials Research (BMR) Program
&
Battery500 Consortium Program

Released December 2018
for the period of July – September 2018

Approved by

Tien Q. Duong, Program Manager
Advanced Battery Materials Research Program & Battery500 Consortium Program
Vehicle Technologies and Electrification Program
Energy Efficiency and Renewable Energy

TABLE OF CONTENTS

Advanced Battery Materials Research Program

Battery500 Consortium Program

TABLE OF FIGURES

TABLE OF TABLES

A MESSAGE FROM THE ADVANCED BATTERY MATERIALS RESEARCH AND BATTERY500 CONSORTIUM PROGRAM MANAGER

This is the last quarterly report for fiscal year 2018, covering efforts made from July 1st through September 30th. By all accounts, it was a highly productive year. The Advanced Battery Materials Research (BMR) principal investigators and their colleagues made significant contributions to the technical community. The group published 182 peer reviewed journal articles, 161 technical presentations, and filed 8 patents in the areas of novel electrode materials, predictive modeling, and advanced diagnostic tools. A complete summary of FY 2018 progress will be available in the Vehicle Technologies Office Annual Progress report in upcoming months (http://energy.gov/eere/vehicles/vehicle-technologies-office-annual-progress-reports).

A few notable achievements from the BMR investigators this quarter are summarized below:

- **Lawrence Berkeley National Laboratory (Persson's Group)** was able to successfully simulate the diffusion coefficient of $LiPF_6$ using classical molecular dynamic simulations and to show behavior consistent with experiments, including the higher transference number at high salt concentrations.
- **Pacific Northwest National Laboratory (Wang's Group**) used high-resolution scanning transmission electron microscopy to demonstrate the coupling among electrochemical, thermal, and mechanical processes during degradation of layered cathode materials.
- **Argonne National Laboratory (Markovic and Curtiss' Group)** made density functional theory calculations on the LLZO ceramic and concluded that niobium is more likely to substitute on zirconium sites near the surface or lithium interface, whereas tantalum is uniformly distributed surface to bulk. This explains why Nb-doped LLZO is more reactive.
- **Stanford University (Cui's Group)** employed dark-field light microscopy to visualize sulfur electrochemistry *in operando*. Employing visible light as a benign probe, an ether-based liquid electrolyte was studied noninvasively by enhancing the sensitivity to small features on a flat background using dark-field illumination. The group was able to directly observe multiple new phenomena in Li-S batteries for the first time, including the electrochemical generation of metastable liquid sulfur at room temperature.
- **University of Pittsburg (Kumpta's Group)** observed that current collectors of metals that form lithium alloys can provide zero or minimal nucleation barriers (that is, zero nucleation underpotential) for Li-metal plating.

Highlights from the Battery500 Consortium team include:

- **Keystone Project 1 (Electrode Architectures):** Team members from University of California at San Diego developed a new approach to quantify the amount of "dead" lithium buried within a cycled lithium anode. This technique will aid in fundamental understanding of the cycling behavior of lithium metal in various electrolytes.

- **Keystone Project 3 (Cell Fabrication, Testing, and Diagnosis):** A 350 Wh/kg Li-metal prototypic pouch cell demonstrated greater than 94% capacity retention after 150 cycles.

We encourage you to follow our progress as we proceed in FY 2019. Our next report is expected to be available in March 2019.

Sincerely,

Tien Q. Duong

Tien Q. Duong
Manager, Advanced Battery Materials Research Program & Battery500 Consortium Program
Vehicle Technologies and Electrification Program
Energy Efficiency and Renewable Energy
U.S. Department of Energy

TASK 1 – Liquid/Polymer Solid-State Electrolytes

Summary and Highlights

The BMR Program goal is to develop long-life batteries superior to commercial Li-ion systems in terms of cost, vehicle range, and safety. The BMR Program addresses the fundamental problems of electrode chemical and mechanical instabilities that have slowed development of affordable, high-performance, automotive batteries. The aim is to identify electrode/electrolyte materials that yield enhanced battery performance and lead to greater acceptance of electric vehicles (EVs). Currently, the U. S. Department of Energy (DOE) Vehicle Technologies Office (VTO) supports ten projects in the BMR Program under this Electrolytes Task. These projects can be categorized into three general topics:

- **Liquid.** The projects for liquid electrolyte aim to develop electrolyte formulations, based on fluoro-chemistries, to achieve significantly improved operating voltage, increased durability, and increased energy density of Li-ion batteries at a reasonable cost. Nonaqueous polyelectrolyte solutions with high Li^+ transference numbers will be developed to achieve high rate capabilities at room temperature. In addition, electrolytes with new polymer binders bearing a pentafluorophenyl group on the backbone will be designed, synthesized, and tested.
- **Polymer.** The targets of polymer electrolyte (PE) projects include inorganic/polymer and polymer/gel hybrid electrolytes that have flexibility, mechanical strength, thermal stability, high ionic conductivity, stable interfaces against lithium metal, and polysulfide-trapping capability enabling energy density Li-S batteries, with comparable cycle life.
- **Self-Forming & Self-Healing.** The self-forming, self-healing electrolyte projects are focused on developing and implementing Li-metal-based metal fluorite and metal iodide batteries, capable of energy densities > 400-500 Wh/kg and 1000 Wh/L.

Highlights

At the Daikin group, they have successfully used Auger Electron Spectroscopy (AES) depth profiling to determine the elemental composition and thickness of the solid electrolyte interphase (SEI) layer in nickel-rich cathode materials (NMC-622). They found that as the surface adventitious carbon and SEI layer is sputtered through the depth profile experiment, the carbon signal decreases and the oxygen and transition metal (TM) Auger signal becomes increasingly evident. Elementally, a pristine cathode and electrochemically cycled cathode are identical. Preliminary analysis suggests the thickness of the NMC-622 cathode with fluorinated electrolyte is 24-29 nm.

The University of California (UC) Berkeley group has investigated the transport properties of a sulfonated polysulfone/poly(ethylene glycol) copolymer (PSf-co-PEG) as a function of polymer concentration, solvent type [ethylene carbonate/dimethyl carbonate (EC/DMC) versus dimethyl sulfoxide (DMSO)], and as a function of added lithium bis(trifluoromethylsulfonyl)imide (LiTFSI) salt. They found that the conductivity of all solutions increases with added small molecule salt, but they see significant differences between EC/DMC and DMSO. The polymer solution without added salt has much lower conductivity in EC/DMC than in DMSO. Further, while the polymer/salt solutions in DMSO have higher conductivity than pure LiTFSI, in EC/DMC the conductivity of the polymer-containing solutions is actually lower than with just LiTFSI. Through direct observation of the ^7Li nuclear magnetic resonance (NMR) peak width, and computational calculations performed in collaboration with Kristin Persson, they find that the reason for this difference is poor dissociation of the sulfonate/lithium ion pair on the polymer backbone.

At Argonne National Laboratory (ANL), to better understand the interactions between LiTFSI salts and new fluorinated solvents synthesized, TFE-PFPE [pentafluoro(2,2,2-trifluoroethoxy)-benzene] and TFE-PFBE [((pentafluoro(2,2,2-trifluoroethoxy) –methyl) -benzene)] in a mixed electrolyte with 1,3 dioxalane (DOL), first principles periodic calculations were performed. The density functional theory (DFT) calculations indicate that the solvation energies of reaction (1) generally weaken with increasing order of polysulfides, Li_2S_x, (x = 1 to 6). The solvation energies indicate these electrolyte mixtures are expected to be very good anion receptors that will strongly interact with polysulfides, especially the low order polysulfides, to form anion receptor complexes. At higher order (x = 4 and 6), the solvation energies of the TFE-PFBE:DOL electrolyte are larger than that of the TFE-PFBE:DOL electrolyte; that is, they are more negative, consistent with the experimental results.

The University of Maryland (UMD) group used the hybrid electrolyte synthesized before to assemble a lithium symmetrical cell. The cell was successfully cycled at 3 mA/cm^2 for 500 cycles without dendrite penetrating through the hybrid electrolyte to meet the Go/No-Go milestone.

At University of Washington (UW), the group made all-solid-state or semi-solid-state Li-S cells for testing. They found that capacity loss corresponds to a major increase in overpotential, particularly during the latter half of charge and initial half of discharge. Alleviation of this overpotential corresponds to recovery of some capacity after cycle 20, and the charge/discharge voltage profiles are relatively stable after this point. This observation led them to believe that the major cause of capacity loss in this system is not related to dissolution and diffusion of Li_2S_x species, as in most other Li-S cells, but rather premature voltage decline to the lower cutoff caused by large overpotential. In addition, they tested performance of their self-healing separators in Li-S cells. The best cell performance was achieved using PP binder with a 3:1 naphthalene diimide:pyrene (NDI:Py) ratio, which displayed > 75% capacity retention after 75 cycles, as compared to < 50% for the polyvinylidene fluoride (PVDF) control (Coulombic efficiency of both cells was > 99% for all but the first several cycles). This corresponds to almost 400 mAh/g more gravimetric specific capacity remaining in the PP cells.

At West Virginia University (WVU), three types of cross-linked polymers (CLPs) were first prepared without adding of Succinonitrile (SN) plasticizer, and mechanical properties of these CLPs were tested. The poly(ethylene glycol) methacrylate (PEGMA) [1 wt% poly(ethylene glycol) diacrylate (PEGDA)] CLP demonstrated the lowest Young's modulus of 1.62 MPa due to low cross-linking density. The PEGDA and pentaerythritol tetraacrylate (PETA) CLP showed relatively higher modulus of 17.8 and 69.5 MPa, respectively. PETA/PEGDA-SN60 and PETA/PEGDA-SN70 exhibited typical cross-linked polymer behavior with high Young's modulus of 36.7 and 20.1 MPa, while PETA/PEGDA-SN80 showed plastic behavior with high elongation yielding and low Young's modulus of 7.3 MPa. In addition, the hydrogen-treated $Li_{0.5}La_{0.5}TiO_3$ (LLTO)-based composite electrolyte PVDF-hexafluoropropylene (HFP)/LiTFSI/H-LLTO exhibited a stable voltage window up to 6 V versus Li/Li+, which indicates that this solid composite electrolyte could meet the requirements of most high-voltage lithium batteries.

The Stanford group has tested the effects of dielectric constant, surface energy on the exchange current density using poly(ethylene oxide) (PEO), polyurethane (PU) and PVDF, PVDF and PVDF-HFP, and poly dimethylsiloxane (PDMS). They found that the swelling, ionic conductivity, or resistance of the film did not follow any discernable trend. However, they observed that the exchange current increased with dielectric constant of the polymer coating. PVDF-HFP contains a high density of polarizable fluorinated groups and has a higher dielectric constant of 15. PVDF-HFP also exhibited the highest measured exchange current. PDMS has a much lower dielectric constant of 2.7 because of the nonpolar nature of the siloxane chemistry and exhibited the lowest exchange current measured. The other polymers tested have intermediate dielectric constants, and their exchange current densities fell in between that of PVDF-HFP and PDMS. In addition, they tested the Coulombic efficiency (CE) of the polymer coatings, as this is one of the most important factors for Li-metal electrode performance. An average CE was measured by depositing a fixed reservoir of lithium, cycling a fixed 1 mAh cm^{-2} capacity for 10 cycles, and then stripping all of the remaining lithium. They found that while CE is generally higher for polymer coatings that promote larger sized lithium deposits (PVDF-HFP, PVDF, and PDMS), lower surface energy appears to be the best parameter that was recorded in this study for predicting high cycling CE.

The Lawrence Berkeley National Laboratory (LBNL) group, for the first time, was able to hit the limiting current of 4.5 mA/cm^2 without the cell shorting immediately. In all of the group's previous experiments on block copolymer electrolytes (CPEs), cells shorted well before the limiting current was reached.

At Stony Brook University (SBU), a cell containing a solid electrolyte composed of 80% LiI/20% LiI(HPN)$_2$ was charged to 5% capacity by a step-wise charging process. Examination of the recovered electrodes by X-ray diffraction (XRD) depicted several peaks appearing at 2-theta values of 8.6°, 16.9°, 25.3°, 33.8°, 42.4°, and 51.4°, and can be assigned to the crystallographic planes of I$_2$-LiI(HPN)$_2$ (for example, 001, 002, 003, 004, 005, and 006). These peaks indicate a layered atomic arrangement of iodine atoms along the lattice c direction of LiI(HPN)$_2$. These results confirm the formation of the desired metal anode and iodine cathode. The results affirm project success for meeting the September 2018 Go/No-Go metric.

At Rutgers, they continued the research and development (R&D) of the 12-V, self-forming architecture they initiated at the end of last quarter. They reported on the first phase of improvement of the 12-V cell architecture through the design optimization at the electrode level and layout. They found that thinner electrodes that are also of smaller width, show higher capacity, and further enhance utilization. First-cycle voltage profile shows that the reduced positive electrode volume and its increased surface area enable shortened diffusion paths that make the chemistry more accessible, resulting in improved performance for the new configuration. They have achieved an output of 12 V in a single unit cell of small dimension. To date, they have achieved a stack energy density of a self-formed cell of > 580 Wh/L and a positive electrode energy density of 3900 Wh/L at 2.5 V and plan to exceed this in the 12-V architecture next quarter.

Task 1.1 – Advanced Lithium-Ion Battery Technology: High-Voltage Electrolyte
(Joe Sunstrom, Ron Hendershot, and Alec Falzone, Daikin)

Project Objective. The project objective is to identify electrolyte formulations, based on fluoro-chemistries, that will allow significantly improved operating voltage, increased durability, and increased energy density of Li-ion batteries at a reasonable cost. The project seeks to understand the conditions under which the electrolyte degrades, the effect on battery performance, and solutions that can overcome current limitations of the electrolyte. Gassing in Li-ion batteries is one of the most common failure mechanisms and poses the greatest safety risk in consumer devices. This project aims to investigate gas composition as a function of cathode material, electrolyte formulation, and operating voltage, and proposes optimal cell compositions at decomposition voltages.

Project Impact. Developing an understanding of the operating conditions in which gasses form in Li-ion batteries enables the project to propose optimized cell compositions, which operate at higher voltages for a longer period. Different fluorinated electrolyte components and additives may suppress and/or eliminate gas generation at or above hypothesized decomposition voltages. To investigate these topics, it is imperative that the project utilize multiple approaches, including, but not limited to: cathode material, electrolyte composition, operating voltage, and cycle number.

Approach. The evolving composition of the electrolyte in the battery will be examined by various analytical instruments to study volatiles [gas chromatography – mass spectrometry (GC-MS)/thermal conductivity detector (TCD)], liquid [liquid chromatography MS (LC-MS)], and solid [time-of-flight secondary ion mass spectrometry (TOF-SIMS), thermogravimetric analysis MS (TGA-MS), X-ray photoelectron spectroscopy (XPS), and AES] electrolyte decomposition products during battery operation. In the first year, the team addressed the gas composition and kinetics for both hydrocarbon and fluorocarbon as a function of several charge/discharge conditions. In the second year, the project will transition into analysis of the solid-state electrolyte (SSE) decomposition components of its tested batteries to obtain valuable information about SEI layer formation and how it manifests change in both the anode (graphite) and cathode (LCO and NMC).

Out-Year Goals. Work will progress toward understanding how electrolyte formulation and cell operation affect SEI layer formation/properties. Specifically, measurements of thickness and elemental composition as a function of fluorinated electrolyte composition and voltage will be performed. Understanding the SEI layer and other solid-state components of Li-ion batteries will provide valuable information on the required surface properties for increased performance at high voltage.

Collaborations. The project has collaborated with Physical Electronics (PHI) USA for cathode film characterization utilizing TOF-SIMS.

Milestones

1. Film thickness versus time/voltage complete – Milestone 2.1. (December 2018; In progress)
2. Film composition (elemental) versus time/voltage complete – Milestone 2.2. (December 2018; In progress)

Progress Report

One method for determining the elemental composition and thickness of the SEI layer in nickel-rich cathode materials (NMC-622) uses AES depth profiling. The sputter rate of standard amorphous carbon films was determined last quarter, and the project has shifted focus to investigate 200-mAh pouch cells cycled at 4.6 V alongside an uncycled cathode. Figure 1 displays an AES survey scan of an uncycled NMC-622 cathode (left) and cycled NMC-622 cathode both before and after depth profile experiments.

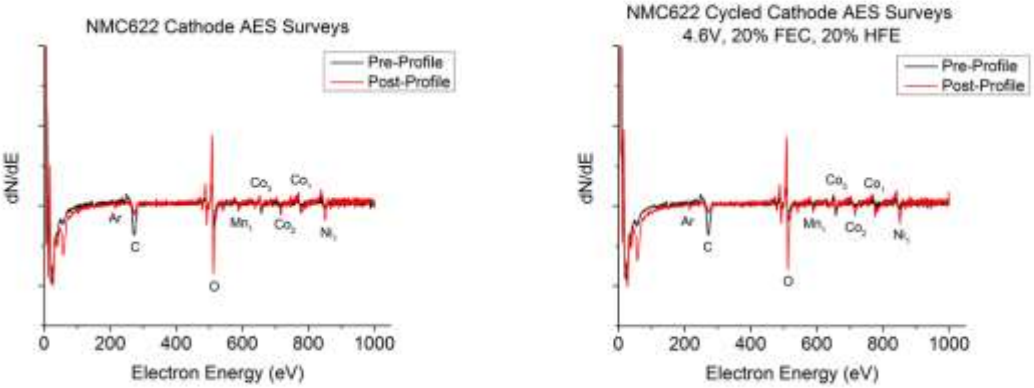

Figure 1. Auger electron spectroscopy (AES) survey scans of NMC-622 cathodes before (black) and after (red) AES depth profile experiments using an Ar(g) sputter gun.

As the surface adventitious carbon and SEI layer is sputtered through the depth profile experiment, the carbon signal decreases and the oxygen and TM Auger signal becomes increasingly evident. Elementally, a pristine cathode and electrochemically cycled cathode are identical. However, the SEI layer's thickness can be deconvoluted by comparing the number of sputter cycles it takes to diminish the carbon signal of the cycled NMC-622 cathode to the pristine material.

A data set of 6 independent depth profiles (Figure 2) from each cathode (cycled versus uncycled) has been compiled, and the thickness of the SEI layer will be determined from the calibrated sputter rate of amorphous carbon films (≈ 1 nm/cycle). Preliminary analysis suggests the thickness of the NMC-622 cathode with fluorinated electrolyte is 24-29 nm.

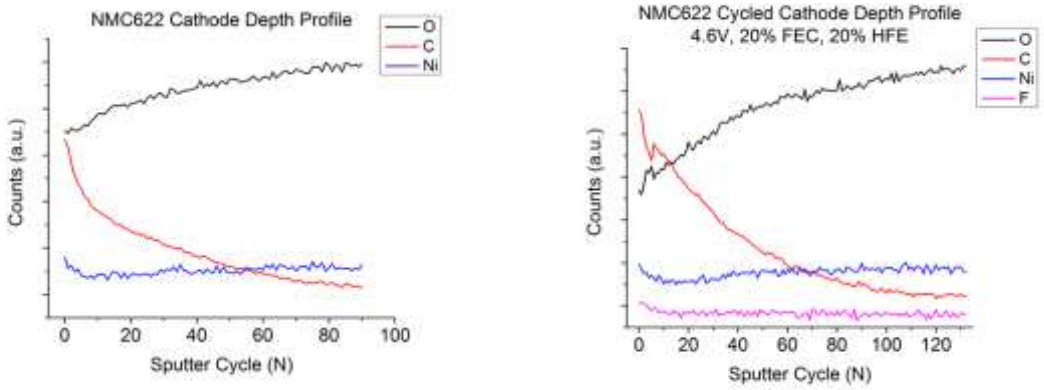

Figure 2. Auger electron spectroscopy depth profile of a pristine cathode (left) and cycled cathode (right). Residual carbon signal is from below the surface of interest.

One of the PIs, A. J. Falzone, presented the project's work at the Solid State Gordon Research Conference at Colby-Sawyer College in New Hampshire in July. In addition, TOF-SIMS analysis was initiated at PHI in Chanhassen, Minnesota. Initial efforts are focused on comparing the SEI layer on NMC-622 cathodes cycled at 4.6 V to those at 4.2 V, with either a hydrocarbon (EMC/EC) or fluorinated (EMC/FEC/HFE) electrolyte.

Patents/Publications/Presentations

Presentation

- 2018 Solid State Chemistry Gordon Research Conference (GRC), New London, New Hampshire (July 22–27, 2018). "Advancing Lithium Ion Battery Technologies: Development of a High-Voltage Electrolyte"; A. J. Falzone, J. Sunstrom, R. Hendershot, C. Meserole, E. Grumbles, A. Haque, and M. Costa.

Task 1.2 – Multi-Functional, Self-Healing Polyelectrolyte Gels for Long-Cycle-Life, High-Capacity Sulfur Cathodes in Lithium-Sulfur Batteries

(Alex Jen and Jihui Yang, University of Washington)

Project Objective. The project objective is to develop self-healing and polysulfide-trapping polyelectrolyte gels containing room-temperature ionic liquid (RTIL) for the Li-S battery system. The battery design will be able to achieve gravimetric and volumetric energy densities of ≥ 800 Wh/kg and ≥ 1000 Wh/L, respectively.

Project Impact. The Li-S battery system is currently hampered by poor capacity retention, primarily caused by dissolution of polysulfide reaction intermediates in typical organic electrolytes, as well as poor electrical contact between insulating sulfur and the conductive carbon matrix. This project aims to produce a high-capacity, long-cycle-life Li-S battery system by using rational molecular design strategies to address each capacity loss mechanism directly. A long-cycle-life Li-S battery system with the capability of doubling Li-ion energy density would enable production of lighter, longer range EVs at a cost that is affordable to the average U. S. household.

Approach. The team will develop Li-S coin cells that utilize self-healing, interpenetrated ionomer gel electrolytes in both the cathode and separator. The team will synthesize necessary starting materials and fabricate components of these gels while testing their relevant electrochemical and mechanical properties. All components will be combined into interpenetrating structures, which will be tested both alone and in cell configurations. Device performance data will be collected and used to further optimize designs of both material and cell, culminating in an optimized Li-S battery design capable of doubling the energy density of traditional Li-ion batteries. During the first year, the team is focusing on (1) synthesis of a variety of precursors for gel electrolytes, (2) fabrication and testing of both baseline materials and novel materials made from these precursors, and (3) iterative validation and improvement of design principles through both materials and device testing.

Out-Year Goals. Work will progress toward developing structure-property relationships for the self-healing, interpenetrated gel ionomer electrolyte and its individual components, as well as successful incorporation of such an electrolyte into a working Li-S cell. The team plans to demonstrate significant improvements in both capacity and retention when using the project's novel materials, as compared to state-of-the-art baseline systems.

Collaborations. This project funds work at the UW. Dr. Alex Jen, principal investigator (PI), focuses on design, synthesis, and testing of novel materials, as well as device-based verification of design principles. Dr. Jihui Yang (co-PI) focuses on optimization of device fabrication and testing, as well as investigation of failure mechanisms in devices using novel materials. Pacific Northwest National Laboratory (PNNL) facilities will be used for detailed study of device operation.

Milestones

1. Select a particular self-healing gel formulation (set of organic starting materials) for continued study based on electrochemical and mechanical properties. (Q2, FY 2018; Completed)
2. Provide detailed cell performance data for concept cells containing currently-best materials designs. (Q4, FY 2018; Completed)

Progress Report

Multifunctional Ionomer Gels and Gel Cathode. Following work on solvate ionogel (SIG) structure and properties, as well as the project's discovery that SIGs can be wetted and cured into a porous Celgard separator, the team developed a procedure to fabricate so-called "gel cathodes" based on sulfur/carbon composites. In this process, a S/C composite (prepared by melt-diffusion) and Super C65 additive (10 wt% total solids) is blended into a slurry with SIG precursor liquid [PEGDMA, Li(G4)TFSI, azobisisobutyronitrile (AIBN) initiator, and dioxane] replacing typical ingredients N-methyl-2-pyrrolidone (NMP) and PVDF. The slurry is then blade coated on aluminum foil under inert atmosphere, then placed in a sealed glass mold and cured at 80°C (Figure 3). This results in formation of a SIG *in situ* around the solid particles, functioning as both the binder and the electrolyte. The cured film may then be punched into circular cathodes for the construction of Li-S cells.

Figure 3. Photo of a cured gel cathode film inside of a sealed glass mold.

The team has fine-tuned this process, producing all-solid-state or semi-solid-state Li-S cells to test viability of the project's strategy. These cells consisted of gel cathodes, excess lithium foil, and either gel composite separators, containing SIGs cured into Celgard 2500 (as previously described), or Li(G4)TFSI-based liquid electrolytes wetted into Celgard 2500. Example cell data is shown in Figure 4 below. The team noted unusual cycling behavior that is quite different from a typical Li-S cell with organic liquid electrolyte: capacity loss occurs gradually, in a roughly linear fashion, over the first 20 cycles, then *increases* slightly and stabilizes thereafter. The capacity loss corresponds to a major increase in overpotential, particularly during the latter half of charge and initial half of discharge. The alleviation of this overpotential corresponds to the recovery of some capacity after cycle 20, and the charge/discharge voltage profiles are relatively stable after this point. This observation leads to the belief that the major cause of capacity loss in this system is not related to dissolution and diffusion of Li_2S_x species, as in most other Li-S cells, but rather premature voltage decline to the lower cutoff caused by large overpotential. The team is working to understand the origin of this overpotential and fine-tune the fabrication processes to further improve reproducibility.

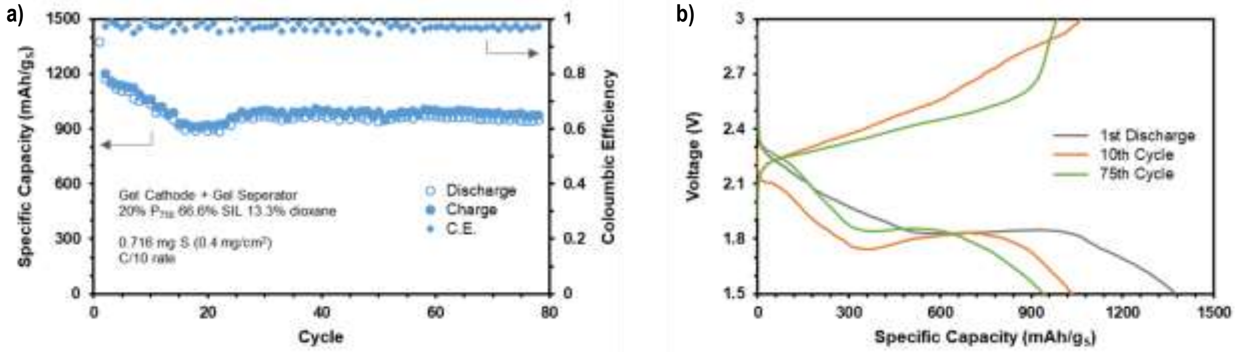

Figure 4. (a) Cycling performance of an all-solid-state Li-S cell with a gel cathode and gel composite separator at C/10 rate (0.067 mA/cm^2). Capacity loss occurs gradually over the first 20 cycles, followed by recovery and stabilization. Coulombic efficiency averaged about 97% per cycle (note: no $LiNO_3$ or any other anode-passivating additives were present in this cell). (b) Selected voltage profiles for the gel cathode Li-S cell. Overpotential grew notably during the initial 20 cycles, coinciding with capacity loss, but was reduced by the time of capacity stabilization. The team also noted the total absence of an initial plateau during the first discharge, indicating all-solid-state conversion of S_8 into long-chain Li_2S_x species.

Self-Healing Materials. Following previous characterization of the PENDI-350/triPy (PP) self-healing polymer system, including its tunable mechanical/self-healing behavior and usefulness as a Li^+ conductor, the team attempted to characterize effects of this material on a Li-S battery system. Performance improvement was expected from the two primary functions of PP: the polysulfide-trapping effect of the PEG and naphthalene diimide (NDI) moieties, and resistance to/self-healing of cracks formed during cycling. To isolate the former effect (polysulfide trapping) for study, the team has fabricated low-loading (~1 mg_S/cm^2) cathodes using either PVDF, PENDI-350, or various combinations of PENDI-350/triPy as binders. The low loading ensures that mechanical stresses play a minor role in cell performance compared to chemical processes in the cathode. These cathodes were then cycled in a Li-S system to compare their performance.

The team varied the molar ratio of NDI:pyrene (Py) units in the binder (6:1, 3:1, 2:1, 1:1, or 0% Py) by adjusting the amounts of PENDI-350 and triPy added to cathode slurries. Cathode films containing PENDI-350 alone, or only 6:1 NDI:Py, cracked easily after drying; however, all other formulations produced smooth, uniform films. The best cell performance was achieved using PP binder with a 3:1 NDI:Py ratio (Figure 5), which displayed > 75% capacity retention after 75 cycles, as compared to < 50% for the PVDF control (CE of both cells was > 99% for all but the first several cycles). This corresponds to almost 400 mAh/g more gravimetric specific capacity remaining in the PP cells. Notably, all PP formulations, even the more brittle ones, enhanced capacity retention compared to PVDF. The charge/discharge rate capability of cathodes with the 3:1 PP binder formulation was also slightly better than the PVDF control, with almost no drop in capacity observed up to 1C rate. The team is working to fabricate and test high-loading (> 5 mg_S/cm^2) cathodes with this PP binder formulation, to observe whether the self-healing properties of this supramolecular polymer result in additional performance improvement for cells with practical thickness.

As an additional test of polysulfide trapping ability in the project's system, the team added a saturated solution of Li_2S_8 (~ 10mM) in Li(G4)TFSI to powdered PVDF, PEO (M_w ~ 3,000kDa), and PENDI-350. Additional Li(G4)TFSI was then stirred in, and the resulting solution was syringe filtered to remove the polymers (all essentially insoluble in Li(G4)TFSI). The team observed a much lighter color for the solution that had been in contact with PENDI-350 more than either PEO or PVDF, indicating a strong interaction between PENDI-350 and Li_2S_x species, which tends to remove them from solution, that is, polysulfide trapping. Further characterization of this effect is ongoing.

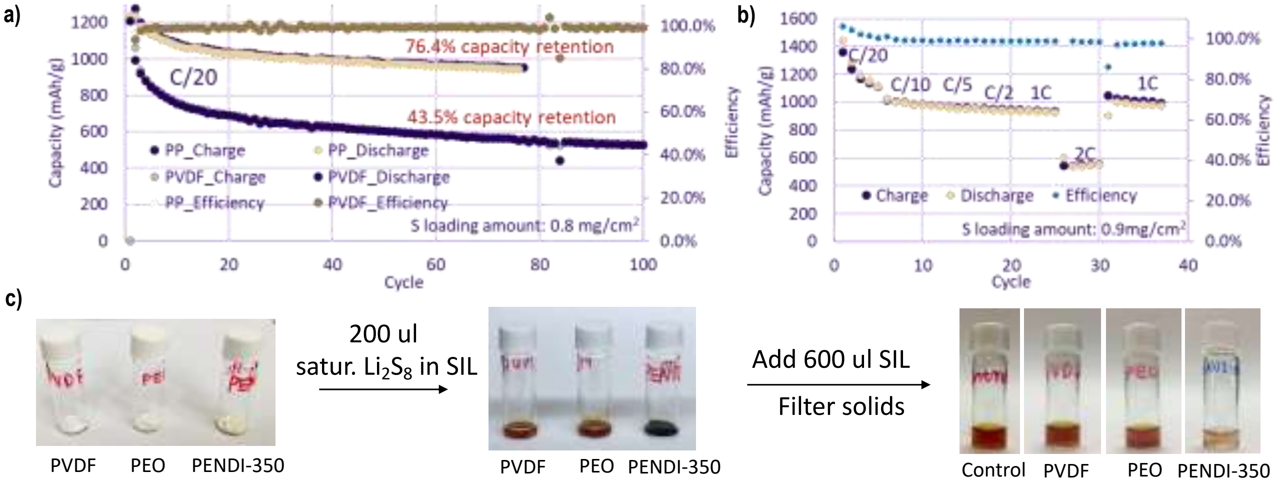

Figure 5. (a) Cycling performance of sulfur cathodes with PENDI-350/triPy (PP) binder [3:1 naphthalene diimide: pyrene (NDI:Py) molar ratio] as compared to polyvinylidene fluoride (PVDF) at C/20 rate. A striking improvement in capacity retention is obtained due to the polysulfide trapping ability of PP, resulting in 400 mAh/g more capacity remaining in the PP cell after 75 cycles. (b) Rate performance of cathodes with PP binder (3:1 NDI:Py). Virtually no reduction in capacity or efficiency is observed up to 1C rate. (c) Visual test of polysulfide trapping in NDI-containing PENDI-350 as compared to PVDF and poly(ethylene oxide). The polymers all turn dark reddish-brown following addition of a Li_2S_8 solution in Li(G4)TFSI due to absorption of polysulfides by the polymers. After filtering out the insoluble solids, the solution which was in contact with PENDI-350 is considerably lighter than the others.

Patents/Publications/Presentations

Publications

- Hubble, D., J. Qin, F. Lin, I. A. Murphy, S.-H. Jang, J. Yang, and A. K.-Y. Jen. "Designing Lithium Solvate Ionogels with Very High Conductivity and Lithium Transference Number." In peer review at *Journal of Materials Chemistry A.*
- Qin, J., F. Lin, D. Hubble, Y. Wang, Y. Li, I. A. Murphy, S.-H. Jang, J. Yang, and A. K.-Y. Jen. "Tuning Self-Healing Properties of Stiff, Ion-Conductive Polymers." In preparation.
- Li, Y.,* I. A. Murphy,* Y. Chen, F. Lin, X. Wang, S. Wang, D. Hubble, S.-H. Jang, K. T. Mueller, C. Wang, A. K.-Y. Jen, and J. Yang. "Surface Functionalization of Mesoporous Carbon for Polysulfide Trapping in Lithium Sulfur Batteries" (*co-first author). In preparation.

Presentation

- BMR Electrolytes Meeting, Berkeley, California (October 11–12, 2018): "Multifunctional, Self-Healing Polyelectrolyte Gels for Long-Cycle-Life, High-Capacity Sulfur Cathodes in Li-S Batteries"; D. Hubble and J. Qin.

Task 1.3 – Development of Ion-Conducting Inorganic Nanofibers and Polymers
(Nianqiang (Nick) Wu, West Virginia University; Xiangwu Zhang, North Carolina State University)

Project Objective. The project objective is to develop SSEs based on the highly conductive inorganic nanofibrous network in the polymer matrix for lithium batteries.

Project Impact. The research team will conduct R&D on solid-state inorganic nanofiber-polymer composite electrolytes that will not only provide higher ionic conductivity, improved mechanical strength, and better stability than the PEO polymer electrolyte, but also exhibit better mechanical integrity, easier incorporation, and better compatibility with the Li-metal anode than the planar ceramic membrane counterparts. The proposed inorganic nanofiber-polymer composite electrolytes will enable practical use of high-energy-density, high-power-density Li-metal batteries, and Li-S batteries.

Approach. Integration of the highly Li^+-conductive inorganic nanofiber network into the polymer matrix not only provides the continuous Li^+ transport channels, but also kinetically inhibits crystallization from the amorphous state of polymer electrolyte. The inorganic nanofibers will be fabricated with an electrospinning technique; the ionic conductivity of inorganic nanofibers will be improved by chemical substitution or doping. Highly ionic-conductive polymers will be developed by cross-linking and/or creation of a block-copolymer structure. The composition and microstructure of the composite electrolyte will be designed to suppress the lithium dendrite formation.

Out-Year Goals. Work will progress toward synthesis of the inorganic nanofibers and the polymer matrix. The goal is to find the optimal synthetic route to achieve the desirable conductivity.

Collaborations. This project funds work at WVU and North Carolina State University (NCSU). Dr. Nianqiang (Nick) Wu at WVU serves as PI, and Dr. Xiangwu Zhang at NCSU acts as co-PI. Peng Zheng and Xuefei Gao (Ph.D. student at WVU), Hui Yang (Postdoctoral Fellow at WVU), Botong Liu (Ph.D. student at WVU), Chaoyi Yan (Ph.D. student at NCSU), and Mahmut Dirican (Postdoctoral Fellow at NCSU) contributed to the project.

Milestones

1. Synthesize the inorganic nanofiber-polymer composite electrolytes by *in situ* polymerization of polymer on the surface of inorganic nanofibers – Subtask 2.1. (Q4, FY 2018; Completed)
2. Characterize the microstructure of composite electrolytes, and study the nanofiber-polymer interface – Subtask 2.2. (Q3, FY 2018; Completed)
3. Measure the temperature-dependent ionic conductivity of composite electrolytes, the transference number, and the electrochemical stability window – Subtask 2.3. (Q4, FY 2018; Completed)
4. Measure the mechanical properties such as the Young's modulus, the shear modulus, and the tensile and shear strengths – Subtask 2.4. (Q4, FY 2018; Completed)
5. Study the geometry (length, diameter) and surface functional groups of nanofibers on the overall performance of composite electrolytes – Subtask 2.5. (Q4, FY 2018; Completed)
6. Study the effects of different types of polymer on the overall performance of composite electrolytes – Subtask 2.6. (Q4, FY 2018; 90% Complete)
7. Optimize the fiber-to-polymer ratio in composite electrolytes – Subtask 2.7. (Q4, FY 2018; Completed)

Progress Report

This quarter, the group developed a new type of solid-state polymer electrolyte based on SN/LiTFSI, achieving ionic conductivity of 8.3×10^{-4} S cm^{-1}, which reached the milestone of electrolyte in Year 2. The electrochemical window and mechanical stability of the hydrogen-treated LLTO based composite electrolyte was measured.

Development of Inorganic Nanofibers-Polymer Composites

Plastic-Crystal Based Solid Polymer Electrolytes

The nitrile groups (-C≡N) comprise good solvation capability and have strong interaction with Li^+, contributing to enhanced ion mobility. Succinonitrile (Figure 6a), as a typical nitrile material, is a solid nonionic and highly polar plastic-crystalline plasticizer. Due to the presence of trans-gauche isomerism involving rotation of molecules at central C-C bonds of SN, SN/Li-salt based solid polymer electrolytes provide high ionic conductivity at room temperature. SN/LiTFSI solid electrolyte was prepared by melting SN and dissolving LiTFSI in SN at 80℃, where the amount of lithium salt was controlled at a molar ratio ([SN]/[Li^+]) of 10:1. At room temperature, the SN/LiTFSI solid electrolyte demonstrated low impedance of 11.3 Ω, corresponding to high ionic conductivity of 2.1×10^{-3} S cm^{-1}.

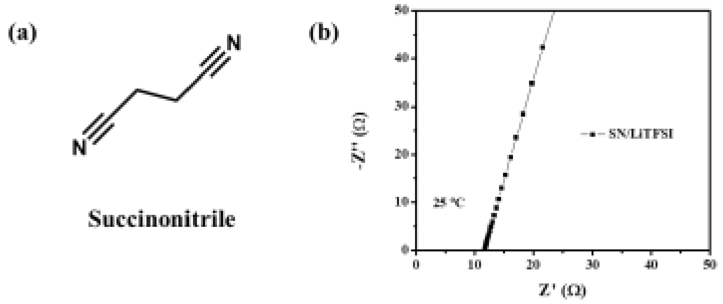

Figure 6. (a) Structure of succinonitrile (SN) and (b) electrochemical impedance spectroscopy (EIS) profile of SN/LiTFSI (10 mol%) solid polymer electrolyte.

Due to the poor mechanical properties of SN/LiTFSI solid polymer electrolyte, a mechanically robust polymer network is critical to practical application of SN-based solid polymer electrolyte in batteries. Three types of CLP were first prepared without adding SN plasticizer, and mechanical properties of these CLPs were tested. Figure 7 shows the structures of different monomers used in three different CLPs. PEGMA (1 wt% PEGDA) CLP demonstrated the lowest Young's modulus of 1.62 MPa due to the low cross-linking density. PEGDA and PETA CLPs showed relatively higher modulus of 17.8 and 69.5 MPa, respectively.

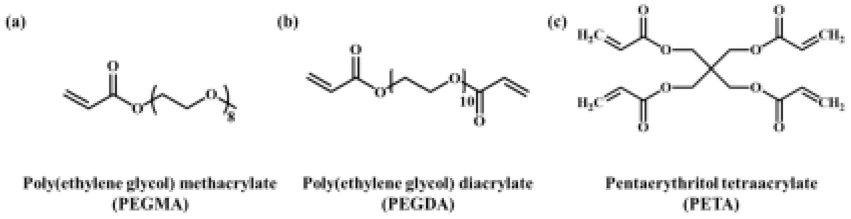

Figure 7. Structure of (a) PEGMA, (b) PEGDA, and (c) PETA monomers.

The prepolymer solution composed of PEGDA and PETA (1:1) monomers were mixed with SN plasticizer and LiTFSI lithium salt to fabricate solid polymer electrolytes. Based on different SN plasticizer amounts (from 50 to 80 wt%, based on the total weight of solid polymer electrolyte) the solid polymer electrolytes were denoted as PETA/PEGDA-SN-50, 60, 70, and 80, respectively. PETA/PEGDA-SN80 demonstrated the lowest impedance of 28 Ω and highest ionic conductivity of 8.3×10^{-4} S cm^{-1} at room temperature, as shown in Table 1. PETA/PEGDA-SN60 and PETA/PEGDA-SN70 exhibited typical CLP behavior with high Young's modulus of 36.7 and 20.1 MPa, while PETA/PEGDA-SN80 showed plastic behavior with high elongation yielding and a low Young's modulus of 7.3 MPa.

Table 1. Room-temperature ionic conductivities of PETA/PEGDA-SN solid polymer electrolytes.

Samples	SN ratio (%)	Ionic Conductivity (S/cm) (at 25°C)	Young's modulus (MPa)
PETA/PEGDA-SN50	50	3.9×10^{-5}	-
PETA/PEGDA-SN60	60	9.7×10^{-5}	36.7
PETA/PEGDA-SN70	70	3.4×10^{-4}	20.1
PETA/PEGDA-SN80	80	8.3×10^{-4}	7.3

Electrochemical Performance of the Symmetric Li | PVDF-HFP/LiTFSI/H-LLTO | Li Cell

The hydrogen-treated LLTO-based composite electrolyte PVDF-HFP/LiTFSI/H-LLTO exhibited a stable voltage window up to 6 V versus Li/Li^+, as shown in Figure 8a, which indicates that this solid composite electrolyte could meet the requirements of most high-voltage lithium batteries. Figure 8b shows the time-dependent voltage profile. At room temperature, Li|PVDF-HFP/LiTFSI/H-LLTO|Li cell stabilized at ~ 340 mV without short-circuiting in 260 h under 0.5 mA/cm² at room temperature.

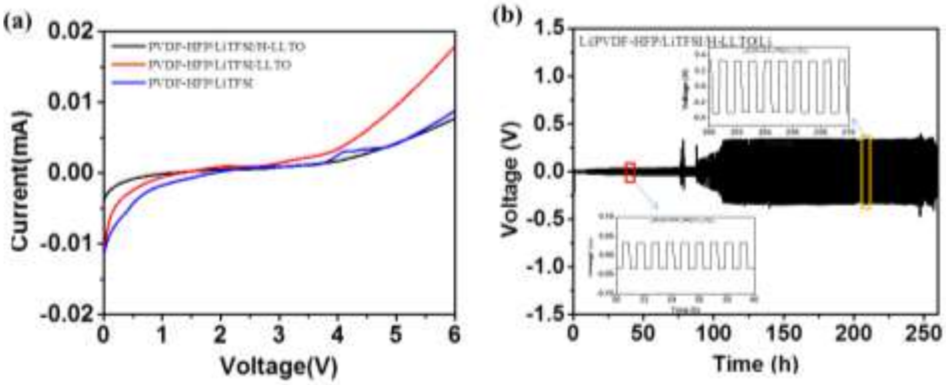

Figure 8. (a) Linear sweep voltammetry curve of the H-LLTO-based electrolyte membrane to show the electrochemical stability window in the range of 0–6 V. (b) Voltage profile of Li|PVDF-HFP/LiTFSI/H-LLTO|Li with a current density of 0.5 mA/cm².

Patents/Publications/Presentations

The project has no patents, publications, or presentations to report this quarter.

Task 1.4 – High Conductivity and Flexible Hybrid Solid-State Electrolyte
(Eric Wachsman, Liangbing Hu, and Yifei Mo, University of Maryland)

Project Objective. The project objective is to develop flexible hybrid electrolyte with garnet nanofibers to achieve the following: (1) flexible, with greater mechanical strength (~ 10 MPa) and thermal stability than polymer electrolytes; (2) high room-temperature ionic conductivity, ~ 0.5 mS/cm; (3) stable interface with lithium metal and effective blocking of lithium dendrites at current densities up to 3 mA/cm^2; and (4) battery performance with Li-S chemistry with an energy density of ≥ 450 Wh/kg (and ≥ 1000 Wh/L) and maintaining ≥ 80% of capacity up to 500 cycles.

Project Impact. Instability and/or high resistance at the interface of lithium metal with various solid electrolytes limit(s) the use of the metallic anode for batteries with high energy density, such as Li-air and Li-S batteries. The critical impact of this endeavor will be focused on developing a new type of SSE that is highly conductive, highly flexible, and electrochemically stable. The new SSE will enable Li-metal anodes with excellent interfacial impedance and blocking of lithium dendrite formation.

Approach. The project will synthesize garnet nanofibers, fill the porous region with polymer electrolyte, and characterize the flexible hybrid membrane properties. The flexible hybrid SSE microstructure will be determined using focused ion beam / scanning electron microscopy (FIB/SEM) and integrated with electrochemical methods to investigate the properties and stability with Li-metal anode.

Out-Year Goals. The project will develop a fundamental understanding of the mechanism of Li-ionic diffusion in garnet nanofibers and their mechanical properties, as well as these properties for hybrid garnet-fiber/polymer hybrids. Work will progress toward study of the electrode assembly during electrochemical cycling of the anode.

Collaborations. This project funds work at UMD, College Park. Dr. Eric D. Wachsman (PI) will focus on optimizing the garnet network to achieve high ionic conductivity and flexibility using FIB/SEM and electrochemical impedance spectroscopy (EIS) characterization. Dr. Liangbing Hu (co-PI) focuses on synthesis of the hybrid electrolyte and test for Li-metal anode with the hybrid electrolyte. Dr. Yifei Mo (co-PI) will lead efforts on computational modeling of the garnet nanofiber hybrid electrolytes for fundamental mechanistic understanding.

Milestones

1. Fully characterize electrochemical, mechanical, and thermal properties of hybrid SSE. (Q1, FY 2018; Completed December 2017)
2. Fabricate hybrid SSE with 20-µm thickness, and understand the Li-hybrid SSE interface through Li-SSE-Li symmetric cells. (Q2, FY 2018; Completed March 2018)
3. Understand lithium stripping and plating in thin SSE at a current density of 3 mA/cm^2 without shorting. (Q3, FY 2018; Completed June 2018)
4. *Go/No-Go Decision*: No lithium dendrites at 3 mA/cm^2 for 500 cycles. (Q4, FY 2018; Completed September 2018)

Progress Report

Hybrid electrolyte was fabricated as the project did before. In brief, 3D garnet framework was prepared by template method, and polymer electrolyte was infiltrated into the as-prepared porous garnet framework for several times to fill the pores and form parallel lithium-ion conducting routes, including: garnet phase, polymer phase, and their interfaces. The hybrid electrolyte was used to assemble a symmetrical cell with two pieces of lithium metal on both sides. Stainless steel discs were then pressed onto the lithium metal as current collectors. The cell was finally sealed in coin cell and tested using the Arbin charging/discharging station at room temperature and different current densities.

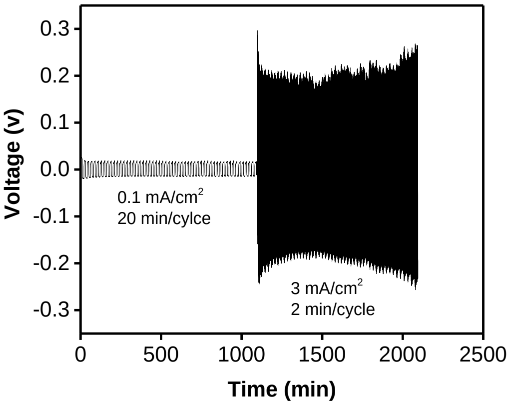

Figure 9. Cycling of the symmetrical cell of lithium metal/hybrid electrolyte/lithium metal assembly.

Figure 9 shows the electrochemical cycling performance of the symmetrical cell for the entire testing process. The cell was first cycled under low current density of 0.1 mA/cm^2 for ~ 18 hours to stabilize the lithium metal/hybrid electrolyte interfaces. The cell shows stable and uniform lithium stripping/plating behavior as flat cycling plateaus were observed during the stabilization procedure under low current density. After stabilization, the cell was cycled at high current density of 3.0 mA/cm^2 for 500 cycles. The enlarged plot is shown in Figure 10. As current density was increased by 30 times, overpotential of the cell increased correspondingly. After interfacial stabilization for a few cycles, the cell voltage was stable at 0.2 V for continuous cycling. Therefore, the cell was successfully cycled at 3 mA/cm^2 for 500 cycles without dendrite penetrating through the hybrid electrolyte to meet the Go/No-Go milestone.

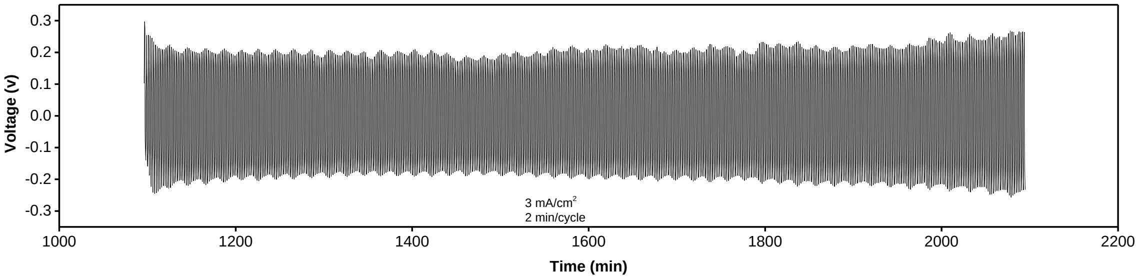

Figure 10. Cycling of lithium metal/hybrid electrolyte/lithium metal symmetrical cell at 3 mA/cm^2 for 500 cycles without lithium dendrite penetration.

Patents/Publications/Presentations

Presentation

- ANL (September 6, 2018): "Beyond Dendrites, Cycling Li-Metal Across Garnet at High Current Densities"; E. D. Wachsman.

Task 1.5 – Self-Forming Thin Interphases and Electrodes Enabling 3D Structured High-Energy-Density Batteries
(Glenn Amatucci, Rutgers University)

Project Objective. The project objective is to develop and implement a novel *in situ* formed Li-metal-based metal fluoride battery that will enable packaged 10-mAh batteries of energy densities > 1000 Wh/L and > 400 Wh/kg at 12 V.

Impact. Successful realization of 3D batteries formed *in situ* with a practical approach to large-scale fabrication would address some of the DOE EV performance goals, including: (1) areal capacity increase, (2) improved rates, and (3) designs to enable high-voltage unit cells.

Approach. The project is divided into two main tasks that focus on advance of the self-forming chemistry concurrent to cell design and fabrication. The self-forming chemistry task is comprised of three subtasks encompassing the negative and positive reactive current collectors, and the bi-ion glass conductor. The cell design and fabrication target development and integration of the bipolar configuration to achieve the 12-V single-cell goal.

Out-Year Goals. Work will continue toward improving reactive current collectors and cell design to optimize electrochemical performance of the cell stack in terms of energy density both gravimetric and volumetric, as well as capacity retention upon cycling. A secondary focus will be implementation of bipolar design within the cell structure.

Collaborations. All project tasks will be performed at Rutgers University.

Milestones

1. Establish negative reactive current collector compositions that enable high efficiency of lithium plating and stripping in excess of 90% during the *in situ* formation step and > 95% during subsequent cycles. (Q2, FY 2018; Completed)
2. Establish optimal type and composition of bi-ion conductors that achieve ionic conductivities in excess of 1 x 10^{-4} S/cm after *in situ* formation. (Q3, FY 2018; Completed)
3. Establish cell-stack design with 75% utilization of the positive reactive current collector and 12 V. (Q1, FY 2019; In progress)
4. *Go/No-Go Decision*: Achieve self-formed cell-stack of at least 750 Wh/L and 200 Wh/kg, and > 80% capacity retention after 20 cycles at a rate of C/10. Achieve an output voltage of 12 V. (In progress)

Progress Report

This quarter, the group continued R&D of the 12-V self-forming architecture initiated last quarter. While the initial cell architectures explored were limited to 8 V, optimization of the cell reorientation to simplify transport pathways enabled successful achievement of an electrolytically formed cell with 12-V output voltage. These 12-V architectures were fabricated reproducibly, charged to an excess of 12 V, and subsequently successfully discharged. However, positive electrode utilization was poor since these initial cells were fabricated as baseline designs without any of the chemical and structural improvements developed for the single self-formed cells reported over the past two years. As previously discussed, diffusion limitations induced electrochemically inactive pockets of materials, thereby preventing full access to the cell's theoretical capacity. Herein, the team reports on the first phase of improvement of the 12-V cell architecture through the design optimization at the electrode level and layout. This was executed with variations in the electrode design, aspect ratio, thickness and electrode width.

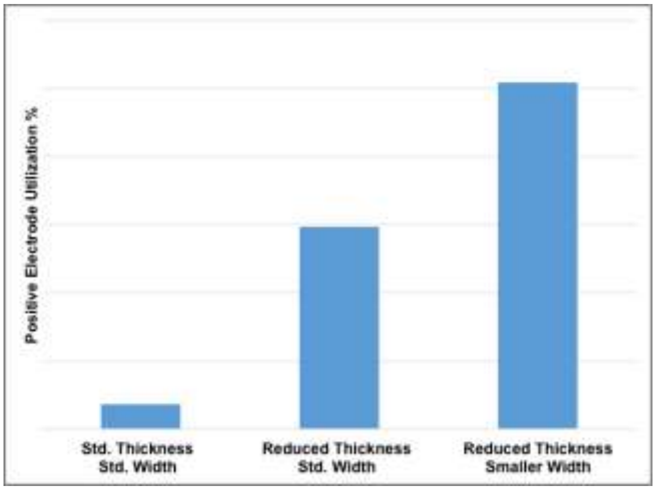

Figure 11. Positive electrode utilization of 12-V architectures as a function of cell design modifications that include variation of the electrode thickness and width charged to 13.5 V. By decreasing the aspect ratio of the electrodes and thereby increasing surface area, enhanced diffusion properties enabled access to previously electrochemically inactive areas, leading to higher utilization.

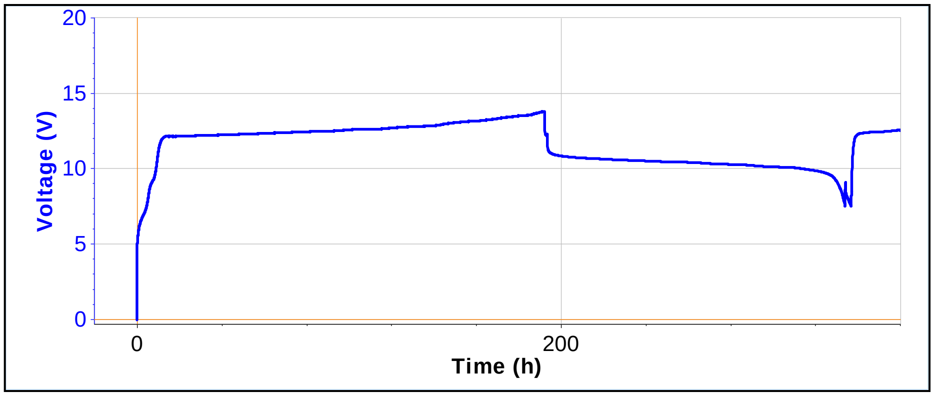

Figure 12. First-cycle voltage profile for self-formed 12-V cell with improved transport pathways due to cell design modification including reduced thickness and width. The cell was charged to 13.75 V before undergoing a stepped discharge protocol down to 7.5 V.

Decreasing the positive electrode thickness of the 12-V baseline architecture by a factor of three did not have significant impact on capacity, but increased positive electrode utilization. This clearly supports the fact that within the initial electrode design, the core of the active material is not participating in the electrochemical reaction in the baseline 12-V configuration. This is consistent with the project's novel chemistry development from previous quarters focused on transport within the bulk. These improved nanostructured architectures have yet to be implemented to the 12-V cells. Thinner electrodes that are also of smaller width show higher capacity and further enhanced utilization, as depicted in Figure 11. First-cycle voltage profile is illustrated in Figure 12, showing that the reduced positive electrode volume and its increased surface area enable shortened diffusion paths, making the chemistry more accessible and resulting in improved performance for the new configuration.

In addition to transport concerns, discontinuity in electrolyte coverage could also prevent full utilization of the positive electrode material. There was a physical break in the continuity of the reactive electrolyte that the team did not discover until finer analysis. Such an issue was addressed herein by increasing thickness of the reactive electrolyte to ensure proper coverage. This significantly improved the multifunctional positive electrode utilization of the 12-V cell to approximately 40% inclusive of the percentage of the electrode that needs to be retained as a current collector.

In summary, the team achieved an output of 12 V in a single unit cell of small dimension. They believe they can exceed 100 V within very small architectures. However, for safety and broad application, 24 or 48 V may be the most desired output.

To date, the project has achieved a stack energy density of a self-formed cell of > 580 Wh/L and a positive electrode energy density of 3900 Wh/L at 2.5 V; the plan is to exceed this in the 12-V architecture next quarter.

Moving forward with the 12-V architecture, the multicomponent nanolayered structured architectures the team developed this year that achieved 63% utilization on evaluation in a more traditional stacked arrangement will be integrated into the 12-V cell designs to further improve performance including utilization, capacities, and energy densities. The group will also focus on achieving performance within the 12-V architecture, which exceeds that of the lower voltage benchmark cells. The cycling protocols and chemistry combinations will be optimized to achieve the remaining milestones. This includes incorporation of the hybrid designs that have demonstrated C/10 rate utilization.

Patents/Publications/Presentations

The project has no patents, publications, or presentations to report this quarter.

Task 1.6 – Dual Function Solid-State Battery with Self-Forming, Self-Healing Electrolyte and Separator
(Esther Takeuchi, Stony Brook University)

Project Objective. The project objective is to demonstrate a solid-state rechargeable battery based on a Li-metal anode and iodine cathode with a self-forming, self-healing electrolyte and separator with high gravimetric and volumetric energy density.

Project Impact. This program will enable demonstration of the proposed rechargeable battery with improved power capability, high energy density, and a self-forming, self-healing SSE/separator. Technical insight will be gained regarding improved conductivity of the solid lithium iodide (LiI) based electrolyte, power capability of the proposed system, the self-healing nature of the LiI layer, the nature of the electrode-electrolyte interfaces, and feasibility of the system to reach the DOE targets.

Approach. The proposed concept is a dual function rechargeable solid-state battery utilizing LiI combined with silver iodide (AgI) as the electrolyte, with lithium metal (and small quantities of silver metal) as the anode and iodine as the cathode with a self-forming, self-healing separator/electrolyte. The battery will be assembled in the discharged state where the anode and cathode will be created during the first formation (charge) step. Initially, silver ion (Ag^+) will diffuse toward the negative electrode and be reduced to silver metal (Ag^0), and iodine ion (I^-) will be oxidized to elemental iodine (I_2) at the cathode side. As the formation of the battery continues, lithium ion (Li^+) will form a Li-metal layer at the anode, with generation of iodine at the cathode. LiI will remain and serve as both the separator and electrolyte.

Out-Year Goals. This is a multiyear program where the effort is divided into three major tasks.

- Year 1 involves electrolyte preparation and characterization including preparation of SSEs and conductivity measurements.
- Year 2 will focus on cell construction and testing including both *in situ* and *ex situ* analysis.
- Year 3 will focus on cell characterization. Under the program, cycle life, efficiency, energy density, and the functional capacity of cells will be determined.

Collaborations. This project collaborates with Amy Marschilok and Kenneth Takeuchi of SBU.

Milestones

1. Prepare construction A cells with the three most conductive electrolytes from Subtask 2.1.0. (June 30, 2018; Completed)
2. *Go/No-Go Decision*: Formation of Li^0, Ag^0 at anode and iodine at cathode with charging. (September 30, 2018; Completed)
3. Determine functional capacity and energy density of construction A cells. (December 30, 2018; Initiated)

Progress Report

Formation of Li^0, Ag^0 at Anode and Iodine at Cathode

This quarter's milestone was identification of the formation of lithium metal and silver metal at the anode and iodine at the cathode upon charge. Figure 13a depicts a schematic of the Li/I_2 battery detailing the *in situ* generation of the lithium anode and iodine cathode after an initial charge. The cell was charged using a step-wise approach (5, 10, and 20 $\mu A/cm^2$); see Figure 13b. After completion of the charging process, the solid electrolyte was recovered and investigated via XRD.

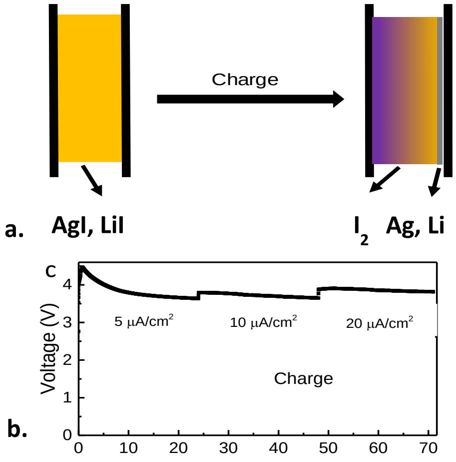

Figure 13. (a) Schematic of LiI battery: as-assembled (left) and after charge (right). (b) Example of step-wise charge profile.

As a demonstration of the feasibility in forming an *in situ* metal anode and iodine cathode, exemplative cells containing a solid electrolyte of reagent-grade *X*I, where *X*=Ag or Li, and supported by stainless steel spacers were constructed, charged, and investigated by XRD. XRD of the anode side of the charged silver(I) iodide-containing solid electrolyte (Figure 14a) confirmed the presence of elemental silver at the anode, as evidenced by several peaks that may be attributed to the 111, 200, and 220 crystallographic planes of the face-centered cubic silver crystals, respectively. Analysis of the cathode side (Figure 14b) confirmed the presence of iodine, evidenced by the appearance of peaks that may be ascribed to the 020 and 112 crystallographic planes of the orthorhombic iodine crystals. The diffraction pattern of the cathode of the LiI containing pouch cell (Figure 15a) revealed peaks consistent with the 020, 111, 112, 113, and 201 crystallographic planes of the iodine crystals. Peaks consistent with lithium can be observed on the anode side (Figure 15b).

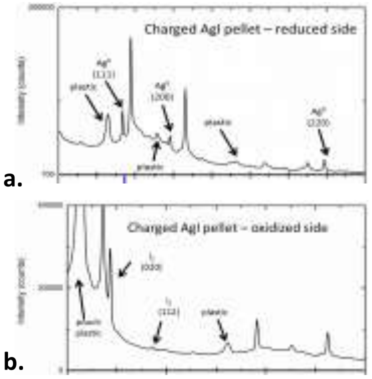

Figure 14. X-ray diffraction of negative (a) and positive (b) electrode of AgI pouch cell.

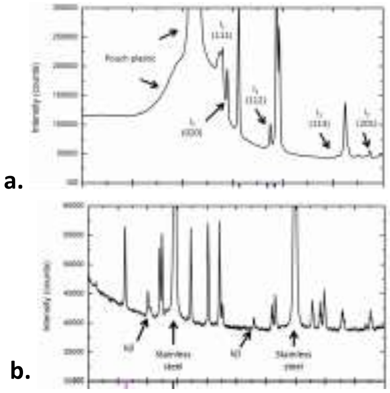

Figure 15. X-ray diffraction pattern of positive (a) and negative (b) electrode of LiI after charge.

A cell containing a solid electrolyte composed of 80% LiI/20% $LiI(HPN)_2$ was charged to 5% capacity by the aforementioned step-wise charging process. Examination of the recovered electrodes by XRD (Figure 16) depicted several peaks appearing at 2-theta values of 8.6°, 16.9°, 25.3°, 33.8°, 42.4°, and 51.4° and can be assigned to the crystallographic planes of I_2-$LiI(HPN)_2$ (for example, 001, 002, 003, 004, 005, and 006).[1-2] These peaks indicate a layered atomic arrangement of iodine atoms along the lattice *c* direction of $LiI(HPN)_2$. These results confirm the formation of the desired metal anode and iodine cathode. The results affirm project success for meeting the Go/No-Go metric.

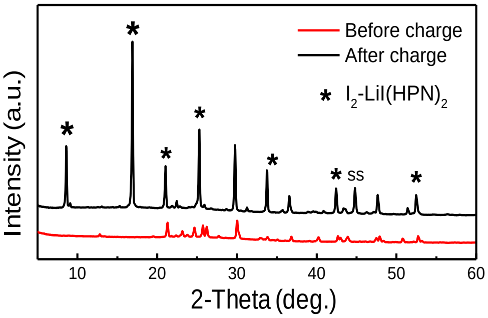

Figure 16. X-ray diffraction of positive and negative electrode of LiI-LiI(HPN)$_2$ after charge.

1. Liu, F.-C., Z. Shadike, F. Ding, L. Sang, and Z.-W. Fu. *Journal of Power Sources* 274 (2015): 280–285.
2. Wang, H., H. Li, B. Xue, Z. Wang, Q. Meng, and L. Chen. *Journal of American Chemical Society* 127 (2005): 6394–6401.

Patents/Publications/Presentations

The project has no patents, publications, or presentations to report this quarter.

Task 1.7 – High-Conductivity, Low-Temperature Polymer Electrolytes for Lithium-Ion Batteries (Bryan D. McCloskey, University of California at Berkeley)

Project Objective. Design of electrolytes with enhanced transport properties compared to conventional liquid organic electrolytes is key to improving the rate at which a Li-ion battery can be discharged or charged. Ideally, electrolytes would allow high mobility for lithium ions and disallow mobility of inactive ions (for example, the counteranion of the Li^+). However, current liquid electrolyte compositions usually provide higher mobility for the counteranion than Li^+, which results in high concentration polarization that disallows fast charging, particularly in batteries that employ thick porous electrodes, as is necessary for EVs to provide high energy densities. The project objective is to develop a high Li^+ transference number (t_{Li}, the fraction of ionic current carried by Li^+ in an electrolyte of uniform composition) polymer-based electrolyte that, when used in a Li-ion battery, can support current rate capabilities sufficient for EV propulsion at room temperature.

Impact. Development of practical high t_{Li} polymer-based electrolytes for Li-ion batteries would enable safer Li-metal and graphitic anode cycling and thicker porous electrode designs, leading to improved specific and volumetric battery energy densities consistent with the EV Everywhere Grand Challenge. High-energy anode and cathode materials, such as lithium metal, silicon, and high-voltage layered or spinel structures, could be enabled by electrolytes with high t_{Li} and large operating voltage windows, such as those based on sulfones, as proposed here.

Approach. Lowering the operating temperature of polymer electrolytes has been cited as an important challenge to their viability as Li-ion battery electrolytes. The project will address this challenge by using Li^+ neutralized anionically charged polymers as salts in conventional liquid solvents. Using these so-called polyelectrolyte solutions, initial results indicate that the project can access t_{Li} values typical of single-ion conducting polymer electrolytes ($t_{Li} > 0.9$) and conductivity values (> 1 mS/cm at room temperature) that approach those of traditional battery electrolytes.

Out-Year Goals. The optimization of transport and stability properties of these polyelectrolyte systems, through understanding of appropriate polymer and solvent design, is the objective. The goal is to develop new polyelectrolyte compositions that provide superior transport properties (specifically, higher t_{Li} and conductivity) than conventional liquid electrolytes and enable use of high-energy electrode materials, such as lithium metal.

Collaborations. Collaborations on this project include Vince Battaglia (porous electrode preparation) and Kristin Persson (atomistic modeling) at LBNL.

Milestones

1. Complete COMSOL modeling to identify target transference number and conductivities for electrolytes that enable efficient fast charging (~ 3 C). (Q1, FY 2018; Completed October 2017)
2. Complete synthesis and physical characterization of polysulfone and PEO-based ionomers of various molecular weights. Progress measure: Publish a comprehensive article on understanding of design criteria of high transference number/high conductivity electrolytes. (Q2, FY 2018; Completed February 2018)
3. Complete transport measurements for polyelectrolyte solutions comprised of various molecular weight polymers. *Go/No-Go Decision*: Switch polymer chemistries if optimized polyelectrolyte solution transference number is less than 0.9 and conductivity at room temperature is less than 0.1 mS/cm. (Q3, FY 2018; Completed June 2018)
4. Complete polyelectrolyte solution cycling measurements using Li-metal electrodes to confirm that high transference number electrolytes suppress dendrite formation. (Q4, FY 2018; On schedule)

Progress Report

Work focused on continued investigation of fundamental polyelectrolyte solution properties to inform the design of high transference number solutions in a battery-relevant EC/DMC blend solvent, as opposed to DMSO, as has been used previously.

The vast majority of polyelectrolyte solution literature has investigated properties of water-based solutions, with very few studies focused on nonaqueous transport properties. No study has reported behavior of any charged polymer dissolved in EC/DMC. In general, polyelectrolyte theory would suggest that the dielectric constant of the solvent is the most important factor determining solution behavior, and thus the team would expect EC/DMC to behave similarly to the DMSO solutions previously studied. As DMSO co-intercalates with lithium into graphite electrodes, ideally EC/DMC would be used as solvent. To investigate the transport properties of an EC/DMC solution, the team utilizes a sulfonated polysulfone/poly(ethylene glycol) copolymer (PSf-co-PEG). The project investigates the transport properties of this polymer as a function of polymer concentration and solvent type (EC/DMC versus DMSO), and as a function of added LiTFSI salt (Figure 17). The conductivity of these solutions is plotted here for DMSO and EC/DMC. The team finds that the conductivity of all solutions increases with added small molecule salt ("LiTFSI Added" on the x-axis), but significant differences exist between EC/DMC and DMSO. The polymer solution without added salt has much lower conductivity in EC/DMC than in DMSO. Further, while the polymer/salt solutions in DMSO have higher conductivity than pure LiTFSI (the "0M Polymer" line), in EC/DMC the conductivity of the polymer-containing solutions is actually lower than with just LiTFSI. Through direct observation of the ^{7}Li NMR peak width, and computational calculations performed in collaboration with Kristin Persson, the team finds that the reason for this difference is poor dissociation of the sulfonate/lithium ion pair on the polymer backbone. This study indicates the need for alternative, charge delocalized anion chemistries to enable carbonate solvent-based polyelectrolyte solutions.

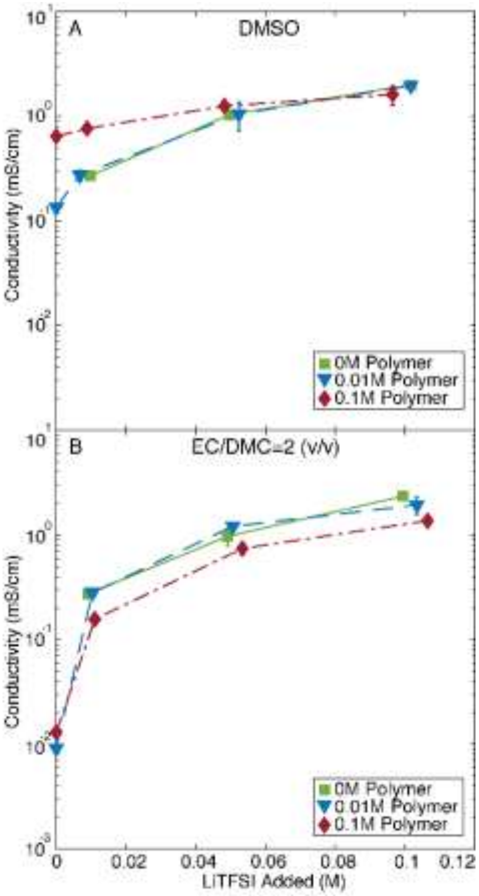

Figure 17. Conductivity of Li⁺-neutralized sulfonated PSf-co-PEG polymer solutions with added LiTFSI salt. Polymer concentration is reported as sulfonate concentration.

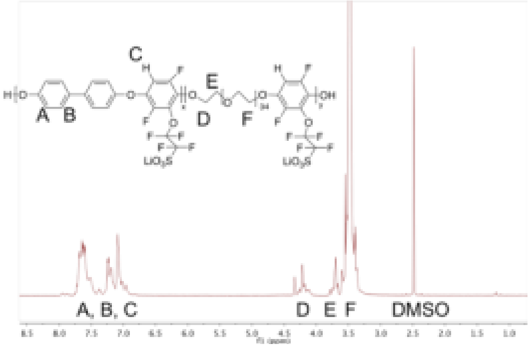

Figure 18. H nuclear magnetic resonance spectrum of a new ionomer that imparts improved ion dissociation in EC/DMC mixtures.

To address the clear need for an alternative polymer chemistry, the team synthesized a monomer containing a fluorinated, sulfonated side chain first synthesized by Oh et al. in 2016 (Figure 18, *Chemistry of Materials* 28: 188–196). The project has successfully incorporated this monomer into a polymer with PEG as shown in proton NMR spectra. An initial test found that the polymer with 40 mol% PEG is soluble in EC/DMC at least to 0.1 M and has a conductivity of 0.12 mS/cm, an order of magnitude higher than the PSf-co-PEG previously discussed. Further purification and characterization are necessary to fully verify this result, and deconvolute the aromatic ring region of the NMR spectra, which will be the focus of the first milestone in FY 2019.

This quarter, the team also began to work on cell cycling measurements with lithium metal to investigate the benefits of the high transference number polyelectrolyte solutions previously synthesized. Unfortunately, this work was hampered by inconsistencies between cells and has thus required significant time in process development of cell fabrication. The team anticipates completion of this milestone by the second quarter of FY 2019.

Patents/Publications/Presentations

Publication

- Diederichsen, K. M., K. D. Fong, R. Terrell, K. A. Persson, and B. D. McCloskey. "Investigation of Solvent Type and Salt Addition in High Transference Number Nonaqueous Polyelectrolyte Solutions for Lithium-Ion Batteries." *Macromolecules.* Accepted.

Presentations

- 256th American Chemical Society (ACS) Meeting, Symposium on Designing Polymers for Electrochemical Applications, Boston, Massachusetts (August 2018): "Ion Transport in Ionomers and Polyelectrolyte Solutions for Lithium Batteries." Invited.
- GRC, Polymer Physics, Mount Holyoke College, South Hadley, Massachusetts (July 2018): "Designing Polymer-Based Electrolytes with High Lithium Ion Transference Number and Conductivity." Invited.
- GRC, Polymer Physics, Mount Holyoke College, South Hadley, Massachusetts (July 2018): "Investigation of Solvent Type and Salt Addition in High Transference Number Nonaqueous Polyelectrolyte Solutions." Poster.

Task 1.8 – Advanced Polymer Materials for Batteries (Zhenan Bao and Yi Cui, Stanford University)

Project Objective. This project will develop new polymer materials for batteries. The team will develop polymer coatings with specific mechanical properties that can accommodate the volume expansion and contraction of the Li-metal anode associated with deposition and stripping (charging and discharging).

Project Impact. The cycling stability and CE of Li-metal electrodes will be increased by implementation of a polymer-based protective layer that functions as an artificial SEI with desired properties. The improved performance will enable further development toward practical utilization of Li-metal anodes with higher cycling efficiency and less susceptibility to dendrite-based failure.

Approach. The project uses soft polymer coatings with dynamic crosslinking to give the resulting polymers liquid-like rheological properties and stretchable and self-healing properties. In previous work, the project has shown that such coatings resulted in uniform deposition/stripping of lithium metal and improved cycling stability of Li-metal electrodes. To understand the design rules for effective polymer coatings, the team chose a few representative polymers to systematically understand structure property relationships. Here, the team investigates the correction between surface energy of the polymer and exchange current for lithium deposition.

Out-Year Goals. Work will progress toward the correlation between dielectric constant and exchange current. These findings will enable further understanding and development of various polymer coatings for protecting Li-metal anodes.

Collaborations. There are no active collaborations this quarter.

Milestones

1. Explore the effects of various commercial polymers on lithium nucleation and interfacial kinetics. (Q1, FY 2018; Completed)
2. Develop polymer coating to mechanically suppress lithium dendrites and improve cycle life. (Q2–Q3, FY 2018; Completed)
3. Understand effects of polymer coating properties such as dielectric constant and surface energy, among others, on lithium electrochemistry and electrode performance. (Q3–Q4, FY 2018; Completed)

Progress Report

For this study, the project systematically chose several different polymers that have been previously used in battery applications. PEO is a common solid polymer electrolyte, and PU and PVDF are common gel electrolytes. Additionally, PVDF and PVDF-HFP are also common binder materials for composite electrodes. PDMS was tested because it has been used previously as a coating to stabilize lithium metal. Last quarter, the team investigated effects of polymer chemistry and thickness on the morphology of Li-metal coating. This quarter, the team investigated the effects of dielectric constant, surface energy on the exchange current density.

Exchange Current Density. Initially, the team presumed that the difference in nuclei size was a result of changes in the nucleation overpotential, as per classical nucleation theory. However, they found that the differences in the overpotential for the lithium nucleation event measured from the galvanostatic charging were not enough to explain the variation in nuclei size, let alone their shape or morphology (Table 2). This galvanostatic nucleation overpotential is a combination of all of the different overpotential components present in the coin cell including competition between the double layer capacitance and the nuclei growth. To more accurately characterize the electrochemical processes occurring in the system, the team turned to measuring the lithium exchange current density, which reflects the direct interaction of the polymer coating with the Li-metal surface and can provide more precise information about the overpotential in the system. Generally, lower values of the exchange current density mean that the surface of the lithium metal is inhibited or passivated, and in the field of electrodeposition inhibition represents the degree to which additive molecules absorb to the active metal surface and suppress the reduction reaction. In the case of the control system (ether electrolyte with 1 wt% $LiNO_3$), the $LiNO_3$ acts as an inhibitor, which promotes the growth of rounded lithium particles and improves the CE. For lithium deposition on polymer-coated electrodes, the specific polymer coatings take on the role of inhibitors because they are directly in contact with the lithium surface at the onset of and throughout deposition. Thus, the exchange current densities measured would ideally represent the level of inhibition or the strength of absorption and interaction of the polymers with the as-deposited lithium metal and provide some relation to the lithium morphology observed.

Table 2. Properties of the polymer coatings in the battery environment.

Polymer	Overpotential[a] [mV]	j_0 [b] [mA/cm^2]	Swelling [%]	σ [c] [mS/cm]	Size [um]
PU	76.8	20	595.0	0.10	0.54
PVDF-HFP	80.2	39	27.2	0.07	2.85
PEO	87.8	22	Soluble	0.27	0.41
PDMS	121.3	5	28.0	0.10	1.26
SHP	129.9	27	Soluble	0.15	0.26
PVDF	151.0	27	27.5	0.06	3.32

[a] Nucleation overpotential determined from galvanostatic cycling. [b] Exchange current density. [c] Ionic conductivity.

It is challenging to accurately measure the exchange current density in traditional coin cell geometries because of SEI forming reactions that occur on the surface of the lithium metal. Fast sweep rates would allow this limitation to be overcome, but are generally not possible due to mass transport limitations. Here, the team utilized a homebuilt microelectrode, a technique known to overcome the mass transport limitations, to perform cyclic voltammetry (CV) sweeps at high rates of 200 mV/s. At these high sweep rates, the freshly deposited lithium is in direct contact with the polymer coating because the short timescale (~ 2 s) of the scan minimizes any reactions of the lithium metal and electrolyte that may occur. These quick scan rates prevent resistive SEI formation from influencing the experiment and provide accurate measurement of the exchange current density, which reflects how the polymer coating interacts with the Li-metal surface.

Table 3. Surface and electrical properties of polymers used in this study.

Polymer	γ^{a} [mJ/m^2]	κ^{b}	$j_0{}^{c}$ [mA/cm^2]	CE^{d} [%]
DOL/DME	-	-	27	98.80 (±0.69)
PDMS	14.6 (±0.95)	2.77 (±0.30)	5 (±2.0)	99.42 (±0.05)
PEO	43.7 (±0.47)	5.42 (±0.35)	22 (±3.4)	98.71 (±0.05)
PU	40.8 (±2.5)	6.56 (±0.52)	20 (±5.5)	98.51 (±0.18)
PVDF	34.8 (±1.4)	10.0 (±1.75)	27 (±6.32)	99.11 (±0.15)
PVDF-HFP	31.0 (±1.5)	15.2 (±0.31)	39 (±10.6)	98.98 (±0.62)
SHP	38.6 (±0.43)	8.76 (±1.24)	27 (±5.4)	97.93 (±0.05)

^{a} Surface energy. ^{b} Dielectric constant at 100 Hz. ^{c} Exchange current density. ^{d} Coulombic efficiency.

EIS is sometimes used to measure the charge transfer resistance and exchange current, but the team has found that the charge transfer resistances measured from Li||Li symmetric coin cells and by microelectrode could differ by orders of magnitude (0.1 mA/cm^2 vs. 10s of mA/cm^2). This discrepancy is because the high-frequency AC used in EIS does not cause significant amounts of lithium deposition. Thus, the kinetics probed by EIS here are mostly of Li$^+$ transport.

Tafel plots are created from the high-rate CV scans, and the exchange current density (j_0) is extracted from the cathodic slope. Typical exchange current densities for lithium in liquid electrolytes are 27 mA cm^{-2} for DOL/DME with 1 M LiTFSI and LiNO$_3$ (Table 3) and 35 mA cm^{-2} for EC/DEC with 1 M LiPF$_6$. The polymer coatings tested here show exchange currents both lower and higher than these values, indicating that the materials the team has selected cover a broad range of properties. PEO and PU both exhibit a low j_0 around 20 mA cm^{-2} and similarly contain ether groups throughout their backbones that may coordinate strongly with Li$^+$. In comparison, the self-healing polymer (SHP) coatings show a higher j_0 of 26.9 mA cm^{-2} and have a combination of polar hydrogen The chemically similar fluorinated PVDF and PVDF-HFP both show higher j_0 of 27.2 mA cm^{-2} and 39.1 mA cm^{-2} respectively. Consistent with literature, the team finds that PDMS promotes the growth of moderate-sized lithium particles, and when examining the exchange current they measured a very low j_0 of 4.7 mA cm^{-2}.

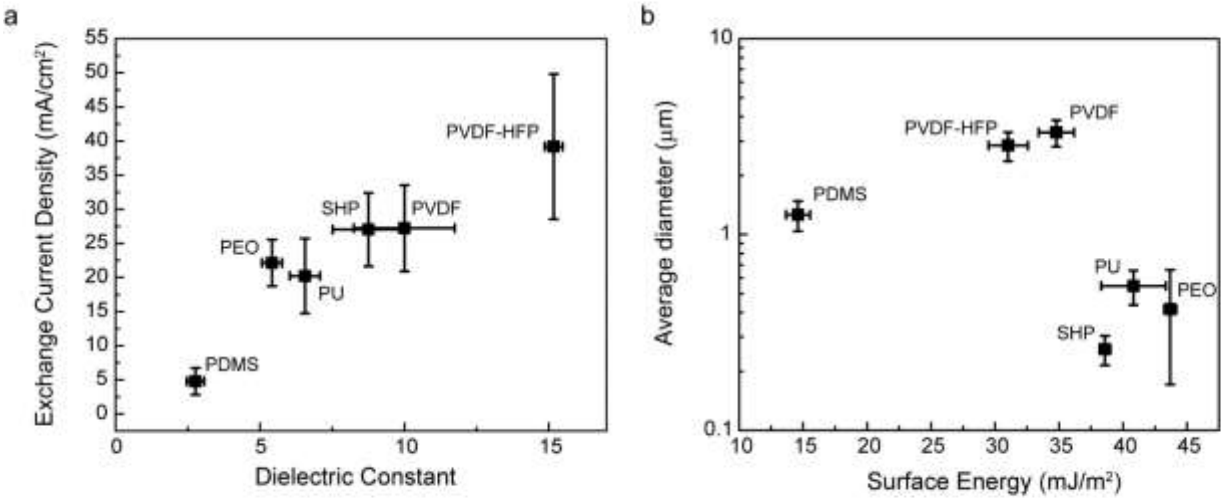

Figure 19. (a) Exchange current density plotted against dielectric constant for various polymer coatings measured via microelectrode. (b) The average diameter of the lithium deposited under various polymer coatings plotted against the surface energy of those coatings. Error bars represent the standard deviation for all samples measured.

Exchange Current, Surface Energy, and Lithium Particle Size. As mentioned above, the mechanical properties of the polymer coating and the overpotential measured from galvanostatic deposition could not accurately predict the size of the lithium particles that were deposited. The team also found that the swelling, ionic conductivity, or resistance of the film did not follow any discernable trend (Table 2). However, they observed that the exchange current increased with dielectric constant of the polymer coating (Table 3 and Figure 19a). PVDF-HFP contains a high density of polarizable fluorinated groups and has a higher dielectric constant of 15. PVDF-HFP also exhibited the highest measured exchange current. PDMS has a much lower dielectric constant of 2.7 because of the nonpolar nature of the siloxane chemistry and exhibited the lowest exchange current measured. The other polymers tested have intermediate dielectric constants and their exchange current densities fell in between that of PVDF-HFP and PDMS. The team hypothesizes that the relationship between dielectric constant and exchange current is due to the better solvation of Li^+ ions at the lithium-polymer interface from improved charge screening by the high dielectric constant coatings. This allows for easier dissolution and solvation of the lithium from the metal electrode surface and could also increase the concentration of Li^+ ions available for deposition locally. These phenomena would cause an increase in exchange current between the Li-metal surface and the electrolyte and are different effects from the adsorption-based inhibition that happens in the case of low concentration additives added to electrolyte solutions.

The team also noticed that in general, the size of lithium deposits increased for the polymer coatings with higher exchange current. However, PDMS presents a notable exception. Even though it has a very low exchange current due to a low dielectric constant, the lithium deposited under the PDMS coating grows into large particles around 1.26 μm in size. When the team reexamined the relationship between deposit size and other polymer properties, they found that PU, PEO, and SHP coatings all had high surface energy and promoted the growth of small lithium particles around 100-400 nm in size (Figure 19b). The higher surface energy coatings should have enhanced adhesion to the Li-metal surface compared to the lower surface energy polymers, and this stronger polymer-Li interaction serves to stabilize the Li-polymer interface. When both surface energy and exchange current are considered as relevant parameters, the anomalous size of the lithium in the presence of the PDMS coating can be understood. The low surface energy of PDMS (14.6 mJ m^{-2}) resulted in a larger average particle size than the other polymers with low dielectric constants, but smaller than the ~3 μm particles from intermediate surface energy, high dielectric constant PVDF, and PVDF-HFP.

This combined dependence of the lithium particle size on both surface energy and exchange current becomes clear when the energetics of the nucleation process are analyzed. A critical radius (r_{crit}) for lithium nucleation can be found by examining the free energy for nucleating a new particle (ΔG_{nuc}). This free energy is the combination of the free energy for the bulk species (ΔG_{bulk}) and the energy required to create the new lithium surface (ΔG_{surf}):

$$\Delta G_{nuc} = \Delta G_{bulk} + \Delta G_{surf} \quad (1)$$

$$\Delta G_{nuc} = -\frac{zF|\eta|}{V_{molar}} V + \Gamma * SA \quad (2)$$

where z is the number of electrons transferred, F is Faraday's constant, η is the overpotential, V_{molar} is the molar volume of lithium, Γ is the interfacial energy of the Li-metal surface, V is the volume of the nuclei, and SA is the surface area of the nuclei. The maximum in this function with respect to size of the new particles represents the transition from small unstable clusters to stable larger nuclei. Assuming that the nuclei are spherical and differentiating with respect to the radius of the nuclei yields the following as the critical radius size.

$$r_{critical} = \frac{2\Gamma V_{molar}}{zF|\eta|} \quad (3)$$

From equation 3, one can see that changes in both Γ and η can affect the critical size of the nuclei. Γ can be defined in terms of the surface energies of the two materials in contact. It is expressed as the following:

$$\Gamma = \gamma_{Li} + \gamma_{poly} - 2\Phi\left(\gamma_{Li}\gamma_{poly}\right)^{\frac{1}{2}} \quad (4)$$

where γ_{Li} is the surface energy of the lithium metal, γ_{poly} is the surface energy of the polymer coating, and Φ is an interaction parameter for the two species. By expanding equation 4 with a Taylor series around the center of the surface energy data collected here (γ_{poly} = 30 mJ m^{-2}), the team finds that the second order and higher terms are two orders of magnitude smaller than the linear term and that the first order term is negative. Therefore:

$$\Gamma \propto -\gamma_{poly} \quad (5)$$

The Butler-Volmer equation describes how the exchange current relates to the overpotential. At high overpotential it reduces to the Tafel equation shown below for the case of a cathodic process.

$$-\eta = -A \ln\left(\frac{j}{j_0}\right) \quad (6)$$

$$-\eta \propto -\ln\left(\frac{j}{j_0}\right) \quad (7)$$

where A is known as the Tafel slope and j is the current density. From these two evaluations, it is seen that the nuclei size scales with both the surface energy of the polymer and the exchange current:

$$r_{crit} \propto \frac{-\gamma_{poly}}{\left|\ln\left(\frac{j}{j_0}\right)\right|} \quad (8)$$

As surface energy increases, the particle size decreases. Furthermore, as exchange current increases, the ratio of j/j_0 decreases, which causes the overpotential to decrease. This decrease in overpotential causes an increase in the size of the nucleating lithium particles.

In addition to the scaling described above, high dielectric constants and corresponding high exchange currents serve to decrease the lithium nucleation rate through decreased overpotential (equation 9) and increase the size of nucleation exclusion zones, resulting in more sparsely packed, larger lithium deposits. The nucleation rate (J) can be written as:

$$J = K_1 \exp\left(-\frac{K_2}{\eta^2}\right) \quad (9)$$

where and K_1 and K_2 are constants that are practically independent of the overpotential. Nucleation exclusion zones refer to the local deformations in the electric field that occur near the newly formed lithium nuclei and cause an ohmic drop in the potential around the new nuclei. This potential drop prevents new nuclei from forming and is related to the exchange current. At high exchange current densities, the screening of the nuclei is poor and so the exclusion zones are large, leading to the growth of only the initial nuclei and thus larger particles. It should be noted, however, that these effects still enable relatively dense lithium deposits without compromising the lithium coverage of the electrode.

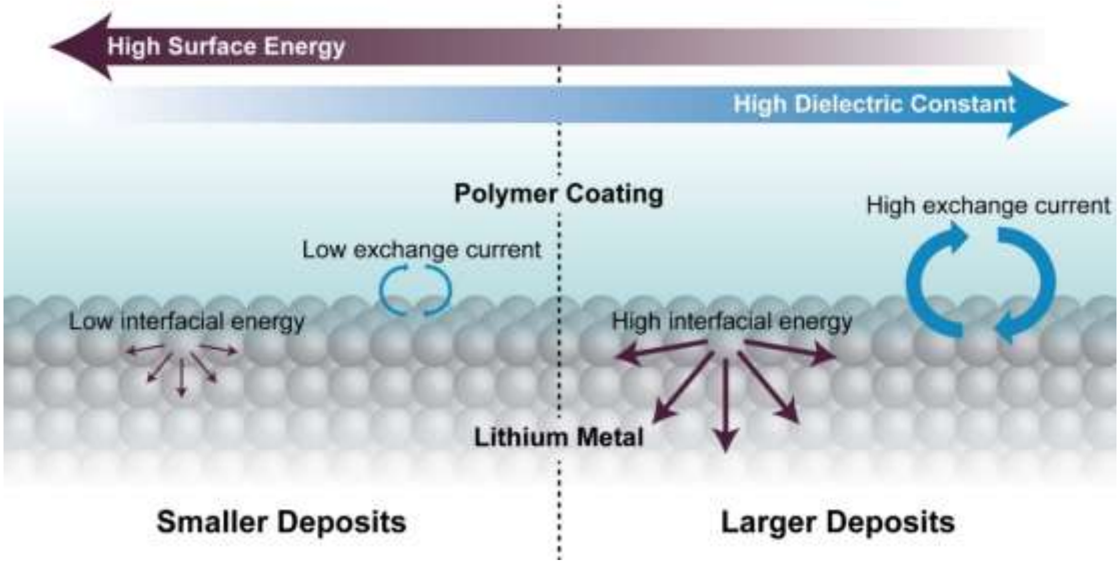

Figure 20. Schematic of the factors influencing Li-metal deposition through a polymer coating. Low surface energy coatings give rise to higher interfacial energies and encourage the growth of large surface area particles. Additionally, high dielectric constant polymers have higher exchange currents and promote larger Li-metal deposits.

Simultaneously, polymers with low surface energies have a weaker interaction with the lithium metal, and therefore do not reduce the polymer-Li interfacial energy as much as high surface energy polymers. With increased interfacial energy, the lithium will deposit as larger particles to minimize surface area and reduce the total energy of the Li-polymer interface. This phenomenon was suggested by Archer et al. in their calculations for polymer systems with immobilized anions. Intuitively, both the chemical and ionic properties of the interface between the polymer coating and the Li-metal surface should influence the lithium deposition and growth. There should be interplay between the effects of polymer surface energy and exchange current; the swollen polymer coating at the lithium interface serves critical roles in the deposition process as both a surface inhibitor and also as a localized electrolyte, mediating both charge-transfer and ionic transport. It may be the case that there is some cooperative inhibition behavior between the $LiNO_3$ and the polymer coatings, as has been observed in traditional electrodeposition systems. Further study of these cooperative effects should be pursued using the framework presented here. Figure 20 schematically illustrates the effects of the exchange current and interfacial energy on the lithium particle size, as described through the polymer dielectric constant and surface energy. In general, larger lithium particles deposited under polymer coatings correspond to polymers with high dielectric constant and low surface energy.

Cycling Efficiency. Finally, the team tested the CE of the polymer coatings, as this is one of the most important factors for Li-metal electrode performance. An average CE was measured by depositing a fixed reservoir of lithium, cycling a fixed 1 mAh cm^{-2} capacity for 10 cycles, and then stripping all of the remaining lithium. Most of the coatings exhibited CEs around 98%, which is similar to the control case of the ether-based electrolyte. Notably, the PDMS coatings achieved a higher CE of 99.13%. There was no clear relationship between exchange current density and cycling CE. However, when the team orders the polymers by decreasing reactivity, an upward trend in the CE is observed (Figure 21). The reactivity of the different polymer coatings was estimated from their relative bond strengths. This is consistent with the present understanding that sub-100% efficiency of Li-metal deposition/stripping is considered to be the result of parasitic side reactions, and highlights the importance of polymer reactivity as an additional parameter. The team also finds that while CE is generally higher for polymer coatings that promote larger sized lithium deposits (PVDF-HFP, PVDF, and PDMS), lower surface energy appears to be the best parameter that was recorded in this study for predicting high cycling CE.

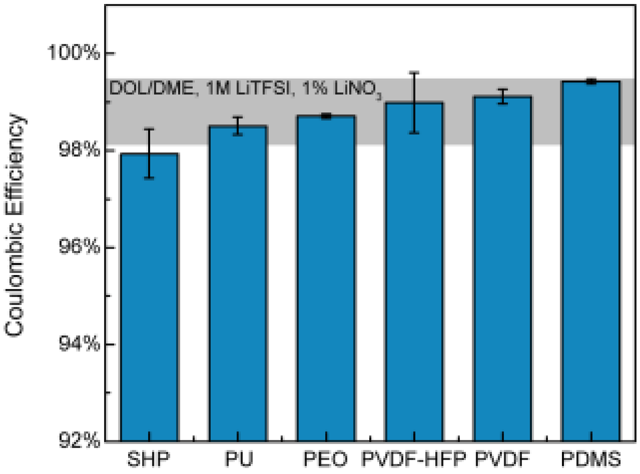

Figure 21. Coulombic efficiency (CE) of various polymer coatings. The horizontal axis is ordered in decreasing volume density of reactive groups. The gray bar represents the CE of bare copper electrodes in DOL/DME electrolyte with 1 M LiTFSI and 1% LiNO$_3$.

Conclusions from the Studies. By examining the initial stages of lithium deposition and growth in the presence of polymer coatings, the team has found that the chemistry of a polymer coating has significant impact on lithium electrodeposition. The chemical functionality of a polymer coating resulted in different local Li-deposit morphology, but coating mechanical properties, including modulus and flowability, and uniformity are still very important for the global deposition quality. The team additionally found that the dielectric constant, and thus the solvation environment of the Li$^+$ ions, of the respective coatings determines the exchange current in the presence of polymer coatings. Furthermore, the size of the lithium particles is dependent on both the dielectric constant, due to effects of the exchange current on nucleation, and surface energy, due to energetics of the Li-polymer interface, of the polymer coatings. Finally, both coating thickness and reactivity should additionally be considered, as they both have large effects on coating performance. Moving forward, new coatings should be designed with high dielectric constant, low surface energy, and low reactivity. Ideally, a coating would also be soluble in nonpolar solvent or amenable to melt processing below lithium's T_m at 180°C. This would allow for direct coating on the Li-metal surface, which is important for fabrication of practical Li-metal batteries that are unlikely to be anode-less. The insight provided here should serve as a starting point for further systematic investigation into soft organic coatings that can potentially help to enable the uniform and reversible deposition of lithium metal at high rates and over long times.

Patents/Publications/Presentations

Publication

- Lopez, J., A. Pei, J. Y. Oh, G.-J. N. Wang, Y. Cui, and Z. Bao. "Effects of Polymer Coatings on Electrodeposited Lithium Metal." *Journal of American Chemical Society* 140 (2018): 11735–11744.

Presentation

- 256th ACS Meeting – *Eastman Chemical Student Award Winner* (August 19, 2018): "Understanding the Influence of Polymer Properties on the Stability of High Capacity Silicon and Lithium Metal Anodes"; J. Lopez, A. Pei, J. Y. Oh, G.-J. N. Wang, Y. Cui, and Z. Bao.

Task 1.9 – Improving the Stability of Lithium-Metal Anodes and Inorganic-Organic Solid Electrolytes (Nitash Balsara, Lawrence Berkeley National Laboratory)

Project Objective. The project objective is to establish a new hybrid electrolyte that will be stable against cells with a Li-metal anode.

Project Impact. Polymer electrolytes offer increased stability in lithium batteries in comparison to more widely used liquid electrolytes. Nanostructured electrolytes containing both soft, ion-conducting domains and rigid nonconducting domains offer the opportunity to tune both mechanical and electrical properties separately. Such electrolytes are conveniently made by block copolymer self-assembly. Most of the block copolymer electrolytes studied thus far comprise organic polymer chains for both the conducting and rigid domains. The team hopes to synthesize new electrolytes that simulataneously have high transport properties and have greater stability against lithium in comparison to organic diblock copolymers.

Approach. First, the team synthesizes hybrid diblock copolymers by incorporating monomers that contain an inorganic component. Then electrolytes are prepared by mixing these diblock copolymers with salt. Electrochemical and mechanical characterization of these materials is performed before carrying out cycling X-ray tomography experiments. The combination of these approaches enables rational design of materials that exhibit improved stability against lithium metal.

Out-Year Goals. The project will synthesize a new hybrid electrolyte that is designed to be stable against lithium metal. The material is a block copolymer wherein acryloisobutyl polyhedral oligomeric silsesquioxane (POSS) is covalently bonded to the chain. The second block is a conventional polymer electrolyte, PEO. Electrochemical characterization of this polymer will include measurement of all transport properties including conductivity, diffusion coefficient, and the transference number. The stability against lithium metal will be evaluated by CV, while its applications as an electrolyte will be evaluated and visualized using cycling X-ray tomography experiments on symmetric Li-hybrid-Li cells.

Collaborations. There are no active collaborations this quarter.

Milestones

1. Synthesis of POSS-PEO block copolymer hybrid electrolyte. (Q1, FY 2018; Completed)
2. Measurement of conductivity of the hybrid copolymer. (Q2, FY 2018; Completed)
3. Measurement of diffusion coefficient and transference number of electrolytes. (Q3, FY 2018; Completed)
4. Completion of the first Li-electrolyte-Li tomography experiments. (Q4, FY 2018; Completed)

Progress Report

Milestone 4 has been completed. A triblock copolymer of POSS-PEO-POSS (molecular weight 5k-35k-5k) was synthesized, an electrolyte membrane was cast and electrochemically characterized, and the first Li-electrolyte-Li tomography experiments were completed. The electrolyte membrane was cast with LiTFSI salt concentration r = [Li]/[EO] = 0.04. Data are summarized below.

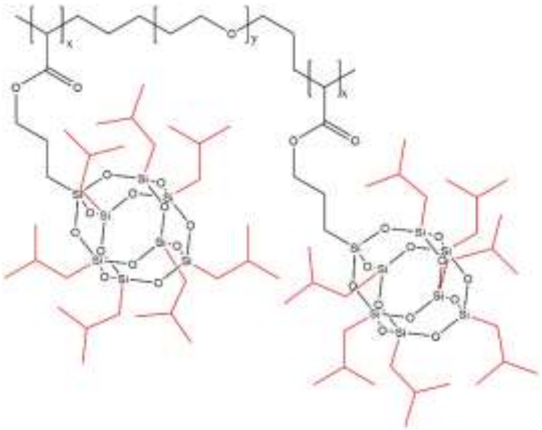

This 30-μ-thick solid organic-inorganic polymer electrolyte was sandwiched between two Li-polymer-Li cells and polarized to electrodeposit lithium from one electrode to the other. The current density was increased systematically. The membrane forming character of the organic-inorganic hybrid electrolyte was exceptional, leading to low interfacial impedance, relative to typical values in all-organic block copolymer electrolytes.

For the first time, the team was able to hit the limiting current of 4.5 mA/cm^2 without the cell shorting immediately. In all of the project's previous experiments on block copolymer electrolytes, cells shorted well before the limiting current was reached. Also of note, the estimate of limiting current is based on complete characterization of solid polymer electrolytes using the Newman approach. At the limiting current, the cell did short, as predicted by theory. The X-ray microtomography results show that the cell failed due to the formation of a single dendritic defect. Further analysis of failure modes in the project's novel organic-inorganic solid electrolytes are in progress.

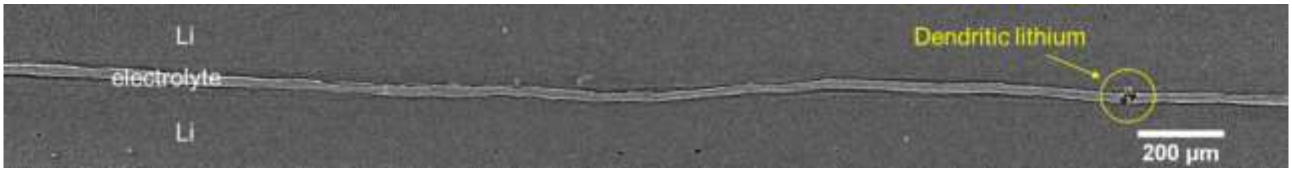

Figure 22. Slice through a volume imaged using X-ray tomography showing a well-fabricated cell and uniform electrolyte membrane. The dendritic defect causing cell failure is identified.

Patents/Publications/Presentations

Publication

- Maslyn, J. A., W. S. Loo, K. D. McEntush, H. J. Oh, K. J. Harry, D. Y. Parkinson, and N. P. Balsara. "Growth of Lithium Dendrites and Globules through a Solid Block Copolymer Electrolyte as a Function of Current Density." Revised manuscript sent to *Journal of Physical Chemistry* 201.

Task 1.10 – Electrolyte/Binder for High Efficiency Lithium-Sulfur Battery: New Materials Design and Computation (Larry A. Curtiss, Zhengcheng Zhang, and Ahn Ngo, Argonne National Laboratory)

Project Objective. Lithium-sulfur batteries have received great attention because sulfur exhibits an order of magnitude higher theoretical capacity than that achievable with intercalation-type cathode materials in Li-ion batteries and is considered as a promising battery chemistry to power long-range, low-cost EVs. Sulfur is abundant in nature and nontoxic, which leads to low cost of the cell and environmental benefits. However, low active material utilization and poor cycle life hinder the practical application of Li-S batteries. The objective of this project is to develop new electrolyte materials to help overcome these challenges and enable high-efficiency Li-S batteries for vehicle application.

Project Impact. The development of novel functional electrolytes tailored for Li-S electrochemistry will enable improved materials utilization and longer cycle life as needed to take advantage of the high potential capacity of Li-S batteries to power long-range, low-cost EVs.

Approach. This project takes a new approach, combining organic synthesis and quantum chemistry computations to obtain an in-depth understanding of the interaction of the discharged lithium polysulfides with the electrolyte solvents and the lithium salt, aiming to develop new electrolyte materials for Li-S batteries. Based on the team's previous study, the fluorinated-ether-based electrolytes have shown very limited Li_2S_x solubility, and at the same time could effectively passivate the lithium anode surface affording a reversible electrochemistry with high CE. However, the low active material utilization compromises its advantages of high theoretical capacity and energy density. To overcome this, the team will investigate boron-containing fluorinated polyethers as a new class of electrolytes for Li-S batteries. To further improve the cycle life, the project also proposes to design and synthesize new polymer binders bearing a pentafluorophenyl group on the backbone. First principles DFT and wave-function based quantum chemistry methods will be employed to provide accurate atomic/molecular level insight into the experimental studies. The team will also employ *ab initio* molecular dynamics (AIMD) simulations of the solvents for different finite temperatures and concentrations. The AIMD simulations will provide information on the structures of the electrolytes based on the fluorinated ethers synthesized in the experimental part of this project.

Out-Year Goals. The out-year goals are to find electrolytes that promote longer cycle life through electrolytes to reduce material loss.

Collaborations. This project engages in collaboration with Prof. Amin Salehi at University of Illinois at Chicago (UIC).

Milestones

1. Design, synthesis, and characterization of fluorinated solvents and studies of physical properties. (Q3, FY 2018; Completed)
2. Quantum chemical calculations of the binding energies of lithium polysulfides (Li_2S_x) with new solvents. (Q4, FY 2018; Completed)

Progress Report

The rapid capacity fade that occurs in Li-S batteries during repeated cycling due to the gradual loss of active materials requires new electrolytes designed to enhance sulfur utilization. Last quarter, the team reported on two new ether solvents containing a pentafluorophenyl group designed to have a strong electron-withdrawing effect of fluorines on the benzene ring to interact with polysulfides, especially the low order polysulfides, to form anion receptor complexes. To better understand the interactions between LiTFSI salts and new fluorinated solvents synthesized here, TFE-PFPE and TFE-PFBE in a mixed electrolyte with 1,3 DOL, first principles periodic calculations have been performed.

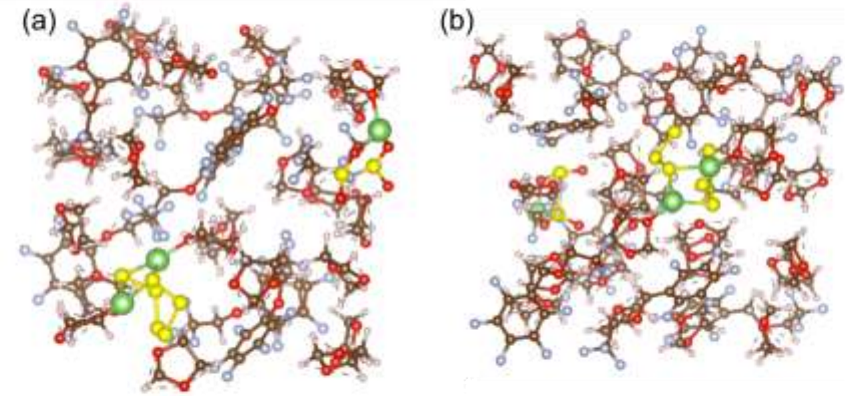

Figure 23. Snapshots from density functional theory calculations show Li_2S_4 species in the electrolytes (a) TFE-PFPE:DOL and (b) TFE-PFBE: DOL.

The first principles calculations are based on plane wave basis sets and projector-augmented wave (PAW) pseudopotentials. The exchange-correlation functional was treated within the generalized gradient approximation (GGA) of Perdew-Burke-Ernzerhof (PBE). The team employed supercells in the computations consisting of salts and solvent molecules including (a) an electrolyte mixture containing 24 DOL molecules and 7 TFE-PFPE (or 13 TFE-PFBE) molecules and (b) LiTFSI at a 1.2 M concentration. The electrolyte optimized structures are obtained by volume relaxation calculations using experimental densities. All molecules were initially randomly arranged inside the simulation box.

The optimized structures and energetics of polysulfide species, Li_2S_x, in the above described electrolyte mixtures (S") with LiTFSI as the salt, were calculated by DFT. The following reaction energy was determined:

$$Li_2S_x + S'' \rightarrow Li_2S_x\text{-}S'' \quad (1)$$

The results of calculations of the reactions for the different polysulfide species in the two electrolytes are given in Table 4.

Table 4. Solvation energies of the lithium polysulfide species in two fluorinated solvent mixtures according to reaction (1).

Electrolyte mixture	Li_2S	Li_2S_2	Li_2S_4	Li_2S_6
1:2 TFE-PFPE:DOL and 1.2 M LiTFSI	-3.1	-1.9	-1.0	-0.9
1:2 TFE-PFBE:DOL and 1.2 M LiTFSI	-2.6	-1.0	-1.3	-1.2

The DFT calculations indicate that the solvation energies of reaction (1) generally weaken with increasing order of polysulfides, Li_2S_x, (x =1 to 6). The solvation energies indicate these electrolyte mixtures are expected to be very good anion receptors that will strongly interact with polysulfides, especially the low order polysulfides, to form anion receptor complexes. At higher order (x = 4 and 6), the results in Table 4 demonstrate that the solvation energies of the TFE-PFPE:DOL electrolyte are larger than the TFE-PFBE:DOL electrolyte, that is, are more negative. This is consistent with the project's experimental results that TFE-PFBE is a stronger anion receptor than TFE-PFPE. The adjacent oxygen in the TFE-PFPE donates electrons to the benzene ring through the p-π conjugation, therefore decreasing the anion receptive strength of the solvents.

Patents/Publications/Presentations

The project has no patents, publications, or presentations to report this quarter.

TASK 2 – DIAGNOSTICS

Summary and Highlights

To meet the goals of the VTO Multi-Year Program Plan and develop lower-cost, abuse-tolerant batteries with higher energy density, higher power, better low-temperature operation, and longer lifetimes suitable for the next-generation of EVs, hybrid EVs (HEVs), and plug-in hybrid EVs (PHEVs), there is a strong need to identify and understand structure-property-electrochemical performance relationships in materials, life-limiting and performance-limiting processes, and various failure modes to guide battery development activities and scale-up efforts. In pursuit of batteries with high energy density, both high cell operating voltages and demanding cycling requirements lead to unprecedented chemical and mechanical instabilities in cell components. Successful implementation of newer materials such as silicon anode and high-voltage cathodes also requires better understanding of fundamental processes, especially those at the solid/electrolyte interface of both anode and cathode.

This Task takes on these challenges by combining model system, *ex situ*, *in situ*, and *operando* approaches with an array of the start-of-the-art analytical and computational tools. Three subtasks are tackling the chemical processes and reactions at the electrode/electrolyte interface. Researchers at LBNL use *in situ* and *ex situ* vibrational spectroscopy and far- and near-field scanning probe spectroscopy to understand the structure of active materials and the physio-chemical phenomena at electrode/electrolyte interfaces, particularly those of the high-voltage cathodes. GM is developing a number of *in situ* diagnostic techniques, including atomic force microscopy (AFM), nanoindentor, dilatometer, and stress-sensor, to be combined with atomic/continuum modeling schemes to investigate and understand the coupled mechanical/chemical degradation of the SEI layer on Li-metal anode. ANL aims to first understand the pathways/mechanisms of the parasitic reactions of the electrode/electrolyte interfaces and then stabilize them by developing functional surface coating and electrolyte additives. Subtasks at Brookhaven National Laboratory (BNL) and PNNL focus on the understanding of fading mechanisms in electrode materials, with the help of synchrotron-based X-ray techniques (diffraction and hard/soft X-ray absorption) at BNL and high-resolution transmission electron microscopy (HRTEM) and spectroscopy techniques at PNNL. UC San Diego (UCSD) is developing advanced diagnostic tools, including scanning transmission electron microscopy / electron energy loss spectroscopy (STEM/EELS), *operando* Bragg coherent diffraction imaging (BCDI) and *ab initio* computation, to probe anion redox and oxygen evolution in Li-excess NMC materials. At LBNL, model systems of electrode materials with well-defined physical attributes are being developed and used for advanced diagnostic and mechanistic studies at both bulk and single-crystal levels. These controlled studies remove the ambiguity in correlating a material's physical properties and reaction mechanisms to its performance and stability, which is critical for further optimization. The final subtask at Stanford University / Stanford Linear Accelerator Center (SLAC) develops and utilizes a correlative X-ray microscopy platform to investigate the lithiation dynamics and understand factors that determine the rate capability and degradation mechanisms in cathode materials. The diagnostics team not only produces a wealth of knowledge that is key to the development of next-generation batteries, it also advances analytical techniques and instrumentation that have a far-reaching effect on material and device development in a variety of fields.

Highlight. PNNL (Wang's Group) used high resolution scanning transmission electron microscopy to demonstrate the coupling among electrochemical, thermal, and mechanical processes during the degradation of layered cathode materials.

Task 2.1 – Model System Diagnostics for High-Energy Cathode Development (Guoying Chen, Lawrence Berkeley National Laboratory)

Project Objective. This project will use a rational, nonempirical approach to design and synthesize next-generation high-energy, high-voltage cathode materials. Combining a suite of advanced diagnostic techniques with model cathode materials and model electrode/electrolyte interfaces, the project will perform systematic studies to achieve the following goals: (1) obtain new insights into solid-state chemistry, particularly cationic and/or anionic redox activities during charge and discharge of high-capacity lithium TM oxides, (2) gain fundamental understanding on cathode/electrolyte interfacial chemistry and charge transfer process as a function of operating voltage, (3) reveal performance- and stability-limiting properties and processes in high-energy, high-voltage cathodes, and (4) develop strategies to mitigate the structural and interfacial instabilities.

Impact. The project will improve the commercial viability of next-generation high-energy cathode materials. The findings will enable more stable high-voltage cycling of existing Li-TM oxides as well as development of novel high-capacity cathode materials for advanced Li-ion batteries.

Approach. The project will prepare crystal samples of Li-stoichiometric and Li-excess TM oxides with well-defined physical attributes. It will perform advanced diagnostic and mechanistic studies at both bulk and single-crystal levels. Global properties and performance of the samples will be established from the bulk analyses, while the single-crystal-based studies will utilize time- and spatial-resolved analytical techniques to probe the material redox transformation process and failure mechanisms under battery operating conditions.

Out-Year Goals. In the out-years, the project will obtain fundamental knowledge on performance-limiting physical properties, phase transition mechanisms, parasitic reactions, and transport processes that prevent cathode materials from delivering higher capacities and achieving more stable cycling at high voltages. It will develop approaches to mitigate cathode structural and interfacial instabilities during high-voltage operation. Further, it will design and synthesize optimized Li-TM oxide cathodes as well as novel high-energy electrode materials.

Collaborations. This project collaborates with the following: G. Ceder, K. Persson, M. Doeff, B. McCloskey, and P. Ross (LBNL); V. Srinivasan (ANL); D. Nordlund and Y. Liu (Stanford Synchrotron Radiation Lightsource, SSRL); C. Wang (PNNL); C. Grey (Cambridge); and A. Huq and J. Nanda (Oak Ridge National Laboratory, ORNL).

`Milestones

1. Characterize oxygen activities during charge/discharge and extended cycling of Li-TM oxides and understand effect on cathode structural and electrochemical reversibility. (Q1, December 2017; Completed)

2. Investigate analytical techniques to determine the kinetics of anion redox process, and evaluate factors influencing rate capability of Li-TM oxide cathodes. (Q2, March 2018; Completed)

3. Apply advanced diagnostic techniques to investigate the reactivities of model oxide surfaces and understand their impact on oxide performance and safety. (Q3, June 2018; Completed)

4. *Go/No-Go Decision*: Reveal the impact of oxide chemistry and particle morphology on the extent of reversible oxygen redox versus lattice oxygen loss; understand how to fine tune oxygen activities at high voltages. *No-Go* if the processes of reversible oxygen redox and lattice oxygen loss cannot be decoupled with diagnostic studies. (Q4, September 2018; Completed with a Go decision)

Progress Report

It is now well recognized that oxygen redox is enabled by excess lithium in certain TM oxides. This quarter, the project evaluated the strategy of using oxide chemistry to fine tune oxygen redox activities in the cation-disordered $Li_{1.4-x}Nb_{0.4-x}Mn_{0.2+2x}O_2$ system. Unlike the layered Li- and Mn-rich (LMR) compounds where stoichiometry is largely fixed, in the rock-salt structure lithium and TM cations share the same crystallographic sites, which makes it feasible to adjust the TM/Li ratio and, subsequently, the contribution of TM and oxygen redox. Here, two new oxides with a composition of $Li_{1.2}Nb_{0.2}Mn_{0.6}O_2$ and $Li_{1.4}Nb_{0.4}Mn_{0.2}O_2$ were prepared for comparative studies with the $Li_{1.3}Nb_{0.3}Mn_{0.4}O_2$ model system previously investigated. The samples were synthesized using the same molten-salt method, which produced large uniform crystals with a similar particle size of ~ 5 µm (Figure 24a/d). Rietveld refinement of the synchrotron XRD and neutron diffraction patterns (Figure 24b/c/e/f) confirms the cation-disordered rock-salt crystal structure free of impurities.

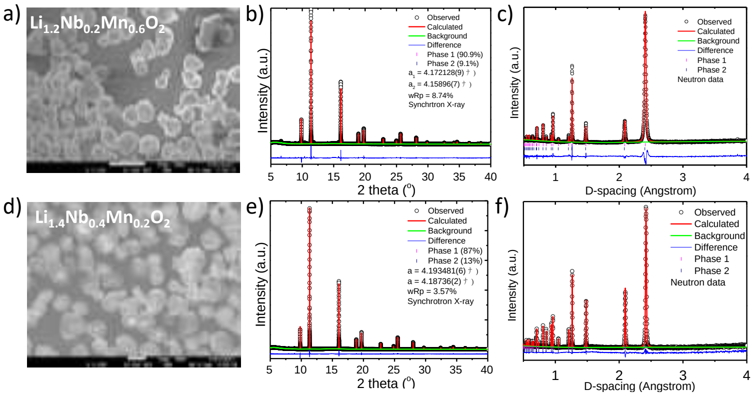

Figure 24. Scanning electron microscopy images (a/d) and Rietveld refinement of (b/e) synchrotron X-ray diffraction patterns and (c/f) neutron diffraction patterns of as-synthesized $Li_{1.2}Nb_{0.2}Mn_{0.6}O_2$ and $Li_{1.4}Nb_{0.4}Mn_{0.2}O_2$ samples. The X-ray wavelength is 0.414 Å.

Figure 25a compares the 1st cycle voltage profiles of the oxide half cells cycled at 10 mA/g between 1.5 and 4.8 V. As the manganese content (x) increases in $Li_{1.4-x}Nb_{0.4-x}Mn_{0.2+2x}O_2$, charge capacity obtained from the slopy region below 4.2 V also increases, with approximately 80, 120, and 180 mAh/g for $x = 0$, 0.1, and 0.2, respectively. On the other hand, charge capacity obtained from oxygen oxidation in the pleteau region above 4.2 V increases with lithium content and decreases with the manganese content, with approximately 300, 200, and 100 mAh/g for $x = 0$, 0.1, and 0.2, respectively. Although the highest initial charge capacity was obtained on $x = 0$, both discharge voltage and capacity were lower compared to that of $Li_{1.3}Nb_{0.3}Mn_{0.4}O_2$, suggesting higher hysteresis and lower CE of oxygen redox as compared to that of the manganese redox. For $x = 0.2$, the

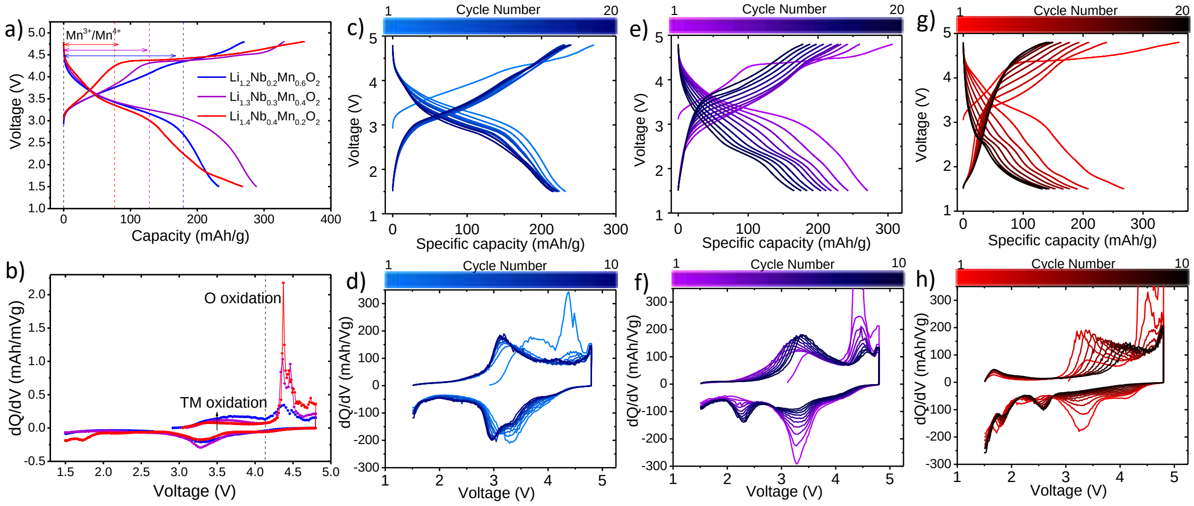

Figure 25. Voltage profiles (a/c/e/f) and incremental capacity (dB/dB) profiles (b/d/f/h) of the half-cells cycled at 10 mA/g. Images (a-b) were collected during the first cycle. Images (c-d, e-f, g-h) were from $Li_{1.2}Nb_{0.2}Mn_{0.6}O_2$, $Li_{1.3}Nb_{0.3}Mn_{0.4}O_2$, and $Li_{1.4}Nb_{0.4}Mn_{0.2}O_2$ cells, respectively.

lower initial charge capacity also led to a lower discharge capacity. The effectiveness of using Li/TM ratio to manipulate 1st cycle manganese and oxygen redox is further shown in the dQ/dV profiles in Figure 25b. While the intensity of the manganese oxidation peak gradually increased along with the manganese content, that of the oxygen oxidation peak decreases.

Figure 25c-h compares the cycling stability of the $Li_{1.4-x}Nb_{0.4-x}Mn_{0.2+2x}O_2$ oxide cathodes. With the highest manganese redox contribution in $Li_{1.2}Nb_{0.2}Mn_{0.6}O_2$, the cathode maintained its initial discharge capacity of ~ 230 mAh/g during the first 20 cycles (Figure 25c). On the dQ/dV profiles (Figure 25d), the anodic and cathodic peaks experienced little voltage shift and current decay after the 1st cycle, suggesting high redox reversibility and cycling stability. On the other hand, the charge and discharge profiles of $Li_{1.4}Nb_{0.4}Mn_{0.2}O_2$ cathode changed significantly with cycling (Figure 25g), and the discharge capacity decreased from 270 to 140 mAh/g during the first 20 cycles, a near 50% reduction. On the dQ/dV profile (Figure 25h), the anodic peak gradually shifted toward higher voltage at an approximate rate of 150 mV per cycle. The primary cathodic peak suffers from significant decay, and after a mere 4 cycles, it was replaced by two lower-voltage cathodic peaks with much smaller current. Comparing to the electrochemical performance of $Li_{1.3}Nb_{0.3}Mn_{0.4}O_2$ (Figure 25e/f), performance degradation in $Li_{1.4}Nb_{0.4}Mn_{0.2}O_2$ is significantly worse. The observed differences suggest that in Li-rich rock-salt oxides, capacity contribution from TM and oxygen redox can be readily tuned via cation stoichiometry, which subsequently impacts the balance between capacity and stability. Such correlation offers an opportunity in designing electrode materials with minimized performance issues associated with utilizing the high capacity brought on by oxygen redox.

Patents/Publications/Presentations

Publications

- Shin, Y., W. H. Kan, M. Aykol, J. K. Papp, B. McCloskey, G. Chen, and K. A. Persson. "Alleviating Oxygen Evolution from Li-Excess Oxide Materials through Theory-Guided Surface Protection." *Nature Communications* 9, no. 4597 (2018). doi: 10.1038/s41467-018-07080-6.
- Chen, D., W. H. Kan, and G. Chen. "Understanding Performance Degradation in Li-Rich Rock-Salt Cathodes." Under review (2018).

Task 2.2 – Interfacial Processes – Diagnostics
(Robert Kostecki, Lawrence Berkeley National Laboratory)

Project Objective. This collaborative project will develop and apply advanced experimental methodologies to study and understand the mechanism of operation and degradation of high-capacity materials for rechargeable cells for PHEV and EV applications. The objective is to develop and apply *in situ* and *ex situ* far- and near-field optical multi-functional probes to obtain detailed insight into the active material structure and physio-chemical phenomena at electrode/electrolyte interfaces at a spatial resolution corresponding to the size of basic chemical or structural building blocks. The goal is to design new diagnostic techniques and experimental methodologies capable of unveiling the structure and reactivity at hidden or buried interfaces and interphases that determine material, composite electrode, and full-cell electrochemical performance and failure modes.

Project Impact. Instability and/or high resistance at the interface of battery electrodes limits electrochemical performance of high-energy-density batteries. A better understanding of the underlying principles that govern these phenomena is inextricably linked with successful implementation of high-energy-density materials in Li-ion and Li-based cells for PHEVs and EVs. The proposed work constitutes an integral part of the concerted effort within the BMR and supports development of new electrode materials for high-energy rechargeable cells.

Approach. The pristine and cycled composite electrode and model thin-film electrodes will be probed using various surface- and bulk-sensitive techniques, including FTIR, attenuated total reflectance (ATR)–FTIR, near-field infrared (IR) and Raman spectroscopy and microscopy, and scanning probe microscopy to identify and characterize changes in materials structure and composition. Novel *in situ/ex situ* far- and near-field optical multifunctional probes in combination with standard electrochemical and analytical techniques are developed to unveil the structure and reactivity at interfaces and interphases that determine materials electrochemical performance and failure modes.

Out-Year Goals. In the out-years, the project aims to: (1) determine the degradation mechanism(s) of high-voltage cathodes; and (2) propose and test effective remedies to intrinsic interfacial instability of these materials and composite electrodes.

Collaborations. Electrode materials and composite electrodes tested under different cycling regimes by M. Doeff (LBNL) and C. Ban (National Renewable Energy Laboratory, NREL) will be studied. The diagnostic studies will be carried out in sync with differential electrochemical mass spectrometry (DEMS) analysis by B. McCloskey (LBNL) and other diagnosticians in the BMR program. He will also work closely with V. Battaglia (LBNL) to obtain samples from full-cell cycling experiments.

Milestones

1. Controlled growth of model thin-film electrodes by pulsed laser deposition (PLD) as model system for fundamental electrochemical studies. *Go/No-Go Decision*: Stoichiometric thin films produced with sub-nanometer roughness. (Q1, FY 2018; Completed December 2017)
2. Characterize bulk and surface structure of model PLD thin films and the relation to electrochemical properties. *Go/No-Go Decision*: Electrochemical performance of model system in line with that of bulk materials. (Q2, FY 2018; Completed March 2018)
3. Characterize chemistry of electrolyte decomposition at model PLD thin-film electrodes with near-field technique. (Q3, FY 2018; Completed June 2018)
4. Determine electrochemical impedance contribution from interface between organic electrolyte and electrode active material. *Go/No-Go Decision*: Development of model electrodes with high electrochemical stability and low impedance. (Q4, FY 2018; Completed)

Progress Report

This quarter, the team analyzed impedance of organic film formation on the thin-film NMC-532 model electrode after electrochemical cycling and washing in DEC. The thin-film NMC-532 electrode was cycled in the CV regime between 2-4.7 V in 1 M $LiPF_6$ in EC:DEC (1:2 wt%) electrolyte against Li-foil anode. Then, it was washed by DEC for 5 min to expose a homogeneous inner cathode electrolyte interfacial (CEI) layer (for details, see previous reports). To evaluate CEI layer contribution to the electrode impedance, the team designed and built a new experimental setup (Figure 26). The system was assembled by sandwiching dry NMC electrode between two flat metal current collectors. The impedance measurements were carried under argon atmosphere.

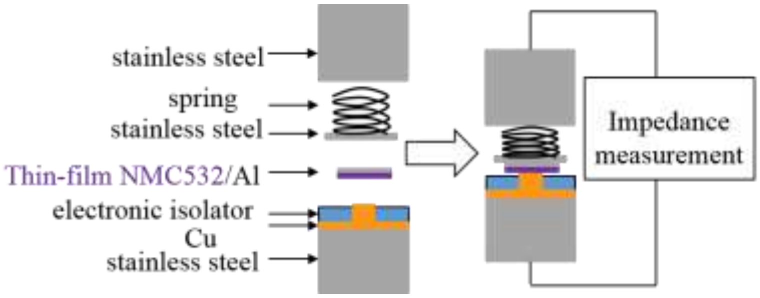

Figure 26. Experimental setup for impedance measurements of the NMC electrode under argon atmosphere.

The real part of AC impedance at 0.1 Hz of the pristine model thin-film NMC-532 electrode and after 3 cycles and 10 cycles in 1 M $LiPF_6$ in EC:DEC is shown in Figure 27a. The electrode impedance increases gradually from 0.5 Ω for the pristine electrode, to 1 and 3 Ω after 3 and 10 cycles, respectively. To correlate these impedance results with the observed organic inner layer formation, corresponding ATR-FTIR spectra of the thin-film NMC-532 electrode after 3 and 10 cycles were recorded and normalized versus Al_2O_3 background peak at 900 cm^{-1} (Figure 27b). The increased intensity of -C-O vibration at ca. 1300 and 1150 cm^{-1} indicates that the thickness of the inner layer that consists of β-diketone, LiEDC, or $ROCO_2Li$ increase with cycling. The semi-quantitative electrode impedance/CEI film thickness correlation directly demonstrates the detrimental effect of electrolyte oxidation and surface film formation on the NMC cathode long-term electrochemical performance. This concludes the project's efforts toward completing the fourth quarter milestone.

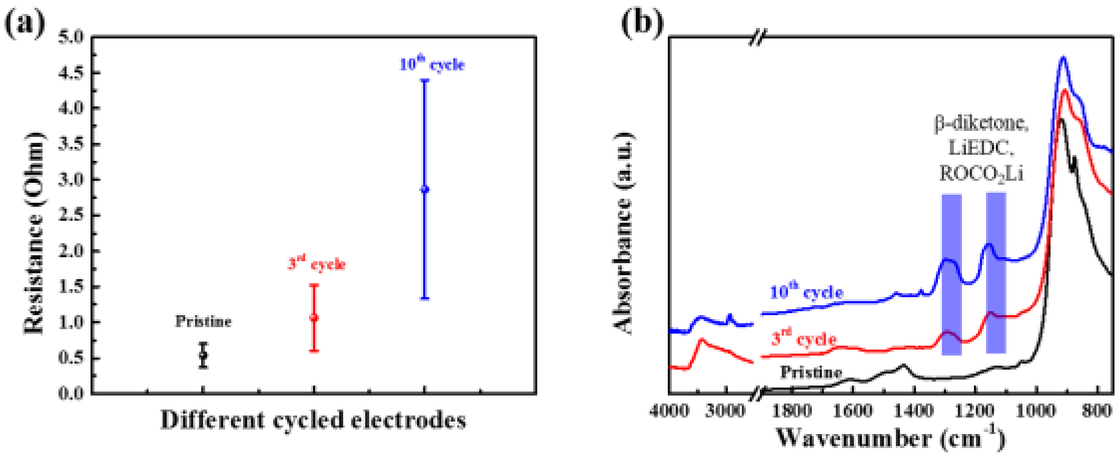

Figure 27. (a) Real-part AC impedance at 0.1Hz (b) attenuated total reflectance – Fourier transform infrared spectra of thin-film NMC-532 electrodes: pristine and after 3 and 10 cycles.

Patents/Publications/Presentations

Publications

- Two manuscripts are in preparation.

Presentation

- 2nd International Conference on Electrochemical Energy Science and Technology (EEST) 2018, Niagara Falls, Canada (August 13–17, 2018): "Understanding Charge and Mass Transport across Interfaces and Interphases in Rechargeable Batteries"; Robert Kostecki. Keynote lecture.

Task 2.3 – Advanced *In Situ* Diagnostic Techniques for Battery Materials
(Xiao-Qing Yang and Seongmin Bak, Brookhaven National Laboratory)

Project Objective. The primary project objective is to develop new advanced *in situ* material characterization techniques and to apply these techniques to support development of new cathode and anode materials for the next generation of Li-ion batteries for PHEVs. To meet the challenges of powering the PHEV, Li-ion batteries with high energy and power density, low cost, good abuse tolerance, and long calendar and cycle life must be developed.

Project Impact. The VTO Multi-Year Program Plan describes the goals for battery: “Specifically, lower-cost, abuse-tolerant batteries with higher energy density, higher power, better low-temperature operation, and longer lifetimes are needed for development of the next-generation of HEVs, PHEVs, and EVs.” The knowledge gained from diagnostic studies through this project will help U. S. industries develop new materials and processes for new generation Li-ion batteries in the effort to reach these VTO goals.

Approach. This project will use the combined synchrotron-based *in situ* X-ray techniques (XRD; and hard and soft X-ray absorption spectroscopy, or XAS) with other imaging and spectroscopic tools such as HRTEM and MS to study the mechanisms governing performance of electrode materials.

Out-Year Goals. In the out years, the project will complete development of diagnostic techniques using X-ray pair distribution function (x-PDF), XRD, and XAS combined with neutron diffraction and neutron PDF (n-PDF), as well as STEM imaging and transmission X-ray microscopy (TXM) for cathode materials studies. It will then apply these techniques to study the structural changes of various new cathode materials.

Collaborations. The BNL team will work closely with material synthesis groups at ANL (Drs. Shin and Amine) for the high-energy composite and at PNNL for the Si-based anode materials. The project will also collaborate with industrial partners at GM and Johnson Controls, as well as with international collaborators.

Milestones

1. Complete the *in situ* TXM studies of $LiCoO_2$ cathode materials during charge-discharge cycling to evaluate the inhomogeneity of the charged (discharged) states among a large number of material particles and using a data mining technique to detect the under (over) reacted minority regions (particles). (Q1, December 2017; Completed)

2. Complete the neutron diffraction studies of $LiCoO_2$ as high-energy-density cathode material at high-voltage charge in comparison with the pristine state. (Q2, March 2018; Completed)

3. Complete the PDF studies of $LiCoO_2$ using both x-PDF and n-PDF probes to study the mechanism of anionic redox reaction in such widely used commercial cathode materials for Li-ion batteries and explore the potential of using this material for high-energy-density cell applications. (Q3, June 2018; Completed)

4. Complete the experimental design, data collection, and analysis of 3D STEM tomography studies of high-energy-density $Li_{1.2}Ni_{0.15}Co_{0.1}Mn_{0.55}O_2$ cathode materials at pristine state and after multiple cycling. (Q4, September 2018; Completed)

Progress Report

This quarter, the fourth milestone for FY 2018 was completed. BNL focused on experimental design, data collection, and analysis of 3D STEM tomography studies of high-energy-density $Li_{1.2}Ni_{0.15}Co_{0.1}Mn_{0.55}O_2$ cathode materials at pristine state and after multiple cycles, especially on the studies of structure change associated with oxygen loss during cycling. To clarify the origin of pores observed in STEM images, STEM-EELS mapping of a concealed pore and an exposed pore was performed, as shown in Figure 28. Figure 28a shows the STEM-EELS mapping results over a concealed pore in bulk and the exposed pore at the surface of the particle. The EELS map of the concealed pore shows that there is only a very thin shell of Mn^{2+} build-up around the pore (Figure 28a). Since a significant number of small pores was observed in the pristine sample before cycling, it is assumed these internal concealed pores are formed during synthesis and thus changed their sizes and shapes during cycling due to the oxygen release initiated near them. In contrast, for the opposite extreme situation in an exposed pore, the entire pore surface area is exposed to the electrolyte; as shown in Figure 28b, a thick layer of spinel/rock-salt structure phase was formed through the interaction between the pore surface and the electrolyte. The EELS relative concentration mapping shows that there is a significant increase in manganese relative concentration close to the surface volume. Based on the observed increased number of pores with large volume size, the team can speculate that a large number of pores are not completely concealed or exposed, but partially exposed internal pores with oxygen pathways nearby in the form of microstructural defects such as dislocation, grain boundaries, and micro cracks. During cycling, these partially exposed internal pores will grow in size and number, together with those completely exposed pores at the surface, contributing to the propagation of the structural phase transitions, facilitating the further oxygen loss and self-feed of further microstructural defect formations, and accelerating voltage fade.

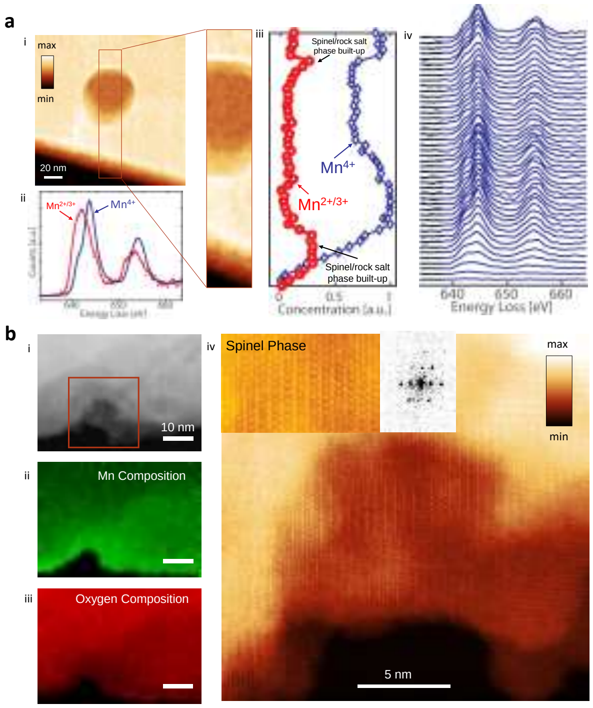

Figure 28. Spatially resolved electron energy loss spectroscopy (EELS) mapping of concealed pore and exposed pore. (a) Scanning transmission electron microscopy (STEM) - EELS mapping of a concealed pore. (i) Annular dark-field (ADF) - STEM image of a concealed pore. (ii) The reference spectra used for linear composition of the manganese L2,3 spectra in (iv). (iii) The linear decomposition coefficient as a function of the vertical spatial location. (iv) The EELS spectra of manganese L2,3 edges across the surface and the concealed pore. (b) STEM-EELS mapping and atomic-resolution imaging of an exposed pore. (i) ADF-STEM image of an opened pore. (ii–iii) The manganese (ii) and oxygen (iii) composition extracted from quantification of the EELS map. (iv) Atomic resolution image of the open pore.

Patents/Publications/Presentations

Publications

- Bak, S-M., Z. Shadike, R. Lin, X. Yu, and X-Q. Yang. "*In Situ*/*Operando* Synchrotron-Based X-Ray Techniques for Lithium-Ion Battery Research." *NPG Asia Materials* (2018). doi: 10.1038/s41427-018-0056-z; Publication Date (Web): July 3, 2018.
- Hu, E., X. Yu, R. Lin, X. Bi, J. Lu, S-M. Bak, K-W. Nam, H. L. Xin, C. Jaye, D. A. Fischer, K. Amine, and X-Q. Yang. "Evolution of Redox Couples in Li- and Mn-rich Cathode Materials and Mitigation of Voltage Fade by Reducing Oxygen Release." *Nature Energy* 3 (2018): 690–698. doi: 10.1038/s41560-018-0207-z; Publication Date (Web): July 30, 2018.
- Wang, F., W. Sun, Z. Shadike, E. Hu, X. Ji, T. Gao, X-Q. Yang, K. Xu, and C. Wang. "How Water Accelerates Bivalent Ion Diffusion." *Angewandte Chemie*. doi: 10.1002/anie.201806748; Publication Date (Web): July 31, 2018.
- Piao, J-Y., Y-G. Sun, S-Y. Duan, A-M. Cao, X-L. Wang, R-J. Xiao, X-Q. Yu, Y. Gong, L. Gu, Y. Li, Z-J. Liu, Z-Q. Peng, R-M. Qiao, W-L. Yang, X-Q. Yang, J. B. Goodenough, and L-J. Wan. "Stabilizing Cathode Materials of Lithium-Ion Batteries by Controlling Interstitial Sites on the Surface." *Chem* 4, no. 7 (July 12, 2018): 1685–1695. doi: 10.1016/j.chempr.2018.04.020.
- Yue, X-Y., W-W. Wang, Q-C. Wang, J-K. Meng, Z-Q. Zhang, X-J. Wu, X-Q. Yang, and Y-N. Zhou. "CoO Nanofiber Decorated Nickel Foams as Lithium Dendrite Suppressing Host Skeletons for High Energy Lithium Metal Batteries." *Energy Storage Materials* 14 (2018): 335–344. doi: 10.1016/j.ensm.2018.05.017; Publication Date (Web): September 2018.

Presentation

- 256th ACS Meeting, Boston, Massachusetts (August 19–23, 2018): "Using Synchrotron X-Ray and Neutron Based Scattering and TXM Imaging Techniques to Study the New Cathode Materials for Batteries"; E. Hu, S-M. Bak, X-Q. Yang*, X. Yu, X. Huang, M. Ge, Y. Chu, Z. Shadike, R. Lin, H-S. Lee, Y. Guo, and Y. Liu. Invited.

Task 2.4 – Advanced Microscopy and Spectroscopy for Probing and Optimizing Electrode-Electrolyte Interphases in High-Energy Lithium Batteries
(Shirley Meng, University of California at San Diego)

Project Objective. The proposed research aims to develop advanced microscopy and spectroscopy tools to probe, understand, and optimize the anion activities that govern the performance limitations such as capacity and voltage stabilities in high-energy Li-excess TM (such as nickel, cobalt, manganese) oxides cathode materials. The approach uniquely combines atomic resolution STEM, EELS, *operando* BCDI, and first-principles computation to probe anion redox and oxygen evolutions in Li-excess NMC materials. Furthermore, the project will track the lithium and oxygen dynamics under electrochemical testing via *operando* neutron diffraction, which will enhance understanding of the overall structural changes due to anion activities. Ultimately, this will hone in on the synthesis efforts to produce the modified materials with optimum bulk compositions and surface characteristics at large scale for consistently good performance. The above-mentioned characterization tools will be extended to diagnose various anode types, such as Li-metal anode.

Project Impact. If successful, this research will enable *operando* imaging at the single-particle level by advanced microscopy imaging and high-energy-resolution oxygen K-edge EELS. This work will provide an in-depth understanding of anion activities in high-voltage electrode materials, which can lead to significant improvement in stabilizing operation voltage and electrode-electrolyte interface for future generation high-energy-density electrodes.

Approach. This unique approach combines STEM/EELS, *operando* BCDI, and *ab initio* computation as diagnostic tools for probing anion redox and oxygen evolutions in Li-excess NMC materials. This allows for pinning down the atomistic/molecular mechanism of anion oxidation and determining the speciation compositions and surface characteristics for enabling high rate and long life in the proposed materials. Neutron enables the characterization of bulk material properties to enhance and further optimize high-energy electrode materials.

Out-Year Goals. The goal is to probe and control defects generation due to oxygen activity in the high-energy composite cathodes and to characterize electrode/electrolyte interface in lithium anodes so that their cycle life and efficiency can be significantly enhanced.

Collaborations. This work funds collaborations on EELS (Miaofang Chi, ORNL); neutron diffraction (Ken An, ORNL); and soft XAS (Marca Doeff, LBNL). It supports collaborative work with Zhaoping Liu and Yonggao Xia at Ningbo Institute of Materials Technology and Engineering in China. It also supports collaboration with the Battery500 Consortium.

Milestones

1. Benchmark electrode performance of bulk and surface modified Li-excess NMC. (Q2, March 2018; Completed)
2. Conduct BCDI and STEM/EELS characterization of modified Li-excess NMC single particle. (Q3, June 2018; Completed)
3. Propose strategies to optimize the anion activities in Li-excess NMC cathode materials. (Q4, September 2018; Completed)

Progress Report

The Impact of Defects Generation on the Structure Metastability and Voltage Decay for Li-Rich Layered Oxide (LRLO) after Electrochemical Cycling

A previous report demonstrated that dislocations are generated and accumulated in the structure of LRLO material during electrochemical cycling. The nucleation of line defects dramatically modifies the local lithium environment by perturbing the sequence of oxygen layers. The influence of the oxygen stacking sequence on the system energy in LRLO material was investigated by first-principles calculations. For simplicity, a supercell model composed of three-formula units of $Li_{11}Ni_2Mn_5O_{18}$ was used for LRLO structure with different oxygen stacking sequences (Figure 29a). Oxygen stacking sequence changes from ABCABC (O_3) to ABAB (O_1) were considered since these transformations are easily accomplished via gliding of the MO_2 layers. In the energetically most favorable O_3 structure, all lithium octahedral sites share edges with TM octahedral sites. The partial transition to O_1 induces unfavorable face sharing between lithium and TM octahedral sites, thus raising the Gibbs free energy of the system (see Figure 29b). The Gibbs free energy for O_1 stacking is higher than that of O_3 stacking for almost all tested delithiation compositions. This energy penalty is greater at high lithium concentration simply because more face-sharing sites are filled. Note, that the slope of the Gibbs free energy as a function of lithium concentration is a rough estimate for the average voltage. This results in a smaller average voltage for the structure with more defects (see Figure 29c). In short, the highly cycled LRLO material is trapped in a metastable state with an energetically unfavorable local lithium environment, which is mainly responsible for the issue of voltage decay. Based on the mechanistic description above, defects elimination is the key factor to achieve structure reversibility and voltage recovery. An external driving force, such as heat treatment, is necessary to enable the system to cross over the energy barrier to relax to the stable state, as indicated by the blue arrows in Figure 29d.

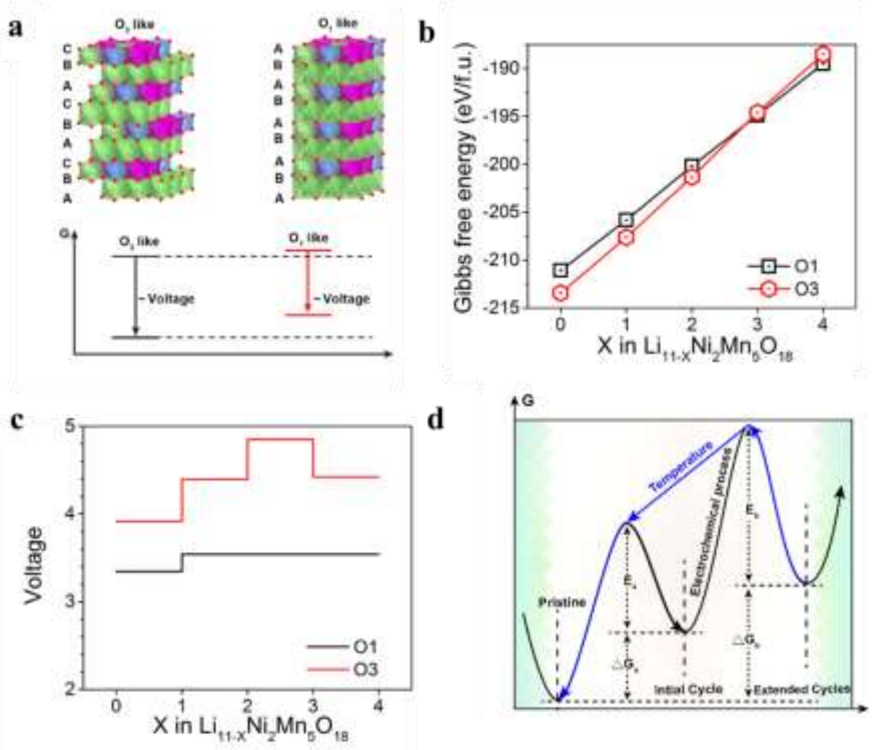

Figure 29. Correlation between voltage decay and defects generation. (a) Schematic illustration of free energy differences due to different oxygen stacking sequences (green, Li; red, O; purple, Mn; blue, Ni). (b) The Gibbs free energy for each delithiation composition of the supercell with O_3 and O_1 stacking. (c) Calculated voltage of supercell $Li_{11-x}Ni_2Mn_5O_{18}$ ($0 \leq x \leq 4$) for stacking sequence O_3 and O_1. (d) Schematic illustration of the Gibbs free energy profiles for the conversion between pristine and cycled Li-rich layered oxide.

Influence of Metal-Ion Electrolyte Additive on Electrochemically Deposited Lithium Metal

To disclose the effect of Cs^+ and Zn^{2+} electrolyte additives, cryo transmission electron microscopy (cryo-TEM) and XPS were applied to explore the nanostructure of the electrochemically deposited lithium metal (EDLi). The cryo-TEM results in the last report demonstrate that both Cs^+ and Zn^{2+} electrolyte additives influence the property of the solid-state interphase of the lithium metal rather than its bulk. The above observations were further confirmed by the surface sensitive XPS, obtaining the chemical compositions of the SEI. The presence of copper signal in the survey spectra (Figure 30a) and metallic lithium in the lithium 1s spectra (Figure 30b) indicates an ultra-thin surface film from the Cs^+-containing electrolyte, consistent with the SEI measured by cryo-TEM. Figure30a/c demonstrate less fluorine species in Cs^+ than in the Zn^{2+}-containing electrolyte, which could be due to the thinner SEI film thickness formed in Cs^+-containing electrolyte. The SEI from all electrolytes is composed of inorganic compounds (for example, LiF, Li_2O and Li_2CO_3 in Figure 30c) and organic species (for example, esters, ethers, and carboxylates in Figure 30d). Some oxygenated fluorines ($Li_xPO_yF_z$) were observed when Cs^+ and Zn^{2+} were added in the electrolyte (Figure 30c). In addition, both ions are found to be partially reduced since there is a weak signal from metallic cesium (Figure 30e) and a strong signal from metallic zinc (Figure 30f). The latter confirms the presence of LiZn alloy on the surface of the EDLi.

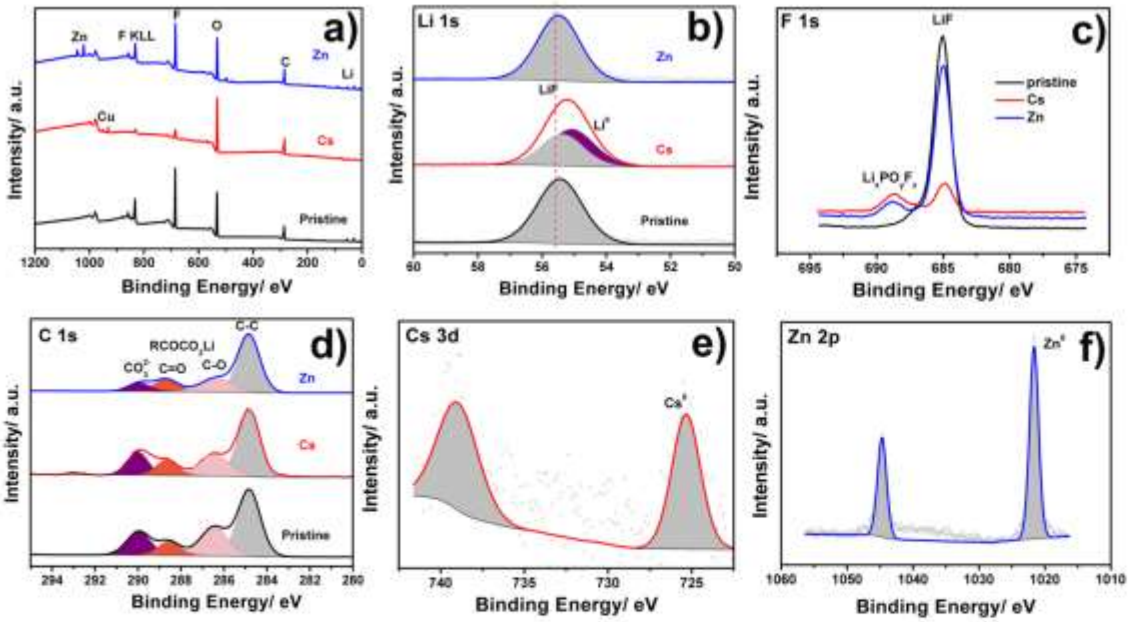

Figure 30. Compared X-ray photoelectron spectra of the survey (a), Li 1s (b), F 1s (c), C 1s (d), Cs 3d (e), and Zn 2p (f) with the deposited lithium metal from the pristine, Cs^+, and Zn^{2+} containing electrolytes

Patents/Publications/Presentations

Publications

- Singer, A., M. Zhang, Y. S. Meng, et al. "Nucleation of Dislocations and Their Dynamics in Layered Oxides Cathode Materials during Battery Charging." *Nature Energy* 3 (2018): 641.
- Qiu, B., M. Zhang, Y. S. Meng, et al. "Structural and Voltage Recovery for Practicability of Anionic Redox in Li-Rich Layered Oxide Cathode Material." *Nature Communications*. Under review.
- Wang, X., Y. Li, and Y. S. Meng. "Cryogenic Electron-Microscopy for Characterizing and Diagnosing Batteries." *Joule* (2018). Accepted.

Task 2.5 – *In Situ* Diagnostics of Coupled Electrochemical-Mechanical Properties of Solid Electrolyte Interphases on Lithium Metal Rechargeable Batteries

(Xingcheng Xiao, General Motors; Brian W. Sheldon, Brown University; Yue Qi, Michigan State University; and Y. T. Cheng, University of Kentucky)

Project Objective. The project objective is to develop a comprehensive set of *in situ* diagnostic techniques combined with atomic/continuum modeling schemes to investigate and understand the coupled mechanical/chemical degradation of the SEI layer/lithium system during lithium cycling. The goal of this understanding is to develop a new coating design strategy to achieve dendrite-free high cycle efficiency and extend the cycle life of high-energy-density batteries with lithium as the anode for EV application.

Project Impact. The fundamental understanding of the coupled mechanical/chemical degradation of the SEI layer during lithium cycling will enable the project to identify the desirable mechanical properties on SEI/lithium as a system and the specific transport properties that enable the homogenous lithium stripping/plating while avoiding the mossy structure. Furthermore, it will allow the project to develop a highly impactful strategy to protect lithium metal and achieve dendrite-free high cycle efficiency, which can dramatically increase the energy density of lithium batteries for EV applications.

Approach. Different *in situ* techniques, including AFM, nano-indentor, dilatometer, and stress-sensor, will be developed to investigate the mechanical compatibility between SEI and soft lithium and the relationship between surface morphology and current density distribution that results in an inhomogeneous lithium plating/stripping process. Multiple strategies will be developed to tailor the mechanical and transport properties of SEI and to properly engineer the protective coating/lithium interface.

Out-Year Goals. The out-year goals involve using *in situ* electrochemical tools to reveal failure mechanisms of SEI/lithium as a whole electrode system, including correlating mechanical failure mechanisms of SEI/lithium, morphology evolution, cycle efficiency, and transport properties of SEI. Then, the project will develop continuum framework to establish the failure modes of SEI layer on lithium metal and provide the governing mechanical/material properties of SEI responsible for the critical failure mode based on the experimental results and atomic scale simulation.

Collaborations. Prof. Huajian Gao (Brown University) and Dr. Qinglin Zhang (GM) will be the key researchers involved in continuum simulation and postmortem analysis. Dr. Chongmin Wang (PNNL), Dr. Wangli Yang (LBNL), and Dr. Jie Xiao will be collaborators on advanced *in situ* analysis and electrolyte additives.

Milestones

1. A continuum model of SEI growth, which can predict potential SEI failure modes and incorporate them into the continuum model. (Q1, December 2017; Completed)
2. The impact of lithium deposition induced stress on lithium morphology and cycle efficiency. (Q2, March 2018; Completed)
3. The mechanical properties of SEIs measured by nanoindentation and the SEI composition measured by XPS. (Q3, June 2018; Completed)
4. Interface adhesion energy calculations; and predication of where interface delamination will occur. Lithium plating kinetics at a lithium/single-component SEI/electrolyte interface predicted by molecular dynamics (MD) simulation. (Q4, September 2018; Completed)

Progress Report

Complete Interface Adhesion Energy Calculations at Li/Li_2CO_3, Li/LiF Interfaces and Predict Where Interface Delamination Will Occur

Based on surface energy results and construction rules described in the method section, two LiF/Li and two Li_2CO_3/Li interfaces were constructed. Since lithium is rather isotropic, the two lowest energy surfaces, (001) and (110), are both considered in the interface model. On the other hand, LiF and Li_2CO_3 are rather anisotropic, so only the single orientation with the lowest surface energy was considered for each. The interfacial mismatches are less than ~ 3% for all interface supercells, and the strain energy contribution to the total interface formation energy is small (less than 3%, except one interface). Both Li/Li_2CO_3 and Li/LiF interfaces have relatively small work of adhesion. The work of adhesion at the interface is also lower than the decohesion energy of each phase, indicating interface delamination will occur under tensile stress.

Table 5. Density functional theory calculated energetics for different fully-relaxed interfacial supercells in comparison with the fracture energy of the bulk materials.

	Li(001)/ Li_2CO_3(001)	Li(110)/ Li_2CO_3(001)	Li(001)/ LiF(001)	Li(110)/ LiF(001)
Interfacial Energy (J/m^2)	0.498	0.573	0.747	0.803
Work of Adhesion (J/m^2)	0.167	0.124	0.093	0.065
Strain Energy (mJ/m^3)	52.711	6.248	16.342	1.121
Strain Energy Contribution (%)	11.73%	1.32%	2.99%	0.23%
Decohesion energy of each phase (J/m^2)	Li(001) 0.96	Li(001) 1.02	Li(001) 0.96	Li(001) 1.02
	Li_2CO_3(001) 0.36		LiF(001) 0.72	

Predict Lithium Plating Kinetics at a Li/Single-Component SEI/Electrolyte Interface

The first step to determine the Li-plating kinetics is to determine the electrochemical equilibrium, which changes in the different electrolyte. The half reaction at the Li/SEI/electrolyte interface can be written as

$$Li^{+}(sol) + e^{-}(s) \leftrightarrow Li^{0}(\mathrm{s}) \quad (1),$$

where the Li+ ions dissolved in the electrolyte are reduced by the electrons, e^{-}, on the electrode to produce the Li^0 atoms depositing to the Li-metal electrode (forwarding reaction). The thermodynamic driving force is given by

$$\Delta G = \Delta G^{0} + F\phi - RTlna_{Li^{+}} \quad (2),$$

where DG^0 is the standard free energy change for the electrode reaction (1) on a zero charged Li-metal. F is the Faraday constant. ϕ is the Galvani potential on the Li-metal electrode (assuming the potential in the electrolyte to be the zero). α_{Li+} is the activity of Li+ in the electrolyte, which depends on temperature, solvent, and the concentrations of ions. At the electrochemical equilibrium, the forward and backward currents are equal, or in other words, the chemical potential of Li$^+$ in the electrolyte equals to the chemical potential of a reduced Li^0 in the electrode, thus

$$\Delta G = \Delta G^{0} + F\phi^{0} - RTlna_{Li^{+}} = 0 \quad (3),$$

where ϕ^{0} is the equilibrium potential. During the charge or discharge process, the thermodynamic driving force for the reaction can also be expressed as,

$$\Delta G = F(\phi - \phi^{0}) = F\eta \quad (4),$$

where h is the overpotential. If h < 0, the Li^+ is reduced (plating); whereas if h > 0, the Li^0 is being oxidized to Li^+ (stripping). The charge transfer reaction in equation 1 can be rewritten to include the insulating effect of the SEI layer, assuming Li^+ dissolved in the solvents. One can compute or measure each energy term in the thermodynamic cycle like the following:

$$\Delta G^0 = -E_f(V_{Li}) - E_{vap} - E_{ion} + W_f + E_{sol}(Li^+) \quad (5)$$

Because the solvation energy of Li^+ in EC is 5.5 eV, larger than that in DOL (5.06 eV), ΔG^0 is 1.26 eV for lithium in EC and 0.82 eV in DOL. Negative charges must be applied to lithium metal to reach the electrochemical equilibrium. Assuming $a_{Li^+} \sim 1M$, the equilibrium potential ϕ^0 is -1.26 eV for lithium in EC and -0.82 in DOL, suggesting the Li-metal surface has less excess electron density at $\eta = 0$. This might be the fundamental reason for less SEI growth in ether-based electrolytes.

A SEI/Li Composite Model for Stress Generation during Lithium Plating/Stripping

Stress measurement on uniformly deposited lithium under asymmetric cycling reveals that the in-plane compressive stress built up during lithium plating is not mainly contributed from the deposited lithium metal. To interpret the origin of the plating-induced stress, a porous structure of SEI with multiple types of conductive paths that lithium atoms can flow into was proposed, as shown in Figure 31.

To simplify the analysis, only the conductive paths that connect to the top surface of the lithium metal have been considered due to their accessibility to the electrons from the Li-metal side, as shown in Figure 31. The SEI is assumed to be fully passivated and thus have a constant thickness H. The average distance between the conductive paths is set to L. During plating, lithium atoms on the Li-metal surface flow into the conductive paths due to the difference in chemical potential, creating compressive stress in the SEI layer.

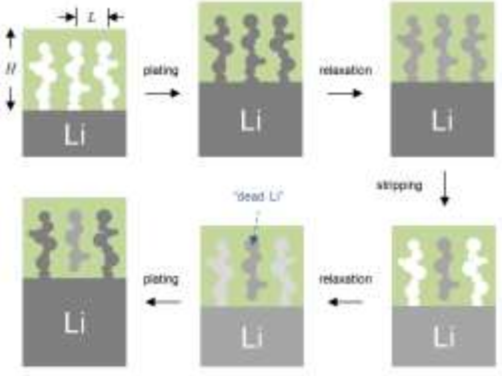

Figure 31. Schematic of lithium flow between the conductive paths and Li-metal surface during plating/stripping cycles.

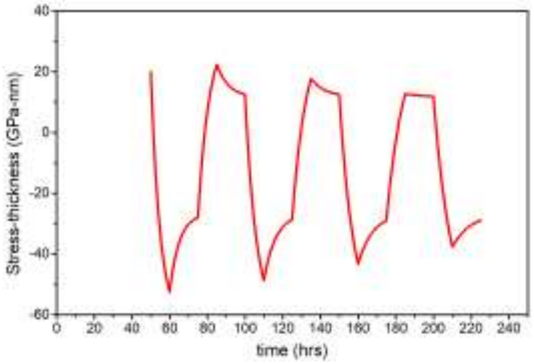

Figure 32. Stress-thickness evolution predicted from the kinetic model.

A kinetic model based on the aforementioned mechanisms has been developed, inspired by a model for stress generation during thin film growth. The stress evolution during each plating, open circuit voltage (OCV) hold, or stripping process takes the following form,

$$\sigma(t) = \left(\sigma_i + \frac{\Delta\mu}{\Omega}\right)\exp\left[-C_s\Gamma\frac{E\alpha\Omega^2}{(1-\nu)HL^2kT}\cdot t\right] - \frac{\Delta\mu}{\Omega} \quad (6)$$

Where σ_i represents the initial stress; $\Delta\mu$ the chemical potential difference between the lithium surface and conductive path; cesium the concentration of mobile lithium on the surface; Γ the transition rate between the surface and the conductive path; α a geometric shape factor; Ω, E, and ν the atomic volume, Young's modulus, and Poisson's ratio of lithium, respectively; κ the Boltzmann constant, and T the temperature.

With parameters calibrated from the experimental data, the kinetic model predicts the stress-thickness evolution, as plotted in Figure 32, which is in good agreement with the results from the stress measurements. This model can account for the build-up of the compressive/tensile stress during plating/stripping, the observed stress relaxation during OCV hold, as well as the decrease in the magnitude of the stress variation during cycling, which supports the conclusion that the main contribution of the induced stress during lithium plating is from SEI, rather than lithium metal.

Patents/Publications/Presentations

Patents

- Xiao, X., B. Li, H. Gao, and K. Guo. Coating System Design for Lithium Electrode Protection, P045909, 2018.
- Li, B., X. Xiao, J. Xu, and Q. Zhang. Surface Treatment of Li Metal for Rechargeable Batteries, P044686, TMS, 2018.
- Li, B., and X. Xiao. A Reinforced Siloxane Coating for Lithium Metal Electrodes, P047263, 2018.

Publications

- Guo, K., W. Zhang, B. W. Sheldon, and H. Gao. "Concentration Dependent Properties Lead to Plastic Ratcheting in Thin Island Electrodes on Substrate under Cyclic Charging and Discharging." *Acta Materialia*, submitted (2018).
- Liu, Y., K. Guo, C. Wang, and H. Gao. "Wrinkling and Ratcheting of a Thin Film on Cyclically Deforming Plastic Substrate: Mechanical Instability of the Solid-Electrolyte Interphase in Li-ion Batteries." *Journal of the Mechanics and Physics of Solids*. In press.
- Liu, Z., P. Lu, Q. Zhang, X. Xiao, Y. Qi, and L. Q. Chen. "A Bottom-up Formation Mechanism of Solid Electrolyte Interphase (SEI) Revealed by Isotope-Assisted Time-of-Flight Secondary Ion Mass Spectrometry (TOF SIMS)." *Journal of Physical Chemistry Letters* 9, no. 18 (2018): 5508–5514.

Presentations

- 10th European Solid Mechanics Conference, Bologna, Italy (July 3, 2018): "Mechanical Degradation and Optimization of Solid Electrolyte Interphases in Li Ion Batteries"; B. W. Sheldon.
- 256th ACS Meeting, Boston, Massachusetts (August 21, 2018): "Chemo-Mechanical Degradation and Optimization of Solid Electrolyte Interphases in Li Ion Batteries"; B. W. Sheldon.
- Society of Engineering Science Annual Meeting, Madrid, Spain (October 10, 2018): "Chemo-Mechanical Degradation of Solid Electrolyte Interphases in Li Ion Batteries"; B. W. Sheldon.
- Detroit Section of the Electrochemical Society, Seminar (September 13, 2018): "*In Situ* Mechanical Characterization for Understanding the Coupled Electrochemical-Mechanical Behavior of Battery Materials"; Yang-Tse Cheng.
- 2018 Beyond Lithium Ion XI, Cleveland, Ohio (July 2018): "Mechanical Behavior of Li Metal Electrodes Studied by Environmental Nanoindentation"; Y. Wang, D. Dang, M. Wang, X. Xiao, and Y-T. Cheng. Poster.

Task 2.6 – Microscopy Investigation on the Fading Mechanism of Electrode Materials (Chongmin Wang, Pacific Northwest National Laboratory)

Project Objective. The objective is to use a combination of *ex situ*, *in situ*, and *operando* HRTEM and spectroscopy to probe the fading mechanism of layer structured cathode under high-voltage operating condition. To complement the HRTEM study, *in situ* liquid cell SIMS and atom probe tomography (APT) will also be used to gain structural and chemical evolution of electrodes and correlate the structural and chemical evolution with battery performance.

Project Impact. The proposed characterization work focused on atomic level structural and chemical analysis and direct correlation with battery fading properties. The work can be directly used to guide the designing of electrode materials with tailored microstructure and chemistry for enhanced properties of increasing the energy density of Li-ion batteries and to accelerate market acceptance of EVs, especially for PHEV as required by the EV Everywhere Grand Challenge.

Approach. This project will use the unique *ex situ* and *in situ* TEM methods to probe the structure of Li-ion batteries, especially a biasing liquid electrochemical cell that uses a real electrolyte in a nano-battery configuration. It will also use various microscopic techniques, including *ex situ*, *in situ*, and especially the *operando* TEM system, to study the fading mechanism of electrode materials in batteries. This project will be closely integrated with other R&D efforts on high-capacity cathode and anode projects in the BMR Program to: (1) discover the origins of voltage and capacity fading in high-capacity layered cathodes, and (2) provide guidance for overcoming barriers to long cycle stability of electrode materials.

Out-Year-Goals. This project has the following out-year goals:

- Conduct multi-scale (ranging from atomic-scale to mesoscale) *ex situ*/*in situ* and *operando* TEM investigation of failure mechanisms for energy-storage materials and devices. Perform atomic-level *in situ* TEM and STEM imaging to help develop fundamental understanding of electrochemical energy-storage processes and kinetics of electrodes.
- Extend the *in situ* TEM capability for energy storage technology beyond lithium ions, such as Li-S, Li-air, Li-metal, sodium ions, and multi-valence ions.

Collaborations. This project collaborates with Michael M. Thackeray and Jason Croy (ANL); Guoying Chen (LBNL); Jagjit Nanda (ORNL); Chunmei Ban (NREL); Khalil Amine (ANL); Donghai Wang (Pennsylvania State University); Arumugam Manthiram (University of Texas at Austin, UT Austin); Wei Tong (LBNL); Gao Liu (LBNL); Yi Cui (Stanford University); Jason Zhang (PNNL); Jun Liu (PNNL); Xingcheng Xiao (GM); Shirley Meng (UCSD); and Stan Whittingham (State University of New York – Binghamton).

Milestones

1. Resolve the vacancy injection mechanism into the LM-NMC during the battery cycling and its correlation with battery fading mechanism. (Q2, March 31, 2018; Completed)
2. The functioning mechanism of electrolyte additive on the solid-liquid interphase in NMC cathode. (Q3, June 30, 2018; Completed)
3. Atomic level understanding of the mechanism of intergranular and intragranular cracking in NMC. (Q4, September 30, 2018; Completed)

Progress Report

The key new information of this work is to use *in situ* HRTEM to directly demonstrate the coupling effect among electrochemically induced thermal and mechanical effects, leading to fading of the cathode in a more severe way than that resulting from the simple addition of each factor.

Electrochemically driven functioning of a battery inevitably induces thermal and mechanical effects. A vast amount of work has been done in terms of elucidating the role of each of these three factors on performance of rechargeable batteries, such as thermal management and analysis of mechanically induced failure. However, during battery operation, these three factors exist simultaneously and then are coupled and collectively govern performance of the battery. However, this coupling effect, whether favorable or detrimental, has not yet been explicitly elucidated.

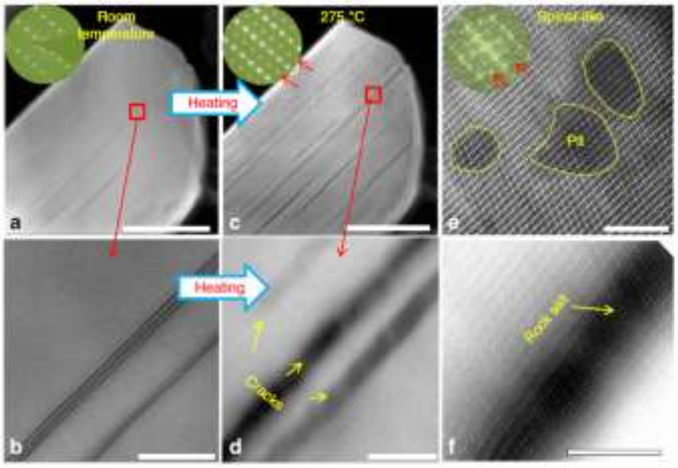

Figure 33. *In situ* heating-induced crack nucleation and propagation. The $LiNi_{0.6}Mn_{0.2}Co_{0.2}O_2$ (NMC-622) was delithiated by charging to 4.7 V versus lithium metal. (a-b) High-angle annular dark field (HAADF) images from delithiated NMC-622 before heating (room temperature). (c–f) HAADF images after heating to 275°C. Selected area electron diffraction (SAED) patterns and fast Fourier transformation images in (a/c/e) show the overall lattice change during heating. (d/e/f) Local lattice structure change at crack regions and crack-free regions. The scale bars are 200 nm in (a) and (c); 10 nm in (b) and (d); and 4 nm in (e) and (f).

This project uses high-resolution STEM to demonstrate such a coupling effect among the electrochemically induced thermal and mechanical effects. By integrating *in situ* TEM, *in situ* XRD, and modeling, a coupling effect on the intragranular cracking of a Ni-rich $LiNi_{0.6}Mn_{0.2}Co_{0.2}O_2$ (NMC-622) layered cathode is demonstrated. It has been noticed that supplying a thermal perturbation to the delithiated $LiNi_{0.6}Mn_{0.2}Co_{0.2}O_2$ will lead to the nucleation and propagation of intragranular cracks in the lattice, often in an explosive way, as shown in Figure 33. It shows that *in situ* heating of delithiated NMC-622 particles, even at the first delithiation from the pristine state, leads to explosive nucleation and propagation of intragranular cracking. Such a phenomenon is absent in fully discharged particles (with lithium being reinserted). Combining *ex situ* and *in situ* TEM observations with chemomechanical modeling reveals that, in response to the temperature raise, electrochemically induced phase inhomogeneity and oxygen evolution cause, respectively, thermal stress and internal pressure, which constitute the two primary driving forces for the intragranular cracking. The present observation demonstrates that the intimate coupling of the electrochemical, thermal, and mechanical processes leads to a much more severe effect on degradation of the cathode.

Characteristically, the heating-induced intragranular cracking is accompanied with surface phase transformation and oxygen gas release. Taken together, the observed intragranular cracking resembles the popcorn fracture mechanism under heating. The studies offer insights into how the electrochemical process triggers thermal and mechanical processes in battery operation, and how these effects are intimately coupled and mutually strengthened in the degradation of layered cathode materials. The fundamental understanding also sheds light on mitigation of degradation of battery materials under complicated electrochemical and thermomechanical conditions.

Patents/Publications/Presentations

Publication

- Yan, P., J. Zheng, T. Chen, L. Luo, Y. Jiang, K. Wang, M. Sui, J-G. Zhang, S. Zhang, and C. Wang. "Coupling of Electrochemically Triggered Thermal and Mechanical Effects to Aggravate Failure in a Layered Cathode." *Nature Communications* 9 (2018): 2437.

Presentation

- 256th ACS Meeting, Analysis of Materials for Energy Storage Symposium, Boston, Massachusetts (August 19–23, 2018): "*In Situ* TEM Observation on the Correlation of Electrochemical Properties with Structural and Chemical Evolution of Electrode Materials in Rechargeable Batteries"; C. M. Wang.

Task 2.7 – Understanding and Mitigating Interfacial Reactivity between Electrode and Electrolyte (Khalil Amine and Zhonghai Chen, Argonne National Laboratory)

Project Objective. To understand the pathway/mechanism of parasitic reaction between electrode materials and electrolyte for beyond Li-ion chemistries, and to stabilize the electrode/electrolyte interface for long life and safe battery chemistries.

Project Impact. The project is designed to have several areas of impact:

- To maximize the practical energy of battery chemistries beyond lithium ion,
- To improve the life and roundtrip energy efficiency of battery chemistries using S-based cathodes, and O_2-based cathodes, and
- To stabilize the lithium/electrolyte interface for high-energy-density lithium battery chemistries.

Approach. The project approach is multi-fold: (1) fundamental investigation of the pathway/mechanism of parasitic reactions between electrolytes and electrode materials, (2) rational mitigation of parasitic reactions based on the identified reaction pathway, (3) developing functional surface coating and electrolyte additives to suppress the chemical reactions between electrolytes and electrode materials, and (4) formulating new electrolyte to control the direct electrochemical reaction of electrolyte components.

Out-Year-Goals. When the electrode electrolyte interface is stabilized, the following results can be achieved:

- A cell with energy density of 600 Wh/kg, and
- A battery capable of operating for 500 cycles with low capacity fade.

Collaborations. The project collaborates with Dr. Gui-Liang Xu and Dr. Ang T. Ngo of ANL and with Prof. Chunsheng Wang of UMD.

Milestones

1. Synthesis of S/C composite cathode materials for Li/S batteries. (Q1, FY 2018; Completed)
2. Electrochemical characterization of S/C cathode. (Q2, FY 2018; Completed)
3. Investigation of the kinetics of parasitic reactions at the interface of S/C cathode. (Q3, FY 2018; Completed)
4. Investigation of the impact of sulfur load on both the electrochemical performance and kinetics of parasitic reactions. (Q4, FY 2018; Completed)

Progress Report

The dissolution of lithium polysulfide in the nonaqueous electrolytes during charge/discharge cycling of Li/S batteries has been widely considered the major contribution of low CE and poor life performance of Li/S batteries. Therefore, it is a widely adopted strategy to encapsulate the sulfur active material inside highly porous electric conductive medium, like nanoporous carbons, to reduce the direct exposure of lithium polysulfide toward the electrolyte. This quarter, the team investigated the dependence of the electrochemical performance of S/C composite cathode on the sulfur loading, with activity focusing on the kinetics of the shuttle reaction (see Figure 34).

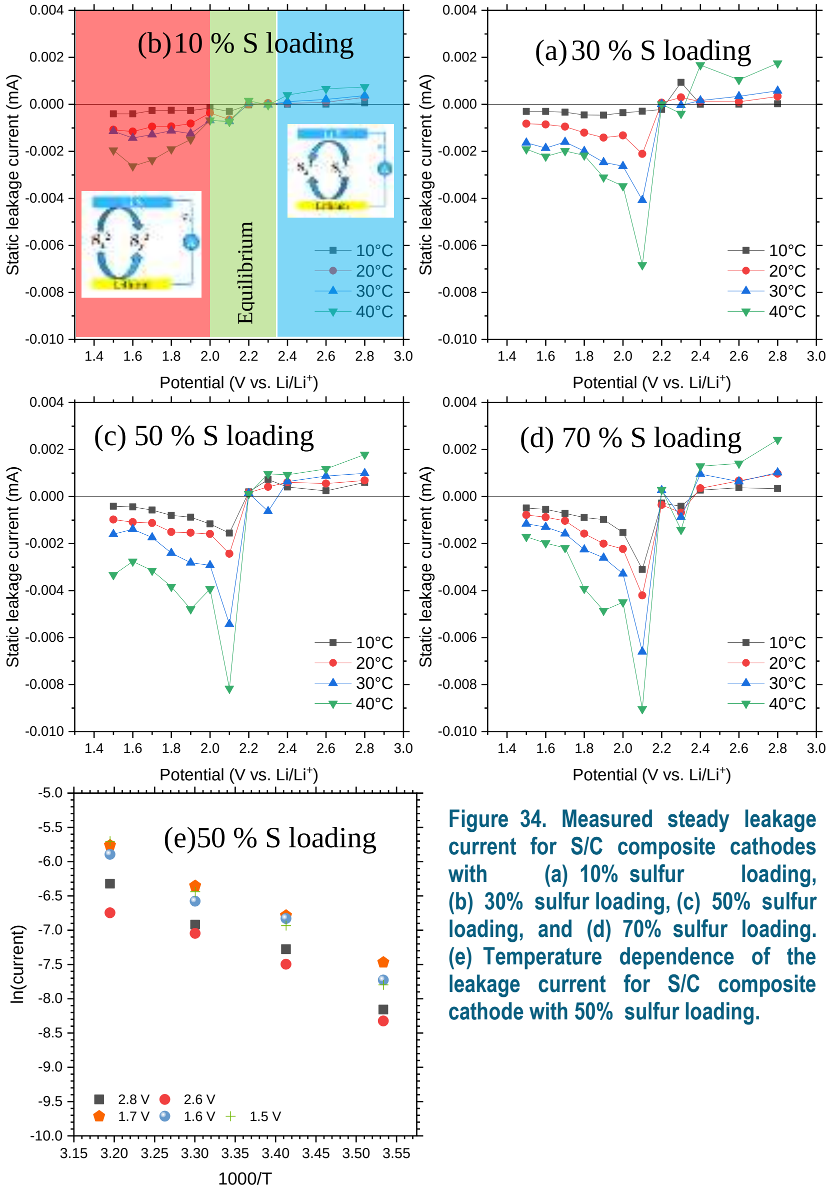

Figure 34. Measured steady leakage current for S/C composite cathodes with (a) 10% sulfur loading, (b) 30% sulfur loading, (c) 50% sulfur loading, and (d) 70% sulfur loading. (e) Temperature dependence of the leakage current for S/C composite cathode with 50% sulfur loading.

Figure 34 shows that there is no clear change on the dissolution mechanism of lithium polysulfide with a simple change in the percentage of sulfur in S/C composite cathodes. However, they all show clear dependence on the working potential the cathode. Using the cathode with 10% sulfur loading as an example, the redox shuttle showed a minimal effect at a potential near 2.2 V versus Li$^+$/Li (~ zero steady leakage current). When the potential is lower than 2.2 V versus Li$^+$/Li, a negative leakage current was developed, resulting from the redox shuttle effect of dissolved lithium polysulfide in the electrolyte. Impressively, the steady leakage current goes to a positive territory when the potential is higher than 2.2 V versus Li$^+$/Li. Figure 34e shows the temperature dependence of the measured steady leakage current at different potential. It is clearly shown that the reaction at a low potential (for example, 1.5 V, 1.6 V, and 1.7 V) has a similar activation energy to that reaction at 2.8 V. This implies that the redox shuttle reactions within the load potential region and the high potential region have the same chemical characteristics, but with reversed reaction direction. It also implies that the middle region at around 2.2 V is an equilibrium region of the chemical potential of sulfide anion in electrolyte and in the solid phase.

Patents/Publications/Presentations

The project has no patents, publications, or presentations to report this quarter.

Task 2.8 – Correlative Microscopy Characterization of Electrochemical Hotspots in Oxide Electrodes (Yi Cui, William Chueh, and Michael Toney; Stanford/SLAC)

Project Objective. This project aims to develop and utilize a correlative microscopy platform to investigate the lithiation dynamics of LMR-NMC and NCA, with the specific goal of understanding factors that determine the rate capability and degradation mechanisms at the single primary particle length scale. By developing a nanoscale and single-particle understanding of lithiation, the project addresses specific engineering problems including electrochemical hotspot, electrode utilization, safety, and capacity/voltage fade.

Project Impact. Fundamental insights from this new diagnostic capability are expected to increase the power density and cycle life of oxide electrodes by improving electrode utilization, reducing electrochemical hotspots, decreasing capacity and voltage fade, and enhancing safety, which all improve the viability of Li-ion batteries for vehicle transportation. By understanding lithiation at the single-particle level, this project’s success will contribute to improving on-vehicle battery management, such as charging/discharging protocol, and state-of-charge and state-of-health monitoring.

Approach. This project aims to develop a correlative microscopy platform to investigate the lithiation dynamics of LMR-NMC and NCA, with the specific goal of understanding factors that determine the rate capability and degradation mechanisms at the single primary particle length scale. On recharging time, the specific phenomena to be addressed include nonuniform current distribution and the correlation between surface property and the local lithiation rate. On degradation, phenomena to be addressed include correlating local chemistry and phases to capacity and voltage fading.

Out-Year Goals. Develop X-ray microscopy to investigate NMC and LMR-NMC cathodes at the single primary particle and single secondary particle level.

Collaborations. Commercial battery electrode particles are being supplied by Samsung.

Milestones

FY 2016

1. Development of correlative microscopy platform for imaging LMR-NMC cathodes. (Achieved)

FY 2017 – 2018

1. Synthesis and characterization of well-faceted NMC and NMC particles. Demonstrate *in situ* single particle imaging with spectro-ptychography of NMC. (Achieved)
2. Use of correlative microscopy platform for imaging LMR-NMC and NMC cathode hotspots. (Achieved)
3. Spectro-imaging of single NMC particles. (Ongoing)
4. *Ex situ* variable temperature (-20°C to +80°C) spectro-imaging of LMR-NMC particles. (Ongoing)

Progress Report

When tin is substituted into Li_2IrO_3 to make solid-solution phase $Li_2Ir_{1-y}Sn_yO_3$ (LISO), the electrochemistry changes dramatically and becomes typical of that of anion redox active materials (Figure 35a). Regardless of tin content, when charged beyond $Ir^{5.5+}$, LISO exhibits a new plateau at ~ 4.35 V, followed by a large voltage drop on the subsequent discharge, a permanently sloped voltage profile, and voltage hysteresis that persists even at open circuit. Despite the drastic changes to the voltage profile, LISO25 (y=0.25) exhibits reasonable capacity retention with cycling (74.5% after 192 cycles). The new high voltage plateau, in conjunction with the additional reversible capacity well beyond 1.5 e- per Ir (Figure 35a), indicates the presence of a reversible redox partner beyond $Ir^{4+}/Ir^{5.5+}$.

In addition to this high-voltage redox partner, the average and local structural behavior of LISO differs from that of Sn-free LIO, as reported in the second quarter. As first demonstrated by McCalla et al., a substantial degree of cation site disorder develops in LISO after first delithiation. Figure 35b quantifies the extent of site disorder in LISO25 before and after electrochemical cycling with either a 4.25 V or 4.60 V cutoff. As shown schematically in Figure 35b, the team assumes that each in-plane and out-of-plane antisite defect results in a corresponding vacant M site. They therefore quantify the total amount of disorder by the fraction of V_M, which reaches between 7.5±0.4% (assuming all Ir_{Li}) and 10.2±0.6% (assuming all Sn_{Li}) after a single cycle between 4.60-2.50 V, approximately evenly split between in-plane and out-of-plane antisite defects (since low concentrations of Sn_{Li} and Ir_{Li} have an identical effect on the Bragg peak intensity, XRD cannot be used to differentiate between the migrating species). This translates to at least 40.8% of tin having migrated in fully charged LISO assuming all Sn_{Li}. Since the total accessed capacity is approximately the same between LIO and the various LISO compositions, by substituting with tin the team can conclude that the structural disordering is not due to inherent structural instability at low lithium contents. Furthermore, the disordering appears to be associated with the new redox partner giving rise to the high voltage plateau: the disorder in LISO25 after a full cycle is dramatically greater than in both LIO after the first cycle and LISO25 after a single cycle between 4.25-2.50 V, which are both zero within experimental error. Out-of-plane refinement of the fully charged O1 structure shows that the disorder is increased substantially at 4.60 V, providing a direct connection between the new redox partner, electrochemical irreversibility, and the onset of cation disordering.

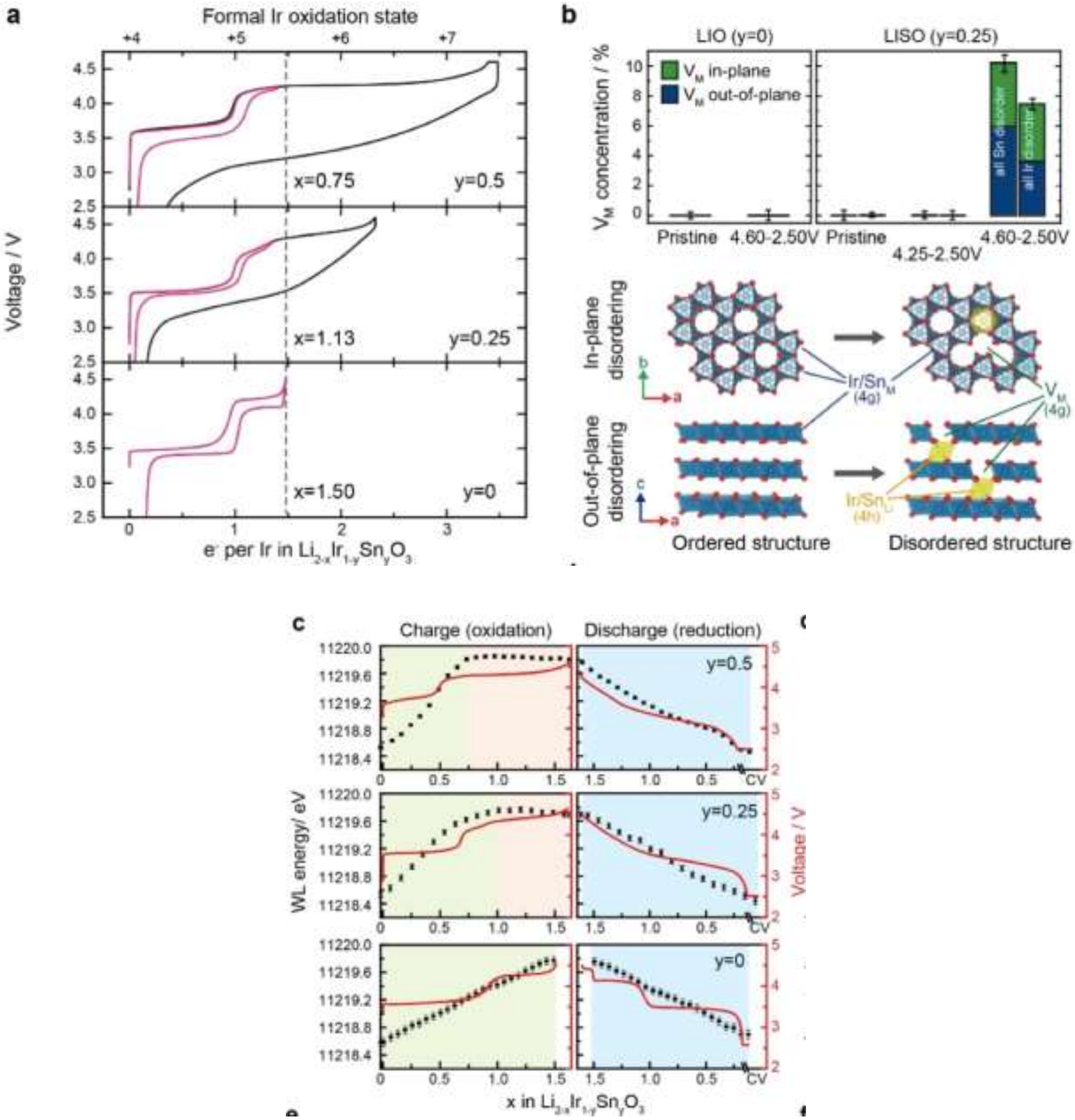

Figure 35. (a) Charge/discharge profiles of $Li_{2-x}Ir_{1-y}Sn_yO_3$ (y=0, 0.25, 0.5) under a constant current density (C/10 rate) for a full cycle (black) and for an approximately 1.5 electron per iridium per f.u. cycle (pink). (b) In-plane and out-of-plane disorders quantified by iterative X-ray diffraction Rietveld refinement for the LISO25 (y=0.25) cycled in 4.60-2.50 V and 4.25-2.50 V and LIO cycled in 4.60-2.50 V, quantified by the total V_M concentration. The scheme illustrates the in-plane (top) and out-of-plane (bottom) structural disordering mechanisms resulting in V_M, with the migrated cation octahedron shaded yellow and the Wyckoff positions indicated in parentheses. (c) *Operando* transmission X-ray absorption near-edge structure spectra of Ir L3 edge for the first cycle showing the continuous iridium oxidation up to 4.25 V, no shift beyond 4.25 V, and the continuous iridium reduction during discharge.

Patents/Publications/Presentations

Publication

- Hong, J., W. E. Gent, P. Xiao, K. Lim, D.-H. Seo, J. Wu, P. M. Csernica, C. J. Takacs, D. Nordlund, C.-J. Sun, K. H. Stone, W. Yang, D. Prendergast, G. Ceder, W. C. Chueh, and M. F. Toney. "Metal-Oxygen Decoordination Stabilizes Anion Redox in Li-rich Oxides." Submitted (2018).

Presentations

- GRC, Batteries, Ventura, California (February 25, 2018): "Coupling Between Oxygen Redox and Cation Migration Explains Unusual Electrochemistry in Lithium-Rich Layered Oxides"; W. E. Gent, K. Lim, Y. Liang, J. Hong, M. McIntire, Q. Li, S-J. Ahn, J. H. Song, J-H. Park, S-K. Doo, D. Kilcoyne, D. Vine, A. Mehta, S. Ermon, W. Yang, D. Prendergast, M. F. Toney, and W. C. Chueh. Poster
- Royal Society Materials Challenges for Sustainable Energy Technologies, London, United Kingdom (September 19, 2018); W. C. Chueh.
- Hoover Institution, Washington, D. C. (September 18, 2018); W. C. Chueh.
- 5th Solid-State Chemistry & Ionics (SCI) Workshop, Fukuoka, Japan (September 11, 2018); W. C. Chueh.

TASK 3 – MODELING

Summary and Highlights

Achieving the performance, life, and cost targets outlined by VTO will require moving to next-generation chemistries, such as higher capacity Li-ion intercalation cathodes, silicon and other alloy-based anodes, Li-metal anode, and sulfur cathodes. However, numerous problems plague development of these systems, from material-level challenges in ensuring reversibility to electrode-level issues in accommodating volume changes, to cell-level challenges in preventing cross talk between the electrodes. In this task, a mathematical perspective is applied to these challenges to provide an understanding of the underlying phenomenon and to suggest solutions that can be implemented by the material synthesis and electrode architecture groups.

The effort spans multiple length scales from *ab initio* methods to continuum-scale techniques. Models are combined with experiments, and extensive collaborations are established with experimental groups to ensure that the predictions match reality. Efforts also focus on obtaining parameters needed for the models, either from lower-length scale methods or from experiments. Projects also emphasize pushing the boundaries of the modeling techniques used to ensure that the task stays at the cutting edge.

In the area of intercalation cathodes, effort is focused on understanding working principles of high nickel layered materials with an aim of understanding structural changes and associated changes in transport properties. Coatings, an effective strategy for high-voltage operation, are being explored with the aim of providing a rational design approach for new coating materials. Focus is also paid both to assembling porous electrodes with particles to predict conduction behavior and to developing tools to measure electronic conduction.

Efforts also continue in predicting transport properties of liquid electrolytes, especially in the superconcentrated regime and understanding the nature of the silicon anode behavior.

In the area of Li-metal anodes, the focus is on understanding how materials can be designed to prevent dendrite growth using continuum modeling approaches, combined with calculations on mobility in solid conductors. The results are used to guide materials development by providing the properties needed to prevent dendrites while also achieving the energy and power goals. Models are also starting to examine the role of the SEI on the morphology of the dendrite and to describe the mechanical-electrochemical coupled effects that are critical for dendrite formation in both polymer and ceramic materials. In the area of sulfur cathodes, the task is aimed at modeling the dissolution-precipitation process and tracking the morphological changes during cycling.

Highlight. The Persson Group (LBNL) was able to successfully simulate the diffusion coefficient of $LiPF_6$ using classical MD simulations and show behavior consistent with experiments, including the higher transference number at high salt concentrations.

Task 3.1 – Design of High-Energy, High-Voltage Lithium Batteries through First-Principles Modeling (Kristin Persson, Lawrence Berkeley National Laboratory)

Project Objective. This project supports VTO programmatic goals by developing next-generation, high-energy cathode materials and enabling stable cathode operation at high voltages through target particle morphology design, functional coatings, and rational design of electrolytes. The end-of-project goals include: (1) novel disordered, high-rate Li-excess cathodes, (2) new fundamental understanding of the cathode/electrolyte interface and the factors that control the interfacial chemistry and interfacial impedance, (3) critical surface and coating design and optimization strategies that will improve cycling of Li-ion battery cathodes, and finally (4) understanding of the factors that govern stability in nonaqueous electrolytes for Li-ion and Li-S systems.

Project Impact. To enhance performance of Li-ion systems, improvements on the cathode and the electrolyte side are needed. This project is aimed to result in an improved understanding of the atomistic mechanisms underlying surface behavior and performance of the Li-ion cathode materials, with the ultimate goal being to suggest strategies, such as coatings, surface protection, and particle morphology design. Furthermore, fundamental studies of electrolyte stability, as a function of solvent and salt concentrations, and components will be conducted.

Approach. First-principles calculations, both static and dynamic approaches, are used to model solid-state electrode material thermodynamics and kinetics. Liquid electrolytes are modeled through coupled classical MD and first-principles methods to accurately capture solvation structure as well as reactivity of the liquid system.

Out-Year Goals. Stable interfaces will be determined by focusing initially on degradation mechanisms related to release of surface oxygen at high charge. Tuning particle morphology and coating materials—both of crystalline as well as amorphous structure—will be explored using the Materials Project. For electrolyte development, work will be aimed toward understanding atomistic interactions underlying the performance of lithium electrolytes, specifically elucidating the solvation structure (as a function of salt concentration) and its impact on stability of different liquid constituent species.

Collaborations. This project is highly collaborative between BMR PIs G. Chen (LBNL), G. Ceder (LBNL), and V. Srinivasan (ANL). Cathode design and synthesis will be performed by Chen and Ceder, surface design by Persson, and electrolyte design and testing by Persson and Srinivasan.

Milestones

1. Finish modeling of $LiAsF_6$ in weakly dissociating solvent. Identify concentration limit causing change in Li^+ solvation structure between contact-ion-pair and solvent separated species. (Q1, December 2017; Completed)
2. Finish modeling of $LiPF_6$ in weakly solvating solvent. Identify concentration limit causing change in Li^+ solvation structure between contact-ion-pair and solvent separated species. (Q2, March 2018; Completed)
3. Model dielectric constant of complex Li^+ electrolytes using MD. (Q3, June 2018; Completed)
4. *Go/No-Go Decision*: Test algorithm against experimental results to assess whether the project's model can quantitatively capture change in dielectric behavior as a function of concentration and different solvation structures. If not, change approach. (Q3, June 2018; Completed)
5. Present simulated kinetic and thermodynamic evaluations of lithiation mechanisms of amorphous silicon and SiO_2. (Q4, September 2018; Completed)

Progress Report

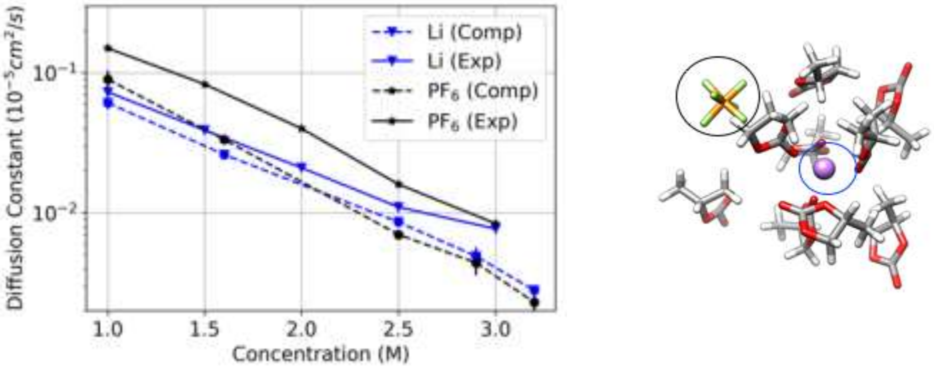

Figure 36. Diffusion constants of Li^+ and PF_6^- in propylene carbonate (PC solutions) from concentrated (1 M) to superconcentrated (~ 3 M) regimes. Illustrative snapshot of a solvated Li+ cation cluster in superconcentrated solution is shown on the right.

Using classical MD simulations, the team computed transport properties of the charge conducting species in $LiPF_6$ – propylene carbonate electrolyte using the Einstein relation; this compared favorably to existing experiments. Notably the ratio of $D_{Li^+}/D_{PF_6^-}$ increases at higher salt concentrations, demonstrating that the project's computational model can reproduce dynamics of promising higher transference number electrolytes.

In prior reports, the team discussed properties of silicon anodes as a precursor to studying binary silicon alloy anode systems, specifically the Si-Sn alloys. Previous studies on Si-Sn anodes by Dahn et al. show promise with improved initial CE and capacity retention. Here, the team uses AIMD to simulate liquid melts and amorphous configurations of the $Si_{1-y}Sn_y$ system throughout the composition range y = {0, 0.1, 0.2, …, 0.9, 1}. Observed structural motifs suggest that the synthesis of these alloys may present challenges due to the system's tendency to maximize Si-Si and Sn-Sn bonding. This is consistent with data reported by the Materials Project (www.materialsproject.org) in which all crystalline Si-Sn polymorphs are unstable and have only been experimentally synthesized under high pressures, and phase diagrams of Si-Sn wherein silicon and tin are miscible only at high temperature.

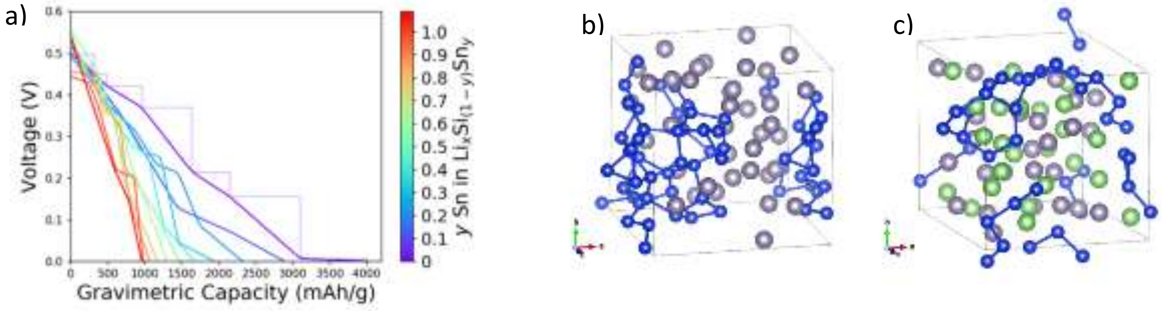

Figure 37. (a) Voltage profile for lithiation of amorphous $Si_{1-y}Sn_y$ and representative structures of (b) SiSn and (c) LiSiSn.

With the same AIMD simulation methodology, the team also studied the $Li_xSi_{1-y}Sn_y$ systems. In these systems, they again do not observe homogeneity, rather the presence of nonpercolating silicon aggregates, Li_xSi, and Li_xSn regions. In the lithiated Si-Sn alloys, the team finds the addition of tin to have two major effects: fragmenting the silicon networks and introducing tin regions into the structure.

Patents/Publications/Presentations

The project has no patents, publications, or presentations to report this quarter.

Task 3.2 – Addressing Heterogeneity in Electrode Fabrication Processes (Dean Wheeler and Brian Mazzeo, Brigham Young University)

Project Objective. The project goal is to better understand connections between fabrication conditions and undesired heterogeneity of thin-film electrodes by means of new NDI techniques and computer models.

Project Impact. This work will result in new diagnostic and modeling tools for rapidly and conveniently interrogating how well homogeneity has been maintained in electrodes during fabrication and in subsequent cycling. Real-time measurement of heterogeneity will enable manufacturer quality control improvements. The measurement and modeling tools will further enable researchers to compare different electrodes, improve formulations and processes, and anticipate cell performance of new designs.

Approach. Two NDI techniques will be developed or improved that will characterize electrochemical and mechanical uniformity of the electrodes. The first tool will be a flexible contact probe on a polymer substrate for rapidly measuring local electrical conductivity across electrodes of any geometry. The second tool will be a new acoustic probe that measures local elasticity and density of the composite film. These two prototyping efforts will be tied together by a particle-based microstructure model that allows prediction and correlation of electrode conductive and mechanical properties with fabrication conditions.

Out-Year Goals. This project was initiated October 2016 and concludes September 2019. Overall goals by fiscal year are as follows:

- **2017.** Fabricate first-generation flexible conductivity probe and proof-of-concept of acoustic probe. Improve microstructure model to match experiment.
- **2018.** Integrate flex probe with test fixtures suitable for assessment of large or continuous samples. Demonstrate measurement of localized ionic conductivity.
- **2019.** Assess affect of heterogeneity on cell charge and discharge performance. Further improve accuracy and reliability of probe and modeling technologies.

Collaborations. Ram Subbaraman and Jake Christensen (Bosch), Daniel Abraham (ANL), Steve Harris (LBNL), Bryant Polzin (ANL), and Chisu Kim (Hydro-Quebec, HQ) have provided battery materials for analysis. Other collaborations and the transfer of this technology to interested parties are being pursued.

Milestones

1. Integrate flex probe with off-the-shelf CNC positioning system to enable interrogation of large-format electrode films. (Q1, December 2017; Completed)
2. Integrate flex probe with prototype rolling apparatus to enable interrogation of continuous-roll electrode films. (Q2, March 2018; Completed)
3. *Go/No-Go Decision*: Demonstrate that localized conductivity probe has adequate reliability for continued development. Criteria: Localized ionic conductivity probe can match macroscopic results for a representative electrode sample. (Q3; Completed)
4. Quantify the durability of multiple flex probes to validate suitability for industrial use. (Q4; Completed)

Progress Report

To complete the fourth milestone of FY 2018, tests were performed to determine the durability of the flexible conductivity microprobes. The probe was used to perform 1,000-sampling-point tests on a commercial Li-ion electrode. Images of the probes were taken between such tests, and the electrical data were also analyzed to determine degradation of the flexible probe. Figure 38 shows the image progression of the probe lines over the duration of these tests. As shown, slight degradation was shown over the course of a total of 10,000 points, which demonstrates high durability, given that typical tests encompass several hundred points. The electrical data also showed that the probe lines consistently obtained good contact with the Li-ion electrode.

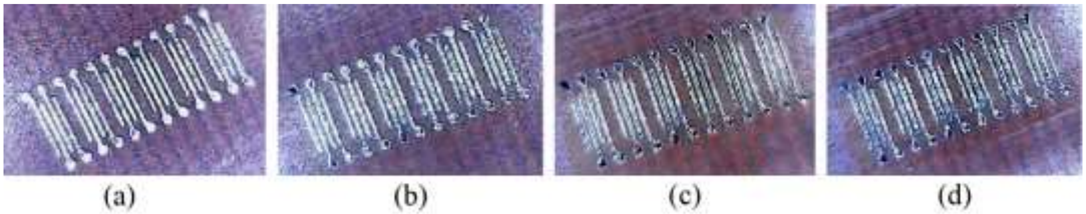

Figure 38. Optical microscope images of probe surface (a) before durability tests, (b) after a total of 3,000 sampling points, (c) after a total of 7,000 points, and (d) after a total of 10,000 points.

A microprobe was used to measure the ionic resistance of seven electrodes of different average MacMullin numbers, a measure of how easily ions can move through the electrode. The MacMullin number was determined using the blocking-electrolyte method over the whole film. On each electrode, 30 locations were chosen randomly, and each location yielded a different ionic resistance using the microprobe, due to the heterogeneity of the electrode. Figure 39 shows the average ionic resistance (by microprobe; vertical axis) of each electrode versus its MacMullin number (by blocking electrolyte method; horizontal axis), with a parity line showing the proportional level of agreement between the two methods. The trend shows that the microprobe measurement has the potential to distinguish electrodes of different tortuosity, though continuing work in FY 2019 will be needed to make the method more quantitative. The method is also able to quantify the degree of heterogeneity in ionic transport for a given electrode.

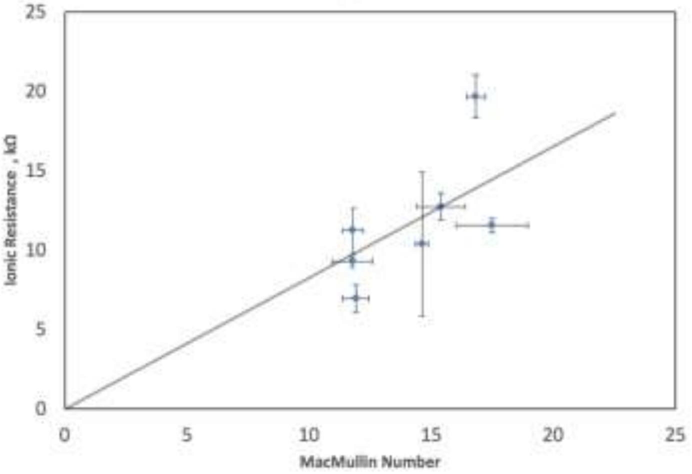

Figure 39. Average MacMullin number versus localized ionic resistance for seven different electrode films.

Patents/Publications/Presentations

Publication

- Pouraghajan, F., H. Knight, M. Wray, B. Mazzeo, R. Subbaraman, J. Christensen, and D. Wheeler. "Quantifying Tortuosity of Porous Li-Ion Battery Electrodes: Comparing Polarization-Interrupt and Blocking-Electrolyte Methods." *Journal of the Electrochemical Society* 165 (2018): A2644–A2653.

Task 3.3 – Understanding and Strategies for Controlled Interfacial Phenomena in Lithium-Ion Batteries and Beyond
(Perla Balbuena and Jorge Seminario, Texas A&M University; Partha Mukherjee, Purdue University)

Project Objective. The project objective is to evaluate and characterize interfacial phenomena in lithiated silicon and Li-metal anodes and to develop guidelines for potential solutions leading to controlled reactivity at electrode/electrolyte interfaces of rechargeable batteries using advanced modeling techniques based on first principles.

Project Impact. Understanding SEI growth on constantly evolving silicon surfaces and on highly reactive Li-metal surfaces is expected to define the electrolyte properties required in high-performance cells. Strategies to control the silicon anode instability and pulverization issues and the well-known safety and short effective lifetimes of Li-metal anodes will be developed by tuning the electrolyte composition, structure, dynamic, and stability, as well as that of the electrode morphology and interactions with the electrolyte, based on multiple characterizations of interfacial phenomena.

Approach. A comprehensive multiscale modeling approach, including first-principles *ab initio* static and dynamics, classical MD, and coarse-grained mesoscopic models, will focus on the roles of the electrolyte's chemical, structural, and dynamical properties and of the electrode micro- and nano- structure on the formation and evolution of the SEI layer and the associated electrochemical performance on silicon and on Li-metal anodes.

Out-Year Goals. Work will progress toward characterizing lithiation and SEI formation at silicon surfaces as well as the subsequent cracking and reforming events under the most realistic modeling conditions. Similarly, the project will investigate electrolyte effects on reactivity and dendrite formation in Li-metal surfaces. The project aims to capture how the chemistry of the various electrolyte components (mainly liquids, but also solid polymers and gels) affects the main issues that influence the electrode performance.

Collaborations. This project funds work at Texas A&M University (TAMU). Prof. G. Somorjai (UC Berkeley), Prof. Shahbazian Yassar (UIC), and Dr. Vijayakumar Murugesan (PNNL) have also contributed to the project.

Milestones

1. Complete analysis of effects of Li-substrate interactions on lithium deposition. (Q1, FY 2018; Completed)
2. Complete study of SEI reactions over lithium deposits. (Q2, FY 2018; Completed)
3. Complete analysis of operating conditions on dendrite growth. (Q3, FY 2018; Completed)
4. Complete evaluation of co-deposition effects. Establish comparisons with experimental trends. (Q4, FY 2018; Completed)

Progress Report

Effects of Sodium and Potassium Substitutions on a Li (100) Surface on Lithium Electrodeposition. DFT analysis was carried out to investigate effects of other metal substitutions on the electrodeposition of lithium cations on a Li-metal slab (100) surface. Substitution of one sodium atom on the top lithium surface was found to be thermodynamically stable. The insertion of a lithium cation in a location surrounding the sodium atom was also favorable, leading to hollow-site adsorption. Various initial configurations were tested, and the results indicated partial reduction of the cation and electron accumulation in the vicinity of the deposited lithium. Comparing the reduction of the lithium cation in the all-Li versus the Na-substituted surface, the reduction in the Na-substituted surface is slightly less favorable. Increasing the sodium concentration on the surface (4 atoms forming a square were substituted out of 16 total surface atoms, a 4-fold increase in sodium surface concentration compared to the initial case), it is found that thermodynamically the lithium cation prefers to be out of the high-Na concentration area. Again, the cation is partially reduced, as found in the case of pure lithium surface. When the complete top lithium layer is substituted by sodium atoms, a decrease of the surface reactivity is clearly detected upon lithium cation deposition. Similar observation was done when the sodium atoms were added, forming a surface defect. The co-deposition of sodium and lithium cations was also investigated, where lithium is preferably reduced to sodium. However, adding one monolayer on top of the sodium monolayer restores the reductive properties of lithium. In another DFT experiment, the ionic concentration on the surface was increased. It was found that the reactivity is largely controlled by increasing the ionic concentration. Potassium was also substituted on the surface, and the substitution was found to be thermodynamically favorable. Similarly to sodium, potassium substitution decreases the surface reactivity. However, the potassium atom is too large to make a smooth monolayer on top of lithium.

Electrolyte and Coating Effects on Lithium Deposition: Shielding Effect of Nonparticipating Cations. Nonuniform Li-ion flux results in heterogeneous lithium electrodeposition, which could lead to dendrite growth. The growth of lithium dendrite is self-enhanced; lithium dendrite grows rapidly through the electrolyte and eventually connects the two electrodes together, resulting in short circuiting. Thus, it is critical to suppress lithium dendrite growth for safe battery operation. One strategy is adding nonparticipating positive ions to the electrolyte. These ions prefer to reside at the dendrite tip, forming a protective layer, which resists the Li-ion approach to the dendrite tip, enabling uniform lithium deposits. To examine this effect, the team developed a mesoscale model, which incorporates lithium electrodeposition on the anode surface and the shielding effect of positive ions. In this model, Li^+ ions transport through the electrolyte and are reduced at the electrolyte-anode interface. To compensate for the lithium consumption, new Li^+ ions are therefore added to the electrolyte domain from the upper boundary. The calculation runs until 3800 lithium atoms are deposited on the electrode substrate. Lithium dendrites form in the center region, and a large Li-ion flux is established in the vicinity of the dendrite tip. This growth accelerates across the cell during deposition. Subsequent analysis illustrates the shielding effect of the nonparticipating cations. Due to the presence of these ions, the strong repulsive forces will prevent Li^+ ions from approaching the dendrite and receiving electrons from the anode. As a result, Li^+ ions are driven to other regions and react with the anode. In this study, three cases are taken into account. The dendrite growth rate is reduced to 60%, 30%, and 20% of the original rate, with increased concentration of nonparticipating ions. It can be seen that as the dendrite growth rate is reduced, the dendrite height is significantly reduced and the deposition thickness of adjacent region becomes larger, indicating a relatively uniform electrodeposition. Thus, suppression of lithium dendrite growth can be achieved by reducing lithium dendrite growth kinetic, such as adding positive ions. The addition of nonparticipating cations results in the reduction of ionic transport near the protrusion on Li-metal anode. It was inferred that Li^+ transport away from the dendrite due to electrostatic shielding results in reduced current density at the dendrite, inhibiting its growth.

SEI Layer Formation Near Nucleation of Dendrites. New MD simulations using reactive force fields are carried out to investigate the initial stages of SEI formation near the sites of dendrite nucleation (showed in the previous report). Work is in progress and will be detailed in the next report.

Patents/Publications/Presentations

Publications

- Qin, X., M. Shao, and P. B. Balbuena. "Elucidating Mechanisms of Li Plating on Li Anodes of Lithium-Based Batteries." *Electrochimica Acta* 264 (2018): 485–494.
- Tewari, D., Z. Liu, P. B. Balbuena, and P. P. Mukherjee. "Mesoscale Understanding of Lithium Electrodeposition for Intercalation Electrodes." *Journal of Physical Chemistry C* 122, no. 37 (2018): 21097–21107.
- Han, J., and P. B Balbuena. "First-Principles Calculations of Oxidation Potentials of Electrolytes in Lithium-Sulfur Batteries and Their Variations with Changes in Environment." *Physical Chemistry Chemical Physics* 20 (2018): 18811–18827.
- Hao, F., A. Verma, and P. P. Mukherjee. "Mesoscale Complexations in Lithium Electrodeposition." *ACS Applied Materials & Interfaces* 10 (2018): 26320.
- Hao, F., A. Verma, and P. P. Mukherjee. "Mechanistic Insight into Dendrite-SEI Interactions for Lithium Metal Electrodes." *Journal of Materials Chemistry A*. doi: 10.1039/C8TA07997H (2018).
- Galvez-Aranda, D. E., A. Varma, K. Hankins, J. M. Seminario, P. P. Mukherjee, and P. B. Balbuena. "Chemical and Mechanical Degradation and Mitigation Strategies for Si Anodes: Multiscale Modeling." *Journal of Power Sources*. Under review.

Presentations

- NREL, Denver, Colorado (June 26, 2018): "Addressing Main Issues of Lithium-Sulfur Batteries"; P. B. Balbuena.
- NREL, Denver, Colorado (June 26, 2018): "Solid Electrolyte Interphase Cracking and Dendrite Formation in Silicon Anodes of a Li-Ion Nanobattery"; J. M. Seminario.
- Beyond Lithium Ion XI (July 25, 2018): "First Principles Analysis of Interfacial Stability of Solid-State Electrolytes at the Lithium-Metal Anode Surface"; P. B. Balbuena. Invited.
- Battery500 Seedling Projects Meeting Review (August 1, 2018): "Identification of Efficient and Stable Solid-Solid Electrochemical Interfaces for Li-S Batteries"; P. B. Balbuena.
- 69th Annual Meeting of the International Society of Electrochemistry (ISE), Bologna, Italy (September 6, 2018): "Molecular Dynamics Simulations of Solid Electrolytes for Li-Ion NanoBatteries"; J. M. Seminario.
- BMR Li-S Deep Dive Meeting, Austin, Texas (September 5, 2018): "Update on Li/S Batteries"; P. B. Balbuena.
- BMR Modeling Meeting, ANL, Chicago, Illinois (September 25, 2018): "Understanding and Strategies for Controlled Interfacial Phenomena in Li-Ion Batteries and Beyond"; P. B. Balbuena, J. M. Seminario, and P. Mukherjee.

Task 3.4 – Electrode Materials Design and Failure Prediction
(Venkat Srinivasan, Argonne National Laboratory)

Project Objective. The project goal is to develop a continuum-based mathematical model to (i) investigate the impact of SEI layer on the growth of dendritic protrusions, and (ii) elucidate the deposition mechanism and deposit morphology observed on top of the carbon substrate in Li-S battery cathodes. Mechanical stiffness and transport mechanism of lithium through the SEI layer can significantly affect the nucleation of dendritic protrusions on top of Li-metal anodes. Effectiveness of protective layers in preventing the growth of lithium dendrites can also be studied by using this methodology. Next-generation, high-energy-density Li-S batteries experience limited capacity due to cathode surface passivation because of the precipitation of Li-sulfides during the discharge process. Understanding the morphology of precipitates can significantly help to develop strategies that can minimize the surface passivation and improve the practical specific capacity of Li-S batteries. The main focus will be to develop microscale models capable of successfully capturing the multiscale multiphysics phenomena that occur during Li-metal and Li-sulfide deposition processes.

Project Impact. Based on the work conducted as part of this project, better understanding of the different mechanisms responsible for degradation in Li-metal anodes and Li-S batteries can be developed. Based on these understandings, different strategies can be devised to minimize the impact of degradation mechanisms and enhance the performance and lifetime of next-generation Li-ion batteries.

Project Approach. The approach used here is to develop mesoscale models, based on continuum modeling, to describe the critical processes in the materials and combining them with electrochemical, microscopic, and spectroscopic data to ensure parameter estimation and model validation. The model is then used to provide insights on the impact of material properties on performance and life, and guidance for design of new materials.

Out-Year Goals. At the end of this project, mathematical models will be developed that can capture the impact of diffusivity, conductivity, transference number, solubility, and mechanical stiffness of various species on the morphology of lithium and Li-sulfide deposits on top of Li-metal and carbon substrates, respectively.

Collaborations. This project has no collaborations this period.

Milestones

Incorporate SEI Layer in Li-Metal Dendrite Model

1. Incorporate SEI layer in lithium dendrite growth model and analyze its influence on growth of dendritic protrusions. (Q1, December 31, 2017; Completed)
2. Evaluate the impact of mechanical properties and thickness of SEI layer on propensity for dendrite growth. (Q2, March 31, 2018; Completed)

Mathematical Model for Sulfur Redistribution

3. Develop a model to examine the precipitation process of lithium sulfide during battery discharge. (Q3, June 30, 2018; Completed)
4. Develop a mathematical model to describe surface morphology evolution in sulfur cathode. (Q4, September 30, 2018; In progress)

Progress Report

Develop a Mathematical Model to Describe Surface Morphology Evolution in Sulfur Cathode. During the discharge of Li-S batteries, surface passivation of carbon cathode due to the deposition of lithium sulfide (Li_2S) is considered to be a major bottleneck preventing the realization of large capacity. Extremely low electronic conductivity of Li_2S films (~10^{-13} S/m) increases the polarization loss as the carbon cathode surface gets covered by the precipitate, and the cell experiences a premature end of discharge. Last quarter, a phase-field-based computational model was developed for capturing the precipitation and dissolution of Li_2S during discharge and charge process. According to the developed phase-field model, Li_2S precipitates form due to the reaction between Li^+ cations and S_2^{2-} anions. Since S_2^{2-} gets generated through the reduction of S_4^{2-}, the concentration of S_2^{2-} should depend strongly on the concentration of S_4^{2-}, or its solubility. Figure 40 demonstrates the impact of S_4^{2-} solubility on the evolution of Li_2S film thickness during discharge and charge processes. During discharge, decreasing the solubility of S_4^{2-} helps to delay the surface passivation by precipitation of Li_2S film. Similarly, lower solubility of S_4^{2-} slows down the dissolution process during charge.

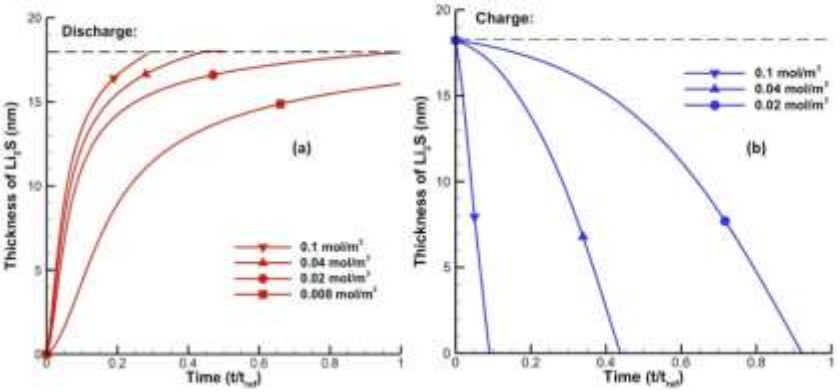

Figure 40. Effect of the S_4^{2-} solubility on the evolution of Li_2S film thickness on top of carbon substrate. (left) During discharge, decreasing the solubility of S_4^{2-} helps to delay surface passivation. (right) Similarly, at the time of charge, decreasing S_4^{2-} solubility slows down the dissolution of Li_2S film.

In collaboration with Partha Mukherjee and his group (Purdue University), the impact of pore size distribution, that is, a range of curvatures, on the Li_2S precipitation process has been investigated. A spontaneous direction for change is the one that lowers down total free energy, which depends on the curvature related interfacial energy. Such complexations change the equilibrium (that is, solubility) for different curvatures (Figure 41, left). A particulate structure (Figure 41, right) has a positive curvature, while a sponge like porous structure has a negative curvature. For a positive curvature structure, further precipitation increases the interfacial area (and energy) and makes it less favorable. This reflects as increased solubility (Figure 41, left) and reduced rate of precipitation (Figure 41, right). A negative curvature structure experiences reduction in interfacial energy upon precipitation, and deposition becomes more spontaneous. Understanding the effect of surface morphology on the precipitation of Li_2S successfully completes the milestone for the fourth quarter.

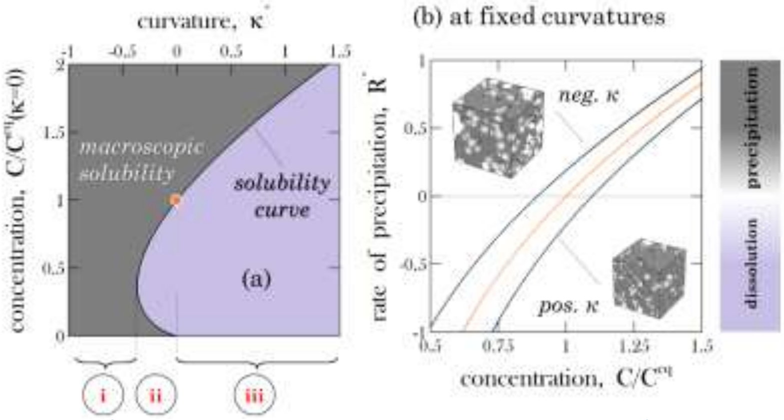

Figure 41. Curvature alters the precipitation–dissolution process. (left) Phase-map identifying equilibrium solubility as a function of curvature. Positive curvature helps increase solubility. (right) Curvature also alters rates for precipitation-dissolution reaction. Positive curvature slows the rate of precipitation.

Patents/Publications/Presentations

Publication

- Barai, P., K. Higa, and V. Srinivasan. "Impact of External Pressure and Electrolyte Transport Properties on Lithium Dendrite Growth." *Journal of the Electrochemical Society* 165, no. 11 (2018): A2654–A2666.

Task 3.5 – First-Principles Calculations of Existing and Novel Electrode Materials (Gerbrand Ceder, Lawrence Berkeley National Laboratory)

Project Objective. The main project objectives are as follows: (1) develop very high-capacity, layered cathodes with high structural stability (> 250 mAh/g) and high surface stability; (2) clarify the role that Li-excess and cation disorder play in capacity and structural stability; (3) develop predictive modeling of oxygen charge transfer and oxygen loss, and find ways to make oxygen redox beneficial in terms of increase capacity; and (4) develop materials with engineered surface passivation that does not lead to impedance increase.

Project Impact. The project will lead to insight in how Li-excess materials work and ultimately to higher capacity cathode materials for Li-ion batteries. The project will help in the design of high-capacity cathode materials that are tolerant to TM migration.

Approach. Thermodynamic evaluation of the project systems is done using configurational Monte Carlo (MC) simulations, based on a cluster expansion Hamiltonian parametrized on the basis of first-principles DFT calculations. Voltages and intercalation curves are calculated with GGA+U; if highly accurate results are required, hybrid functionals (HSE) are used. Phase diagrams are calculated with the Materials Project infrastructure based on high-throughput computations. Configurational disorder for elevated temperature and off-stoichiometry is modeled with either point defect models (when off-stoichiometry is small) or with the cluster expansion for larger disorder. Compounds were synthesized by mechanochemical ball-milling, and experimental characterization is used to evaluate existing and novel materials.

Out-Year Goals. Future goals include the following: (1) develop higher capacity Li-ion cathode materials, and novel chemistries for higher energy density storage devices, and (2) guide the field in the search for higher energy density Li-ion materials.

Collaborations. This project collaborates with K. Persson (LBNL), C. Grey (Cambridge), G. Chen (LBNL), and B. McCloskey (UC Berkeley).

Milestones

1. Assess, through modeling, the viability of fluorination of disordered-rocksalt cathodes to reduce the oxygen activity. (Q1, FY 2018; Completed)
2. Synthesize one partially fluorinated cathode material and demonstrate fluorination through NMR, TEM, XRD, or other characterization tool. (Q2, FY 2018; Completed)
3. Demonstrate viability of reducing TM valence in Li-excess materials to create higher capacity (for example, use Mn^{2+} or V^{3+} or more Ni^{2+}). (Q3, FY 2018; Completed)
4. Demonstrate capacity > 200 mAh/g in a novel fluorinated disordered rocksalt. (Q4, FY 2018; Completed)

Progress Report

The team synthesized $Li_{1.143}Mn_{0.286}V_{0.572}O_2$ (ST-LMVO), $Li_{1.171}Mn_{0.343}V_{0.486}O_{1.8}F_{0.2}$ (ST-LMVF20), $Li_{1.133}Mn_{0.400}V_{0.467}O_{1.8}F_{0.2}$ (MR-LMVF20) and $Li_{1.23}Mn_{0.255}V_{0.515}O_{1.8}F_{0.2}$ (LR-LMVF20) using high-energy ball-milling in an argon atmosphere. As shown in Figure 42, obtained capacities are lower than theoretical ones. Note that the lithium theoretical capacity is based on the lithium content of each composition, while the TM theoretical capacity is based on the total capacity of the $Mn^{2+/4+}$ and $V^{4+/5+}$ couples. Figure 42 indicates that fluorination increases both lithium and TM theoretical capacity from ST-LMVO to ST-LMVF20. By increasing the TM content from ST-LMVF20 to MR-LMVF20, theoretical capacity becomes lower and leaves the fraction of theoretical capacity obtained unchanged. For the LR-LMVF20 structure, the team can see that the observed capacity becomes much closer to the theoretical value. In general, these trends illustrate that the limit on the performance of these compounds is not related to the accessibility of TM redox. Actually, distribution of lithium site energies in the disordered compounds can explain the observed sub-theoretical capacity.

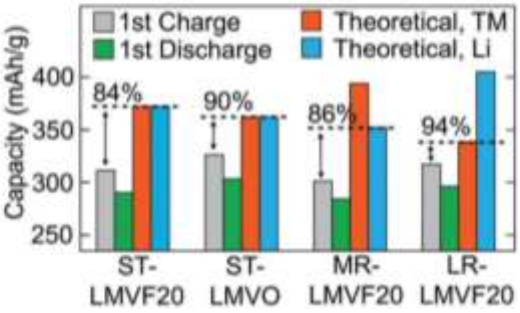

Figure 42. Comparison between observed and theoretical capacities for ST-LMVF20, ST-LMVO, MR-LMVF20, and LR-LMVF20 compounds.

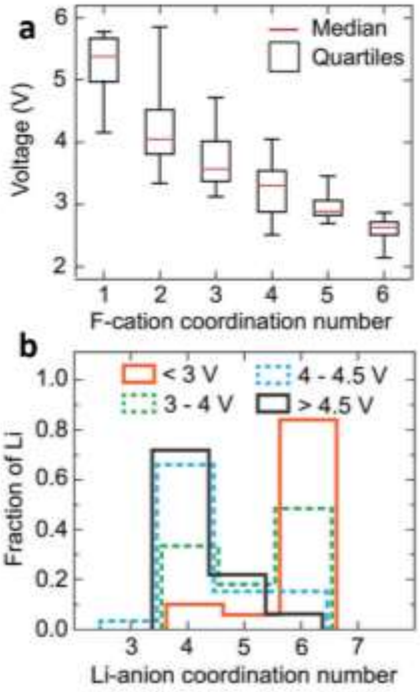

Figure 43. Distribution of (a) F-cation and (b) Li-anion environments by coordination number, among simulated partially charged structures derived from ST-LMVF20, according to the voltage at which they appear.

Figure 43a shows the voltage range over which various fluorine environments, characterized by their F-cation coordination number, appear within the computed, partially delithiated structures obtained from ST-LMVF20. Environments containing fluorine with 1 nearest neighbor nearly always occur above 4.6 V. It shows that for 75% of fluorine sites, the delithiation of a fluorine environment down to 1 remaining nearest neighbor cation needs more than 4.6 V. Fluorine is incorporated into disordered rocksalts at locally Li-rich sites, minimizing the number of high-energy metal–F bonds, while maintaining a sufficiently high entropy to stabilize the dopant in the structure.

Figure 43b shows the Li-anion coordination number as a function of voltage for computed structures obtained from the delithiation of ST-LMVF20. The distribution of Li-anion coordination numbers shows that tetrahedral lithium environments will be formed above 4 V. Above 4.5 V, nearly all lithium remaining in the structure exist in a tetrahedral environment. The formation of tetrahedral lithium is a structural relaxation that can lower the lithium site energy. In conclusion, the gettering effect of fluorine doping and formation of high-voltage tetrahedral lithium are two important mechanisms that can explain the observable lithium capacity within a given voltage window.

Reference: Kitchaev, D. A., Z. Lun, et al. *Energy & Environmental Science* (2018).

Patents/Publications/Presentations

The project has no patents, publications, or presentations to report this quarter.

Task 3.6 – Dendrite Growth Morphology Modeling in Liquid and Solid Electrolytes (Yue Qi, Michigan State University)

Project Objective. The project goal is to develop a validated model to predict lithium dendrite morphology evolution in both liquid and solid electrolytes during electrodeposition and stripping to accelerate the adoption of Li-metal electrodes in current and emerging battery technologies. To achieve this goal, the project has four objectives: (1) formulate a general framework that captures the electrochemical-mechanical driving forces for lithium morphology evolution; (2) consider the role of the nm-thin SEI in liquid electrolytes as well as the microstructures of mm-thick solid electrolytes for lithium morphology evolution; (3) connect micron-scale phase-field models and atomic-scale DFT-based simulations via parameter- and relationship-passing to predict lithium dendrite nucleation and growth kinetics and morphology; and (4) validate the key input parameters and main conclusions of the multi-scale model as new capabilities are being developed step-by-step.

Project Impact. This atomically informed, fully coupled, electrochemical-mechanical dendrite morphology evolution model will allow the project to design the desired properties of artificial SEI coatings, the microstructure of solid electrolyte materials, and the corresponding battery operating conditions, so as to avoid dendrite growth during cycling. It will accelerate design of durable and safe lithium anodes for Li-S, Li-air, and all-solid Li-ion batteries. Thus, it directly impacts emerging technologies, such as Li-S, Li-air, and all-solid Li-ion batteries, which aim to meet the DOE target of the high-energy-density battery cells (> 350 Wh/kg) for EV applications and to push the cost below $\$100/\text{kWh}_{\text{use}}$.

Approach. A multiscale model approach is taken to connect micron-scale phase-field models and atomic-scale DFT-based simulations via parameter- and relationship-passing.

Out-Year Goals. The second-year goal is to establish the model to simulate metallic lithium precipitation in solid electrolytes while further developing the understanding of lithium dendrite growth in liquid electrolytes. To reach this goal, mechanical and electrochemical driving forces for lithium dendrite growth in solid electrolytes will be coupled in phase-field model, while DFT is used to address the lithium plating tendency in various solid electrolyte and coating materials. Validation of the model will come from experiments to correlate the distinctive transport properties of artificial SEI layers with their impact on lithium dendrite morphology.

Collaborations. This project collaborates with UMD, Sandia National Laboratories (SNL), PNNL, University of Arkansas, and University of Houston.

Milestones

1. Compare lithium morphology obtained from experiments and modeling. *Go/No-Go Decision*: Determine if effect of SEI on dendrite growth should be modeled implicitly or explicitly. (Q1, December 30, 2017; *Go*)
2. Identify electronic pathway of lithium dendrite growth inside $Li_7La_3Zr_2O_{12}$ (LLZO). (Q2, March 31, 2018; Completed)
3. Identify Li-ion pathway of lithium dendrite growth inside LLZO. (Q3, June 30, 2018; Completed)
4. Develop multiphase multigrain phase-field model that incorporates mechanical and electrochemical driving forces for lithium dendrite growth in polycrystalline solid electrolyte. (Q4, October 31, 2018; In progress)

Progress Report

Figure 44. Solid electrolyte property map.

Solid Electrolyte. To assess the Li-dendrite resistance in solid electrolyte materials, γ and β Li_3PS_4, c-LLZO and t-LLZO and an ALD LiPON form (Li_2PO_2N) were investigated with DFT calculations. The project's previous studies on the lithium nucleation tendency in the c-LLZO have shown that the surface electronic states in LLZO can be the pathway for electron transport and the traps for excess electrons to nucleate metallic lithium. A literature survey of experimental data on c-LLZO and β–Li_3PS_4 revealed that, despite similar Li-ion conductivity, β-Li_3PS_4 sustained higher current density and areal capacity than c-LLZO, indicating the better Li-dendrite resistance of β-Li_3PS_4. Correlating this observation with all the computed basic material properties, including the shear modulus, fracture energy, bulk band gap, surface band gap, and the reduction potential (Figure 44), it seems the Li-dendrite resistance is mainly determined by the surface band gap (the higher the better). Therefore, Li_2PON_2 is even more resistant to Li-dendrite growth.

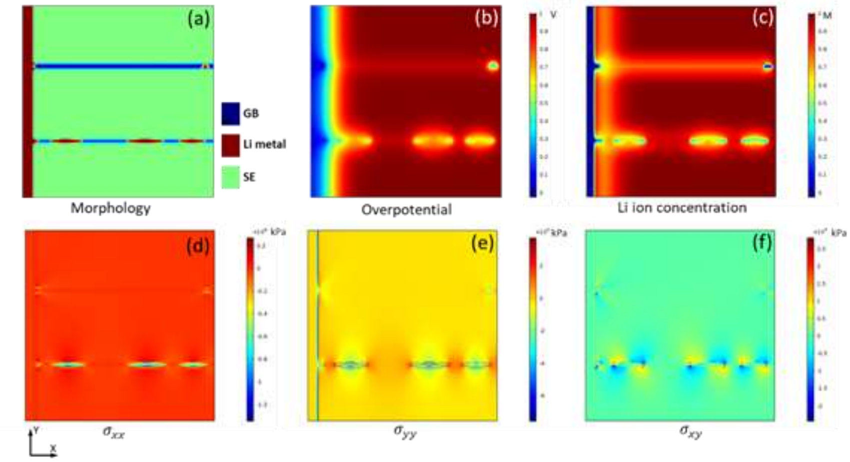

Figure 45. Phase-field simulation results of lithium dendrite growth and nucleation at straight grain boundaries with different widths under constant voltage condition at 100s: (a) Lithium dendrite morphology, (b) overpotential distribution, (c) Li-ion concentration distribution, and (d-f) stress distribution.

The contribution of the surface states to Li-dendrite nucleation and growth needs to be captured in the mesoscale model. The team has formulated the local static electron concentration based on the DOS data calculated from DFT, and then incorporated it into a phase-field model. An explicit nucleation process based on classical nucleation theory was also integrated with the electrochemical-reaction-driven Li-dendrite growth model. The lithium plating process was simulated, and the effect of straight grain boundaries (can also be considered as cracks or pores) was investigated in a solid electrolyte (SE) half-cell system charged under constant voltage (1V) condition, as shown in Figure 45. The dendrite morphology (Figure 45a) demonstrates that isolated lithium dendrite nucleated and grew along the grain boundaries, where the local overpotential (Figure 45b) and Li-ion concentration (Figure 45c) drops due to the formation of lithium metal. The stress distributions (Figure 45d-f) show stress concentration at the Li-metal nucleation tip regions, where large elastic deformation occurs. It also shows higher dendrite nucleation probability and growth rate at narrower grain boundaries due to the higher surface free electron and Li-ion concentration. On the other hand, since Li-metal nucleation and growth at narrow grain boundaries need to overcome larger elastic strain energy barrier compared to the wider grain boundaries, it can be concluded that the electrochemical driving force plays a more dominant role in lithium plating.

Liquid Electrolyte. Sulfur-based electrolyte additive showed improved cyclability, and it was found that the formation of Li_2S in SEI near the Li-metal surface was beneficial.

Patents/Publications/Presentations

Publications

- Cheng, Q., L. Wei, Z. Liu, N. Ni, Z. Sang, B. Zhu, W. Xu, L-Q. Chen, W. Min, and Y. Yang. "*In-Operando*, Three Dimensional, and Simultaneous Visualization of Ion Depletion and Lithium Growth by Stimulated Raman Scattering Microscopy." *Nature Communications* 9 (2018): 2942.
- Li, G., Z. Liu, Q. Huang, Y. Gao, M. Regula, D. Wang, L-Q. Chen, and D. Wang. "Stable Metal Anodes Enabled by Electrokinetic Phenomena." *Nature Energy*. Accepted.
- Liu, Z., P. Lu, Q. Zhang, X. Xiao, Y. Qi, and L.-Q. Chen. "A Bottom-up Formation Mechanism of Solid Electrolyte Interphase (SEI) Revealed by Isotope-Assisted Time-of-Flight Secondary Ion Mass Spectrometry (TOF SIMS)." *Journal of Physical Chemistry Letters* 9 (2018): 5508–5514.
- Li, Y. S., and Y. Qi. "Energy Landscape of the Charge Transfer Reaction at the Complex Li/SEI/Electrolyte Interface." Submitted to *Journal of the American Chemical Society*.
- Z. Liu, Y. Li, Y. Ji, Q. Zhang, X. Xiao, Y. Yao, L.-Q. Chen, and Y. Qi. "Atomically-Informed Phase-Field Modeling of Lithium and Manganese Electrodeposition Morphologies." In preparation.

Presentation

- 256th ACS Meeting, Boston, Massachusetts (August 22, 2018): "Simulation of Lithium Ion Transport through the Complex Electrode/SEI/Electrolyte Interface"; Y. Qi. Invited.

Task 3.7 – First-Principles Modeling and Design of Solid-State Interfaces for the Protection and Use of Lithium-Metal Anodes
(Gerbrand Ceder, UC Berkeley)

Project Objective. The project objective is to determine the design principles that control the solid electrolyte/lithium electrode interfaces by determining the reaction products stemming from pairing solid electrolytes and lithium metal. The project will conduct rigorous analysis based on computing electrolyte phase-diagrams closed and open to lithium. Li-ion transport properties in bulk electrolytes and interfacial products will be assessed through AIMD and nudged elastic band (NEB) calculations. Simultaneously, a robust framework will be developed to identify factors controlling lithium dendrite propagation within solid electrolytes and interfacial products by accounting for irregularities, defects, and grain boundaries, through a model that includes elements of fracture mechanics, thermodynamics, and electrochemistry.

Project Impact. The project will lead to understanding of the complex evolution of lithium metal/SEI during electrochemical cycling. The understanding of this process is necessary to determine design principles to develop reliable all solid-state batteries.

Approach. By incorporating NEB and AIMD methods, high-throughput computation is used to screen candidate solid electrolyte with high electrochemical stability and high ionic conductivity. DFT is used to calculate bulk elastic constants of materials, surface energies, and interface de-cohesion energies of grain boundaries; continuum theory (elastic-plastic-fracture mechanics) is used to assess the resilience of solid electrolytes and grain/particle boundaries toward lithium dendrite growth and propagation. The finite element method is used to couple several physical processes, including electrochemical deposition, ionic diffusion, thermal expansion, and mechanical contacting.

Out-Year Goals. The out-year goals include the following: (1) obtain design criteria for solid electrolytes that can resist unstable lithium propagation by computing elastic properties, surface energies, and decohesion energies, and (2) adapt fracture mechanics models describing crack propagation to lithium dendrite propagation in different scenarios.

Collaborations. There are no collaborative activities this quarter.

Milestones

1. Development of metal-electrolyte electrochemical-mechanical interface model. (Q1, FY 2018; Completed)
2. Stability screening of candidate material for good SSE. (Q2, FY 2018; Completed)
3. Determine critical stress conditions that yield fracture in ceramic electrolytes during lithium deposition. (Q3, FY 2018; Completed)
4. Lithium conductivity screening using AIMD and NEB method to screen for materials with high lithium mobility. (Q4, FY 2018; Completed)

Progress Report

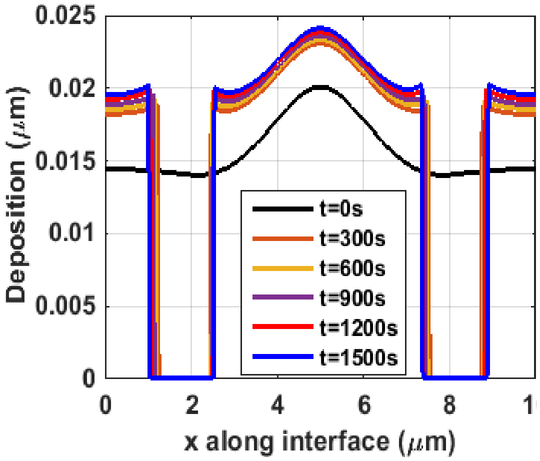

Figure 46. Lithium deposition at Li-metal/SEI at different charging time.

Inhomogeneous Lithium Deposition at Rough Interface. Experimentally, it is observed that the interfacial contact between lithium metal and solid electrolyte (SE) deteriorates during cycling of a solid-state battery (SSB). Inhomogeneous deposition at a rough interface (or defect) is believed to be one of the main reasons for contact loss and for the nucleation and propagation of dendrites in SSB. By using the Finite Element Method, the Li-ion transport in the SE, the electrochemical deposition at Li-metal/SE interface, and the mechanical balance between lithium metal and SE are all coupled together and solved numerically. As shown in Figure 46, Lithium is unevenly deposited along a cosine shape interface. Initially, lithium is plated more at the center of the interface than in other areas. After further deposition at the interface Lithium accumulates at the central area and causes the separation of lithium metal and SE at the low deposition area; The contact loss at the low deposition area causes an increase in current density at the remaining contact area, which causes even larger lithium deposition inhomogeneity. Eventually, more and more contact loss can be observed at the interface (Figure 47).

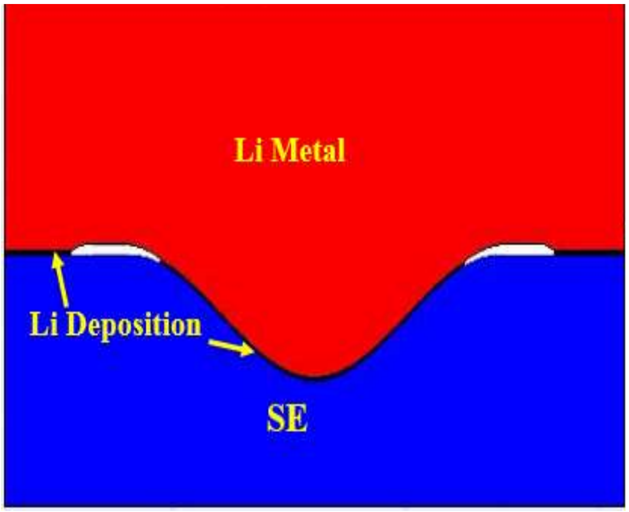

Figure 47. The gap generated at Li-metal/SEI because of inhomogeneous deposition rate.

Loss of Contact Area is Affected by External Pressure and Material Properties. Interfacial contact loss is determined by several factors, including the back-pressure at the cell boundaries during cycling, the material properties of both lithium metal and SE, and the morphology of the interface. A high back-pressure at the boundary can decrease the amount of contact loss. A big enough back pressure can in principle always ensure a perfect interfacial contact during cycling, but too large a back-pressure may also crack the SE and facilitate the growth of dendrites. The project’s study shows that a lower yielding stress of lithium metal can also decrease the amount of contact loss because a softer lithium metal means a higher plastic flow along the Li-metal/SE interface, which can fill in any possible gap generated by the inhomogeneous deposition.

Patents/Publications/Presentations

The project has no patents, publications, or presentations to report this quarter.

Task 3.8 – Large-Scale *Ab Initio* Molecular Dynamics Simulations of Liquid and Solid Electrolytes (Lin-Wang Wang, Lawrence Berkeley National Laboratory)

Project Objective. The project goal is to use large-scale AIMD simulations and other computational approaches to study the discharging mechanism in Li-S battery, especially for polysulfur interaction with liquid electrolyte solvent molecules, and cathode materials, as well as lithium diffusion mechanisms in various systems. The long-term goal is to use such theoretical understanding to provide guidance to develop better electrolyte and cathode systems to overcome the bottlenecks that prevent commercialization of the Li-S battery. One major issue is solvation of Li_2S_n molecules in the electrolyte. The team is working to find the solution to this problem by both understanding the Li_2S_n-electrolyte interaction and discovering better cathode materials for optimal Li_2S_n-cathode binding. Specifically, the team seeks to: (1) develop reliable methods that combine classical force field (CFF) simulations with *ab initio* calculations to study thermal dynamic properties of Li_2S_n in different electrolytes, as well as interactions with different species within the electrolytes; and (2) study Li_2S_n interaction with different cathode materials, especially for 2D cathode materials consisting of light elements in the right-upper corner of the periodic table. The goal is to have sufficient binding energy between the Li_2S_n molecules and the cathode material, so, thermodynamically, the Li_2S_n will not be dissolved in the electrolyte. To study the Li_2S_n-electrolyte interaction, the team needs to accurately calculate the molecule entropy inside the solvent, which is a challenging task. The team plans to combine CFF with *ab initio* calculations for that study. To study Li_2S_n and cathode interaction, the team will calculate the phase diagrams of the systems with different number *n* and will hence obtain the binding energies and voltages at every step of the discharging process.

Project Impact. Making the Li-S battery a commercial reality will have a major impact on society and also help to realize the VTO goal of 500 km per charge for EV. However, the nature of chemical reaction makes it different from the traditional intercalation-based Li-ion battery. The molecular nature of Li_2S_n also allows solvation in the electrolyte. To address these problems, it is essential to have fundamental studies and understandings of the underlying mechanisms. The theoretical simulation can also play an important role in discovering and designing new cathode materials.

Approach. The project uses *ab initio* calculations to study the binding energy of LiS cluster to different substrate. If such binding energy is larger than its dissolution energy, the LiS will be anchored to be substrate and will not be dissolved. Specially designed generated algorithms are used to search for the structures of the amorphous like LiS clusters. The project also developed a special algorithm to study the lithium mobility in such amorphous and disordered systems. The team also plans to use bicanonical MD to calculate the solute free energy in the electrolyte.

Out-Year Goals. In the outgoing years, the team will further develop computational methods for more accurate entropy and interaction energy calculations for the electrolyte. This is a critical capability to study the battery system. The team will also explore different cathode materials and morphologies. In particular, there is a vast space to explore using 2D materials as Li-S battery cathodes and using curved amorphous structures to increase capacity. The key is to investigate all the effects and competitions of different reactions.

Collaborations. The project will collaborate with G. Liu's group for cathode design. It has also collaborated with Prof. F. Pan of Beijing University for lithium battery research in general.

Milestones

1. Set up the Li_2Sn calculation with charge polarization model (CPM) solvent model without explicit solvent molecule. (Q1 2018; Completed)
2. Carry out Li_2S_n/cathode structure calculations using CPM solvent model, with different cathode structures. (Q2 2018; Completed)

3. Continue the Li2S_n calculation with explicit solvent molecules; carry out direct CFF and AIMD simulations. (December 2018; In progress)
4. Continue calculation of Li_2S_n/cathode binding energies and phase diagrams, discovering new adequate cathode materials and morphologies. (Q4; In progress)

Progress Report

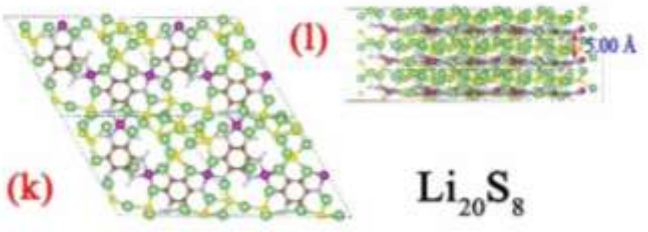

Figure 48. An alternating 2D hexaaminobenzene and Li-S sandwich structure.

The project has continued studying alternating 2D hexaaminobenzene and Li-S layer sandwich structure. This is designed to increase the volumetric energy capacity for such Li-S cathode. One of the structures is shown in Figure 48. The team has optimized the structure and lattice distance for different level of lithiation. They found that when the system is lithiated, the z direction lattice constant can increase by about 7%. One challenge, however, is to calculate the lithium diffusion constant in such a disordered system. This is important to estimate the usability of the system as a Li-S cathode material. The traditional method like the NEB method cannot be used to study the lithium diffusion barrier since the initial and final atomic configurations are not well defined in such a disordered system. The team has developed a lithium pulling method, where a lithium atom is pulled by an external force while an MD simulation is carried out. This will force the lithium to move. By analyzing the energy profile along the path of the lithium, one can estimate the barrier height of the system. The team has tested this approach against different situations. One typical energy profile is shown in Figure 49. In this case, the diffusion barrier is estimated to be 0.58 eV. The team found that the lithium can diffuse along the hole in the perpendicular direction toward the layers, but it is difficult to diffuse along the layers.

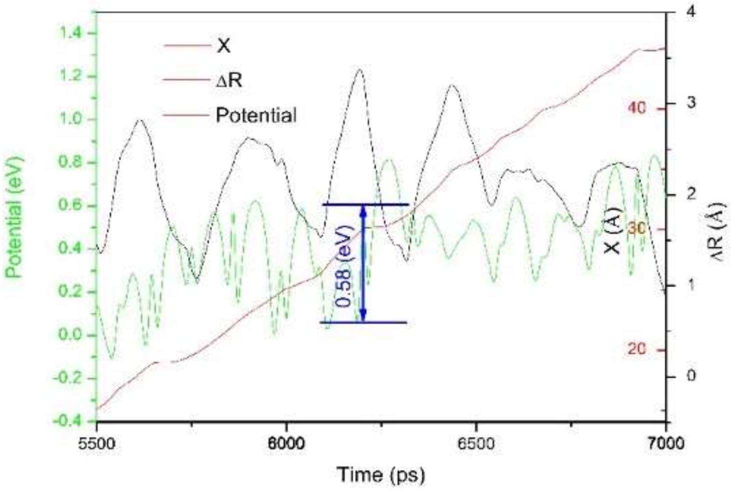

Figure 49. Typical energy profile; diffusion barrier estimated to be 0.58 eV.

The team has also calculated S_n polymer on the gold surface. They found that the gold surface can break the ring of the S_8, and makes it either an open chain or a U-shaped chain with both ends anchored on the gold surface. There is a strong bond between gold and sulfur atoms, stronger than the S-S bond. For example, for the system shown in Figure 50, there are two possible configurations: one is that the 40 S form 5 S_8 rings, and another is that the 40 S form a long chain, with both of its ends bound to the gold (111) hollow site. The single chain is denoted by the green color. The long chain case is about 1 eV lower in energy than the 5 S_8 ring case. When lithium is added to the system, the lithium tends to bind to one end of S-chain, while the other end binds to gold. This is a model system to study what happens when sulfur is bound to the metal surface. Note that, for aluminum, due to the existence of a thin layer of Al_2O_3, there is no strong bonding between S and the substrate. The team likes to study the anchoring of the S chain to the substrate, and gold is one clean system for such study.

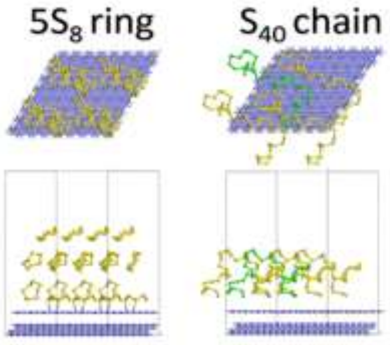

Figure 50. Two possible configurations. (left) 5 S_8 ring. (right) S_{40} chain (green color).

Patents/Publications/Presentations

Publications

- Yang, L., J. Zheng, M. Xu, Z. Zhuo, W. Yang, L.W. Wang, L. Dai, J. Lu, K. Amine, and F. Pan. “Short Hydrogen Bonds on Reconstructed Nanocrystal Surface Enhance Oxygen Evolution Activity.” ACS *Catalysis* 8 (2018): 466.
- Duan, Y., B. Zhang, J. Zheng, J. Hu, J. Wen, D. J. Miller, P. Yan, T. Liu, H. Guo, W. Li, X. Song, Z. Zhuo, C. Liu, H. Tang, R. Tan, Z. Chen, Y. Ren, Y. Lin, W. Yang, C. M. Wang, L. W. Wang, J. Lu, K. Amine, and F. Pan. “Excess Li-Ion Storage on Nanocrystal Reconstructed Surface to Boost Battery Performance.” *Nano Letters* 17 (2017): 6018.
- Wu, J., and L. W. Wang. “2D Frameworks C2N as a Potential Cathode for Lithium Sulfur Batteries: An *Ab Initio* Density Functional Study.” *Journal of Materials Chemistry A* 6 (2018): 2984.
- Li, Y., F. Ma, and L. W. Wang. “Phosphorene Oxides as Promising Cathode Material for Sealed Non-Aqueous Li-Oxygen Battery.” *Journal of Materials Chemistry A* 6 (2018): 7815.
- Gao, G., F. Zheng, F. Pan, and L. W. Wang. “Theoretical Investigation of 2D Conductive Microporous Coordination Polymers as Li-S Battery Cathode with Ultrahigh Energy Density.” *Advanced Energy Materials* 8 (2018): 1801823.

Task 3.9 – *In Operando* Thermal Diagnostics of Electrochemical Cells (Ravi Prasher, Lawrence Berkeley National Laboratory)

Project Objective. Effective heat dissipation in batteries is important for multiple reasons including performance, reliability, and safety. Currently, the thermal management of battery cells is provided at the system level by either forced air or liquid cooling, leading to reduced system-level energy densities and more failure-prone complex system designs. Furthermore, even given theoretically infinite system-level cooling applied to the external battery surface, peak temperature rise within a cell would still easily exceed acceptable threshold values due to the poor thermal transport properties within the cell itself. It has not yet been possible to thermally profile a real cell during operation to provide a spatially resolved map of heat transfer properties throughout the cell. The objective of this research is to create a metrology capable of spatially resolved *in operando* thermal property profiling, and then use this tool to reveal the largest thermal bottlenecks within a functioning Li-ion cell and create a complete materials-level cell thermal model.

Project Impact. The intrinsic thermal resistance of Li-ion cells is currently far higher than the theoretical value predicted by simply combining the known thermal properties of each macro component into an appropriate thermal model. The spatially resolved thermal transport property measurements from this project will reveal what key piece of information is missing. Preliminary data suggest that more than 75% of the total battery thermal resistance may be due to a single interface between the cathode and separator, previously unknown. An accurate understanding of the cell internal thermal transport is necessary to successfully optimize cell thermal performance to meet the challenges of extremely fast charging, mitigating thermal runaway, and improving battery performance, reliability, and safety.

Approach. To accomplish the project goals, the team will utilize two state-of-the-art thermal metrology techniques. They will build an in-house adapted 3ω technique to measure thermal transport properties throughout the bulk of a Li-ion cell while it is in operation, without affecting the operation of the cell. The 3ω system will work by using mm-scale sensors on the electrode current collectors to send variable-frequency thermal waves into the operational battery to quantitatively measure heat transport through different layers and interfaces. The team will also use the ultrafast optical time domain thermoreflectance (TDTR) technique to measure nanoscale thermal transport properties of constituent components of the cathode composite. They will then combine these results to create an “all-scale” accurate thermal model of the cell that—unlike existing models—agrees with the empirical measurements of cell thermal performance.

Out-Year Goals. In outgoing years, the project will design, build, and implement the adapted 3ω metrology. This will involve developing and testing the metrology itself along with accompanying theory, designing compatible battery samples, and finally applying the technique to live cells. The team will use the already built TDTR system at LBNL to measure epitaxially grown cathode materials provided by collaborators. Combined, this will provide enough data to construct and validate a realistic all-scale thermal model of the battery.

Collaborations. This project collaborates with two LBNL groups: V. Battaglia’s for cell assembly for 3-Omega studies, and R. Kostecki’s for pristine battery active material growths for TDTR studies.

Milestones

1. TDTR measurements of ideal battery samples. (Q1, FY 2018; Completed)
2. 3-Omega sensing and heating lines fabricated, and metrology developed. (Q2, FY 2018; Completed)
3. Electrochemical cells with 3-Omega sensors integrated on the electrodes. (Q3, FY 2018; Completed)
4. *Go/No-Go Decision*: Baseline *in operando* thermal diagnostics and measurement with 3-Omega technique performed. (Q4, FY 2018; On schedule)

Progress Report

The team has successfully performed a baseline *in operando* thermal measurement with the 3-Omega technique. The sample is a full Li-ion battery pouch cell, as shown in Figure 51a. The 3-Omega sensors are attached to the cathode side of the battery. During the *in operando* measurement, the battery is being used to power a green LED. The 3-Omega measurement is performed using the sensors' electrical connector shown plugged into the breadboard. The raw data from the measurement is shown in Figure 51b. Initial *operando* measurement attempts failed, as the electrolyte dissolved the insulation and Kapton tape adhesive used within the battery. The team made a new sample using polyethylene foam and "Torr Seal" epoxy instead as insulation. This new version survived the electrolyte, and the team was able to successfully perform *operando* measurements for extended periods of time. They have also extended the minimum possible frequency of measurements from 0.5 Hz down to 0.02 Hz. This significantly increases the frequency range and allows for more deeply penetrating low-frequency thermal waves to better probe all layers in the battery, especially those farthest from the sensor. There are still some noisy points at specific frequencies; however, this is of minimal impact to the overall measurement. For future *operando* measurements, the battery will be connected to a battery cycler so that the team can have more control over the charging and discharging dynamics and perform measurements under different states of charge.

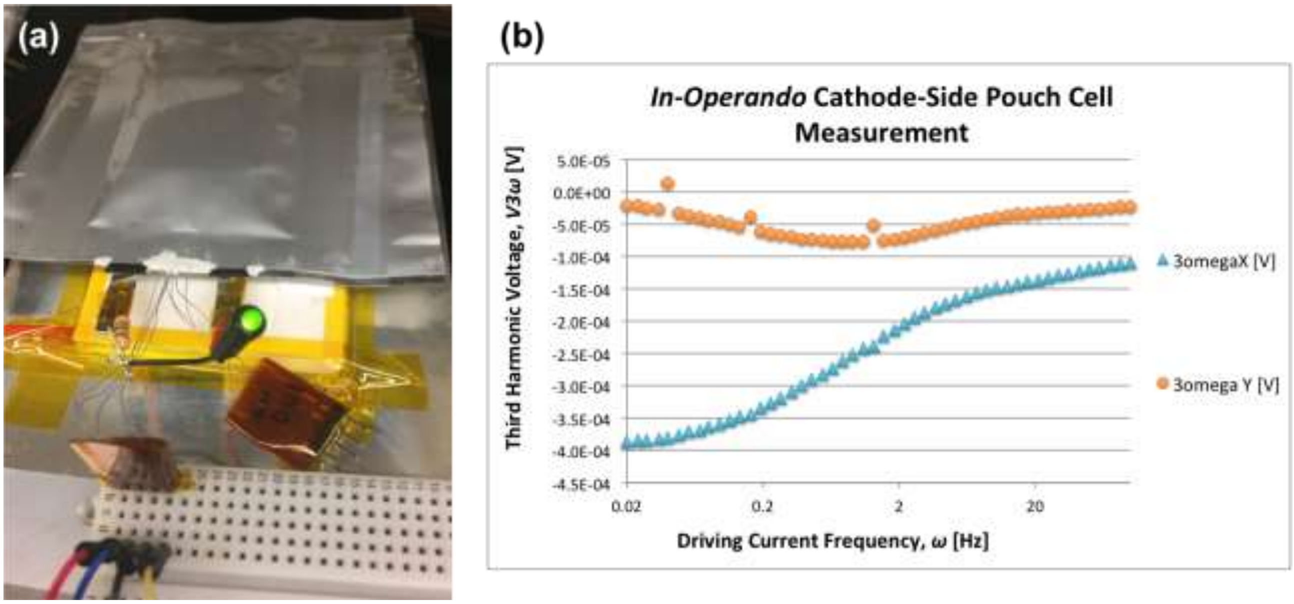

Figure 51. Baseline *in operando* measurement of battery. (a) Battery pouch cell powering LED during 3-Omega measurements. (b) 3-Omega data from the measurement.

Patents/Publications/Presentations

Presentation

- This work was presented at the ASME 2018 International Technical Conference and Exhibition on Packaging and Integration of Electronic and Photonic Microsystems (InterPACK2018).

Task 3.10 – Multi-Scale Modeling of Solid-State Electrolytes for Next-Generation Lithium Batteries (Anh Ngo, Larry A. Curtiss, and Venkat Srinivasan, Argonne National Laboratory)

Project Objective. This project is part of a multi-scale modeling effort to obtain an in-depth understanding of the interaction of the electrode and the solid electrolyte aimed at developing highly efficient SSE batteries for vehicle applications. Input parameters needed for mesoscale (continuum) level calculations are being obtained from atomistic calculations including DFT and classical MD simulations. This atomistic input will enable a multi-scale computational procedure for SSEs that is capable of successfully capturing the physicochemical aspects during charge and discharge process including lithium transport mechanisms, interfacial phenomena during the insertion and extraction of lithium ions, and mechanical deformation of SSE.

Project Impact. A major safety concern experienced with commercially available Li-ion batteries under some scenarios is leakage of the liquid electrolyte, which can potentially catch fire. Replacement of the liquid electrolyte is necessary to decrease the fire hazard and improve safety associated with present-day Li-ion batteries. In addition, use of solid electrolytes provides a path to prevent dendrites in Li-metal anodes, thereby leading to batteries with significantly higher energy density. The impact of this project will be to help in development of good SSEs as a replacement for the commercially used organic liquid electrolytes to improve safety and energy density in Li-ion batteries.

Approach. Parameters needed for mesoscale modeling of grain-interior, grain-boundary, and electrode-electrolyte interface will be calculated by DFT-based calculations along with MC and MD simulations. The calculations will be used to determine properties of the electrode with the solid electrolyte as well as in grain-boundary regions of the solid electrolyte. This will include calculations of structure, stability, ionic conductivity, Young's modulus, fracture toughness, exchange current density, and other properties.

Out-Year Goals. The out-year goals of this work are to calculate other properties such as fracture toughness and include other SSEs and coatings in the multi-scale modeling.

Collaborations. This project collaborates with V. Srinivasan at ANL.

Milestones

1. AIMD of the interface structure of the LLZO solid electrolyte lithium anode and MC simulations of LLZO grain boundaries. (Q2, FY 2018; Completed)
2. Calculations of Young's modulus at grain-interior and grain-boundary region for LLZO solid electrolytes. (Q3, FY 2018; Completed)
3. Calculations of exchange current density at the electrode-electrolyte interface. (Q4, FY 2018; Initiated)

Progress Report

The use of lithium metal in Li-ion batteries requires protection of the lithium surface, such as by a ceramic solid electrolyte to prevent propagation of lithium dendrites that can cause safety problems and capacity fade. Multi-scale modeling of SSEs can provide insight into the mechanism for dendrite growth and other instabilities for guidance on how to improve performance. At the mesoscale (continuum) level of modeling, atomistic-level input is required from theory or experiment to accurately capture physicochemical aspects during charge and discharge processes of a Li-ion battery with a SSE. One of these inputs is the Young's modulus, which is a fundamental property of every material and is important in batteries material research. This constant can provide information as to when a structure will deform.

In this work, the Young's modulus was calculated for bulk regions of LLZO and its grain boundaries. The atomic structure/stoichiometry of LLZO grain boundaries was previously established by MC simulations using about 35,000 atoms. The MC calculations provided the structures of four low-angle grain boundaries [Σ_3(112), Σ_5(210), Σ_5(310), Σ_9(221)]. This quarter, the team used these results to carry out MD simulations with the LAMMPS code and soft bond-valence potentials. About 1,720,000 atoms were used for LLZO to calculate the Young's modulus. The Young's modulus, *E*, can be calculated from tensile stress-strain graphs in the linear regime. The slope of the graph is used to calculate *E* when the material obeys Hooke's law. The team divided it into contributions from the bulk region of the simulation cell and grain-boundary region. The team has strained LLZO in each direction, and a summary of the results is given in Figure 52 for bulk and the Σ_3(112) grain boundary. A linear fit gave an average value of Young's modulus *E*=138 GPa for bulk LLZO and E=117 GPa for the Σ_3(112) grain boundary.

Young's modulus provides an estimation of the deformability of any solid material. This parameter helps to estimate the evolution of stress within solids subjected to a certain amount of deformation. Since ceramic-based SSEs are very stiff, the magnitude of their Young's modulus is also very high (approximately 10- to 15-times larger than that of lithium). Due to lithium deposition, a small amount of deformation at the electrode-electrolyte interface can lead to development of compressive stress, which can significantly impact the state of the electrochemical potential observed at the lithium/ceramic-electrolyte interface. Since evolution of mechanical stress, and effectively Young's modulus, directly affects the overpotential observed during the lithium deposition process, it is very important to estimate the exact magnitude of Young's modulus for the ceramic SSEs for use in multi-scale modeling. Differences in Young's moduli between the bulk and grain boundary of electrolyte can also impact the reaction current observed in each of the phases.

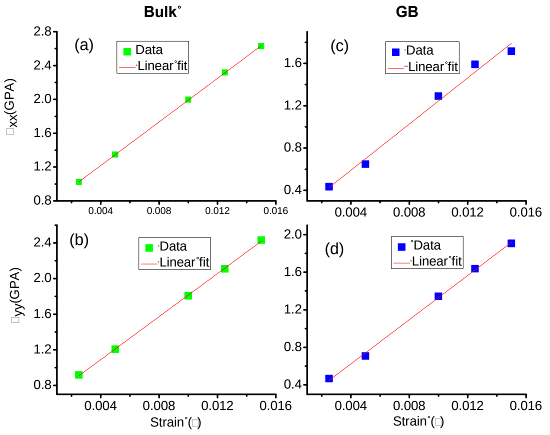

Figure 52. The x, y components of the Young's modulus obtained from the project's model. (a) and (b) are for the bulk region, while (c) and (d) are for grain boundary regions of the Σ_3(112) grain boundary.

Patents/Publications/Presentations

The project has no patents, publications, or presentations to report this quarter.

TASK 4 – METALLIC LITHIUM

Summary and Highlights

The use of a metallic lithium anode is required for advanced battery chemistries like Li-ion, Li-air, and Li-S to realize dramatic improvements in energy density, vehicle range, cost requirements, and safety. However, the use of metallic lithium with liquid and polymer electrolytes has so far been limited due to parasitic SEI reactions and dendrite formation. Adding excess lithium to compensate for such losses effectively negates the high energy density for lithium in the first place. For a long lifetime and safe anode, it is essential that no lithium capacity is lost either (1) to physical isolation from roughening, dendrites, or delamination processes, or (2) to chemical isolation from side reactions. The key risk/limitation for this technology is the gradual loss of lithium over the cycle life of the battery.

The BMR, Battery500, and other DOE programs are addressing this challenge with many innovative and diverse approaches. Key to all is the need for a much deeper analysis of the degradation processes and new strategies to maintain a dense, fully connected lithium and a dendrite-free electrolyte so that materials can be engineered to fulfill target performance metrics for EV application, namely 1000 cycles and a 15-year lifetime, with adequate pulse power. Projecting the performance required in terms of just the lithium anode, this requires a high rate of lithium deposition and stripping reactions, specifically about 30 μm of lithium per cycle, with pulse rates up to 10 and 20 nm/s (15mA/cm^2) charge and discharge, respectively, with little or no excess lithium inventory. This is daunting in the total mass and rate of material transport that must be achieved without failures.

The efficient and safe use of metallic lithium for rechargeable batteries is then a great challenge, and one that has eluded R&D efforts for years. This Task takes a broad look at this challenge for both solid-state batteries and batteries continuing to use liquid electrolytes. For the liquid electrolyte batteries, steady improvement has been realized by PNNL researchers through use of dual lithium salts and organic additives to the typical organic solvent electrolytes to impede lithium corrosion and roughening. Now, MIT is investigating halide and other additives to form self-healing SEI coatings. Engineered coating and 3D-anode structures continue to offer promising results. These include application of various 2D coating materials under investigation at Stanford University and use of 3D-copper-foam structures at University of Pittsburgh. An increasing number of programs are turning to various composites of polymer and ceramic electrolytes to address mechanical and ion transport challenges. ORNL is continuing investigation of spray-coated composite polymer electrolytes, while UT Austin and PNNL are also initiating work in this direction. A breakthrough is needed to promote facile Li-ion transport between the ceramic and organic polymer or liquid electrolytes. Two highly successful programs using ceramic solid electrolytes, specifically the LLZO garnets, were completed. Both demonstrated a great decrease in the area specific resistance (ASR) of the garnet-Li interface, reaching values of just a few ohms. This was accomplished variously using coating to promote wetting, treatments to ensure the surface is free of flaws and contamination, or higher interface areas to decrease the current density. As the ASR decreased, the interface adhesion and the critical current density achievable without forming Li-metal shorts increased. Fundamental aspects of this work on inorganic solid electrolytes are being continued by ANL researchers and others. The last project is focused on the properties of lithium metal itself. Past work using nanoindentation showed that lithium plating under high currents can exert large stresses at the lithium SEI. Following this, ORNL with Michigan Technological University and University of Michigan will initiate work to create lithium stability maps to understand conditions where the lithium morphology becomes difficult to control. Each of these projects involves a collaborative team of experts with the skills needed to address the challenging materials studies of this dynamic electrochemical system.

Highlights. Promising Li-metal cycling was reported using electrolytes of typical organic salt solutions, high concentrated solutions, ceramic-gel composites, and pure dense ceramic and glass electrolytes. It is shown how using thin (20 µm) lithium as one contact can provide a more accurate and rapid assessment of the lithium stability. Several programs also report on the lithium plating reactions.

For the Solid Electrolyte Systems:

- For the LLZO ceramic, DFT calculations predict that niobium is more likely to substitute on zirconium sites near the surface or lithium interface, whereas tantalum is uniformly distributed surface to bulk. This explains why Nb-doped LLZO is more reactive.
- Indentation studies of glassy LiPON electrolyte film will creep under stress. The stress exponent is consistent with viscous flow.
- Dry composite solid electrolytes with a high volume fraction of the ceramic phase show stable cycling when the cathode is also a dry polymer $LiFePO_4$ composite.

Several New Quasi-Solid Electrolyte Systems are Under Investigation:

- A ceramic composite filled with a plasticized polymer gel provides high conductivity of 0.1 mS/cm.
- A hybrid “polymer-in-salt” composite electrolyte with 1 mS/cm conductivity appears stable for lithium metal versus NMC-333 battery cycling.

For Liquid Electrolyte System:

- Concentrated solution, 4 M LiFSI in DME, used with graphene surface coatings demonstrate extended lithium cycling. The coating included wrinkled graphene cage (WGC) and reduced graphene oxide (rGO) containing silicon nanoparticles.
- Suitable current collectors of metals that form lithium alloys can provide zero or minimal nucleation barriers (that is, zero nucleation underpotential) for Li-metal plating.
- Methods to more accurately quantify CE for lithium cycling utilize very thin 20-µm lithium on copper foil for one of the electrodes. This is cycled to a fixed capacity versus thick lithium or an LCO cathode until the small excess lithium is consumed by side reaction or dendrite formation.

Considering the Properties of Lithium Metal:

- The flux of lithium as controlled by diffusion of lattice vacancies may be slower in the metallic lithium than in the ceramic LLZO at high current density. In this case, Li^+ may be forced to plate on already occupied sites leading to “hot-spots.”

Task 4.1 – Lithium Dendrite Prevention for Lithium Batteries (Wu Xu and Ji-Guang Zhang, Pacific Northwest National Laboratory)

Project Objective. The project objective is to enable lithium metal to be used as an effective anode in rechargeable Li-metal batteries for long cycle life at a reasonably high current density. The investigation in FY 2018 will focus on effects of various lithium salt mixtures, inorganic fillers and polymer types on ionic conductivity, lithium CE, Li-anode morphology, and battery performances in terms of long-term cycling stability at room temperature and elevated temperatures and at various current density conditions, rate capability, and low-temperature discharge behavior. The compatibility of such electrolytes with 4-V NMC cathode will be investigated.

Project Impact. Lithium metal is an ideal anode material for rechargeable batteries. Unfortunately, uncontrollable dendritic lithium growth and limited CE during repeated lithium stripping/deposition processes have prevented their practical applications. This work will explore the new hybrid composite electrolytes that can lead to dendrite-free lithium deposition with high CE. The success of this work will increase energy density of Li-metal and Li-ion batteries and accelerate market acceptance of EVs, especially for PHEVs as required by the EV Everywhere Grand Challenge.

Approach. By using some facile cost-effective methods, the exploration and development of new liquid electrolytes, additives, and composite polymer electrolytes with high stability against Li-metal anode and good electrochemical stability will be conducted to further push forward development of high-energy-density rechargeable Li-metal batteries with conventional intercalation cathode materials.

Out-Year Goals. The long-term goal of the proposed work is to enable lithium and Li-ion batteries with > 120 Wh/kg (for PHEVs), 1000 deep-discharge cycles, 10-year calendar life, improved abuse tolerance, and less than 20% capacity fade over a 10-year period.

Collaborations. This project collaborates with C. Wang, PNNL, on characterization by TEM/SEM; B. Polzin, ANL, on electrodes sampling; and H. Xiang, Hefei University of Technology, on LiDFP additive study.

Milestones

1. Develop a lithium salt mixture that has an ambient melting temperature and an ionic conductivity over 1 mS/cm. (Q1, December 31, 2017; Completed)
2. Investigate effects of inorganic fillers and polymers on hybrid composite electrolytes. (Q2, March 31, 2018; Completed)
3. Develop an inorganic/polymeric hybrid composite electrolyte with ionic conductivity over 1 mS/cm and lithium CE over 99%. (Q3, June 30, 2018; Completed)
4. Achieve over 300 cycles for 4-V Li||NMC batteries with ~ 2 mAh/cm^2 cathode loading. (Q4, September 30, 2018; Ongoing)

Progress Report

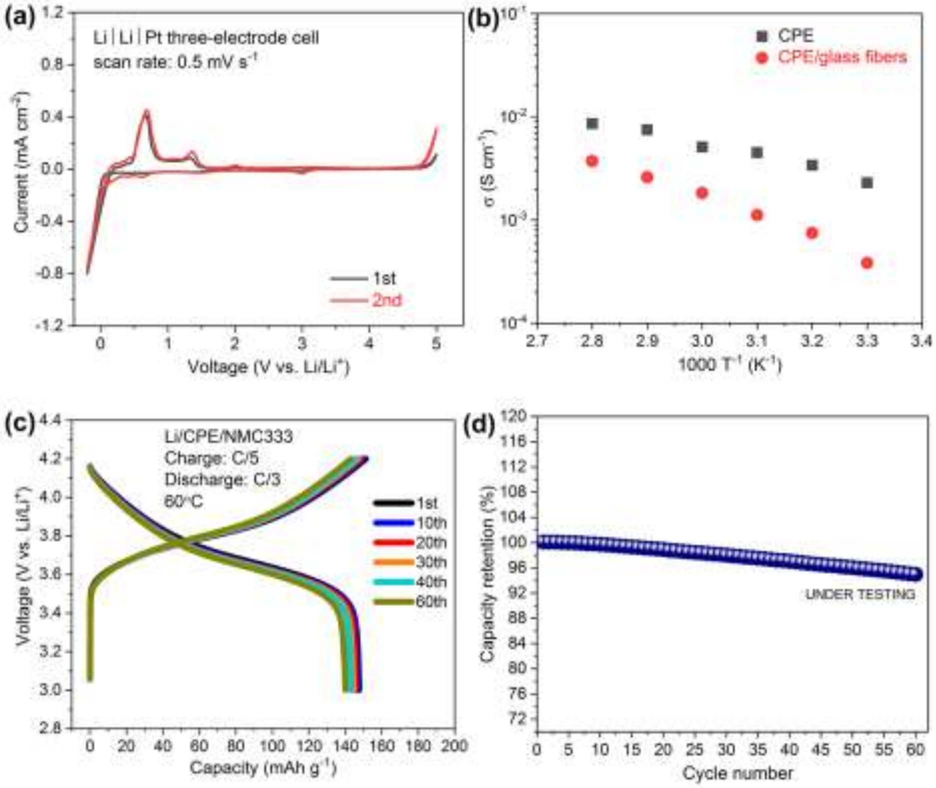

Figure 53. (a) Cyclic voltammetry curves of Li|Li|Pt three electrode cell containing composite polymer electrolyte (CPE) under a scan rate of 0.5 mV s^{-1} in a voltage window of -0.2 V to 5.0 V at room temperature. (b) Temperature dependence of ionic conductivity of CPE and CPE/glass fiber separator. (c) Voltage profiles of a coin cell of NMC-333 cathode (2 mAh cm^{-2}) and Li-metal anode with glass fiber separator (GF-B) soaked with CPE cycled using charge rate of C/5 rate and discharge rate of C/3 at 60°C, where 1C = 2.0 mA cm^{-2}. (d) The corresponding cycling performance of the cell (under continuing test).

This quarter, the team further developed a new kind of hybrid “polymer-in-salt” composite electrolyte for more stable operation of Li-metal battery cycling. Briefly, such a composite polymer electrolyte (CPE) is composed of a lithium salt, a suitable polymer, and a small amount of organic solvent that has been fabricated by using a facile mixing method. The CV curves of Li|Li|Pt three-electrode cell containing the above CPE were tested under a scan rate of 0.5 mV s^{-1} at room temperature in an argon-filled glovebox, and the results are shown in Figure 53a. It clearly demonstrates that the as-prepared CPE is stable at a voltage as high as 4.8 V versus Li/Li^{+}, which is well compatible with the 4-V class batteries. In addition, the team measured its ionic conductivity in CR2032 coin cell set with and without the separator. The ionic conductivity values of the CPE without separator are 2.3 mS cm^{-1}, 3.4 mS cm^{-1}, 4.5 mS cm^{-1}, 5.1 mS cm^{-1}, 7.5 mS cm^{-1}, and 8.6 mS cm^{-1} at 30°C, 40°C, 50°C, 60°C, 70°C, and 80°C, respectively (black squares in Figure 53b). The ionic conductivity values of CPE/glass fiber separator used in coin cell cycling are 0.28 mS cm^{-1}, 0.38 mS cm^{-1}, 0.75 mS cm^{-1}, 1.12 mS cm^{-1}, 1.83 mS cm^{-1}, 2.60 mS cm^{-1}, and 3.72 mS cm^{-1} at 25°C, 30°C, 40°C, 50°C, 60°C, 70°C, and 80°C, respectively (red dots in Figure 53b). This indicates that the ionic conductivity of the CPE/glass fiber separator is capable of working in Li-metal batteries. Furthermore, the coin cells of NMC-333 cathode (with a medium areal capacity loading of 2 mAh cm^{-2}) and Li-metal anode with glass fiber separator (GF-B) soaked with the CPE were cycled using charge rate of C/5 and discharge rate of C/3 at 60°C after two formation cycles. It is seen from Figure 53c-d that the Li||NMC-333 cells based on the CPE have fairly stable cycling and a high capacity retention of 95% after 60 cycles. The cells are under testing, and more details will be disclosed in the next report. It is highly expected to achieve the long-lasting Li-metal cells containing CPE with a cycle life of 300 cycles and a capacity retention of over 80%. Currently, the team is working on further enhancing the ionic conductivity and mechanical capability of the composite polymer electrolytes.

Patents/Publications/Presentations

Presentations

- Beyond Lithium Ion XI, Cleveland, Ohio (July 24–26, 2018): "Lithium Difluorophosphate as a Dendrite-Suppressing Additive for Lithium Metal Batteries"; P. Shi, L. Zhang, H. Xiang, X. Liang, Y. Sun, and W. Xu. Poster.
- BMR Li-Metal Anode Deep Dive Meeting, University of Pittsburgh, Pittsburgh, Pennsylvania (August 28–29, 2018): "Lithium Dendrite Prevention for Lithium Batteries"; W. Xu and J.-G. Zhang.

Task 4.2 – Self-Assembling and Self-Healing Rechargeable Lithium Batteries (Yet-Ming Chiang, Massachusetts Institute of Technology; Venkat Viswanathan, Carnegie Mellon University)

Project Objective. The project objectives are as follows: (1) investigate formation of lithium halide containing SEI, (2) characterize the structure and composition of the SEI surface film and morphology of the electrochemically deposited lithium, and (3) develop combinations of electrolytes (solvents + salts) and electrolyte additives that produce a highly Li-ion conducting, mechanically robust, and self-healing SEI to suppress lithium dendrite formation and improve CE.

Project Impact. Efforts to achieve practical use of the Li-metal anode in rechargeable lithium batteries have long been plagued by lithium dendrite formation and low CE. Lithium dendrites cause battery short-circuits, leading to serious safety hazards. The low CE of Li-metal anodes demands use of excess lithium to offset the lithium loss during cycling, which lowers the overall energy density of the battery. If successful, this project will enable self-forming and self-healing SEI containing alkali and/or alkaline earth halides that can suppress dendrite formation and improve CE. This will eventually enable high-energy-density (> 400 Wh/kg) and long-cycle-life (> 500 cycles, 80% capacity retention) Li-metal batteries.

Approach. The project approach involves the following: (1) identifying suitable combinations of solvents, Li-electrolyte salts, and halide and other additives that can produce highly Li-ion conducting, mechanically robust, and self-healing SEI, (2) using integrated theory and experiment, and (3) assembling and testing symmetric and asymmetric cells and Li-metal batteries comprising a high areal-capacity cathode (> 3 mAh/cm^2) and a capacity-limited Li-metal anode (< 130% lithium excess).

Out-Year Goals. The project will down-select electrolyte compositions, develop designs for prototype full cells of > 10 mAh capacity, and fabricate and deliver cells to DOE-specified laboratories for testing and evaluation.

Collaborations. This project collaborates with 24M Technologies Inc. on 18 cm^2/80 cm^2 pouch cell fabrication and tests.

Milestones

1. Demonstrate Li-Li asymmetric cell using halide additives that outperforms additive-free cell according to criteria in Q3 and Q4. (Q1, December 2017; Completed)
2. Deliver structural and chemical characterization results for baseline halide films on lithium metal. (Q2, March 31, 2018; Completed)
3. Deliver structural and chemical characterization results for self-healed halide films on lithium metal. (Q3, June 30, 2018; Completed)
4. Establish quantitative theoretical criteria for effectiveness and reproducibility in dendrite-suppression experiments. (Q4, September 30, 2018; Completed)
5. *Go/No-Go Decision*: Demonstrate Li-Li symmetric cells that meet established criteria cycling at ≥ 3 mAh/cm^2 at C/5 rate over 30 cycles. (Q1, FY 2019; Completed ahead of schedule)

Progress Report

This quarter, results are reported for two experimental approaches utilized for accurate quantification of CE in development of dendrite-suppression electrolytes. These results have met this quarter's DOE milestone.

The first approach is an asymmetric Li-Li cell test. The asymmetric cell consists of a two Li-metal electrodes that have different thicknesses and areal capacities (Figure 54a). Currently, the working electrode is a 20µm-thick lithium film coated on a copper foil (areal capacity ~ 4.12 mAh/cm^2), while the counter electrode is a 750-µm-thick lithium foil (large excess capacity). The two electrodes are assembled into a CR2032-type coin-cell with a Tonen polyethylene separator and 40-µL of electrolyte. The cell is cycled at a current density of 0.6 mA/cm^2, and the cycling capacity is 3.0 mAh/cm^2 per deposition/stripping cycle. The cell is cycled until the overpotential for lithium stripping spikes and reaches 0.5 V versus Li$^+$/Li, which indicates that there is no further lithium available for stripping at the working electrode (Figure 54b). The 20-µm-thick lithium film originally coated on the copper foil is consumed by side reactions and insulated by a thick SEI layer (that is, "dead lithium"). The average lithium cycling CE of the test cycles is calculated using a method similar to that previously reported by Doron Aurbach et al.: $E_{AVERAGE} = 1 - Q_D/nQ_T$ where Q_T is the cycling capacity (3 mAh/cm^2 in project tests); Q_D is the total lithium capacity ($Q_D = Q_T + Q_{excess} = \sim 7.12$ mAh/cm^2); and n is the number of completed deposition/stripping cycles when the test is stopped. This is a reliable approach for measuring CE and comparing the effect of lithium salts, solvents, and additives (Figure 54c). The final voltage spike (as indicated by the black arrows in Figure 54c) is also used to confirm the absence of short-circuit during the cycling test.

The project also developed a standardized Li-metal full cell test. The Li-metal full cell consists of a high-voltage $LiCoO_2$ cathode (23.0 mg/cm^2 single-side coated on aluminum foil, areal capacity ~ 4.3 mAh/cm^2 when charged to 4.5 V versus Li$^+$/Li), a 20-µm-thick lithium anode coated on a copper foil (areal capacity ~ 4.12 mAh/cm^2), and a single-layer polyethylene separator. The tests are performed inside a temperature chamber set at 30°C ± 0.2°C. The 2025-type coin cell cases made of 316L-grade stainless steel that are used for the tests are stable at high voltage (4.5 V). The full cells are first cycled at 0.1 C rate for 3 cycles and then cycled under the condition of 0.2 C charge to 0.5 C discharge (1 C = 170 mA/g = 3.91 mA/cm^2 in tests). At least three parallel tests are performed for each electrolyte composition. Examples are shown in Figure 55. It is clear that the control electrolyte (1 M $LiPF_6$ EC-DMC, gray data in Figure 55) is ineffective in suppressing dendrite formation. The dual-salt electrolyte [0.6 M LiTFSI-0.4 M LiBOB in EC-EMC (4/6 w) + 0.05 M $LiPF_6$] previously reported by Zheng et al. [*Nature Energy* 2 (2017): 17012; doi: 10.1038/nenergy.2017.12] is effective. The team has also discovered a new additive X that is effective in suppressing dendrite formation and improving cycling performance of Li-metal full cells (Figure 55, green data,) when added to the 1 M $LiPF_6$ FEC-DMC electrolyte previously reported. More details regarding the additive X will be reported in future reports.

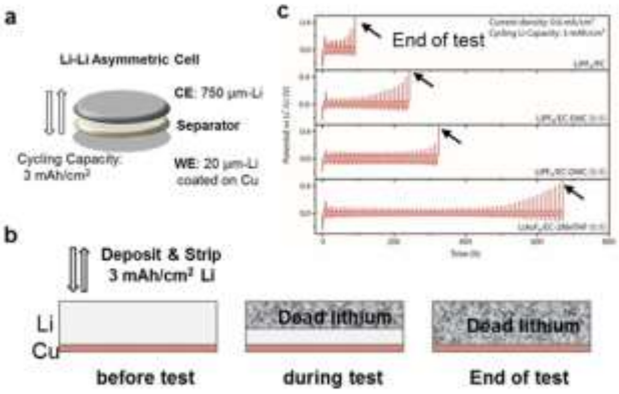

Figure 54. Schematic illustration of the standardized Li-Li asymmetric cell tests.

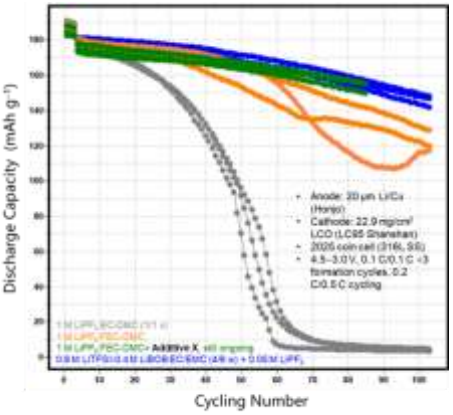

Figure 55. Cycling results of 4 electrolytes from the standardized Li-metal full-cell tests.

Patents/Publications/Presentations

Patent

- Chiang, Y-M., V. Viswanathan, L. Li, V. Pande, D. Krishnamurthy, Z. Ahmad, and W. H. Woodford. "Lithium Metal Electrodes and Batteries Thereof." U. S. Patent Application, US20170288281A1.

Task 4.3 – Engineering Approaches to Dendrite-Free Lithium Anodes (Prashant Kumta, University of Pittsburgh)

Project Objective. This project will yield Li-metal anodes with specific capacity ≥ 2000 mAh/g (≥ 10 mAh/cm^2), ~ 1000 cycles, CE loss ≤ 0.01%, and CE ≥ 99.99% with superior rate capability. The goal is to (1) systematically characterize different approaches for generation of dendrite-free Li-metal anodes while also providing understanding of the scientific underpinnings, and (2) evaluate the microstructure and electrochemical performance of dendrite-free Li-metal anodes. Generation of high-performance, dendrite-free Li-metal anodes will successfully demonstrate generation of novel sulfur cathodes, affording fabrication of Li-S batteries meeting the targeted gravimetric energy densities ≥ 350 Wh/kg and ≥ 750Wh/l with a cost target $125/kWh and cycle life of at least 1000 cycles for meeting the EV Everywhere Grand Challenge blueprint.

Project Impact. Dendrite formation in electrochemical systems occurs due to inhomogeneous current densities coupled with local diffusion gradients, surface roughness, and kinetic roughening. Lithium dendrite formation and growth are, however, not well understood; adding to the complexity is SEI formation. Control and elimination of Li-metal dendrite formation is a veritable challenge. If overcome, it would render universal adoption of Li-anode batteries for stationary and mobile applications. This project is a scientific study of novel approaches to address dendrite formation in Li-anode batteries, electrolyte decomposition, and associated cell failure. Development of dendrite-free, high-performance lithium anodes will enable the use of Li-free cathodes, opening myriad possibilities to push the envelope in terms of cathode capacity and battery energy density.

Approach. This project will explore several approaches focused on engineering new structurally isomorphous metallic alloys combined with engineering the surface of metallic lithium as well as the current collectors, including development of novel high Li-conducting conjugated polymers and composite structures. The unifying theme is to initiate a uniform nucleation with homogenous growth, eliminating preferential reversible plating and de-plating and thus resulting in dendrite-free, high-energy-density Li-metal anodes.

Out-Year Goals. This project comprises three major phases to be successfully completed in three years:

- Year 1 – Synthesis, characterization, and scale-up of suitable porous foams (PF) for use as current collectors for lithium anodes and Li-ion conductor (LIC) materials to prepare multilayer porous foams (MPF).
- Year 2 – Development of Li-rich structurally isomorphous alloy (SIA) anodes. Generation of composite multilayer anodes (CMAs).
- Year 3 – Advanced high-energy-density, high-rate, extremely cyclable cell development.

Collaborations. The project works with Dr. M. K. Datta and Dr. O. I. Velikokhatnyi (University of Pittsburgh) as co-PIs. It also collaborates with Dr. A. Manivannan (Global Pragmatic Materials), XPS analysis; Dr. D. Krishnan Achary (University of Pittsburgh), solid-state magic angle spinning NMR (MAS-NMR) characterization; and Dr. J. R. Gaines (Kurt Lesker), thin-film system fabrication/ characterization.

Milestones

1. Synthesis and testing of SIA electrodes. (Q3, April 2018; Completed)
2. Optimization of MPFs to improve capacity and stability for scaling. (Q4, July 2018; Completed)
3. Synthesis of MPFs exhibiting: specific capacity ≥ 1000 mAh/g (≥ 4 mAh/cm^2), > 400 cycles without cell failure), and initial CE of ≥ 95% with ≤ 0.05% loss per cycle. (December 2018; Ongoing)
4. First-principles investigations into identifying electronically and ionically conductive materials capable of acting as SIA compositions over a range of lithium compositions. (December 2018; Ongoing)
5. Fabrication/characterization of thick electrodes for 10-mAh cell configurations. (December 2018; Ongoing)

Progress Report

In the previous two reports, the concept of surface engineering of lithium metal to control the nucleation and growth of dendritic structures was presented. This quarter, a significant study was performed to identify suitable current collectors as heterogeneous nucleation sites exhibiting zero or minimal nucleation barriers (that is, zero nucleation underpotential) for Li-metal plating. The heterogeneous nucleation feature, described in Figure 56, shows that if the contact angle between lithium metal and the current collector decreases below ~ 20° to 30°, the heterogeneous nucleation barrier, [ΔG_{cr}(het)/ΔG_{cr}(hom)], approaches almost 0, and therefore, the rate of nucleation, J_{het}, is expected to increase significantly. In this condition, it is expected that the nucleation underpotential for Li-metal plating will be minimum, leading to smooth homogeneous surface formation across the current collector if the associated contact angle is well below 30°. Further, in the presence of an efficient nucleant/current collector, the columnar/needlelike growth of lithium metal as well as dendrite formation can also be prevented by inhibiting the rapid and isotropic growth of the nucleated lithium crystal.

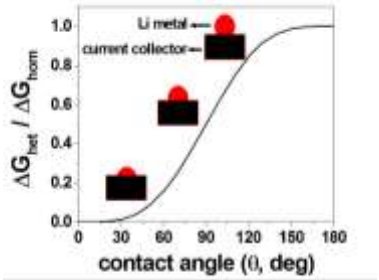

Figure 56. Variation of heterogeneous nucleation barrier with contact angle.

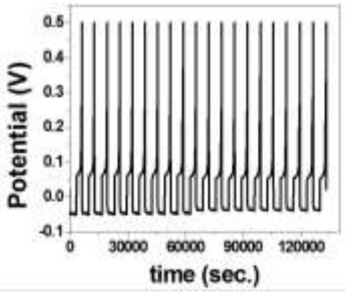

Figure 57. Li-metal plating/stripping behavior of an efficient electrode showing zero nucleation underpotential and invariant growth potential with time and cycle numbers.

This quarter, metal alloys as an efficient nucleant/current collector exhibiting negative heat of mixing (that is, good wetting with lithium metal) and exceptional lattice registry with lithium metal have been synthesized. Figure 57 shows the plating/stripping behavior of one of the synthesized novel current collectors/substrates showing “zero nucleation underpotential” tested at a current density of 0.5mA/cm^2 in the 1M LiPF$_6$ (EC:DEC), whereas the traditional copper current collector (not shown) exhibits a large nucleation under-potential. In addition, the growth potential of lithium metal (Figure 57), cycled at a current density of 0.5mA/cm^2 for 1h, shows no significant change (~ 47 mV) with time or with cycle numbers, suggesting minimal Gibbs-Thomson effect on the growth potential that mainly arises due to formation of high surface area needlelike cellular or dendritic growth of the lithium metal. However, most current collectors that cycle show low CE (≤ 90%, Figure 58) due to the irreversible reactive electrolyte (EC:DEC) side reactions with the current collector resulting in SEI formation. This adventitious side reaction in the novel materials is minimized by further alloying with nonreactive metals to form novel “zero nucleation under-potential” multicomponent alloys inhibiting SEI formation. Figure 59 shows preliminary plating/stripping behavior of such a “zero nucleation underpotential” novel ternary alloy made exhibiting high CE (> 99%) tested at 1 mAh/cm^2 charge capacity and 1 mA/cm^2 current density in EC:DEC based electrolyte. Studies of the lithium growth front morphology when plated at low and high current density (0.5mA/cm^2-2mA/cm^2) and charge capacity (0.5-4 mAh/cm^2) are being investigated. Results will be presented and highlighted next quarter.

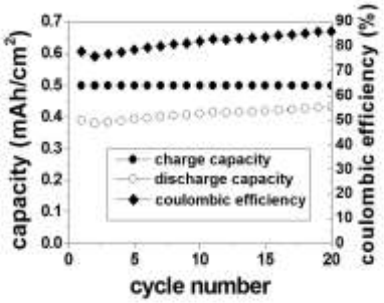

Figure 58. The charge/discharge capacity along with Coulombic efficiency of an efficient electrode.

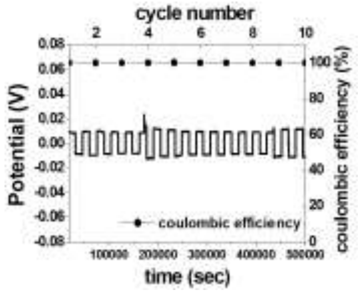

Figure 59. Li-metal plating/stripping behavior of ternary alloy showing high Coulombic efficiency.

Patents/Publications/Presentations

Presentation

- BMR Li-Metal Anode Deep Dive Meeting, University of Pittsburgh, Pittsburgh, Pennsylvania (August 28–29, 2018): “Engineering Approaches to Dendrite Free Li-Metal Anodes”; P. N. Kumta.

Task 4.4 – Nanoscale Interfacial Engineering for Stable Lithium-Metal Anodes (Yi Cui, Stanford University)

Project Objective. This study aims to render Li-metal anode with high capacity and reliability by developing chemically and mechanically stable interfacial layers between lithium metal and electrolytes, which is essential to couple with sulfur cathode for high-energy, Li-S batteries. With the nanoscale interfacial engineering approach, various kinds of advanced thin films will be introduced to overcome issues related to dendritic growth, reactive surface, and virtually "infinite" volume expansion of Li-metal anode.

Project Impact. Cycling life and stability of Li-metal anode will be dramatically increased. The success of this project, together with breakthroughs of sulfur cathode, will significantly increase the specific capacity of lithium batteries and also decrease cost, thereby stimulating the popularity of EVs.

Out-Year Goals. Along with suppressing dendrite growth, the cycle life, CE, and current density of Li-metal anode will be greatly improved (that is, no dendrite growth for current density up to 3.0 mA/cm^2, with CE greater than 99.5%) by choosing the appropriate interfacial nanomaterial along with rational electrode material design.

Collaborations. There are no collaborative activities this quarter.

Milestones

1. Further improve the efficacy of Li-metal protection layers. (Q1, December 2017; Completed)
2. Improve the CE > 99.2%. (Q2, FY 2018; Completed)
3. Demonstrate > 800 cycles of Li-metal anode with stable host and interphase. (Q3, FY 2018; Completed)

Progress Report

High-concentration electrolytes have recently attracted serious research interest. The project team has been able to demonstrate that with only 60 µl of 4 M LiFSI in DME electrolyte per coin cell, Li/Cu cell was able to be stably cycled for over 1000 cycles, with an average CE around 99.3% at a current of 1 mA cm^{-2} and a capacity of 1 mAh cm^{-2} (Figure 60).

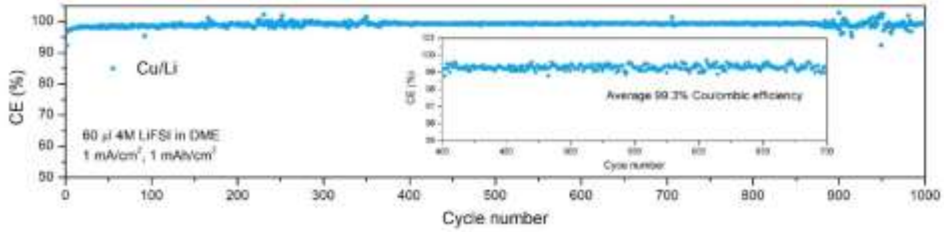

Figure 60. Li/Cu cell cycling performance in 4 M LiFSI in DME.

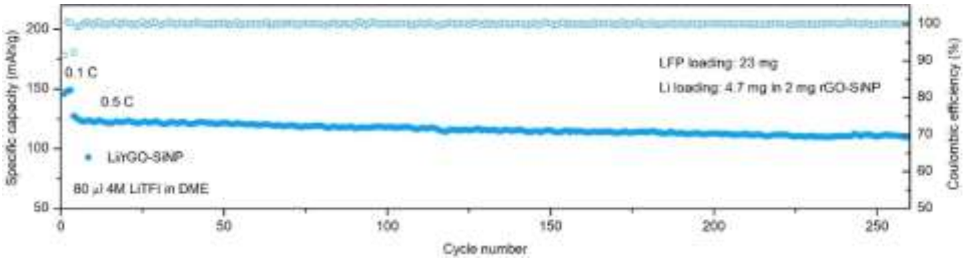

Figure 61. The cycling performance of LiFePO$_4$ (LFP) cathode paired with a lithium / reduced graphene oxide with embedded silicon nanoparticles (Li/rGO-SiNP) anode. The capacity shown here corresponds to that of LFP.

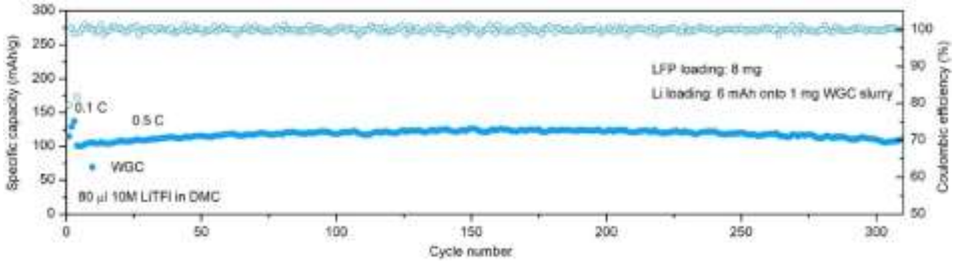

Figure 62. Wrinkled graphene cage / lithium anode with LiFePO$_4$ (LFP) cathode.

This prompted the team to combine novel host structures with these innovations in high-concentration electrolytes, conducting two efforts to demonstrate the idea. First, based on previously reported Li/rGO composite anode, a better rGO with silicon nanoparticles embedded inside was fabricated (Li/rGO-SiNP). The silicon nanoparticles enabled nucleation in between the graphene layers, promoting better performance. The team paired Li/rGO-SiNP with LiFePO$_4$ (LFP) cathode, and it can be stably cycled under 0.5 C for more than 260 cycles (Figure 61). This testing continues.

In another case, the team fabricated a novel WGC as lithium host. This material enables lithium deposition inside the cage and also uniform SEI protection. Paired with LFP cathode, this full cell was able to be cycled over 310 cycles; this work continues (Figure 62).

With the combination of high-concentration electrolyte with various Li-composite anodes, the team anticipates a further improved CE to an applicable level in the near future.

Patents/Publications/Presentations

Publication

- Wang, H., Y. Cui, et al. Pending submission.

Task 4.5 – Composite Electrolytes to Stabilize Metallic Lithium Anodes (Nancy Dudney and X. Chelsea Chen, Oak Ridge National Laboratory)

Project Objective. The project has several objectives: (1) prepare composites of representative polymer and ceramic electrolyte materials to achieve thin membranes that have the unique combination of electrochemical and mechanical properties required to stabilize the metallic lithium anode while providing for good power performance and long cycle life, (2) understand the Li-ion transport at the interface between polymer and ceramic solid electrolytes, which is critical to effective conductivity of the composite membrane, (3) identify key features of composite composition, architecture, and fabrication that optimize performance, and (4) using practical and scalable processing, fabricate thin electrolyte membranes to use with a thin metallic lithium anode to provide good power performance and long cycle life.

Project Impact. A stable lithium anode is critical to achieve high energy density with excellent safety, lifetime, and cycling efficiency. This study will identify key design strategies that should be used to prepare composite electrolytes to meet the challenging combination of physical, chemical, and manufacturing requirements to protect and stabilize the Li-metal anode for advanced batteries. By utilizing well characterized and controlled component phases, design rules developed for composite structures will be generally applicable toward substitution of alternative and improved solid electrolyte component phases as they become available. Success will enable DOE technical targets: 500-700 Wh/kg, 3000-5000 deep discharge cycles, and robust operation.

Approach. This project seeks to develop practical solid electrolytes to provide stable, long-lived protection for the Li-metal anode. Current electrolytes have serious challenges when used alone; oxide ceramics are brittle, sulfide ceramics are air sensitive, polymers are too resistive and soft, and many electrolytes react with lithium. Composites provide a clear route to address these issues. This project does not seek discovery of new electrolytes; rather, the goal is to study combinations of well-known electrolytes. The project emphasizes investigation of polymer-ceramic interfaces formed as bilayers and as simple composite mixtures where effects of interface properties can be readily isolated. In general, the ceramic phase is several orders of magnitude more conductive than the polymer electrolyte, and interfaces can contribute an additional source of resistance. Using finite element simulations as a guide, composites with promising compositions and architectures are fabricated and evaluated for Li-transport properties using AC impedance and DC cycling with lithium in symmetric or half cells. General design rules will be determined for wide application to other solid electrolyte combinations.

Out-Year Goal. The goal is to use advanced manufacturing processes where the architecture of the composite membrane can be developed and tailored to maximize performance and cost-effective manufacturing.

Collaborations. Work is conducted by Dr. Y. Zhang and Dr. X. Chen. Dr. J. Chen (ORNL) assisted with electron microscopic characterization and Dr. R. Ruther (ORNL) with Raman spectroscopy. Electrolyte powders are obtained from Ohara Corporation and Prof. J. Sakamoto (University of Michigan).

Milestones

1. Fabricate a full battery using aqueous spray coating for both the composite electrolyte and cathode incorporating a protected Li-metal anode. (Q4 FY 2017 stretch goal; Completed)
2. Accurately determine the polymer/ceramic electrolyte interface resistance for PEO and Ohara. Revisit effect of DMC on interface ASR. (Q1, FY 2018; Completed)
3. Minimize interface ASR by chemical and mechanical treatment with a goal of < 100 ohm. (Q2, FY 2018; ongoing, as ASR is > 100 ohm)
4. Move beyond model materials like Ohara and PEO, to include polymer gels. Identify promising polymer ceramic systems with interfacial ASR less than 10 ohm. (Q3, FY 2018; In progress – new polymer gel)
5. Assess the feasibility of slurry spray coating to form the thin membrane of new materials. (Q4, FY 2018)

Progress Report

The project obtained $LiFePO_4$ composite cathode from a new collaborator to the program. Two full cells, Li|PE|LFP and Li|PE|CPE|LFP were built using the same protocol as last quarter. Both cells showed much higher capacity (> 110 mAh/g) and much improved stability compared to the cells built with the homemade porous LFP cathode (40-80 mAh/g), at C/20 rate, ~ 70 μA current. As shown in Figure 63, the cell with bilayer electrolyte PE|CPE delivered higher capacity (138 mAh/g) than the one with single-layer polymer electrolyte (120 mAh/g) after cycle 10. The capacity of Li/PE/CPE/LFP cell increased with cycling, whereas that of Li/PE/LFP decreased. The team will continue using the composite LFP cathode due to its superior performance.

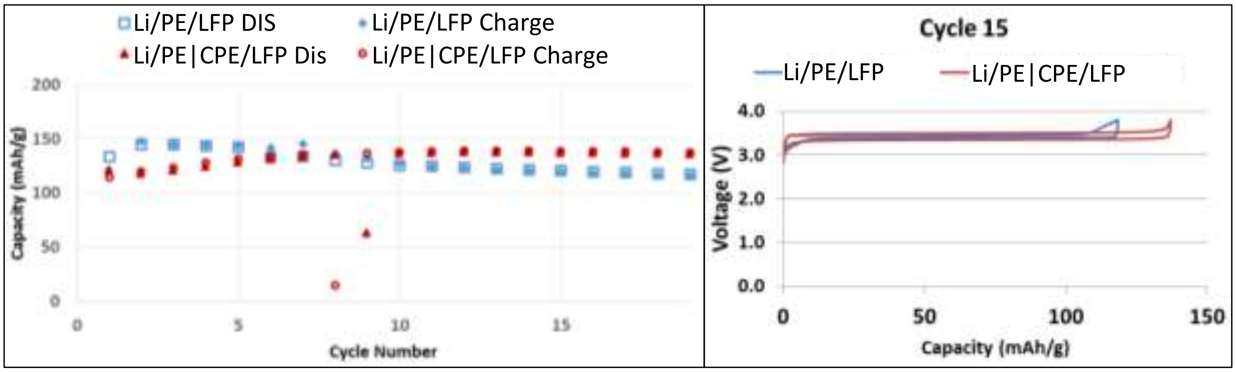

Figure 63. (left) Discharge and charge capacity as a function of cycle number at 75°C. (right) Discharge and charge voltage profile at cycle 15 for Li|PE|LFP cell and Li|PE|CPE|LFP cell. The capacity is normalized to the mass of the composite LFP cathode.

Continuing last quarter's effort of developing composite gel electrolyte, the team investigated the effect of a few gel forming conditions, including two types of ceramic fillers, two types of plasticizers, and different plasticizer contents, on the conductivity of the composite gel electrolyte, as shown in Figure 64. Composite gel-1 and composite gel-2 with two different ceramic fillers exhibited similar conductivity when infused with similar amounts of plasticizer-A. Composite gel-1 with 38 wt% plasticizer-A showed the highest conductivity compared to 10 wt% plasticizer-A and 26-88 wt% of plasticizer-B. The team thus conducted lithium symmetrical cell testing using composite gel-1 +38 wt% plasticizer, as shown in Figure 65. The overvoltage of composite gel-1 (0.035V) was much smaller than that of the polymer gel (0.14V) at 50 μA. Furthermore, lithium symmetrical cell with polymer gel electrolyte could not cycle at 100 μA, while that with composite gel electrolyte is still cycling as of this report.

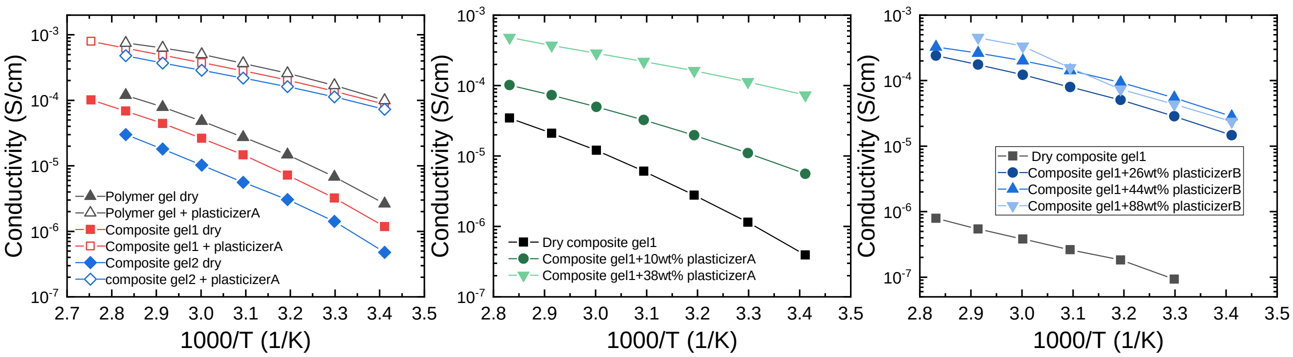

Figure 64. Ionic conductivity as a function of inverse temperature. (left) Comparsion of polymer gel, composite gel with ceramic 1, and composite gel with ceramic 2. All gels were infused with ~ 40 wt% plasticizer-A. (center) Comparision of composite gel-1 with different amounts of plasticizer-A. (right) Comparision of composite gel-1 with different amounts of plasticizer-B.

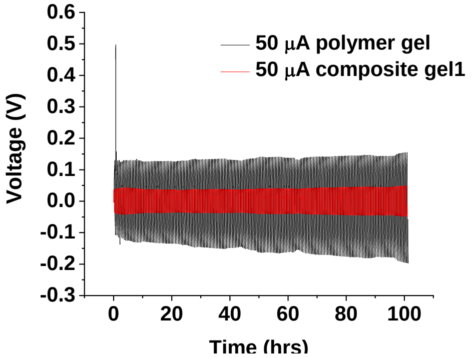

Figure 65. Lithium symmetrical cell cycling using polymer gel and composite gel-1 at 50 μA current at 25°C.

Patents/Publications/Presentations

Publication

- Chen, X. C., A. S. Pandian, X. Liu, K. Liu, F. M. Delnick, and N. J. Dudney.* "Facilitating Ion Transport at the Polymer-Ceramic Electrolyte Interface." Submitted for internal review.

Presentation

- BMR Electrolyte Meeting, Berkeley, California (October 2018): "Composite Electrolyte to Stabilize Metallic Lithium Anodes"; N. J. Dudney, X. C. Chen, Y. Zhang, and F. M. Delnick.

Task 4.6 – Lithium Batteries with Higher Capacity and Voltage (John B. Goodenough, University of Texas at Austin)

Project Objective. The project objective is to develop an electrochemically stable alkali-metal anode that can avoid the SEI layer formation and the alkali-metal dendrites during charge/discharge. To achieve the goal, a thin and elastic solid electrolyte membrane with a Fermi energy above that of metallic lithium and an ionic conductivity $\sigma > 10^{-4}$ S cm^{-1} will be tested in contact with alkali-metal surface. The interface between the alkali-metal and the electrolyte membrane should be free from liquid electrolyte, have a low impedance for alkali-metal transport and plating, and keep a good mechanical contact during electrochemical reactions.

Project Impact. A safe alkali-metal anode that can be plated/stripped reversibly at low resistance and high rates over many thousands of charge/discharge cycles would maximize the volumetric energy density for a given cathode of a rechargeable battery for powering an all-electric road vehicle. Such a battery could also be used for stationary back-up storage of electric power from energy sources other than fossil fuels.

Approach. The project will design, make, and test cells. The approach is to introduce a solid-electrolyte interfacing the anode and a coating on the anode current collector that is wet by a lithium anode. The solid electrolyte should also be wet by the anode to create a bond that is strong enough to constrain the anode volume changes to be perpendicular to the anode/electrolyte interface.

Out-Year Goals. The out-year goal is to develop coin cells that are safe and low-cost with a long cycle life at a voltage $V > 3.0$ V that can compete with the internal combustion engine for powering a road vehicle.

Collaborations. This project collaborates with A. Manthiram at UT Austin and K. Zaghib at HQ.

Milestones

1. Test the cyclability of plating of metallic lithium through a conventional polymer/ceramic or ceramic Li^+ electrolyte. (Q1, FY 2018; Completed)
2. Test relative energies of Cu^+/Cu^0 redox couple and energy of plating/stripping of lithium on/from copper. (Q2, FY 2018; Completed)
3. Test plating/stripping of metallic lithium on a carbon-coated copper current collector with different electrolytes. (Q3, FY 2018; Completed)
4. Demonstrate a low-cost, 3-V cell with a copper current collector as cathode. (Q4, FY 2018; In progress)

Progress Report

The project has made a low-cost, 3-V cell with a copper current collector and dissolved $Cu(ClO_4)$ as the cathode. Compared to the all-solid-state cell configuration in the second quarter, several modifications have been made. First, the electrochemical cell adopts gel-polymer electrolyte membranes (metal salt dissolved in PEG inside PVDF-HFP polymer network) instead of the PEO-based solid electrolyte or regular liquid electrolytes. The gel polymer electrolyte membrane enables room-temperature cell characterizations. Second, as the PVDF-HFP gel polymer membrane cannot block the penetration of lithium dendrites, Li_3N particles were deposited on the anode lithium foil to remove the dendrites by wetting. The lithium dendrites can wet the Li_3N particles via an interfacial charge transfer. The team has confirmed stable charge/discharge cycles of the Li_3N/Li symmetric cell with the gel polymer electrolyte membrane in the middle. All the cells were tested at room temperature.

This quarter, a porous copper foam instead of the copper foil was used as a cathode current collector to increase the electrochemical surface area. The quasi-solid-state cathode electrolyte in contact with the copper metal was LiTFSI/$Cu(ClO_4)_2$ dissolved in PEG inside PVDF-HFP. A separate layer of gel polymer membrane without the copper salt was introduced on top of the lithium anode to avoid a short-circuit. Although the thin copper foil can make very thin and simple cells, (i) the electrochemical area is limited, and (ii) a concentration polarization was observed during discharge, as shown in Figure 66. In contrast, the cathode gel-polymer-electrolyte-impregnating copper foam exhibits stable voltage curves without a notable overpotential during discharge (the black voltage curve in Figure 67), which indicates that the increased surface area is beneficial to reduce effectively the Cu^{2+} diffusion length to and from the copper surface during the redox reactions.

In parallel, the team attempted to enhance the charge transfer kinetics of the Cu-foam electrode by adding carbon black into the cathode polymer network. The voltage curve (red) in Figure 67 shows the benefit of having carbon in the polymer: it shows less voltage polarization during charge and discharge. The carbon can facilitate electronic conduction in the polymer membrane, so charge transfer is less likely controlled by diffusion of Cu^{2+} ions in the gel polymer network. The team is optimizing cathode polymer composition and cell configurations.

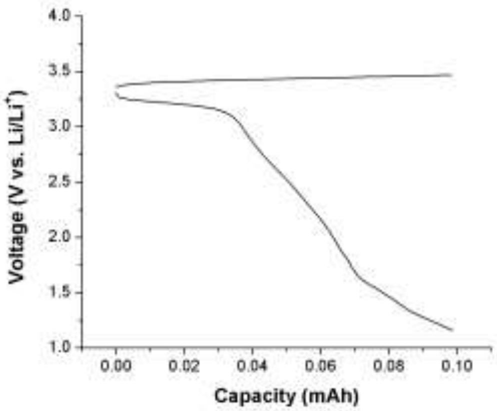

Figure 66. Charge/discharge voltage curves of the LiTFSI/$Cu(ClO_4)_2$ dissolved in PEG inside PVDF-HFP in contact with copper foil. (Current: 20 μA) .

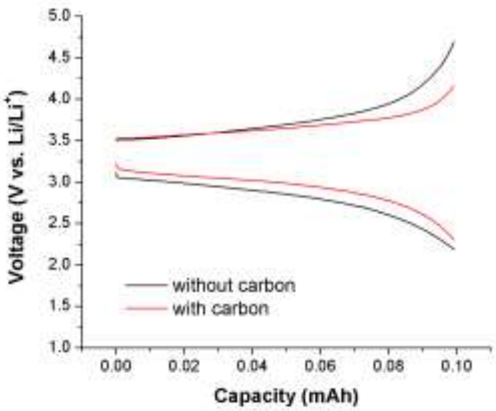

Figure 67. Charge/discharge voltage curves of the LiTFSI/$Cu(ClO_4)_2$ dissolved in PEG inside PVDF-HFP that is impregnated in the copper foam. Carbon was added to the polymer membrane (red curves) to characterize its effect on polarization. (Current: 40 μA).

Patents/Publications/Presentations

The project has no patents, publications, or presentations to report this quarter.

Task 4.7 – Advancing Solid-State Interfaces in Lithium-Ion Batteries (Nenad M. Markovic and Larry A. Curtiss, Argonne National Laboratory)

Project Objective. The project objectives are multifaceted, including development of a new mechanically and chemically stable and Li-ion conductive (≥ 2 x 10^{-4} S/cm at 298 K) solid electrolyte for a solid-state battery encompassing a Li-metal anode, Li-oxide-based cathode, and nonflammable crystalline and amorphous solid electrolytes that can operate at cathode potentials > 5 V (denoted as a S_{Li}-S_{EL}-S_C system).

Project Impact. Protective organic and inorganic compounds can enhance stability of the interface, improve Li-ion interfacial transport, minimize dendrite formation, and increase safety in Li-ion batteries.

Approach. The project proposes to develop and use interdisciplinary, atomic-/molecular-level insight obtained from integrating both experimental- and computational-based methodologies to define the landscape of parameters that control interfacial properties for a new generation of the Li-ion solid-solid battery systems. The strategy will involve transferring knowledge gained from well-characterized thin-film materials to real-world materials. This strategy forms a closed loop wherein the knowledge gained from model systems is used to design more complex, real-world materials, and vice versa. The work will focus on utilizing existing in-house synthesis and characterization methods to enable rapid transition from fundamental science to realistic cells.

Out-Year Goals. The out-year goals are to use and develop the physical and chemical synthesis methods for design of solid-solid interfaces with unique chemical/mechanical/conductivity properties. The proposed work will develop and exploit a variety of *ex situ* and *in situ* experimental optical and surface sensitive techniques and electrochemical methods to explore and explain bulk and interfacial properties of the selected materials. The results will serve to unravel many puzzling bulk and interfacial properties of S_{Li}-S_{EL}-S_C systems, including various types of ceramic and glass materials.

Collaborations. This project funds work at ANL. It will establish collaboration with J. Sakamoto at University of Michigan.

Milestones

1. Development of new synthesis and characterization methods for controlled deposition of lithium on crystalline LLZMO (M = Nb, Ta, Al) materials on the appropriate substrate. (Q1, FY 2018; Completed)
2. Use electrochemical methods to investigate the efficiency as well as charge-discharge cyclability for selected LLZMO materials. Characterize the interface stability of lithium in contact with LLTO solid electrolyte with different orientation. (Q2, FY 2018; Completed)
3. Development of chemical- and physical-based synthesis method to make amorphous Li_2S-P_2S_5 (~ 10^{-3} S/cm at room temperature) and LLZMO solid electrolytes with fast ionic transport of lithium and to elucidate the chemical interaction of lithium with such a glass material. (Q3, FY 2018)
4. Introduce new computational tools for studying interfacial interactions of lithium with solid electrolytes (LLZO) and dopants (Ta, Nb). (Q4, FY 2018; Completed)

Progress Report

Computational Characterization of LLZMO and Its Interaction with Lithium Metal

DFT calculations were performed for LLZMO to elucidate thermodynamic factors that affect reactivity of LLZMO with Li-metal anode. In particular, using XPS and EIS, the team observed considerable differences in Li-induced reactivity of Ta- and Nb-doped LLZO, which is surprising. The LLZMO structure for first-principles calculations is derived from $Li_7La_3Zr_2O_{12}$ with a conventional bulk unit cell of 192 atoms. A partial occupation of lithium sublattices of 24d tetrahedral sites and 96h octahedral sites, with observed experimental occupancies of 0.564 and 0.442, respectively, is modeled by occupancies of 0.542 and 0.448, respectively. The sites were occupied following previous recipes that minimize occupancy of energetically unfavorable nearest-neighbor sites. For the interface with lithium metal, the team used Li-terminated LLZO(100) surface orientation, one of the most stable LLZO surfaces.

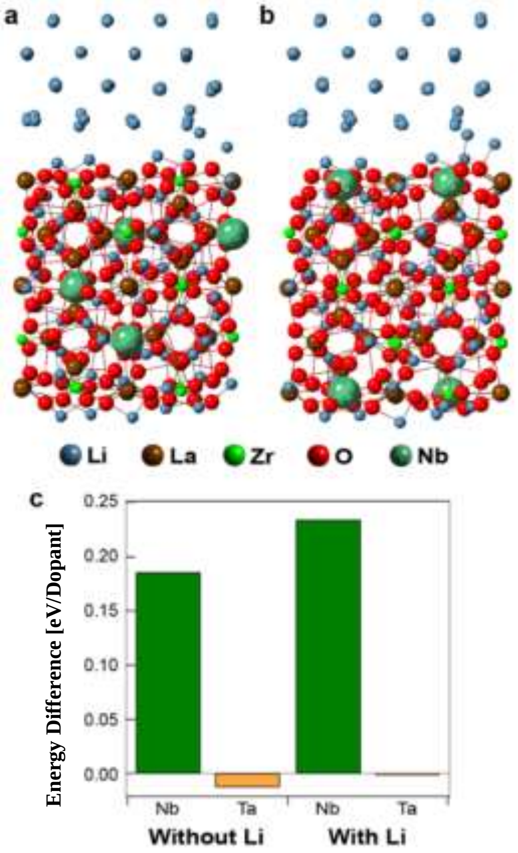

Figure 68. Examples of density functional theory optimized structures with niobium dopants (a) distributed in the bulk and (b) segregated toward the surface for Nb-doped LLZO in contact with lithium. (c) Bar chart showing differences in dopant energy near the surface and in the bulk for niobium- and Ta-doped LLZO without and with lithium present.

They calculated several instances for each dopant, and report averaged energy values, since energy deviations from these averages are, in most cases, below 0.1 eV per dopant atom. The interface energy does not depend considerably on the doping element, which is explained by the fact that the top layer of the surface that interacts with deposited lithium metal consists of lithium and oxygen atoms, with dopant atoms well underneath. This energy is -0.51 J/m^2, -0.52 J/m^2, and -0.55 J/m^2 for average Nb-doped, Ta-doped, and undoped material, respectively.

The team also considered two dopant distributions for each dopant type, with dopants evenly distributed in the bulk or segregated toward the surface (Figure 68a-b), and at least three configurations calculated for each distribution. The team finds that, in the case of Ta-doped LLZO, the average energy of configurations with dopant atoms distributed near the surface versus distributed in the bulk is nearly the same, favoring bulk by less than 0.01 eV/dopant atom both in the presence of lithium on the surface and without lithium metal (Figure 68c). Strikingly, for Nb-doped LLZO, there is strong preference for niobium to be distributed near the surface as compared to distributed in the bulk, both with and without lithium on the surface, with average energy differences for the two distributions of 0.23 eV/dopant and 0.19 eV/dopant, respectively. This clearly indicates niobium has a thermodynamic preference to substitute zirconium sites near the surface of LLZO, whereas tantalum has about the same preference for surface and bulk sites. The preference of niobium to occupy zirconium sites near the surface is slightly stronger in the presence of deposited lithium metal, which suggests that segregation of niobium to the Li-LLZO interface may drive the high degree of Li-induced reactivity of this material. This high degree of reactivity may further lead to the observed propagation of the Li-induced reaction into the solid electrolyte. The findings are complemented by the project’s continuing development of approaches to experimental characterization of buried interfaces between solid electrolyte and electrode. The team shows by XPS that reduction of niobium in Nb-doped LLZO is continuing into the bulk, while for tantalum and aluminum, the reaction is interface-limited. Additionally, XRD shows lattice expansion of Nb-doped LLZO. This work and the established concepts will be extended to other reactivity studies of solid electrolyte/electrode interface on anode side (with amorphous solid electrolytes, such as Li_2S-P_2S_5 completed last quarter) and on cathode side (with $LiCoO_2$ as model system).

Patents/Publications/Presentations

Publication

- Zhu, Y., J. G. Connell, P. Zapol, S. Tepavcevic, J. Sakamoto, L. A. Curtiss, D. D. Fong, J. W. Freeland, and N. M. Markovic. "Surface Chemistry and Intrinsic Stability of Doped Lithium Lanthanum Zirconium Oxides." Submitted to *Advanced Energy Materials*.

Presentation

- BMR Li-Metal Anode Deep Dive Meeting, University of Pittsburgh, Pittsburgh, Pennsylvania (August 28–29, 2018): "Surface Chemistry and Intrinsic Stability of Doped Lithium Lanthanum Zirconium Oxides"; S. Tepavcevic, Y. Zhu, J. G. Connell, P. Zapol, J. Sakamoto, L. A. Curtiss, D. D Fong, J. W. Freeland, and N. M. Markovic.

Task 4.8 – Mechanical and Defect Properties at the Protected Lithium Interface

(Nancy Dudney, Oak Ridge National Laboratory; Erik Herbert, Michigan Technological University; Jeff Sakamoto, University of Michigan)

Project Objective. A new project objective will be to understand the evolution of lithium metal upon cycling in contact with a generic solid electrolyte under various intrinsic and extrinsic conditions. The team plans to construct a set of stability maps that will describe the predominate mass transport process and defect structure evolution in lithium metal. Simple maps may address current density, areal capacity, and layer thickness. Then, maps extending to many other cell designs, interfacial factors, and duty cycle parameters are envisioned. A key activity in FY 2018 will be to develop experimental tools with which to probe lithium morphology in real time. While initial work will focus on experimental characterization, modeling will be introduced to interpret kinetic processes and extrapolate for alternative properties and designs and extended cycling.

Project Impact. Stability maps can guide realistic design choices for solid electrolytes and cell design. Ideally, lithium is deposited and removed uniformly to maintain a fully dense anode in good contact with the solid electrolyte. However, in practice, this may not be realized depending on cycling conditions, nature of the electrolyte, nature of the lithium, and cell architecture. Mapping the lithium defect evolution will offer insight for when, how, and why the lithium structure is altered, along with a much deeper analysis of the degradation. With this insight, the team can realistically project the performance of optimized Li-metal anodes. Materials and cells can be engineered to fulfill the target level of performance for EV batteries, namely 1000 cycles, 15-year lifetime, with adequate pulse power.

Approach. For the initial one-year effort, the project will work to develop experimental tools to probe the lithium structure and its interfaces with mechanical, imaging, and electrochemical methods during mass transport and relaxation. Different constructions for the stability maps will be explored to identify the most useful graphical representation of what is expected to be a rich and detailed analysis of the formation and annealing of lattice and extended defects in the lithium metal.

Out-Year Goals. In the out-years, modeling efforts will be integrated to interpret and extrapolate the results to wide cycling conditions and detailed analysis of the solid electrolytes being used to stabilize the lithium metal.

Collaborations. This project funds work at ORNL, Michigan Technological University, and University of Michigan.

Milestones

1. Characterize *in situ* changes in lithium anode from a single stripping/plating half cycle. (FY 2017; Completed)
2. Identify two experimental tools to probe the defect structure of lithium created under cycling. (Q2, FY 2018; Completed)
3. Cycle lithium under conditions expected to create different defect structures and morphologies to begin creation of stability maps. (Q3, FY 2018; Completed)
4. Design and construct stability diagrams to map the evolution of the defects structure and morphology for lithium metal under a variety of cycling conditions and with different model solid electrolytes. (Q4, FY 2018; In progress)

Progress Report

***In Situ* Neutron Imaging (R. Garcia, University of Michigan).** The neutron imaging experiments were conducted in September 2018 consisting of ^{6}Li metal electrodes paired with $^7Li_{6.25}La_3Zr_2Al_{0.25}O_{12}$ symmetric cells. The LLZO samples consisted of a range of average grain sizes (70-200 µm), large enough to distinguish grain versus grain-boundary transport of ^{6}Li. The cells were cycled below, at, and above the critical current density (CCD) at 80°C, satisfying milestone 3 to address how the defects and morphology change with cycling. Neutron tomography was conducted on all samples. Some cells were cycled *in situ* and below the CCD, and neutron tomography was also conducted *ex situ* on samples where CCD was exceeded. Analysis is under way to correlate physical phenomena at the buried interface with electrochemical behavior.

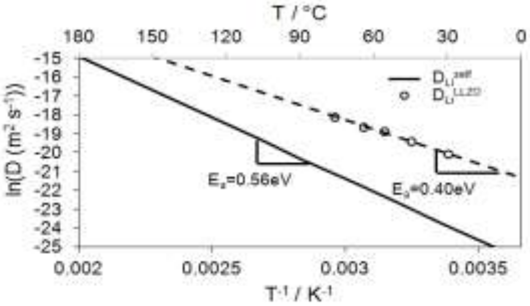

Figure 69. The calculated diffusivity of lithium in LLZO from the Nernst-Einstein equation. The self-diffusivity of lithium is shown for comparison.

Lithium Flux Analysis (Mike Wang, University of Michigan). In this study, it was found that the flux of lithium as controlled by diffusivity (D_{Li} self) will be slower in the metallic lithium t ambient temperature than in LLZO (Figure 69). The team hypothesizes that this flux imbalance could be the origin of "hot spots" that are electrical or mechanical in nature (Figure 70). At low current densities, vacant sites at the Li/LLZO interface should accommodate the lithium deposition (Figure 70a), whereas near the CCD, diffusivity may be insufficient to maintain an adequate number of vacant sites (Figure 70b). At high current densities, Li^+ is forced to plate on already occupied sites leading to "hot-spots" (Figure 70c). Hydrostatic compression in the lithium metal may exacerbate this process (Figure 70d), as suggested by Masias et al. [Masias, F., G-M. Wolfenstine, and J. Sakamoto. *Journal of Materials Science* (2018)].

Nanoindentation Studies (V. Thole, Michigan Technological University). While setting up and testing the project platform for nanoindentation study of the lithium anode for live batteries at different current densities, the team continues to investigate the electrolyte side of the interface. It is fascinating that the glassy electrolyte, LiPON, shows evidence of both creep and recovery processes that may influence the interface with lithium. Creep measurements have been conducted at several temperatures and analyzed as viscoplastic flow behavior described by the constitutive equation $\dot{\varepsilon} = B\,\sigma^n$, where $\dot{\varepsilon}$ is the normalized strain rate, σ the stress, and n the stress exponent. To date, the stress exponent for LiPON films is a high number, ~ 20, and independent of temperature and displacement (Figure 71). A similarly high value has been reported for lithiated amorphous silicon [Berla and Nix, *Journal of Power Sources*, 2015]. Such a high value may be understood as the rearrangement of small atomic clusters in the material, rather than single atoms. The exponent indicates an activated volume of 112 Å^3, whereas a possible cluster unit of LiPON, being 3 Li^+ plus a PO_4^{-3} unit, would occupy 81 Å^3 in the dense glass.

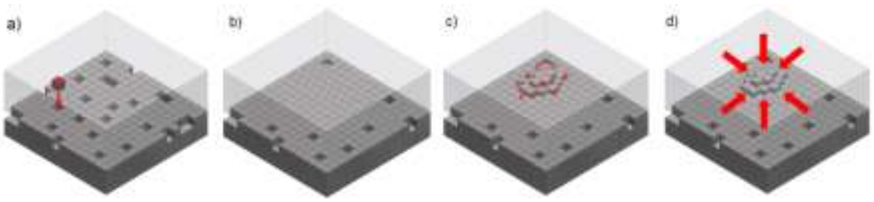

Figure 70. Schematic of Li⁺ deposition at the anode interface with different current density and hydrostatic pressure. Details in text.

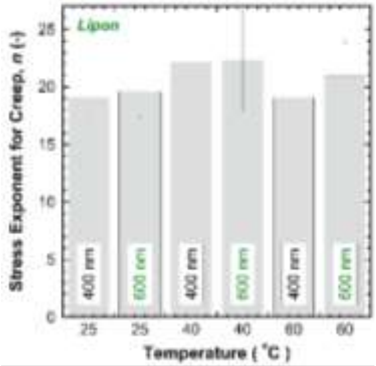

Figure 71. Stress exponent determined for 60-sec constant load measure of creep in LiPON films.

Patents/Publications/Presentations

Publication

- Wang, M., and J. Sakamoto. "Temperature Dependent Flux Balance of the Li / $Li_7La_3Zr_2O_{12}$ Interface." *Electrochemica Acta* (2018). Under review.

Presentations

- Materials Science & Technology 2018 Annual Meeting, Columbus, Ohio (October 14–18, 2018): "Nanoindentation of High Purity Vapor Deposited Lithium Films: A Mechanistic Rationalization of Diffusion-Mediated Flow"; E. Herbert. Invited.
- 256th ACS Meeting, Boston, Massachusetts (August 19–22, 2018): "Interface Stability of Lithium with Lipon and Lipon-Like Electrolytes"; N. Dudney. Invited.

TASK 5 – SULFUR ELECTRODES

Summary and Highlights

Advances in Li-ion technology have been stymied by challenges involved in developing highly reversible capacity cathodes and stable anodes. Hence, there is a critical need for development of alternate battery technologies with superior energy densities and cycling capabilities. In this regard, Li-S batteries have been identified as the next flagship technology, holding much promise due to the attractive theoretical specific energy densities of 2,567 Wh/kg. In addition, realization of the high theoretical specific capacity of 1,675 mAh/g corresponding to formation of Li_2S using earth-abundant sulfur renders the system highly promising compared to other available cathode systems. Thus, the research focus has shifted to developing Li-S batteries. This system, however, suffers from major drawbacks, as elucidated below:

- Limited inherent electronic conductivity of sulfur-based and sulfur-compound-based cathodes;
- Volumetric expansion and contraction of both the sulfur cathode and lithium anode;
- Soluble polysulfide formation/dissolution and sluggish kinetics of subsequent conversion of polysulfides to Li_2S, resulting in poor cycling life;
- Particle fracture and delamination resulting from the repeated volumetric expansion and contraction;
- Irreversible loss of lithium at the sulfur cathode, resulting in poor CE; and
- High diffusivity of polysulfides in the electrolyte, resulting in plating at the anode and consequent loss of driving force for lithium diffusion (that is, drop in cell voltage).

These major issues cause sulfur loss from the cathode, leading to mechanical disintegration. Additionally, surface passivation of anode and cathode systems results in a decrease in the overall specific capacity and CE upon cycling. Consequently, the battery becomes inactive within the first few charge-discharge cycles. Achievement of stable, high capacity Li-S batteries requires execution of fundamental studies to understand the degradation mechanisms in conjunction with devising engineered solutions.

This Task addresses both aspects with execution of esoteric, fundamental *in situ* XAS and *in situ* electron paramagnetic resonance (EPR) studies juxtaposed with conducting innovative applied research comprising use of suitable additives, coatings, and exploration of composite morphologies as well as appropriate engineered strategies. ANL and LBNL use X-ray based techniques to study phase evolution and loss of CE in S-based and S-Se-based electrodes, primarily by the former during lithiation/delithiation while understanding polysulfide formation in sulfur and oligomeric PEO solvent by the latter, respectively. Work from PNNL, University of Pittsburgh, and Stanford demonstrates high areal capacity electrodes exceeding 4 mAh/cm^2. Following loading studies, PNNL performed *in situ* EPR to study reaction pathways mediated by sulfur radical formation. Coating/encapsulation approaches adopted by University of Pittsburgh and Stanford comprise flexible sulfur wire electrodes coated with LIC by University of Pittsburgh, and TiS_2 encapsulation of Li_2S in the latter, both ensuring polysulfide retention at sulfur cathodes. BNL work, on the other hand, has focused on benchmarking of pouch-cell testing by optimization of the voltage window and study of additives such as LiI and $LiNO_3$. *Ab initio* studies at Stanford and University of Pittsburgh involve calculation of binding energies, diffusion coefficients, ionic conductivities, and reaction pathways determination, augmenting the experimental results. Similarly, AIMD simulations performed at TAMU reveal multiple details regarding electrolyte decomposition reactions and the role of soluble polysulfides on such reactions. Using kinetic MC simulations, electrode morphology evolution and mesostructured transport interaction studies were also executed. Studies at PNNL suggest that proper control of electrode porosity/thickness is essential for obtaining high-energy Li-S batteries.

Porosity shows strong dependence on calendering pressure because of low tap densities of electrode components such as sulfur and carbon. Increasing the calendering-pressure from 0.2 to 1.5 ton leads to rapid decrease of electrode porosity, resulting in improvement of electrode volumetric energy density.

Measured electrode volumetric energy density increased from 650 Wh L^{-1} for as-cast electrode (120-μm thick) to 1300 Wh L^{-1} for electrode compressed to 60 μm. Additionally, Pennsylvania State University has shown use of dimethyl disulfide as a functional co-solvent, demonstrating its ability to show an alternate electrochemical reaction pathway for sulfur cathodes by formation of dimethyl polysulfides and lithium organosulfides as intermediates and reduction products. Further, University of Wisconsin at Milwaukee (UWM) has conducted high-performance liquid chromatography (HPLC)-MS studies and has determined the distribution of polysulfides at various discharge and recharge reactions. UT Austin, at the same time, has shown that by integrating polysulfide-filter-coated separators fabricated with cellulose nanofiber, the cells retain 50% of the initial capacity after storing for one year and exhibit a low self-discharge rate of only 0.14% per day.

Each of these projects has a collaborative team of experts with the required skill set needed to address the EV Everywhere Grand Challenge of 350 Wh/kg and 750 Wh/l and cycle life of at least 1000 cycles.

Highlights. This Task reports the following project highlights for this quarter:

- Dr. K. Amine and his group conducted SEM characterization coupled with energy-dispersive X-ray (EDX) mapping on pristine/cycled sulfur cathode, lithium anode and separator to look into the beneficial effects of concentrated polysiloxane electrolytes versus commonly used dilute ether-based electrolytes and observed Li_2S in the separator confirming the migration of polysulfides between the cathode and anode side in case of the ether-based electrolyte. The group also identified signals of sulfur, fluorine, and carbon in the cycled Li-metal electrode and separator that originated from the decomposition of LiTFSI salt to form SEI layer in the ether-based electrolytes, which is one of the first reports on chemical detection of SEI in Li-S batteries.
- Work guided by Dr. P. Balbuena identified lithiated sulfurized-carbonaceous composite ($C_{1.96}N_{0.29}H_{0.13}SLi_{2.50}$) derived by PAN as a promising cathode material for Li-S batteries due to its excellent polysulfide retention and cycling performance. Their latest calculations studied the structural features and lithiation mechanisms of these materials and found evidence of C-S chemical bonding with no formation of long-chain polysulfides during lithiation.
- Researchers in Dr. Y. Cui's group combined dark-field light microscopy (DFLM) and a planar electrochemical cell fabricated on a glass slide to visualize sulfur electrochemistry *in operando*. Using visible light as a benign probe, native ether-based liquid electrolyte was studied noninvasively by enhancing the sensitivity to small features on a flat background using dark-field illumination. Using this technique, they were able to directly observe multiple new phenomena in Li-S batteries for the first time, including the electrochemical generation of metastable liquid sulfur at room temperature, etc.

Task 5.1 – Novel Chemistry: Lithium Selenium and Selenium Sulfur Couple (Khalil Amine, Argonne National Laboratory)

Project Objective. The project objective is to develop a novel S_xSe_y cathode material for rechargeable lithium batteries with high energy density and long life, as well as low cost and high safety.

Project Impact. Development of a new battery chemistry is promising to support the goal of PHEV and EV applications.

Approach. The dissolution of lithium polysulfides in nonaqueous electrolytes has been the major contribution to the low energy efficiency and short life of Li-S batteries. In addition, the insulating characteristics of both end members during charge/discharge (sulfur and Li_2S) limit their rate capacity. To overcome this problem, sulfur or Li_2S is generally impregnated in a carbon-conducting matrix for better electronic conductivity. However, this makes it difficult to increase the loading density of practical electrodes. It is proposed to solve these barriers using the following approaches: (1) partially replace sulfur with selenium, (2) nano-confine the S_xSe_y in a nanoporous conductive matrix, and (3) explore advanced electrolytes with suppressed shuttle effect.

Out-Year Goals. This new cathode will be optimized with the following goals:

- A cell with nominal voltage of 2 V and energy density of 600 Wh/kg.
- A battery capable of operating for 500 cycles with low capacity fade.

Collaborations. This project engages in collaboration with the following: Professor C. Wang of UMD, Dr. Y. Ren and Dr. C. Sun of Advanced Photon Source at ANL, and Dr. L. A. Curtiss at ANL.

Milestones

1. Exploration of novel siloxane-based electrolytes for Li-Se and Se-S systems. (Q1, FY 2018; Completed)
2. Development of high-performance Li/Se-S batteries using optimized siloxane-based electrolytes. (Q2, FY 2018; Completed)
3. Computational modeling on the working mechanism of high-concentration siloxane-based electrolytes. (Q3, FY 2018; Completed)
4. *In situ/ex situ* diagnostic of the cell and electrodes based on high-concentration siloxane-based electrolytes. (Q4, FY 2018; In progress)

Progress Report

This quarter, SEM characterization was conducted, coupled with EDX spectroscopy mapping on pristine/cycled sulfur cathode, lithium anode, and separator to look into the beneficial effects of concentrated polysiloxane electrolytes versus commonly used dilute ether-based electrolytes.

On the Li-anode side, the morphology of the pristine lithium anode is quite flat (Figure 72a). However, after 20 cycles in the dilute ether-based electrolyte, the surface became very rough and porous (Figure 72b), indicating severe Li-metal corrosion by polysulfides. This is because polysulfides are highly soluble in the dilute ether-based electrolytes, which can easily migrate from the cathode side to the Li-anode side. On the other hand, in the case of concentrated polysiloxane-based electrolytes, the surface of lithium remained relatively flat (Figure 72c), implying that the parasitic reactions between polysulfides and the lithium anode are effectively mitigated. This means that the formation of soluble polysulfides in the concentrated polysiloxane-based electrolytes is remarkably suppressed. On the cathode side, after cycling in the dilute ether-based electrolytes, the deposition of Li_2S outside the pores of carbon host can be clearly seen (Figure 72e). There is, however, no obvious morphology change on the surface of the cycled sulfur cathode (Figure 72d-f) when using concentrated polysiloxane-based electrolytes.

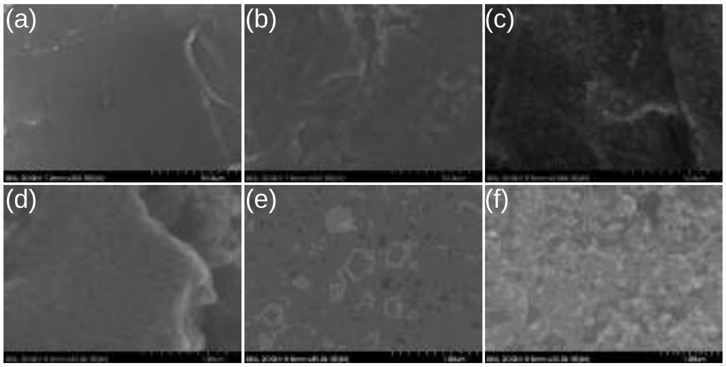

Figure 72. (a-c) Scanning electron microscopy (SEM) images of (a) pristine lithium anode and cycled lithium anode in the (b) dilute ether and (c) concentrated polysiloxane electrolytes. (d-f) SEM images of (d) pristine sulfur cathode and cycled sulfur cathode in the (e) dilute ether and (f) concentrated polysiloxane electrolytes.

Additional evidence comes from the EDX mapping on cycled lithium anode and separator. For cycled lithium anode (Figure 73a), the signal of sulfur, carbon, and fluorine can be clearly seen, and Li_2S can also be found in the separator (Figure 73c), confirming the migration of polysulfides between the cathode and anode side. However, the signals of sulfur, fluorine, and carbon in the cycled lithium metal (Figure 73b) and separator (Figure 73d) are very weak, which originated from the decomposition of LiTFSI salt to form SEI layer.

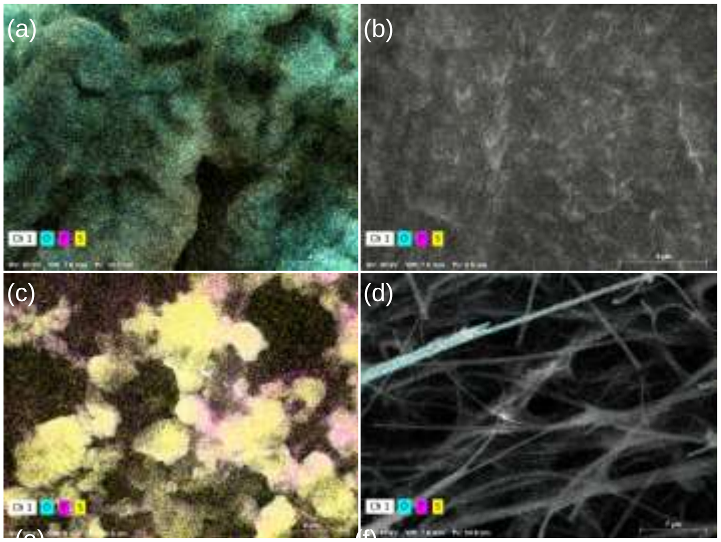

Figure 73. (a-b) Scanning electron microscopy (SEM) energy-dispersive X-ray spectroscopy mapping of cycled lithium anode in the (a) dilute ether and (b) concentrated polysiloxane electrolytes. (c-d) SEM images of cycled separator in the (c) dilute ether and (d) concentrated polysiloxane electrolytes.

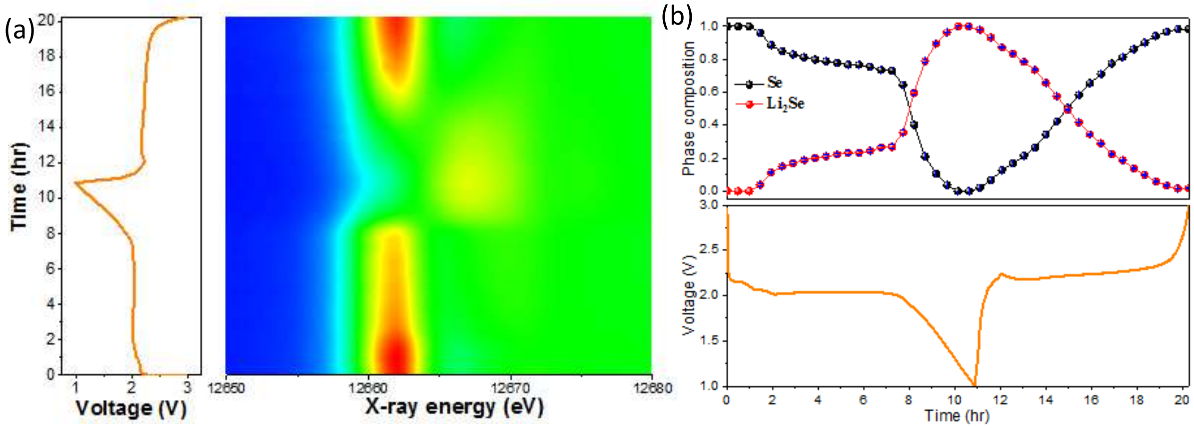

Figure 74. (a) *In situ* selenium K-edge X-ray absorption near-edge structure of Li/Se battery in concentrated polysiloxane-based electrolytes. (b) Corresponding phase composition analysis using linear combination fitting at different charge/discharge states.

Furthermore, *in situ* selenium K-edge X-ray absorption near-edge structure (XANES) was used to probe the valence state changes of selenium during charge/discharge in concentrated polysiloxane-based electrolytes. As shown in Figure 74a, there is no clear edge shift, while the absorption intensity decreased during discharge and then increased during the charge process. This is different from that when cycled in the dilute ether-based electrolytes [*Nano Letters* 16 (2016): 2663–2673]. By selecting standard selenium and Li_2Se as reference, it can be clearly seen that all the spectrum can be fitted well using Se-Li_2Se two phases transition mode. This result indicates that there is very little formation of highly soluble polyselenides during charge/discharge in the concentrated polysiloxane-based electrolytes, which leads to the significant reduction of the shuttle effect and increased capacity retention.

In conclusion, by using concentrated polysiloxane-based electrolytes, the formation of highly soluble polysulfides has been effectively eliminated, which can well protect the cathode structure and lithium anode. The composition of cycled lithium anode will be further investigated by XPS to elucidate the microstructure of the surface layer.

Patents/Publications/Presentations

Publication

- Xu, G. L.; H. Sun, C. Luo, L. Estevez, M. H. Zhuang, H. Gao, R. Amine, H. Wang, X. Zhang, C. J. Sun, Y. Z. Liu, Y. Ren, S. Heald, C. S. Wang, Z. Chen, and K. Amine. "Solid-State Lithium/Selenium-Sulfur Chemistry Enabled via a Robust Solid-Electrolyte Interphase." *Advanced Energy Materials* (2018). Under revision.

Presentation

- BMR Li-S Deep Dive Meeting, Austin, Texas (September 5–6, 2018): "Novel Chemistry for Automotive Application: Lithium-Selenium and Selenium-Sulfur Couple"; G-L. Xu, Z. Chen, and K. Amine.

Task 5.2 – Development of High-Energy Lithium-Sulfur Batteries (Jun Liu and Dongping Lu, Pacific Northwest National Laboratory)

Project Objective. The project objective is to develop high-energy, low-cost Li-S batteries with long lifespan. All proposed work will employ thick sulfur cathode (≥ 2 mAh/cm^2 of sulfur) at a relevant scale for practical applications. The diffusion process of soluble polysulfide out of thick cathode will be revisited to investigate cell failure mechanism at different cycling. The fundamental reaction mechanism of polysulfide under the electrical field will be explored by applying advanced characterization techniques to accelerate development of Li-S battery technology.

Project Impact. The theoretical specific energy of Li-S batteries is ~ 2300 Wh/kg, which is almost three times higher than that of state-of-the-art Li-ion batteries. The proposed work will design novel approaches to enable Li-S battery technology and accelerate market acceptance of long-range EVs required by the EV Everywhere Grand Challenge.

Approach. The project proposes to (1) identify and address key issues of applying high-energy sulfur cathodes including materials, binders, electrode architectures and functional electrode additives, (2) advance mechanism study of sulfur cathode and electrolyte by using *in situ*/*ex situ* techniques and custom-designed hybrid cell setup, and (3) verify effectiveness of the new approaches with coin/pouch cells by using high-loading electrodes (> 4 mg/cm^2), limited lithium (< 200% lithium excess), and lean electrolyte (E/S < 4 µL/mg).

Out-Year Goals. This project has the following out-year goals:

- Fabricate Li-S pouch cells with thick electrodes to understand sulfur chemistry/electrochemistry in environments similar to real application.
- Leverage the Li-metal protection project funded by the DOE and PNNL advanced characterization facilities to accelerate development of Li-S battery technology.
- Develop Li-S batteries with a specific energy of 400 Wh/kg at cell level, 1000 deep-discharge cycles, improved abuse tolerance, and less than 20% capacity fade over a 10-year period to accelerate commercialization of EVs.

Collaborations. This project engages in collaboration with the following: Dr. X-Q. Yang (BNL), Dr. D. Qu (UWM), Dr. X. Xiao (GM), and Dr. J. De Yoreo (PNNL).

Milestones

1. Study of electrolyte compatibility with different carbon host materials and binders and their effects on reversible sulfur utilization. (Q1, December 31, 2017; Completed)

2. Design and demonstration of an electrochemical cell by using ceramics Li$^+$ conductive separator for focused cathode or anode mechanism study for Li-S. (Q2, March 31, 2018; Completed)

3. Study failure mechanism of Li-S cell under lean amount of liquid electrolyte by decoupling the interference of lithium anode using liquid/solid electrolyte hybrid cell. (Q3, June 30, 2018; Completed)

4. Develop functionalized separators to suppress polysulfide shuttle and improve interfacial stability of lithium anode. (Q4, September 30, 2018; Completed)

Progress Report

The study from last quarter indicates that Li-S cells suffer from limited cycle life when high-loading sulfur cathodes (> 4 mg/cm^2) and lean electrolyte amounts (E/S = 4 µL/mg) are used simultaneously. It was identified that most of those failed cells terminated with voltage drops or fluctuation during the charging process, a sign of cell short-circuit. A mechanism study of cell failure under such practical conditions revealed that nonuniform sulfur reactions under lean electrolyte conditions, which are exacerbated by electrolyte consumption upon cycling, lead to localized lithium deposition and stripping; this results in a short-circuit. To circumvent those issues, functionalized separator with double-sided coating was designed and prepared. The coating layers are designed to realize the functions of (1) enhancing sulfur electrode wetting and obtaining uniform electrolyte distribution throughout the electrode, (2) blocking polysulfide shuttle and improving sulfur utilization, and (3) trapping the electrolyte and enhancing reaction uniformity of the lithium anode. Figure 75a shows a cross-sectional SEM image of the double-side coated Celgard separator. One side was coated with a mixture of polymer P1 and carbon nanotube (CNT) with a mass loading of 0.2-0.6 mg/cm^2, which faced toward sulfur cathode in the cell; the other side was coated by an ultra-thin layer of polymer P2, which has a loading of 0.1 mg/cm^2 and contacts the lithium anode in the cell. The P1 polymer has rich carboxyl and nitrogen groups, which help improve electrolyte distribution and slow down polysulfide crossover with the help of CNT, while the P2 polymer has hydroxyl groups and decent chemical stability when contacting the lithium anode. The improved wettability of the coated Celgard separators with electrolyte (1 M LiTFSI/DOL/DME + 0.3 M $LiNO_3$) was demonstrated by comparing the static contact angles (Figure 75b). To verify the polysulfide blocking effects of the coated separator, coin cells using high-loading sulfur cathodes (4 mg/cm^2) and excess amount of electrolyte (E/S = 16) were tested and compared. The separator coating (0.3 mg/cm^2) boosts stable sulfur utilization from 600 mAh/cm^2 to greater than 900 mAh/cm^2 at an optimized weight ratio of P1/CNT = 1:4, indicating the mitigation of polysulfide crossover and irreversible loss. Interestingly, by use of the double-side coated separator, the cell cycle life was doubled when operated at practical conditions (sulfur loading > 4 mg/cm^2 and E/S = 4 µL/mg). As shown in Figure 75d, the cell life was only 20 cycles as a consequence of a short-circuit, but was extended to 45 cycles with only 0.3 mg/cm^2 of coating on the separator. It is believed that the coating of functional polymers enhances uniform electrolyte distribution across the electrode surface. This regulates the reactions of both the sulfur cathode and lithium anode in a more even way. However, the cell failure after 45 cycles was still caused by short circuit as a result of electrolyte consumption and resulting localized reaction current. This double-side coated separator has been applied in the fabrication and testing of high energy Li-S pouch cells.

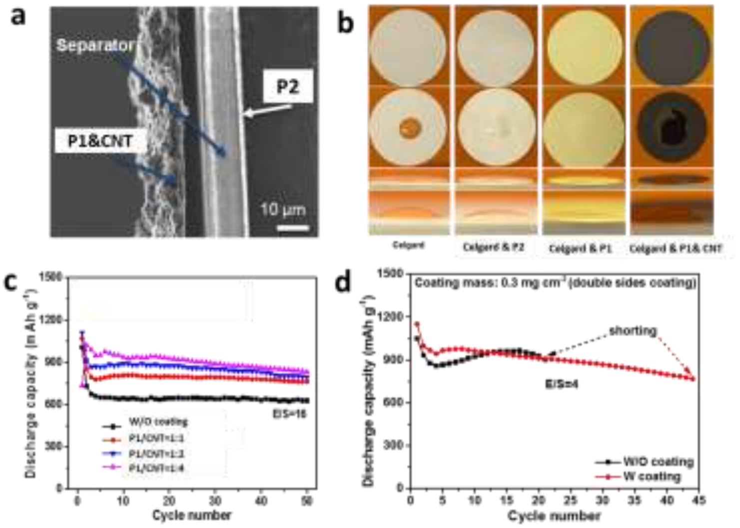

Figure 75. (a) Cross-sectional scanning electron microscopy (SEM) of double-side coated Celgard 2500. (b) Digital photographs of the static contact angles of the coated separators with electrolyte 1 M LiTFSI/DOL/DME+0.3M $LiNO_3$. (3) Effects on separator coating on sulfur utilization rate. (4) Cycling stability of cells at lean electrolyte conditions (E/S= 4 µl/mg) (sulfur loading of electrode: 4 mg/cm^2).

Patents/Publications/Presentations

Presentations

- BMR Li-S Deep Dive Meeting, Austin, Texas (September 5–6, 2018): “Development of High Energy Lithium-Sulfur Batteries”; D. Lu and J. Liu.
- Battery Electric Vehicle Architectures (BEVA) USA 2018 Congress, San Francisco, California (September 2018): Development of High Energy Lithium-Sulfur Batteries: From Materials to Pouch Cell”; D. Lu, J. Xiao, and J. Liu.
- Americas International Meeting on Electrochemistry and Solid-State Science, Cancun, Mexico (September 2018): “Rational Design of High Energy Sulfur Cathodes for Lithium-Sulfur Batteries”; D. Lu, L. Shi, J. Xiao, J. Zhang, and J. Liu.
- Americas International Meeting on Electrochemistry and Solid-State Science, Cancun, Mexico (September 2018): “Sulfide Based Solid Conductor for Lithium-Sulfur Batteries”; D. Lu, Y. Wang, J. Xiao, J. Zhang, and J. Liu.

Task 5.3 – Nanostructured Design of Sulfur Cathodes for High-Energy Lithium-Sulfur Batteries (Yi Cui, Stanford University)

Project Objective. The charge capacity limitations of conventional TM oxide cathodes are overcome by designing optimized nano-architectured sulfur cathodes. This study aims to enable sulfur cathodes with high capacity and long cycle life by developing sulfur cathodes from the perspective of nanostructured materials design, which will be used to combine with Li-metal anodes to generate high-energy Li-S batteries. Novel sulfur nanostructures as well as multi-functional coatings will be designed and fabricated to overcome issues related to volume expansion, polysulfide dissolution, and the insulating nature of sulfur.

Project Impact. The capacity and the cycling stability of sulfur cathode will be dramatically increased. This project's success will make Li-S batteries to power EVs and decrease the high cost of batteries.

Approach. The approach comprises the three main parts shown below, with primary activities listed.

- ***Advanced nanostructured sulfur cathodes design and synthesis:*** (1) Engineer empty space into sulfur cathode to solve the problem of electrode volume expansion; (2) Develop novel sulfur nanostructures with multi-functional coatings for the confinement of sulfur/lithium polysulfides to address the issues of active materials loss and low conductivity; (3) Develop/discover optimal nanostructured materials that can capture the polysulfide dissolved in the electrolyte; (4) Develop space efficiently packed nanostructured sulfur cathode to increase the volumetric energy density and rate capability; and (5) Identify the interaction mechanism between sulfur species and different types of oxides/sulfides, and find the optimal material to improve the capacity and cycling of sulfur cathode.
- ***Structure and property characterization:*** (1) *Ex situ* SEM; (2) XPS analysis; and (3) *In operando* XRD and optical microscopy.
- **Electrochemical testing:** (1) Coin cells and pouch cells and (2) a set of electrochemical techniques.

Out-Year Goals. The cycle life, capacity retention, and capacity loading of sulfur cathodes will be greatly improved (200 cycles with 80% capacity retention, > 0.3 mAh/cm^2 capacity loading) by optimizing material design, synthesis, and electrode assembly.

Collaborations. This project engages in collaboration with the following: BMR PIs; SLAC National Accelerator Laboratory: Dr. M. Toney (*In situ* X-ray); and Stanford: Professor Nix (mechanics) and Professor Bao (materials).

Milestones

1. Elucidate different adsorption mechanisms and probe possible adsorption species. (Q2, FY 2018, January 2018; Completed)
2. Develop multi-functional sulfur cathode binder capable of controlling the polysulfide shuttling and facilitating Li-ion transport. (Q3, FY 2018, April 2018; Completed)
3. Demonstrate the flame-retardant property of binder to improve safety and propose flame-retardant mechanism. (Q4, FY 2018, July 2018; Completed)
4. Build *in situ* characterization platform to monitor nucleation/dissolution of sulfur/Li_2S_n. (Q1, FY 2019, October 2018; Completed)
5. Develop a noninvasive imaging method with sub-micron, sub-second resolution for Li-S battery in label-free, native organic liquid electrolyte. (Q2, FY 2019, January 2019; In progress)

Progress Report

Last quarter, it was demonstrated that ammonium polyphosphate (APP) bestows the sulfur cathode with significantly improved flame-retardant property, thus improving the safety of Li-S batteries. This quarter, the team built an *in situ* characterization platform to monitor nucleation/dissolution of sulfur to provide direct evidence about a long-debated reaction pathway for sulfur.

Probing sulfur electrochemistry has multiple challenges, including the following: (a) sulfur and its reduced species are extremely sensitive to vacuum, electron beam irradiation, and X-ray irradiation, which limits the diagnostic tools one can use; (b) sulfur has a large family of intermediate species connected by interwoven reaction pathways, which could be easily disturbed by added indicators or labels; and (c) the materials easily change upon removing from native electrolyte, hence often requiring *in operando* study.

Here the team combined DFLM and a planar electrochemical cell fabricated on a glass slide to visualize sulfur electrochemistry *in operando* (Figure 76a). Visible light is a benign probe that allows noninvasive study in native ether-based liquid electrolyte, while dark-field illumination was used to enhance the sensitivity to small features on a flat background. Lithium polysulfide (Li_2S_8) was dissolved in DOL and dimethyl ether (DME) and served as the electrolyte and sulfur source. A metal grid electrode (1-μm in line width, 50-nm in height) was deposited on a glass substrate via e-beam lithography and evaporation (Figure 76b-c), while lithium metal placed on the same plane was the counter/reference electrode. During galvanostatic charging/discharging at room temperature (Figure 76d), sulfur deposits onto and strips from the working electrode, while DFLM images of a 180-μm × 135-μm region on the surface of the substrate were captured at 1 frame/second simultaneously. A white light source and a three-color-channel CMOS camera were used to record color information. Using this technique, the team was able to directly observe multiple new phenomena in Li-S batteries for the first time, including the electrochemical generation of metastable liquid sulfur at room temperature, etc.

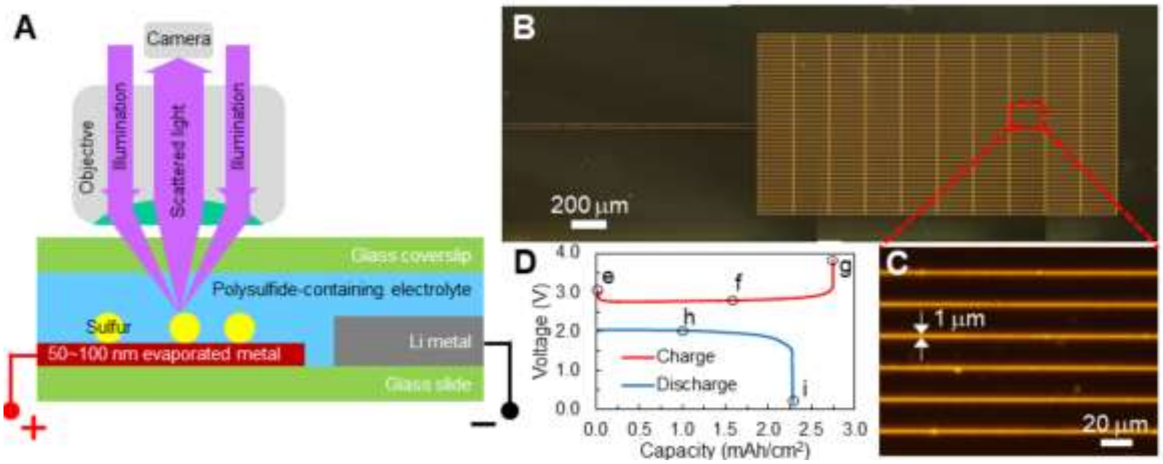

Figure 76. (a) Schematic of the electrochemical cell design that allows *in operando* dark field light microscopy (DFLM) observation. (b-c) DFLM images of the metal grid (50-nm thick, 1-μm wide) fabricated on glass slide as a substrate for the electrochemical cell. (d) Voltage profile of the cell.

Patents/Publications/Presentations

Publication

- Zhou, G., K. Liu, Y. Fan, M. Yuan, B. Liu, W. Liu, F. Shi, Y. Liu, W. Chen, J. Lopez, D. Zhuo, J. Zhao, Y. Tsao, X. Huang, Q. Zhang, and Y. Cui.* “An Aqueous Inorganic Polymer Binder for High Performance Lithium–Sulfur Batteries with Flame-Retardant Properties.” ACS *Central Science* 4, no. 2 (2018): 260–267.

Task 5.4 – Addressing Internal “Shuttle” Effect: Electrolyte Design and Cathode Morphology Evolution in Lithium-Sulfur Batteries
(Perla Balbuena, Texas A&M University; Partha Mukherjee, Purdue University)

Project Objective. The project objective is to overcome the Li-metal anode deterioration issues through advanced Li-anode protection/stabilization strategies including (1) *in situ* chemical formation of a protective passivation layer and (2) alleviation of the “aggressiveness” of the environment at the anode by minimizing the polysulfide shuttle with advanced cathode structure design.

Project Impact. Through formulation of alternative electrolyte chemistries as well as design, fabrication, and test of improved cathode architectures, it is expected that this project will deliver Li/S cells operating for 500 cycles at efficiency greater than 80%.

Approach. A mesoscale model including different realizations of electrode mesoporous structures generated based on a stochastic reconstruction method will allow virtual screening of the cathode microstructural features and the corresponding effects on electronic/ionic conductivity and morphological evolution. Interfacial reactions at the anode due to the presence of polysulfide species will be characterized with *ab initio* methods. For the cathode interfacial reactions, data and detailed structural and energetic information obtained from atomistic-level studies will be used in a mesoscopic-level analysis. A novel sonochemical fabrication method is expected to generate controlled cathode mesoporous structures that will be tested along with new electrolyte formulations based on the knowledge gained from the mesoscale and atomistic modeling efforts.

Out-Year Goals. By determining reasons for successes or failures of specific electrolyte chemistries, and assessing relative effects of composite cathode microstructure and internal shuttle chemistry versus that of electrolyte chemistry on cell performance, expected results are as follows: (1) develop an improved understanding of the Li-S chemistry and ways to control it, (2) develop electrolyte formulations able to stabilize the lithium anode, (3) develop new composite cathode microstructures with enhanced cathode performance, and (4) develop a Li-S cell operating for 500 cycles at an efficiency greater than 80%.

Collaborations. This is a collaborative work combining first-principles modeling (P. Balbuena, TAMU), mesoscopic-level modeling (P. Mukherjee, Purdue University), and synthesis, fabrication, and test of Li/S materials and cells (V. Pol, Purdue University). Balbuena also collaborates with M. Vijayakumar from PNNL.

Milestones

1. Elucidate effects of PS migration and reduction at the anode on overall performance. (September 30, 2018; Completed Q3)
2. Investigate charge reactions of nucleating Li_2S structures. (September 30, 2018; Completed Q2)

Progress Report

Physicochemical Origins of Electrochemical Hysteresis in Li-S Cell. The electrochemical progression is different during charge and discharge operations for a Li-S cell. During discharge, sulfur successively reduces to lower order polysulfides and deposits in the form of solid Li_2S. During charging, since the electrode potential is greater than oxidation potentials for each of the intermediate sulfur species, all the oxidation reactions take place concurrently and start forming solid sulfur from a very early stage. This leads to partial coverage of the Li_2S surface by solid sulfur. Based on the morphologies of Li_2S and solid sulfur, the extent of this coverage varies. For example, a film-type sulfur deposition covers more Li_2S. In the extreme event, freshly deposited sulfur can completely overlap on the remaining Li_2S and prevent its further dissolution in the electrolyte. Such isolated Li_2S cannot be oxidized back to sulfur, and thus amounts to capacity decay. Another factor that further complicates such isolation is the affinity of sulfur to deposit on the backbone substrate (for example, carbon). If the substrate is sulfur-philic, Li_2S isolation is reduced; however, it makes for a more deteriorative surface passivation and in turn increases the overpotentials.

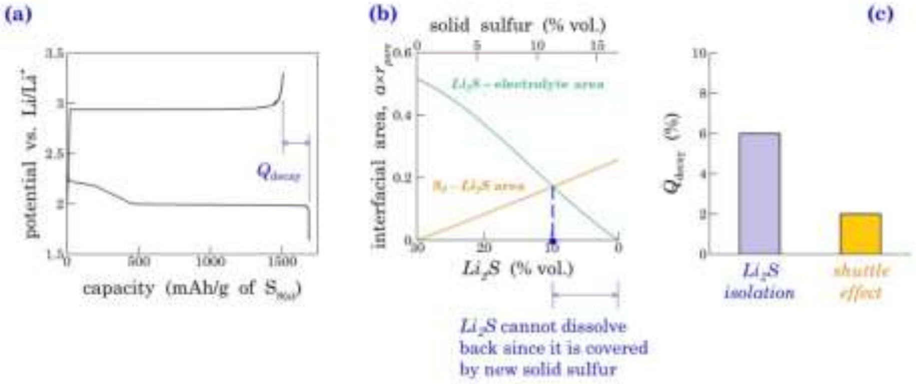

Figure 77. (a) Charge-discharge hysteresis is composed of dissimilar potential profiles and unequal capacities. (b) Dissolution of Li_2S does not often proceed to completion, as freshly precipitated sulfur covers Li_2S surface. (c) Both Li_2S isolation and shuttle effect fundamentally lead to such hysteresis.

In addition to the sulfur isolation effect, shuttle effect also plays a crucial role. As higher-order polysulfides are formed at the cathode (during charging), a concentration drop develops from the cathode to anode and gives rise to diffusional fluxes towards lithium. Simultaneously, the electrolyte phase potential gradient is formed to migrate ions from anode to cathode. Based on the charging current (C-rate), the relative contribution of migration and diffusional fluxes vary and lead to varying degree of shuttle effect contributions.

Lithiated Sulfurized-Carbonaceous Composite $C_{1.96}N_{0.29}H_{0.13}SLi_{2.50}$. The sulfurized polyacrylonitrile composite (SPAN) has emerged as a very promising cathode material for Li-S batteries due to its excellent polysulfide retention and cycling performance. The latest calculations conducted by the team studied the structural features and lithiation mechanisms of these materials. The team found evidence of C-S chemical bonding and no formation of long-chain polysulfides during lithiation. Moreover, at high lithium contents, significant C-Li and N-Li interactions were found that might contribute to an extended lithiation process beyond a Li:S 2:1 molar ratio in SPAN composites (Figure 78). The team's calculations corroborate the experimental findings and pave the way to a rational design of SPAN-based cathodes for Li-S batteries. Currently, the team is aiming to get a better understanding of long-term effects of these C-Li and N-Li interactions during battery cycling.

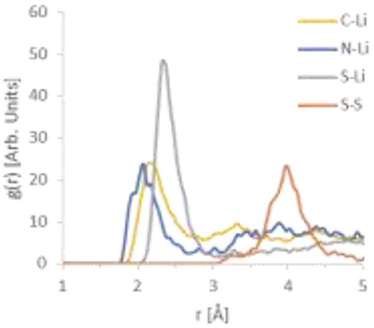

Figure 78. Radial distribution function illustrating the main C-Li, N-Li, S-Li, and S-S interactions.

Patents/Publications/Presentations

Publications

- Mistry, A., and P. P. Mukherjee. "Electrolyte Transport Evolution Dynamics in Li-Sulfur Batteries." *Journal of Physical Chemistry C*, 122 (2018): 18329. doi: 10.1021/acs.jpcc.8b05442.
- Mistry, A., and P. P. Mukherjee. "'Shuttle' in Polysulfide Shuttle: Friend or Foe?" *Journal of Physical Chemistry C*, in press (2018). doi: 10.1021/acs.jpcc.8b06077.
- Perez-Beltran, S., and P. B. Balbuena. "First-Principles Explorations of the Electrochemical Lithiation Dynamics of a Multilayer Graphene Nanosheet-Based Sulfur-Carbon Composite." *Journal of Materials Chemistry A* 6 (2018): 18084–18094.

Presentations

- NREL, Denver, Colorado (June 26, 2018): "Addressing Main Issues of Lithium-Sulfur Batteries"; P. B. Balbuena.
- BMR Li-S Deep Dive Meeting, Austin, Texas (September 5-6, 2018): "Update on Li-S Batteries"; P. B. Balbuena.
- BMR Li-S Deep Dive Meeting, Austin, Texas (September 5-6, 2018): "Mesoscale Complexations in Li-Sulfur Batteries"; P. P. Mukherjee.

Task 5.5 –Investigation of Sulfur Reaction Mechanisms (Deyang Qu, University of Wisconsin at Milwaukee; Xiao-Qing Yang, Brookhaven National Laboratory)

Project Objective. The primary objectives are (1) to conduct focused fundamental research on the mechanism of "shuttle effect" inhibition for the rechargeable Li-S batteries, and (2) to develop electrode and electrolyte systems that can mitigate "shuttle effect" so low self-discharge and long cycle life can be achieved. Special attention will be paid to the following: investigating chemical interactions between additives and dissolved polysulfides, management for solubility of polysulfide ions, formation of SEI layer and dead lithium on surface of lithium anode, and exploration of electrode and cell designs. Through such investigations, the Li-S chemistry will be studied systematically, and scientific understanding of the inhibition mechanism for "shuttle effect" can be well utilized to guide system engineering design. The goal is to develop a practical rechargeable Li-S battery to meet the challenges of powering next-generation EVs beyond Li-ion technologies.

Project Impact. With the unique *in situ* electrochemical-HPLC/MS technique developed in this program, the mechanisms of all reactions in a Li-S cell can be revealed. The interactions between additives and the soluble polysulfides can be investigated in real-time toward mitigation of "shuttle effect." The results will guide development of sulfur cathode and Li-S designs for EVs.

Approach. This project will use *in situ* electrochemical-MS, electrochemical-HPLC/MS, XPS, SEM, and XRD to study electrochemical reactions associated with sulfur electrodes. Electrochemical techniques such as AC impedance, rotation ring disk electrode, and galvanostat will be used to study the electrode process kinetics. The project will use an *in situ* electrochemical optical method to investigate the surface of lithium anode during cycling of a Li-S cell.

One-Year Goals. The one-year goals include the following: (1) complete preliminary investigations of the inhibition mechanism for the "shuttle effect" and evaluation of "shuttle effect" inhibitors, and (2) complete preliminary design and tests of sulfur-containing electrodes and electrolytes.

Collaborations. The PI, D. Qu, is the Johnson Controls Endowed Chair Professor; thus, the UWM and BNL team has close collaboration with Johnson Controls' scientists and engineers. This collaboration enables the team to validate the outcomes of fundamental research in pilot-scale cells. This team has been closely working with top scientists on new material synthesis at ANL, LBNL, and PNNL, with U. S. industrial collaborators at GM, Duracell, and Johnson Controls as well as international collaborators in China, Japan, and South Korea. These collaborations will be strengthened and expanded to give this project a vision on both today's state-of-the-art technology and tomorrow's technology in development, with feedback from the material designer and synthesizers upstream and from industrial end users downstream.

Milestones

1. Complete the investigation and determination of the possible chemical reactions between dissolved polysulfide ions with the materials in a Li-S cell, both active and inactive during the storage, and thus the stability of battery components. (Q1, December 31, 2017; Completed)
2. Complete tabulating the list of materials to be tested as inhibitive additives to mitigate "shuttle effect"; start the tests and develop understanding of the mechanism of such effects. (Q2, March 31, 2018; Completed)
3. Complete testing the inhibitive additives; start to explore and design sulfur-containing electrode materials. (Q3, FY 2018; Completed on June 30, 2018)
4. Complete the preliminary engineering design and test for the new sulfur-containing electrode materials. (Q4, FY 2018; Completed on September 30, 2018)

Progress Report

This quarter, the team continued to synthesize new polymer materials as sulfur cathode and test the synthesized sulfur cathode material. In addition, they started to look for the anode materials that do not react with dissolved polysulfide. The scheme below shows the team's thinking of mitigating the "shuttle-effect" of the dissolved polysulfide ions. The main purposes are first to localize the dissolved polysulfide ions in the cathode matrix, and second to prevent the chemical reactions between the anode and dissolved polysulfide ions. The team is exploring to bond the polysulfide species on the backbone materials, and investigating new anode materials.

$$\boldsymbol{S_8} \cancel{\rightarrow} \boldsymbol{S_8^{2-}} \rightleftarrows \boldsymbol{S_7^{2-}} \rightleftarrows \boldsymbol{S_6^{2-}} \rightleftarrows \boldsymbol{S_5^{2-}} \cancel{\xrightarrow{+Li\,metal}} \rightleftharpoons \boldsymbol{S_4^{2-}} + S_3^{2-} + Li_2S_2 \downarrow + Li_2S \downarrow$$

Prevent dissolution of the polysulfide ions and their reaction with the anode.

The team synthesized a few copolymerized sulfur materials according to the various strategies to localize the polysulfide ions with limited success. The results are tabulated in Table 6. It seems copolymers #1, #6, and #10 had relatively better cyclability than a sulfur cathode, but the initial capacity of all cathodes was lower than that of sulfur cathode. More copolymerized sulfur compounds are being synthesized and tested.

Table 6. Test results of 10 synthesized co-polymers. The control is sulfur cathode with 75% sulfur.

Sulfur Polymer	1st Discharge Capacity (mAh/g)	50th Discharge Capacity (mAh/g)	Retention (%)
1	626	455	72.7
2	623	283	45.4
3	554	253	45.7
4	448	201	44.9
5	905	412	45.5
6	333	249	74.8
7	591	228	38.6
8	345	134	38.8
9	176	69	39.2
10	473	288	61.0
S	672	267	39.7

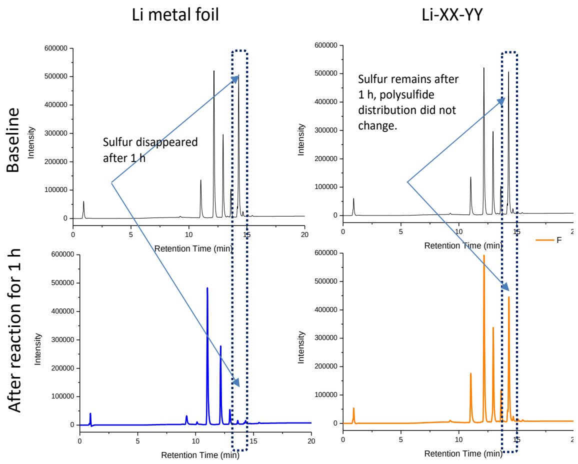

Figure 79. Chemical reaction between Li-containing anode materials with dissolved polysulfide ions detected by liquid chromatography. The anode materials were put in the electrolyte solution with polysulfide ion.

The team also tested a few anode materials and found one composite material that does not react with polysulfide ions as much. The results are shown in Figure 79 in comparison with metallic lithium. After 1 h exposure to the metallic lithium, all the elemental sulfur disappeared. However, under the same condition, the dissolved elemental sulfur remained intact contacting the Li-composite anode. The anode material has specific capacity around 600 mAh/g.

Patents/Publications/Presentations

Publication

- Zheng, D., G. Wang, D. Liu, J. Si, T. Ding, D. Qu, X. Yang, and D. Qu. “The Progress of Li-S batteries – Understanding of the Sulfur Redox Mechanism.” *Advanced Materials Technology*. doi: https://doi.org/10.1002/admt.201700233.

Task 5.6 – Statically and Dynamically Stable Lithium-Sulfur Batteries
(Arumugam Manthiram, University of Texas at Austin)

Project Objective. The project objective is to develop statically and dynamically stable Li-S batteries by integrating polysulfide-filter-coated separators with a protected Li-metal anode through additives or a modified Li_2S cathode with little or no charge barrier during first charge. The project includes demonstration of electrochemically stable cells with sulfur capacities of > 1000 mAh g^{-1} and cycle life in excess of 500 cycles (dynamic stability) along with positive storage properties (static stability) at > 70 wt% sulfur content and ~ 5 mg cm^{-2} loading.

Project Impact. The combination of polysulfide-filter (PS-filter)-coated separator, Li-metal-protection additives, and Li_2S cathode modifications offers a viable approach to overcome the persistent problems of Li-S batteries. This project is systematically integrating the basic science understanding gained in its laboratory of these three aspects to develop the Li-S technology as the next-generation power source for EVs. The project targets demonstrating cells with sulfur capacities of over 1000 mA h g^{-1} and cycle life in excess of 500 cycles along with good storage properties at high sulfur content and loading that will make the Li-S technology superior to the present-day Li-ion technology in terms of cost and cell performance.

Approach. Electrochemical stability of the Li-S cells is improved by three complementary approaches. The first approach focuses on establishment of an electrochemically stable cathode environment by employing PS-filter-coated separators. The PS-filter coatings aim to suppress the severe polysulfide diffusion and improve the redox capability of Li-S cells with high-sulfur loadings. The study includes an understanding of materials characteristics, fabrication parameters, electrochemical properties, and battery performance of the PS-filter-coated separators. The second approach focuses on electrode engineering from two aspects. First, investigation of a Li-metal anode with coating- and additive-supporting approaches is aimed at improving the safety of Li-S cells. Second, research on activated-Li_2S cathode with little or no charge-barrier will promote performance and safety of the C-Li_2S cells. Integration of the first two approaches would create statically and dynamically stable Li-S batteries for EVs.

Out-Year Goals. The overall goal is to develop statically and dynamically stable Li-S batteries with custom cathode and stabilized anode active materials. In addition to developing a high-performance battery system, a fundamental understanding of the structure-configuration-performance relationships will be established. Specifically, the optimization of the electrochemical and engineering parameters of PS-filter-coated separators aims at comprehensively investigating different coating materials and their corresponding coating techniques for realizing various high-performance custom separators. The developed PS-filter-coated separators can be coupled with pure sulfur cathodes with high-sulfur loading and content. Multi-functional PS-filter-coated separators, high-loading sulfur cathodes, stabilized-Li-metal anodes, activated-Li_2S cathodes, and novel cell design are anticipated to provide an in-depth understanding of the Li-S battery chemistry and to realize statically and dynamically stable Li-S batteries.

Collaborations. There are no collaborative activities this quarter.

Milestones

1. Develop Li-metal anodes with high electrochemical stability. (Q1, December 2017; Completed)
2. Develop Li_2S cathodes with low activation barrier and polarization. (Q2, March 2018; Completed)
3. Demonstrate high-loading coin cells and pouch cell prototypes. (Q3, June 2018; Completed)
4. *Go/No Go Decision*: Study cost and environmental impact assessment of the technology. (Q4, September 2018; Completed)

Progress Report

Establishing high-energy-density Li-S batteries relies on the design of electrode substrates that can host a high sulfur loading with reasonably lean electrolyte while still attaining a high electrochemical utilization. For practical application, it is necessary to develop the Li-S technology by transitioning from coin-type cells with small size electrodes to pouch-type cells with electrode sizes similar or close to that of practical battery electrodes.

To develop and assess design of Li-S pouch cells with a high sulfur loading, cathode engineering was focused on this quarter (Figure 80). In addition, the cost and environmental issues involved with high-loading cathode configurations in pouch cells were considered. Thus, a simple S-based active-material composite was used. The active-material composite with pristine sulfur, KetJen Black (KJB), and CNT was prepared through a melt-diffusion process at 155°C. The synthesized active-material composite (S/KJB/CNT) was mixed with additional conductive carbon and polymer binders. The resultant active-material slurry was then coated onto an aluminum foil and dried in a vacuum oven at 50°C. All materials, including active sulfur and other inactive materials, and the heat-treatment methods are similar to those commonly used with Li-S cathodes. Thus, the cathode preparation was made as simple as possible. A simplified cathode-preparation method allows the team to prepare a high volume of cathodes with high repeatability and stability, limiting the cost issues encountered in cathode optimization. The prepared cathode was cut in a size of 47.8 mm x 81.5 mm and had a sulfur content of 65 wt% and a sulfur loading of 6 mg cm^{-2}. In the cell-assembly process, a lithium foil was cut into the same size as the cathode. A sheet of coated separator was then placed between the two electrodes, and the assembled cell was sealed in a plastic film pouch. The E/S ratio was 5 µL mg^{-1}. The assembled cells were rested for 2 h and then cycled in the voltage window of 1.65-2.60 V at a C/20 rate.

Figure 80. Sulfur cathodes fabricated for Li-S pouch cells.

Figure 81a shows the voltage profile of the Li-S pouch cells. After the first cycle, the discharge-charge curves exhibit the typical two-step redox reaction of the Li-S chemistry. The discharge capacity at the first cycle reaches 995 mA h g^{-1}, which corresponds to 60% electrochemical utilization. Considering the larger areal size of the cell (38.9 cm^{2}), the cell still shows outstanding performance. As a reference, the areal size of the regular coin cell is only 1.13 cm^{2}. After 18 cycles, the discharge capacity remains at 661 mA h g^{-1}, which corresponds to a high capacity retention of 66% (Figure 81b), offering a path forward to fabricate Li-S pouch cells with good consistency. This allows the team to avoid the concern of applying a high amount of toxic starting active materials, such as liquid-state polysulfide catholyte that has strong activity or lithium sulfide that has strong sensitivity toward air and moisture. However, the CE is relatively low (~ 80%). The lower CE could be due to severe degradation of the Li-metal anode, which needs to be addressed as part of the future work.

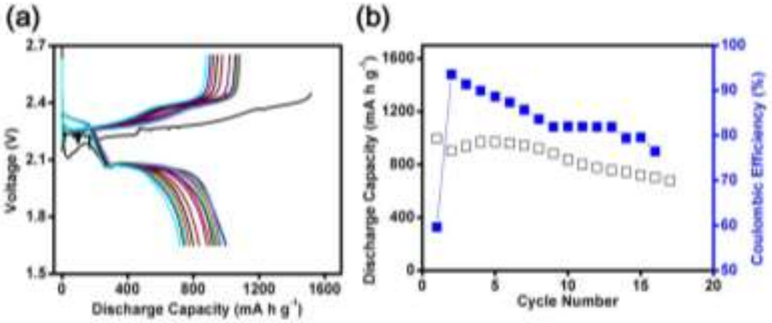

Figure 81. Electrochemical performance of the Li-S pouch cell: (a) voltage profiles and (b) cycling performance.

Patents/Publications/Presentations

Publications

- Luo, L., S.-H. Chung, and A. Manthiram. "Long-Life Lithium-Sulfur Batteries with a Bifunctional Cathode Substrate Configured with Boron Carbide Nanowires." *Advanced Materials* 30 (2018): 1804149.
- Chung, S.-H., K.-Y. Lai, and A. Manthiram. "A Facile, Low-Cost Hot-Pressing Process for Fabricating Lithium-Sulfur Cells with Stable Dynamic and Static Electrochemistry." *Advanced Materials* (2018). doi: 10.1002/adma.201805571.

Presentations

- Hefei University, Hefei, China (July 14–15, 2018): "Next-Generation Rechargeable Battery Chemistries"; A. Manthiram. Invited.
- 3rd International Symposium on Renewable Energy Technologies, Gold Coast, Australia (July 19–22, 2018): "Materials Challenges and Prospects of Electrical Energy Storage"; A. Manthiram. Invited plenary talk.
- 16th Asian Conference on Solid-State Ionics, Shanghai, China (August 5–9, 2018): "Where is Electrical Energy Storage Headed?"; A. Manthiram. Invited plenary talk.
- BMR Li-S Deep Dive Meeting, Austin, Texas (September 5–6, 2018): "Lithium-Sulfur Batteries: Progress, Benchmarks, and Challenges"; A. Manthiram. Invited.

Task 5.7 – Electrochemically Responsive, Self-Formed, Lithium-Ion Conductors for High-Performance Lithium-Metal Anodes

(Donghai Wang, Pennsylvania State University)

Project Objective. The project objective is to develop and deliver an electrochemically responsive self-formed hybrid LIC as a protective layer for Li-metal anodes, enabling Li-metal anodes to cycle with a high efficiency of ~ 99.7% at high electrode capacity (> 6 mAh/cm^2) and high current density (> 2 mA/cm^2) for over 500 cycles. The project will also demonstrate prototype ~ 300 mAh Li-S battery cells with energy densities of ~ 200 Wh/kg and ~ 80% capacity retention for ~ 300 cycles at ~ 80% depth of discharge using Li-metal anodes with this protective layer.

Project Impact. This project aims to develop a new hybrid LIC that enables safe and high-performance Li-metal anodes. The use of these high-performance Li-metal anodes in turn enables Li-S batteries with high energy density and long cycling life. Such anodes can also lead to a 50% increase in the energy density of conventional Li-ion batteries with Li-metal oxide cathodes. Meeting the technical targets will potentially develop a new high-energy-density lithium battery, promote increased adoption of EVs and PHEVs, and reduce petroleum consumption in the transportation sector by helping battery-powered vehicles become accepted by consumers as a reliable source of transportation.

Approach. The novel multiphase organo-Li_xS_y or organo-$Li_xP_yS_z$ hybrid ion conductors with tunable multi-functional organic components and controlled Li_xS_y and $Li_xP_yS_z$ inorganic components will be designed and prepared, and thus enable safe use of lithium metal with high CE. In the second year, the team will develop the 2nd generation of organo-Li_xS_y lithium protection layers with tuned functionality: (1) finding appropriate composition, (2) developing appropriate synthesis and fabrication methods, and (3) optimizing organic components in a protection layer to further improve CE and Li-S battery performance.

Out-Year Goals. Work will progress toward development of the 2nd generation of organo-Li_xS_y lithium protection layers with tuned functionality. Characterization, performance, and compatibility tests on materials and systems will be conducted. Uniform and dendrite-free lithium deposition under the protection of the 2nd generation of organo-Li_xS_y lithium protective layers will be demonstrated, and CE will be further improved.

Collaborations. There are no active collaborations.

Milestones

1. Development of the 2nd generation of organo-Li_xS_y lithium protection layers with tuned functionality. Conduct characterization and performance tests on the materials. (Q1, FY 2018; Completed)
2. Demonstrate uniform and dendrite-free lithium deposition under protection of the 2nd generation of organo-Li_xS_y lithium protective layers. (Q2, FY 2018; Completed)
3. Optimize the 2nd generation of organo-Li_xS_y lithium protective layer and demonstrate lithium anodes cycling with ~ 98.8% CE for ~ 200 cycles. (Q3, FY 2018; Completed)
4. Demonstrate lithium anodes with optimized 2nd generation of organo-Li_xS_y lithium protective layer and ~ 99.2% CE for ~ 300 cycles. (Q4, FY 2018; Completed)

Progress Report

The CE and cycling stability of lithium deposition/dissolution at high current densities and deposition capacities are investigated. The stable hybrid SEI layer fabricated from PSD-90-Ely significantly improves the CE. The cycling performance of lithium deposition/dissolution using PSD-90-Ely is shown in Figure 82. At the current density of 2 mA cm^{-2} and deposition capacity of 2 mA h cm^{-2}, the average CE achieved can be as high as 99% over 250 cycles (Figure 82a). When the capacity of 3 mA h cm^{-2} was applied, the cells delivered a high average CE of 98.9% over 250 cycles (Figure 82b). Especially from 160th cycle to 220th cycle, the average CE is as high as ~ 99.5%. The voltage profiles of lithium deposition/dissolution (Figure 82c) indicate the cells using PSD-90-Ely show lower polarization than those with C-Ely. Moreover, in contrast to the cells using C-Ely, the batteries using PSD-90-Ely show more stable and smaller voltage hysteresis at ~ 47 mV over 200 cycles (Figure 82d). Both the low polarization and the modest and stable hysteresis are mainly due to the durable and flexible SEI layer that enables the compact and uniform lithium deposition leading to thin and uniform SEI to accumulate over the electrode surface.

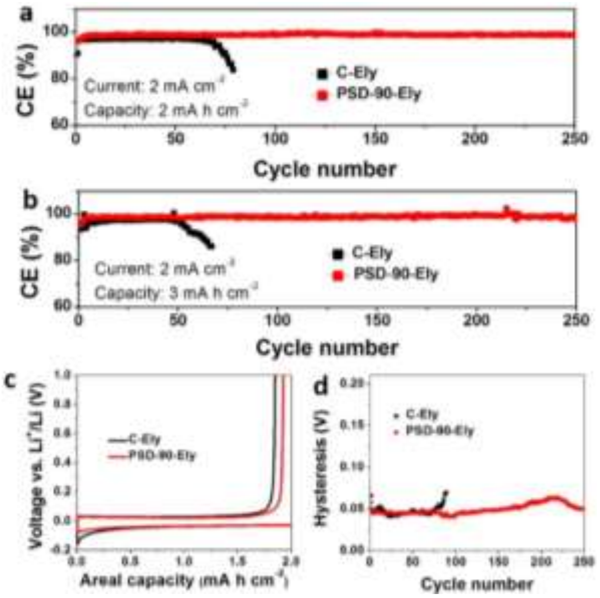

Figure 82. Cycling performances of lithium deposition/dissolution using the PSD-90-Ely and C-Ely at a current density of 2 mA cm^{-2} and a deposition capacity of 2 (a) and 3 mA h cm^{-2} (b). (c) Voltage profiles (the first cycle) and (d) average voltage hysteresis of (b).

At an extremely high capacity and current density (4 mA h cm^{-2} and 4 mA cm^{-2}), the stable hybrid SEI layer still enables improved CE. As shown in Figure 83, a high average CE of ~ 97% can be maintained over 150 cycles. From 95th cycle to 115th cycle, the average CE can reach as high as 99.5%.

After finishing the goals of Budget Period 2, preliminary study was also conducted in Budget Period 3. Polymers containing P_xS_y components (polymer-P_xS_y) were synthesized through the reaction of sulfur anion (S_n^-) containing trifunctional crosslinker lithium polythiophosphate with a chlorine-rich polymer. Then the polymers were directly coated on the substrates (Figure 84); during lithium plating/stripping, the polymers react with

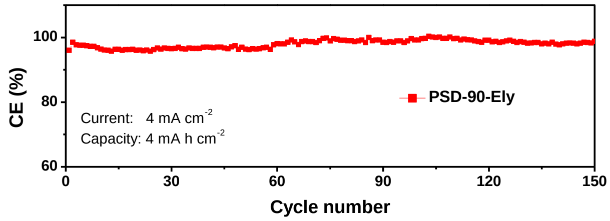

Figure 83. Lithium deposition/dissolution cycling performances of the cells using PSD-90-Ely at a current density of 4 mA cm^{-2} with a deposition capacity of 4 mA h cm^{-2}.

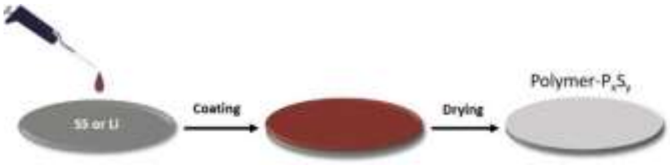

Figure 84. Schematic illustration for the fabrication of polymer-P_xS_y protective layer on substrates.

lithium metal and *in situ* release lithium sulfides and $Li_xP_yS_z$ at the interface of polymer and lithium metal to form organo-Li_xS_y/organo-$Li_xP_yS_z$ composite protection layer. Figure 85 shows the SEM images of the as-prepared polymer-P_xS_y film, which appears to form a very uniform coating layer with a thickness around 7.0 µm.

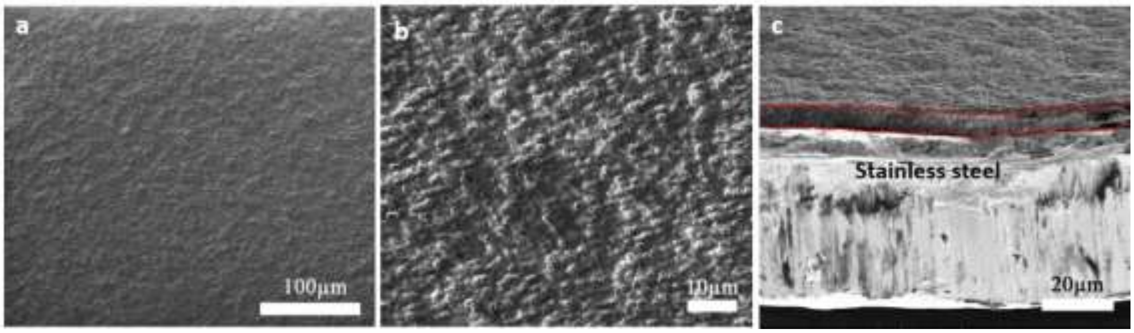

Figure 85. Scanning electron microscopy images of the as-prepared polymer-P_xS_y film on SS foil.

Patents/Publications/Presentations

The project has no patents, publications, or presentations to report this quarter.

Task 5.8 – Materials and Cell Design Optimization for Lithium-Sulfur Battery Technology (Hong Gan, Brookhaven National Laboratory)

Project Objective. Develop a low-cost battery technology for PEV application utilizing the Li-S electrochemical system by incorporating new materials (cathode, electrolyte, additives), consistent with DOE's long-term goals.

Project Impact. The Li-S battery system has gained significant interest due to its low material cost potential (35% cathode cost reduction over Li-ion) and its attractive 2.8x (volumetric) to 6.4x (gravimetric) higher theoretical energy density compared to conventional Li-ion benchmark systems. Commercialization of this technology requires overcoming several technical challenges. This effort will focus on improving the cathode energy density, power capability, and cycling stability by introducing optimized multifunctional cathode additives (MFCA) and multifunctional electrolyte (MFE) and conductive carbon host. The primary deliverable of this project is to boost the sulfur utilization and further improve the energy efficiency and the energy density at the cell level for Li-S battery technology.

Approach. In the past three years, the team successfully completed the project "*Multi-Functional Cathode Additives (MFCA) for Li-S Battery Technology*." The layer structured TiS_2 has been identified as the true MFCA for Li-S cells, which is conductive electronically, active electrochemically, and with ability to adsorb polysulfide. By incorporating all the improvements—including the TiS_2 additive, the formulation optimization, the new binder and new carbon host for high sulfur loading, the electrode processing optimization, the electrode density control, and the electrolyte fill weight control—2032 coin cells with > 4 mAh delivered capacity with excellent cycle life have been demonstrated. This year, the team will build on previous work by incorporating MFE studies, in addition to the cathode material studies to further optimize Li-S cell performance.

Out-Year Goals. To address the system level interactions, one area of research will be the electrolyte and electrolyte additives, since electrolyte is a critical component in the Li-S battery for polysulfide dissolution, lithium anode SEI protection, and cathode interface reaction control. The project will continue to look into electrolytes with reduced polysulfide solubility, and the electrolytes/additives with ability to improve sulfur utilization to achieve long cycle life and high energy-efficiency. Improvement of sulfur utilization and the delivered energy density at the electrode level will also be achieved by introducing the 2D-nano-sheet TiS_2 with reduced particle size and increased Brunauer–Emmett–Teller (BET) surface area for maximized polysulfide–TiS_2 interaction, and by introducing the new carbon host of high pore volume and high BET surface area with controlled particle size distribution for high sulfur loading.

Collaborations. This project collaborates with D. Su (BNL), X. Tong (BNL), Q. Wu and Y-C. K. Chen-Wiegart (SBU, BNL), A. Marschilok (SBU), K. Takeuchi (SBU), and E. Takeuchi (SBU, BNL).

Milestones

1. Electrolyte with low polysulfide solubility. (Q1, December 2017; Completed)
2. Electrolyte additive investigation for improved sulfur utilization. (Q2, March 2018; Completed)
3. Proof-of-concept testing of 2D TiS_2 as MFCA in sulfur electrode. (Q3, March 2018; Completed June 2018)
4. Alternative high pore volume and high BET surface area carbon host investigation. (Q4; Completed September 2018)

Progress Report

As a conductive host, microporous carbon is a key component for sulfur electrode in Li-S batteries. Based on the team's previous research, several key parameters were identified for ideal carbon host in Li-S battery application: (a) particle size in microns for high loading cathode processability; (b) large pore volume for high wt% sulfur encapsulation; (c) large surface area for high rate capability; and (d) high electrode porosity to maximize the electrolyte volume within the electrode stack for good sulfur utilization. Previously, the team selected microporous carbon (A5597) derived from wood [*Electrochimica Acta* 235 (2017): 399-408] for high sulfur loading electrode processability (up to 11 mg/cm^2). However, the sulfur utilization is unsatisfactory, especially at high discharge rate. This quarter, the team identified and evaluated an alternative microporous carbon material (ADV-C) that maintains the particle size in micron scale and at the same time with larger pore volume and larger surface area than that of A5597 for improved sulfur encapsulation and utilization.

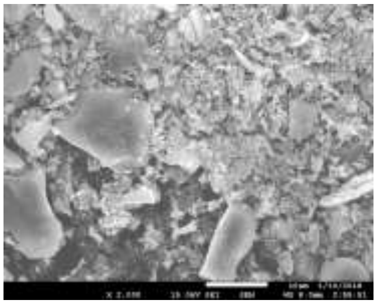

Figure 86. New carbon ADV-C morphology.

New Carbon (ADV-C) Material. The ADV-C material has irregular particle morphology similar to A5597(see Figure 86). However, this alternative carbon exhibits more than double the pore volume (~ 1.9 cc/g) and BET surface area (~ 3000 m^2/g) relative to that of A5597 (~ 0.7 cc/g, ~ 1200 m^2/g). 78 wt% of sulfur was successfully infiltrated into ADV-C with uniform sulfur distribution (Figure 87, EDX mapping). Using this C-S composite material, the team has successfully prepared electrodes with sulfur loading up to 11 mg/cm^2.

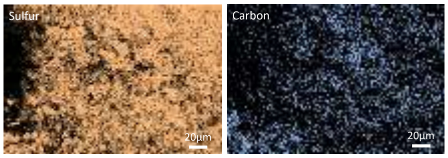

Figure 87. ADV-C sulfur infiltration (S:C = 78:22).

Electrochemical Performance. The ADV-C/S composite electrodes with sulfur loading ~ 5.5 mg/cm^2 were used for coin cell study, with A5597 carbon/S composite electrode as control. As shown in Figure 88, cells built with ADV-C exhibited improved sulfur utilization at both 0.1 mA/cm^2 (56% to 87%) and 2.0 mA/cm^2 (30% to 39%) discharge rates. The cycle life data (after rate test) under 1.0 mA/cm^2 discharge rate are shown in Figure 89. Both types of carbon host afforded stable cycling with only 0.111% and 0.046% capacity fade per cycle over the initial 60 cycles for A5597 and ADV-C, respectively. In addition, higher sulfur utilization is maintained throughout the cycling test for ADV-C versus A5597. Around 1050 mAh/g sulfur utilization is still maintained when the discharge rate is reduced to 0.1 mA/cm^2. In combination with this new carbon host with the electrolyte optimization, similar cycling performance was also observed when an electrode with sulfur loading of 10.7 mg/cm^2 was used (Figure 89), which delivers > 6 mAh/cm^2 at 1.0 mA/cm^2 discharge rate.

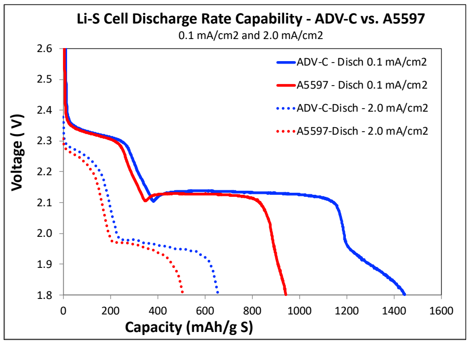

Figure 88. Rate capability.

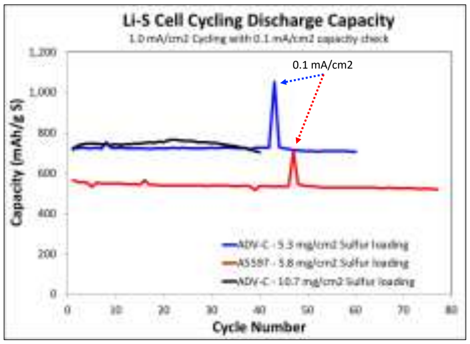

Figure 89. Cycle life at 1.0 mA/cm^2.

These results indicate that the use of microporous carbon with high pore volume, high porosity, high surface area, and micron-scale particle sizes is a promising direction to proceed to achieve high sulfur loading electrode processability, high sulfur utilization at high discharge rate, and long cycle life of Li-S batteries.

Patents/Publications/Presentations

Publications

- Sun, K., M. Fu, Z. Xie, D. Su, H. Zhong, J. Bai, E. Dooryhee, and H. Gan. “Improvement of Li-S Battery Electrochemical Performance with 2D TiS_2 Additive.” *Electrochimica Acta*. Accepted for publication.
- Sun, K., N. Li, D. Su, and H. Gan. “Electrolyte Concentration Effect on Sulfur Utilization of Li-S Batteries.” Manuscript submitted and under review.

TASK 6 – AIR ELECTRODES / ELECTROLYTES

Summary and Highlights

High-density energy storage systems are critical for EVs required by the EV Everywhere Grand Challenge. Conventional Li-ion batteries still cannot fully satisfy the ever-increasing needs because of their limited energy density, high cost, and safety concerns. As an alternative, the rechargeable lithium-oxygen (Li-O_2) battery has the potential to be used for long-range EVs. The practical energy density of a Li-O_2 battery is expected to be ~ 800 Wh kg^{-1}. The advantages of Li-O_2 batteries come from their open structure; that is, they can absorb the active cathode material (oxygen) from the surrounding environment instead of carrying it within the batteries. However, the open structure of Li-O_2 batteries also leads to several disadvantages. The energy density of Li-O_2 batteries will be much lower if oxygen must be provided by an onboard container. Although significant progress has been made in recent years on fundamental properties of Li-O_2 batteries, research in this field is still in an early stage, with many barriers to be overcome before practical applications. These barriers include:

- Instability of electrolytes—The superoxide species generated during discharge or O_2 reduction process is highly reactive with electrolyte and other components in the battery. Electrolyte decomposition during charge or O_2 evolution process is also significant due to high over-potentials.
- Instability of air electrode (dominated by carbonaceous materials) and other battery components (such as separators and binders) during charge/discharge processes in an O-rich environment.
- Limited cyclability of the battery associated with instability of the electrolyte and other battery components.
- Low energy efficiency associated with large over-potential and poor cyclability of Li-O_2 batteries.
- Low power rate capability due to electrode blocking by the reaction products.
- Absence of a low-cost, high-efficiency oxygen supply system (such as oxygen selective membrane).

The main goal of this Task is to provide a better understanding on the fundamental reaction mechanisms of Li-O_2 batteries and identify the required components (especially electrolytes and electrodes) for stable operation of Li-O_2 batteries. PNNL researchers will investigate new approaches to improve stability of Li-metal anode in Li-O_2 batteries and develop thick carbon/catalyst composite air electrodes for practical Li-O_2 batteries. Li-metal anodes will be protected using two approaches: (1) *in situ* formation of a stable SEI layer before Li-O_2 cell operation through various electrolyte formulations and treatment protocols, and (2) *ex situ* formation of stable inorganic/polymeric hybrid electrolyte layers through dip-coating or tape casting method to coat the inorganic/polymeric hybrid electrolyte layer on Li-metal surface. Thick carbon/catalyst composite air electrodes based on CNTs and transient metal oxides such as RuO_2 and with ≥ 4 mg/cm^2 areal loading will be developed. At ANL, new cathode materials and electrolytes for Li-air batteries will be developed for Li-O_2 batteries with long cycle life, high capacity, and high efficiency. The state-of-the-art characterization techniques and computational methodologies will be used to understand the charge and discharge chemistries. Success of this project will establish a solid foundation for further development of Li-O_2 batteries toward practical applications for long-range EVs. The fundamental understanding and breakthrough in Li-O_2 batteries may also provide insight on improving the performance of Li-S batteries and other energy storage systems based on chemical conversion processes.

Task 6.1 – Rechargeable Lithium-Air Batteries
(Ji-Guang Zhang and Wu Xu, Pacific Northwest National Laboratory)

Project Objective. The project objective is to develop rechargeable Li-O_2 batteries with long-term cycling stability. The team has found that the corrosion of Li-metal anode is a critical degradation mechanism of Li-O_2 batteries. Realization of very high energy density of Li-O_2 batteries strongly depends on the stability of Li-metal anodes. In FY 2018, the focus will be on protection of Li-metal anodes for Li-O_2 batteries. Several approaches, including *in situ* and *ex situ* methods, will be used to study the corrosion of Li-metal anode in Li-O_2 cells under different treatment/protection conditions.

Project Impact. Li-air batteries have a theoretical specific energy more than five times that of state-of-the-art Li-ion batteries and are potential candidates for use in next-generation, long-range EVs. Unfortunately, the poor cycling stability and low CE of Li-air batteries have prevented their practical application. This work will explore well-protected Li-metal anodes, new electrolytes, and high-loading air-electrodes that could lead to long cyclability and high CE in high-energy Li-air batteries that can be used in the next-generation EVs required by the EV Everywhere Grand Challenge.

Approach. Li-metal anodes will be protected using *in situ* formation of a stable SEI layer before Li-O_2 cell operation through various electrolyte formulations and treatment protocols and *ex situ* formation of stable inorganic/polymeric hybrid electrolyte layers through dip-coating or tape casting method to coat the inorganic/polymeric hybrid electrolyte layer on Li-metal surface. Thick carbon/catalyst composite air electrodes based on CNTs and transient metal oxides such as RuO_2 and with ≥ 4 mg/cm^2 areal loading will be developed. The lithium anodes and Li-O_2 cells at different stages of cycling (including as-prepared, after discharge, after recharge, and after cycling) will be analyzed by microscopy and spectroscopy techniques such as SEM, EDX, XRD, and XPS.

Out-Year-Goals. The long-term goal is to enable rechargeable Li-air batteries with a specific energy of 800 Wh/kg at cell level, 1000 deep-discharge cycles, improved abuse tolerance, and less than 20% capacity fade over a 10-year period to accelerate commercialization of long-range EVs.

Collaborations. This project collaborates with Chongmin Wang of PNNL on characterization of cycled air electrodes by TEM/SEM.

Milestones

1. Investigate electrolyte additives to form stable SEI layer on Li-metal anode of Li-O_2 batteries. (Q1, December 31, 2017; Completed)
2. Develop inorganic/polymeric composite hybrid electrolyte membranes to protect Li-metal anode in Li-O_2 batteries. (Q2, March 31, 2018; Completed)
3. Develop thick air electrodes of at least 4 mg/cm^2 areal loading for Li-O_2 batteries. (Q3, June 30, 2018; Completed)
4. Evaluate cycling performance of Li-O_2 batteries with protected Li-metal anode and thick air electrode. (Q4, September 30, 2018; Completed)

Progress Report

Although much progress has been made in improving cycling stability of Li-O_2 batteries in recent years, very small mass loading (generally less than 1 mg/cm^2) in these batteries hindered application of high energy density of Li-O_2 batteries. Realization of high-energy-density Li-O_2 batteries relies on effective utilization of high loading air-electrodes with long-lasting cycling stability. This quarter, Li-O_2 cells containing optimized RuO_2/CNTs air cathodes with high loading and Li-metal anodes with or without composite protective membrane (LiTFSI/LLZTO/PVDF) have been tested in 1 M LiTf-TEGDME electrolyte; the corresponding cell design can be found in Figure 90a. Here, glass fiber (GF-B) is used as separator, with thickness of composite polymer membrane ~ 20 µm. After one pre-treatment process to optimize RuO_2/CNTs air electrode, these Li-O_2 cells were cycled in a voltage window between 2.2 V and 4.2 V in 1 M LiTf-TEGDME electrolyte at a current density of 0.1 mA cm^{-2} in O_2 atmosphere at room temperature. From Figure 90b, it can be observed that Li-O_2 cells with optimal air electrode and protected Li-metal anode with composite protective membrane demonstrate better stability over 14 cycles, compared to the poor cycling performance of cells with optimal air electrode and nonprotected Li-metal anode. After 14 cycles, the areal capacity of Li-O_2 cells with composite protective membrane is still more than 4 mAh cm^{-2}. Moreover, capacities of Li-O_2 cells with composite protective membrane on Li-metal anode are higher than those of cells without composite protective membrane on lithium anode; this means that the addition of composite protective membrane on Li-metal surface leads to significant increase in the capacity retention of Li-O_2 cells due to effective protection for Li-metal anode during long-term discharge/charge processes (Figure 90c-d). The well-protected Li-metal anode paired with high loading air-electrode in a nonaqueous Li-O_2 battery has delivered high areal capacity (that is, over 4 mAh cm^{-2}) required for high utilization of lithium metal in each cycle and reliable stabilization of Li-metal anode.

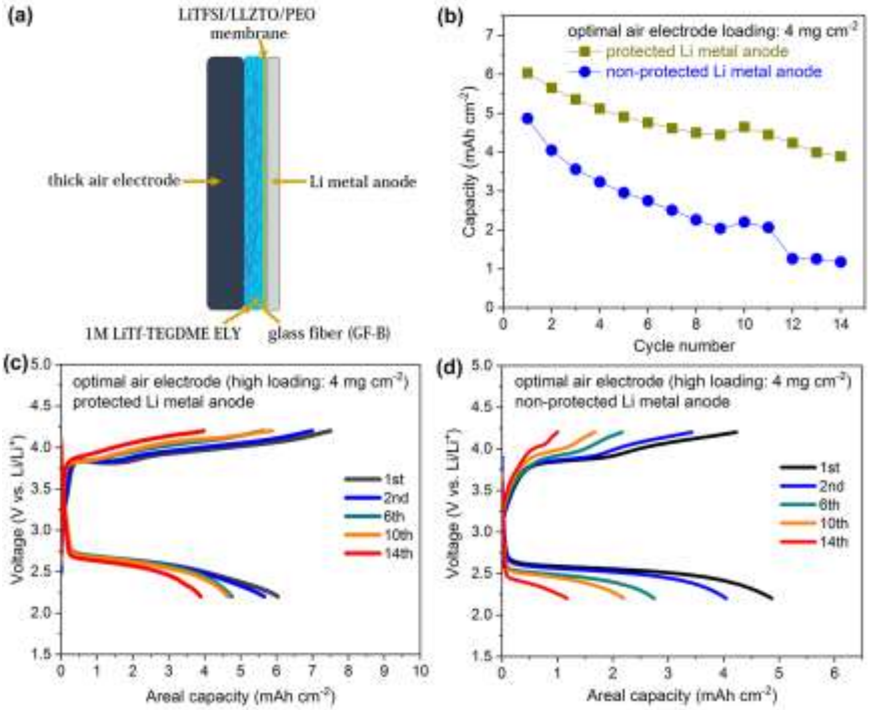

Figure 90. (a) Schematic of high-energy-density Li-O_2 cell design. (b) Cycling performance of Li-O_2 cells containing optimal RuO_2/CNTs air electrodes (high loading: 4mg cm^{-2}) and Li-metal anodes with and without composite protective membrane (LiTFSI/LLZTO/PVDF) cycled in voltage window between 2.2 V and 4.2 V at a current density of 0.1 mA cm^{-2} in 1 M LiTf-TEGDME electrolyte at room temperature. Their corresponding voltage profiles of lithium cells with (c) and without (d) composite protective membrane, respectively.

Patents/Publications/Presentations

Publication

- Liu, B., W. Xu, and J.-G. Zhang.* "Stability of Lithium-Metal Anode in Rechargeable Li-Air Batteries." Chapter for book entitled *Metal-Air Batteries: Fundamentals and Applications*. Wiley, Germany. Published online (2018). https://www.wiley.com/en-us/Metal+Air+Batteries%3A+Fundamentals+and+Applications-p-9783527807666.

Task 6.2 – Lithium-Air Batteries
(Khalil Amine and Larry A. Curtiss, Argonne National Laboratory)

Project Objective. This project will develop new cathode materials and electrolytes for Li-air batteries for long cycle life, high capacity, and high efficiency. The goal is to obtain critical insight that will provide information on the charge and discharge processes in Li-air batteries to enable new advances to be made in their performance. This will be done using state-of-the-art characterization techniques combined with state-of-the-art computational methodologies to understand and design new materials and electrolytes for Li-air batteries.

Project Impact. The instability of current nonaqueous electrolytes and degradation of cathode materials limits performance of Li-air batteries. The project impact will be to develop new electrolytes and cathode materials that are stable and can increase energy density of electrical energy storage systems based on lithium.

Approach. The project is using a joint theoretical/experimental approach for design and discovery of new cathode and electrolyte materials that act synergistically to reduce charge overpotentials and increase cycle life. Synthesis methods, in combination with design principles developed from computations, are used to make new cathode architectures. Computational studies are used to help understand decomposition mechanisms of electrolytes and how to design electrolytes with improved stability. The new cathodes and electrolytes are tested in Li-O_2 cells. Characterization along with theory is used to understand the performance of the materials used in the cell and make improved materials.

Out-Year Goals. The out-year goals are to find catalysts that promote discharge product morphologies that reduce charge potentials and find electrolytes for long cycle life through testing and design.

Collaborations. This project engages in collaboration with Prof. K. C. Lau (UC at Norridge), Prof. Y. Wu (Ohio State University), Dr. D. Zhai (China), and R. Shahbazian-Yassar (UIC).

Milestones

1. Investigation of highly uniform Pt_3Co nanoparticles in biphasic nitrogen-doping cobalt@graphene heterostructures as cathode materials. (Q1, FY 2018; Completed)
2. Computational studies of dependence of stability and composition of discharge products in Li-O_2 batteries on ether-based electrolytes. (Q2, FY 2018; Completed)
3. Use of highly uniform small iridium clusters supported on rGO to study formation of Ir_3Li alloys for lithium-superoxide-based batteries. (Q3, FY 2018; Completed)
4. Investigation of dependence of discharge composition on type of ether used in electrolytes from experimental studies. (Q4, FY 2018; Completed)

Progress Report

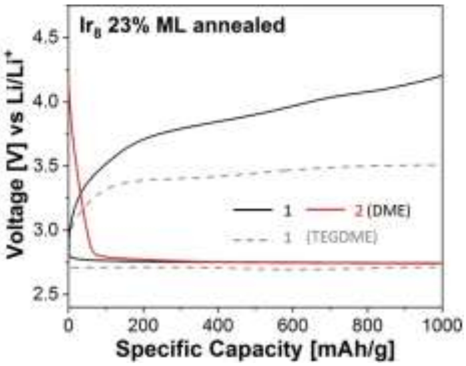

Figure 91. Voltage profile for annealed 23% ML Ir_8-rGO cathode cycled in 1 M $LiCF_3SO_3$ in TEGDME electrolyte (bold lines), overlaid with the same electrode cycled in 1 M $LiCF_3SO_3$ in DME electrolyte (dashed lines).

It has recently been shown that lithium superoxide, which is a good electronic conductor and has a low charge overpotential, can be formed in a Li-O_2 battery using iridium as a catalyst, but little is known about the role of the electrolyte in the lithium superoxide formation. In this work, size-selected subnanometer iridium clusters were used to generate uniformly sized iridium nanoparticles on rGO-based cathodes to gain new insight into whether the electrolyte affects composition of the discharge product and also how it can stabilize the lithium superoxide. The team has examined several aspects, including whether disproportionation depends on ether chain length and whether different electrolytes at the interface can suppress disproportionation. Results are based on both experimental and theoretical investigations.

The first question was investigated by using DME and comparing it with tetraglyme (TEGDME). The Li-O_2 cell was tested under identical conditions with annealed Ir_8 clusters on the cathode surface. The cell was discharged to 1000 mAh/g using 1 M $LiCF_3SO_3$ in DME as the electrolyte and then was charged. The voltage profile is shown in Figure 91 for the first cycle. The cell discharged at ~ 2.7 V similar to the results for TEGDME, but charged at ~ 4.1 V, significantly higher than what was found for TEGDME. These differing charge potentials suggest that the discharge product with DME is different from the LiO_2 formed with TEGDME. This was confirmed when the Ti(IV)OSO_4 based titration technique was used on the DME discharge product. A strong ultraviolet peak was obtained in the ultraviolet-visible spectra, which showed a Li_2O_2 content of 42%.

The team performed computational studies to investigate whether the shorter chain DME solvent favors disproportionation of LiO_2 in solution to form Li_2O_2 as a reason for these differing results. They first carried out density functional calculations to determine whether for DME the interaction of two LiO_2 leading to disproportionation would be more favorable than for TEGDME because of the shorter length of the DME. The results of these calculations indicated that disproportionation should be no more favorable for DME than for TEGDME and would not explain the results. A more likely explanation is the differences in viscosity. TEGDME, due to its long chain length, is more viscous than DME, which may result in much slower lithium cation conductivity in TEGDME compared to DME. Based on various reports of ionic conductivity in related species, the team estimates that the ionic conductivity in DME is about two orders of magnitude larger than in TEGDME. The faster diffusion of Li+ or LiO_2 in DME may enhance formation of LiO_2 dimers for disproportionation in solution, accounting for the preference for Li_2O_2 formation in DME as opposed to TEGDME.

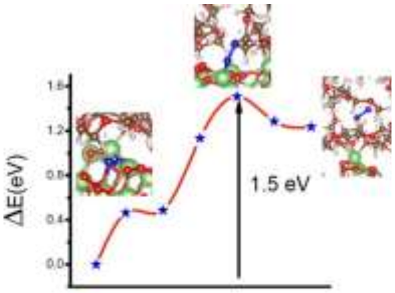

Figure 92. Density functional calculation of the barrier for dissolution of O_2 into the TEGDME from a LiO_2 surface.

The second question the team investigated was the role of the electrolyte in the stability of LiO_2. For this study, they carried out calculations for the barrier to elimination of O_2 from a crystalline surface of lithium superoxide at an interface with DME and TEGDME solvents needed for disproportionation. The barriers were 1.51 and 1.66 eV for TEGDME and DME, respectively. The barrier for TEGDME is shown in Figure 92. This is larger compared to vacuum (0.9 eV), suggesting that the lifetime of LiO_2 will increase significantly in the presence of an electrolyte at the surface. This is consistent with previous experimental studies, which indicated that the presence of a TEGDME-based electrolyte decreases the disproportionation of LiO_2 compared to when it is aged for 24 h in vacuum. In addition, the barriers indicate that LiO_2 disproportionation from the surface in the presence of DME, if it was formed in DME, should be similar to that of TEGDME. This suggests that differences in the stability of solid LiO_2 discharge product in DME and TEGDME are not the reason for it not being observed in DME. Thus, the reason is more likely due to differences in the formation mechanisms in the two electrolytes.

Patents/Publications/Presentations

Publication

- Ma, L., T. Yu, E. Tzoganakis, K. Amine, T. Wu, Z. Chen, and J. Lu. "Fundamental Understanding and Material Challenges in Rechargeable Nonaqueous Li-O_2 Batteries: Recent Progress and Perspective." *Advanced Energy Materials* 8 (2018): 1800348.

TASK 7 –SODIUM-ION BATTERIES

Summary

During FY 2019, the BMR will add five new projects, including several in the area of Na-ion batteries. The Na-ion battery will require investigations to identify optimal electrode materials, electrolytes, separators, and binders to reach its full potential. The BMR program will therefore have a limited effort directed toward identifying Na-ion battery materials that have potential value for vehicle applications. These projects will be included in this new section as they get underway. More detailed information on this BMR Task will be provided in upcoming reports.

Task 7.1 – Exploratory Studies of Novel Sodium-Ion Battery Systems (Xiao-Qing Yang and Seongmin Bak, Brookhaven National Laboratory)

Project Objective. The primary objective of this proposed project is to develop new advanced *in situ* material characterization techniques and to apply these techniques to explore the potentials, challenges, and feasibility of new rechargeable battery systems beyond the Li-ion batteries, namely the Na-ion battery systems for PHEV. To meet the challenges of powering the PHEV, new rechargeable battery systems with high energy and power density, low cost, good abuse tolerance, and long calendar and cycle life need to be developed. This project will use the synchrotron-based *in situ* X-ray diagnostic tools developed at BNL to evaluate the new materials and redox couples, to explore fundamental understanding of the mechanisms governing the performance of these materials.

Project Impact. In the VTO MYPP, the goals for battery are described as: "Specifically, lower-cost, abuse-tolerant batteries with higher energy density, higher power, better low-temperature operation, and longer lifetimes are needed for the development of the next-generation of HEVs, PHEVs, and EVs." The knowledge learned from diagnostic studies and collaborations with U. S. industries through this project will help U. S. industries to develop new materials and processes for new generation of rechargeable battery systems, namely Na-ion battery system in their efforts to reach the VTO goals.

Approach. This project will use the synchrotron-based *in situ* X-ray diagnostic tools developed at BNL to evaluate the new materials and redox couples to enable a fundamental understanding of the mechanisms governing performance of these materials and provide guidance for new material and new technology development regarding Na-ion battery systems.

Out-Year Goals. Complete the synchrotron-based *in situ* XRD and *ex situ* XAS studies of $Na_{0.66}Mn_{0.6}Ni_{0.2}Mg_{0.2}O_2$ as new cathode material for Na-ion batteries during charge-discharge cycling.

Collaborations. The BNL team has been closely working with top scientists on new material synthesis at ANL, LBNL, and PNNL and with U. S. industrial collaborators at General Motors and Johnson Controls, as well as international collaborators.

Milestones

1. Complete i*n situ* XRD and *ex situ* XAS studies and the evaluation of lattice parameter changes of new $NaCrS_2$ layer structured cathode materials during the charge-discharge cycling. (Q1, December 2017; Completed)
2. Complete the synchrotron-based XRD studies with Rietveld refinement of $Na_3VP_3O_9N$, as well as XANES and extended X-ray absorption fine structure (EXAFS) investigation of this new cathode material for Na-ion batteries at pristine and fully charged states. (Q2, March 2018; Completed)
3. Complete the synchrotron-based *in situ* XRD studies of $Na_{0.66}Mn_{0.6}Ni_{0.2}Mg_{0.2}O_2$ as new cathode material for Na-ion batteries during charge-discharge cycling. (Q3, June 2018; Completed)
4. Complete the synchrotron-based XANES studies of $Na_{0.66}Mn_{0.6}Ni_{0.2}Mg_{0.2}O_2$ as new cathode material for Na-ion batteries during charge-discharge cycling. (Q4, September 2018; Completed)

Progress Report

This quarter, the fourth milestones were completed. BNL has been focused on the *in situ* XAS studies of $Na_{0.66}Mn_{0.6}Ni_{0.2}Mg_{0.2}O_2$ (MNM) as new cathode materials for Na-ion batteries. Synchrotron-based XAS was employed to investigate the valence state and local structure changes of the MNM-2 electrode during the charge and discharge process. XANES spectra of manganese and nickel during the first charge, first discharge, and second charge processes are illustrated in Figure 93. Regarding quantitative analysis of the K-edge position of manganese and nickel, Figure 93g shows the change of the half edge energy ($E_{0.5}$) of manganese and nickel deduced by the half-height method. In the first charge process, no edge shift for manganese K-edge XANES can be observed, indicating Mn^{4+} ions are maintained with no valence change during the initial charge. However, the white line for nickel K-edge XANES shifts to higher energy obviously, suggesting that the nickel cations are oxidized to higher valence state during charge. The energy shift of nickel K-edge is about 1.6 eV; it can be roughly estimated that the valence state of nickel is changing from 2+ to 3.3+, compared with the XANES of NiO and $LiNiO_2$ references.

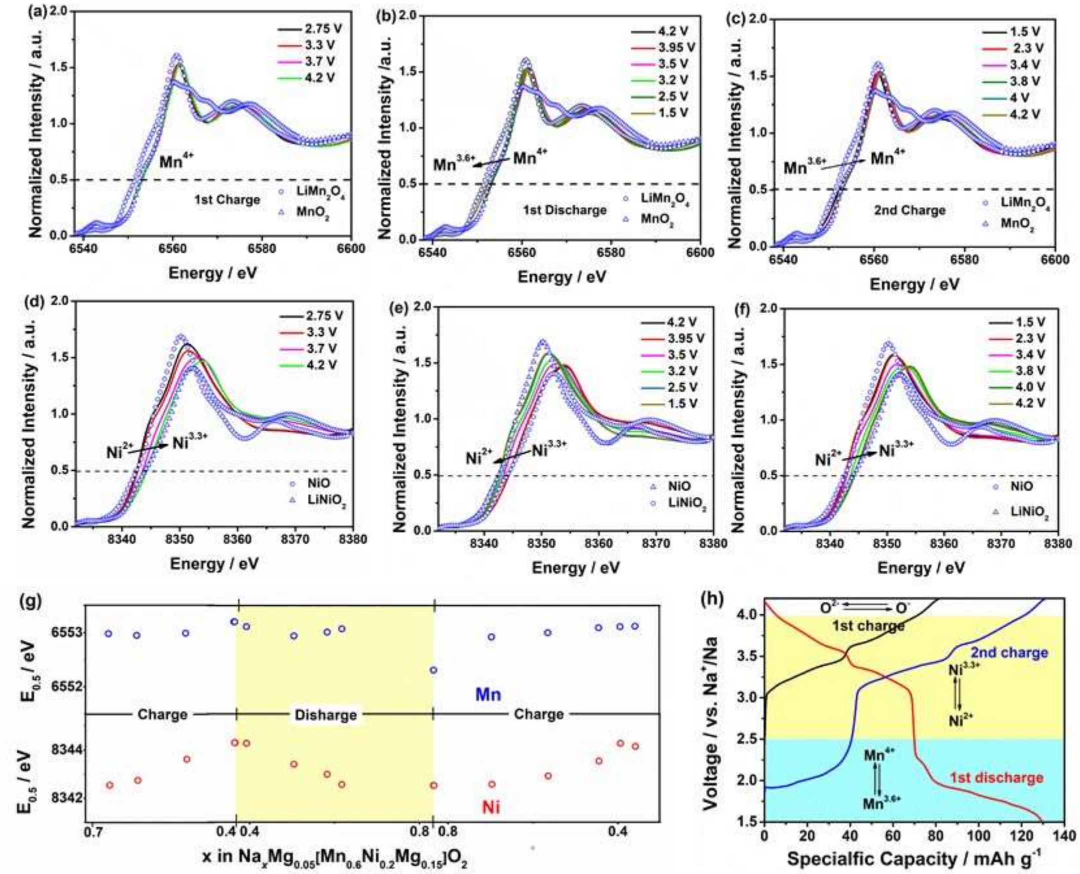

Figure 93. Charge compensation mechanism of MNM-2 during charge and discharge processes. (a-c) Manganese and (d-f) nickel K-edge X-ray absorption near-edge spectroscopy of MNM-2 at various stages during the first charge/discharge and the second charge process, respectively. (g) The half edge energy ($E_{0.5}$) at different content of sodium in $Na_xMg_{0.05}[Mn_{0.6}Ni_{0.2}Mg_{0.15}]O_2$. (h). The charge compensation of different elements contribution during the charge and discharge process.

Patents/Publications/Presentations

Publication

- Xu, S., J. Wu, E. Hu, Q. Li, J. Zhang, Y. Wang, E. Stavitski, L. Jiang, X. Rong, X. Yu, W. Yang, X-Q. Yang*, L. Chen, and Y-S. Hu.* “Suppressing the Voltage Decay of Low-Cost P2-Type Iron-Based Cathode Materials for Sodium-Ion Batteries.” *Journal of Materials Chemistry A*, Advance Article, published on September 24, 2018. doi: 10.1039/C8TA07933A.

Presentation

- 256th ACS Meeting, Boston, Massachusetts (August 19–23, 2018): “Using Synchrotron X-Ray and Neutron Based Scattering and TXM imaging Techniques to Study the New Cathode Materials for Batteries”; E. Hu, S-M. Bak, X-Q. Yang,* X. Yu, X. Huang, M. Ge, Y. Chu, Z. Shadike, R. Lin, H-S. Lee, Y. Guo, and Y. Liu. Invited.

Innovation Center for Battery500
(Jun Liu, PNNL; Yi Cui, Stanford University)

Project Objective. The project aims to develop commercially viable lithium battery technologies with a cell-level specific energy of 500 Wh/kg through innovative electrode and cell designs that enable the extraction of the maximum capacity from advanced electrode materials. In addition to achieving high specific energy, the project aims to be able to achieve 1,000 cycles for the developed technologies.

Project Impact. The Battery500 Consortium will develop the next-generation lithium battery technologies that will significantly increase energy density, improve cycle life, and reduce cost. This will greatly accelerate the deployment of EVs and reduce carbon emission associated with fossil fuel consumption. The consortium will utilize first-class expertise and capabilities in battery research in the United States and develop an integrated and multidisciplinary approach to accelerate development and deployment of advanced electrode materials in commercially viable high-energy batteries. The advances made in this consortium will also benefit the improvement of current Li-ion battery technologies.

Approach. This project will utilize an assortment of national resources located at the national laboratory level and university level. The lithium anode combined with a compatible electrolyte system and two cathodes—one high-Ni $LiNi_xMn_yCo_zO_2$ and another sulfur—will be studied and developed to reach high-energy density. The project focus is to design novel electrode and cell architectures to meet the 500 Wh/kg goal. The consortium will work closely with R&D companies, battery/materials manufacturers, and end users/OEMs to ensure that the developed technologies are aligned with industry needs and can be transitioned to production.

Out-Year Goals. This project aims for the following out-year goals. (1) Integrate materials and components developed in FY 2018 into 1 Ah pouch cell and demonstrate 350 Wh/kg cell with more than 50 charge discharge cycles, and provide analytical results for materials selection, cell design and fabrication, and further refinement for FY 2019. (2) Evaluate the seedling projects for key findings that can be incorporated into the consortium.

Collaborations. The collaboration among consortium team members will be well coordinated by the leadership team, which includes the keystone project leads and co-leads along with PIs at all member institutions. Collaboration with the community outside of this consortium and with industry will be facilitated by the executive committee, the advisory board, and the industry committee.

Milestones

1. Scale up the synthesis capacity of high-Ni-content NMC to 500 g; Incorporate cathode surface modification in coin cells with greater than 2 mAh/cm^2 loading. (Q1, December 2017; Completed)
2. Establish the high-nickel NMC coin cell properties using the materials synthesized by the team and supplied by other sources. Develop stage 1 pouch cell testing protocols and provide updated component parameters toward 350 Wh/kg. Establish baseline properties of Li-S coin cells using parameters required to reach 350 Wh/kg. (Q2, March 2018; Completed)
3. Provide feedback on characterization of new materials and concepts by the characterization team. Develop procedures to identify lithium anode failure in coin cells and pouch cells. (Q3, June 2018; In progress)
4. Establish coin cell performance with 30% weight reduction in the anode current collector. Develop and implement methods to improve and understand cycle and calendar life limitations of pouch cells. (Q4, September 2018; Completed)

Progress Report

The technical portion of this report is organized under three Keystone projects, as presented below.

Keystone Project 1: Materials and Interfaces

High Nickel NMC Cathode Materials

Determine the Origin of 1st Cycle Loss of Capacity of High Nickel NMC and Mitigate It. The discharge capacity of NMC is around 15% lower than the 1st charge capacity. Recouping that loss would make attaining 400 Wh/kg cells more feasible. The team has demonstrated (Figure 94a-c) the following through initial experiments on the NMC-811:

- Cathode active material loading has little if any impact on the 1st-cycle loss. This is important as thicker electrodes are needed to attain higher energy density cells.
- Calendering the electrode slightly reduces this 1st-cycle loss.
- More than half of this 1st-cycle loss can be recovered by a constant voltage discharge at 2.8 V. This behavior is still present after several cycles. This suggests that the last 30% of lithium insertion is diffusion controlled. This is consistent with earlier results showing up to a two-order-of-magnitude decrease in the lithium chemical diffusion coefficient in going from x = 0.3 to x = 0.8 in Li_xMO_2 (JPS 268, 106, 2014).

These results suggest that the team needs to increase the D_{Li} in these materials, and that calendering is important and should be optimized: porosity/electrolyte optimization versus particle contact (see earlier report of UC San Diego group).

Combining calendering and constant current/constant voltage (CC/CV) discharging recovers a little more of the capacity, but there is still around 10 mAh/g loss. This is likely due to irreversible surface changes in the material and/or utilization of a little of the material in forming a surface CEI layer. A coating or artificial CEI may help in eliminating this loss.

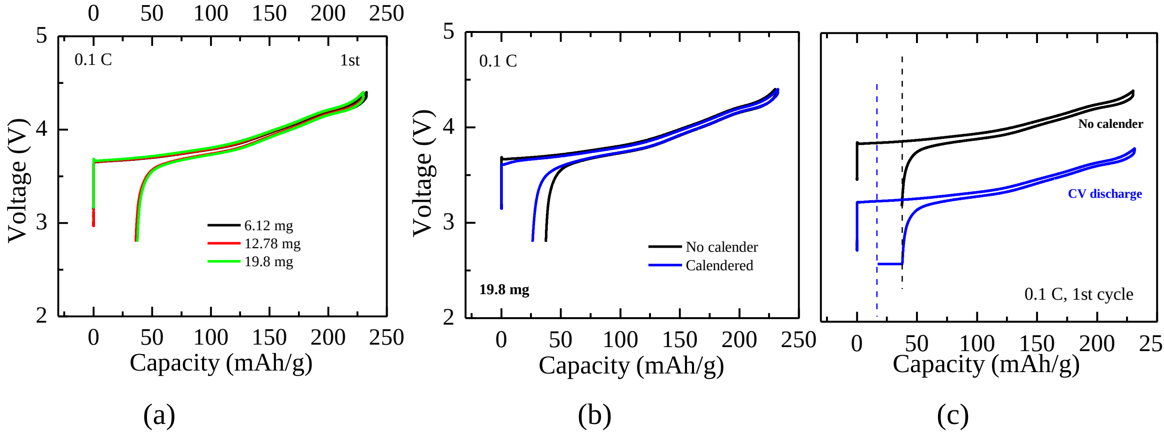

Figure 94. (a) 1st cycle of NMC-811 with three different loadings. (b) Impact of calendering on NMC-811. (c) Impact of constant current / constant voltage discharge on NMC-811. All cells cycled between 4.4-2.8 V.

Evaluate Thermal Stability of High-Nickel NMC. Last quarter, the team showed that in the presence of electrolyte, both delithiated NMC-811 and NCA have similar thermal stabilities. Both decompose at temperatures below 250ºC; the similarity indicates that in an operating battery, NCA does not have a significant thermal stability edge over NMC-811. This quarter, the team determined the thermal stability of a range of four in-house synthesized high-nickel NMCs. They determined the thermal stability both after a charge to 4.3 V and after charging each one to 220 mAh/g, that is, to the same delithiation level. The results are shown in Figure 95.

The results after the 4.3-V charge gave expected results consistent with earlier work; namely, the thermal event decreases in temperature with increasing nickel content from 268°C for $LiNi_{0.5}Co_{0.2}Mn_{0.3}O_2$ to 181°C for $LiNi_{0.94}Co_{0.06}O_2$. However, for the four cathodes charged to roughly the same level of delithiation, 220 mAh/g (80%), the difference is much less: 227°C to 182°C. Thus, thermal stability is determined by both nickel content and degree of delithiation. These results clearly indicate that high-nickel NMC cathodes represent a metastable situation, and emphasize the need for bulk and surface stabilization. This instability is inherent to the NMC material itself and may be acerbated by choice of electrolyte.

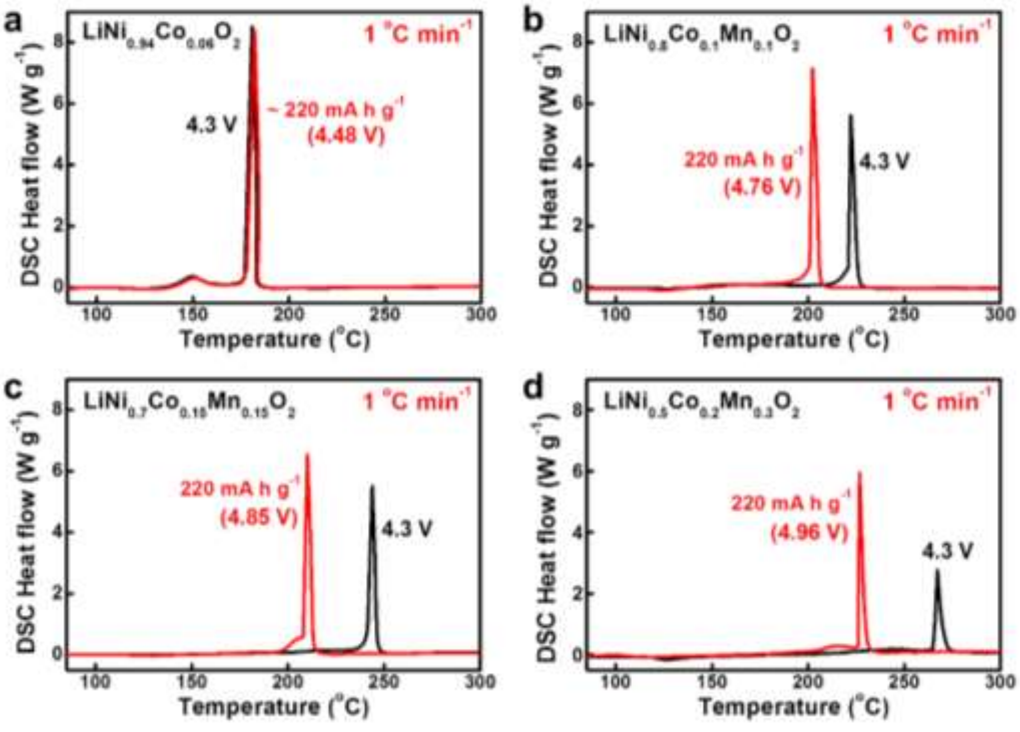

Figure 95. Thermal stability measurements using differential scanning calorimetry of (a) $LiNi_{0.94}Co_{0.06}O_2$ and series of NMC cathodes: (b) $LiNi_{0.8}Co_{0.1}Mn_{0.1}O_2$, (c) $LiNi_{0.7}Co_{0.15}Mn_{0.15}O_2$, and (d) $LiNi_{0.5}Co_{0.2}Mn_{0.3}O_2$ at high states of charge. The cathode samples were retrieved from cells either charged to the same upper cut-off voltage (4.3 V versus Li^+/Li) or to roughly the same extent of delithiation (~ 220 mA h g^{-1} specific capacities corresponding to approximately 80% lithium removal).

New Electrolyte

Electrochemical Performance. The project's newly developed localized high-concentration electrolyte (LHCE) ED1123 exhibits much improved thermal stability than other LHCE reported before. The electrochemical performance of ED1123 was verified in Li||NMC-811 cells. Baseline electrolyte 1M $LiPF_6$ in EC/EMC (3/7) + 2% VC and high concentrated electrolyte (HCE) were presented for comparison. Figure 96a shows that ED1123 has great stability in Li||NMC-811 cell with an average CE of 99.7% and capacity retention of ca. 80% after 300 cycles even with limited lithium (50 µm) used in cells. Baseline and HCE electrolytes show fast capacity decay and cell failure after 30 or 50 cycles, respectively. Beyond the significantly improved long-term cycling stability, Figure 96b-c shows that ED1123 electrolyte also leads to great rate performances. Specific capacity of 135 mAh/g can be achieved at 4C (6 mA/cm^2) charge rate with a discharge rate of C/3, and 170 mAh/g specific capacity is obtained at 4C discharge rate with a charge rate of C/3. These results indicate that ED1123 electrolyte is suitable for fast charge and fast discharge for Li||NMC-811 cells.

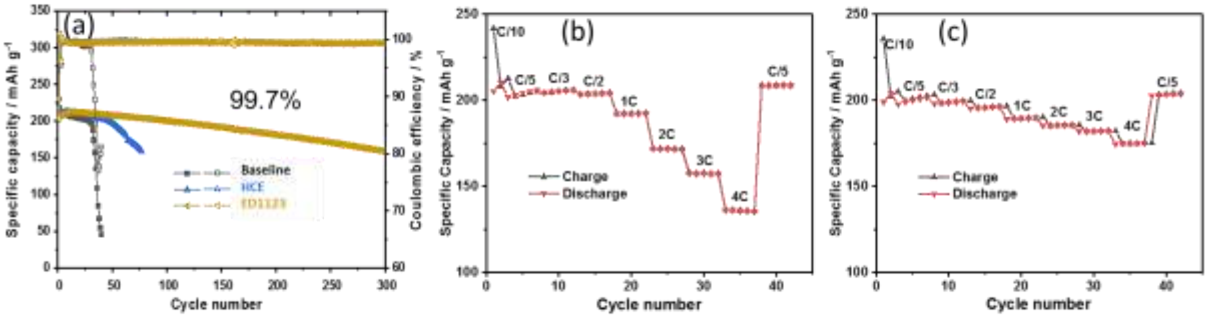

Figure 96. Electrochemical performance of Li||NMC-811 with investigated electrolytes. (a) Cycling performance at C/3 charge/discharge processes. (b) Different charge rate performance in ED1123 electrolyte with constant charge rate of C/3. (c) Different discharge rate performance in ED1123 electrolyte with constant charge rate of C/3. All Li||NMC cells are cycled between 2.8-4.4 V versus Li/Li$^+$.

Minimized Thickness Expansion during Cycling. Lithium consumption and volume expansion caused by Li/electrolyte side reactions are among the biggest barriers for practical use of Li-metal batteries, leading to limited cycle life and severe safety concerns. ED1123 electrolyte has led to significantly reduced lithium consumption and volume expansion over cycling. Figure 97 shows the cross-sectional SEM image of the cycled lithium anode in Li||NMC-811 cells with baseline and ED1123 electrolytes after 100 cycles. In this study, 50-µm-thick lithium metal is used as the anode. After 100 cycles in baseline electrolyte, 50-µm-thick lithium metal is fully utilized, and the final thickness of reacted lithium anode is of ca. 290 µm. In contrast, for lithium anode cycled in the ED1123 electrolyte, two distinguished lithium layers are observed. One layer is nonreacted lithium, which is ca. 48 µm and has the same state as the fresh lithium; the other one is reacted lithium (residue lithium) on the surface of the nonreacted lithium foil. This result indicates that majority of Li-metal foil was not used during cycling. The porous layer shown in Figure 97b is mainly formed by the reaction of electrolyte, and lithium comes from NMC cathode instead of Li-metal anode. This phenomenon will lead to long-term cycle stability of LMBs. The reacted lithium layer (ca. 48-µm thick) collected from Li||NMC-811 cell using ED1123 electrolyte contains large particle size, as shown in Figure 97b, instead of fine particles shown in Figure 97a for the reacted lithium layer collected from Li||NMC-811 cell using baseline electrolyte.

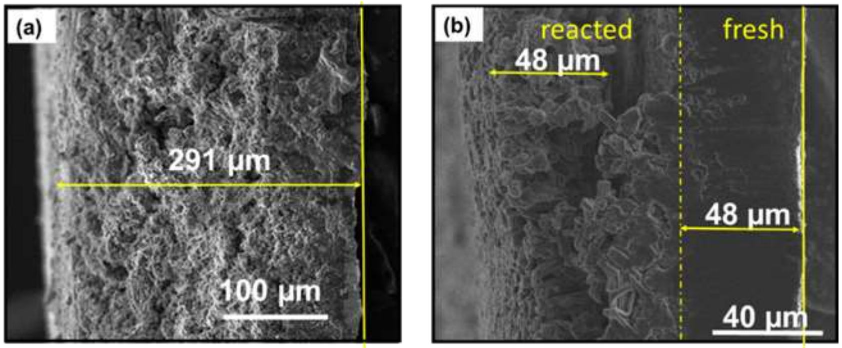

Figure 97. Cross-section of cycled lithium (100 cycles) collected from Li||NMC-811 cells with (a) baseline and (b) ED1123 electrolytes.

Highlights

- Studies show that 1st-cycle loss is independent of cathode loading, but decreased by increased calendering.
- Studies show that thermal instability is a function of both nickel content and degree of lithium removal.
- Newly developed LHCE ED1123 exhibits much improved thermal stability than other LHCE, and electrochemical performance of ED1123 in Li||NMC-811 cells is very good.

Keystone Project 2: Electrode Architecture

The goal of Keystone 2 is to design, model, fabricate, and characterize the effect of electrode architecture on electrode and cell performance in support of reaching the project goal of 500 Wh/kg cell specific energy. Included in this Keystone are architectured design of thick cathodes (UCSD), Li-metal electrode architectures (PNNL and Stanford), inorganic (UT-Austin) and polymer (Stanford) electrolytes, and electrode performance modeling (UW). Highlighted this quarter are recent advancements at UW on electrochemical modeling of lithium deposition and development of transport measurement of thick cathodes at UCSD.

The objective of the work at UW is to model the deposition and stripping of lithium metal by considering the local electrochemistry and mechanical coupling and linking the same to the overall cell voltage response. Effort this quarter focused on developing an electrochemical transport and deposition model for Li/Li symmetric cells and comparing the results with experimental observations. The team developed a one-dimensional (1D) transport model for lithium symmetric cells based on the Poisson-Nernst-Planck (PNP) equations. Further, a preliminary electrode kinetic model is developed by considering regions of lithium deposition with two different reaction rates. These two models are integrated and simulated to obtain the cell-voltage response as a function of time. The model parameters used in the simulation are relevant to the symmetric cell used at the team at SLAC. The comparison with experiment is depicted in Figure 98. The model can fit the initial nucleation-influenced voltage response of the first 'half-cycle.' The model also qualitatively captures the transitions in cell voltage induced by the change in deposition pathways, seen in the third 'half-cycle.' The internal plots of the local overpotential are also depicted, with the transition from 'fast' to 'slow' electrodeposition also being observed. Ongoing work is focused on improving this model fit by achieving more realistic coupling of transport and reaction through a more localized electrodeposition model.

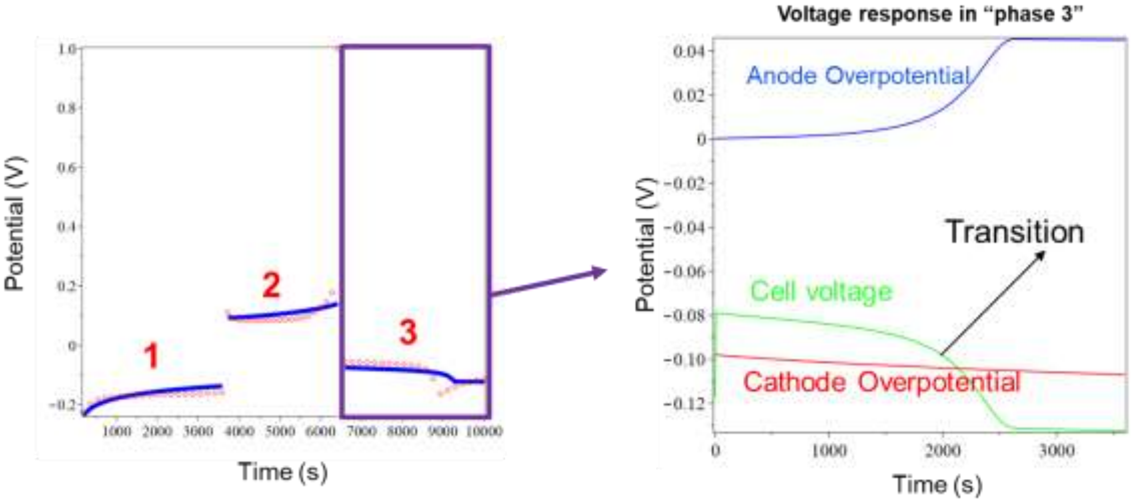

Figure 98. Comparison of predicted cell voltage with experimental data from Stanford Linear Accelerator Center. Phase 1 corresponds to the nucleation and growth of lithium on the bare copper substrate. The transition in Phase 3 is associated with change of stripping from deposit to the slower 'bulk.' When the surface area fraction ϴ of the deposit goes to zero, stripping at the anode occurs from the bulk lithium with a higher polarization.

In the cathode work, UCSD has continued evaluation of thick electrodes. To understand the ion transport through the pores of thick cathodes, the team has previously adopted a method that measures impedance of a porous electrode in the presence of a non-intercalating cation. However, that technique requires the electronic resistance to be negligible as compared to ionic resistance. To circumvent this shortcoming, the team at UCSD developed a DC-based technique to directly measure effective ion conductivity through the electrode thickness. Specifically, a freestanding cathode is sandwiched between two porous polymer separators. This sandwich is in turn placed between two $LiFePO_4$ electrodes. A DC current is applied between the two $LiFePO_4$ electrodes.

The polarization of the cell is then compared to a similar cell, but without the porous cathode in the middle of the stack. Their difference represents the resistance contribution from the porous cathode.

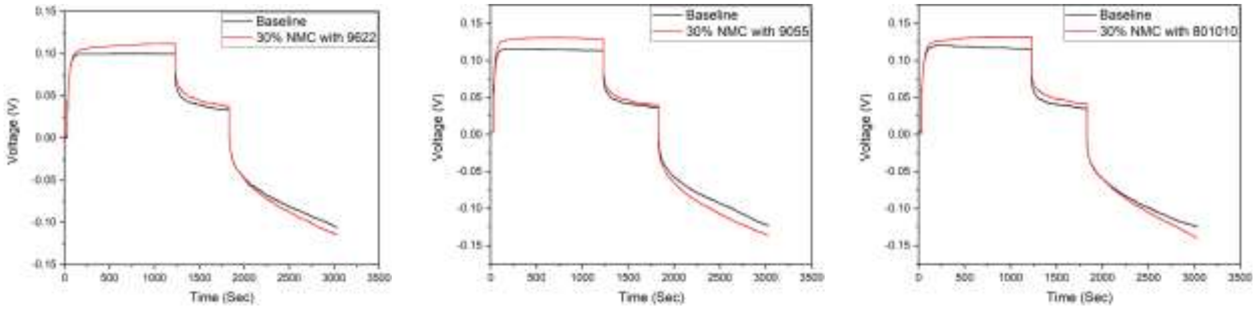

Composition	96:2:2	90:5:5	80:10:10
Effective ionic conductivity	0.208	0.089	0.076

Figure 99. Voltage profiles for testing the cell shown at a constant current of 100 µA for 1200s, followed by a rest of 600s, and a reverse constant current of 100 µA for 1200s. The table summarizes the conductivities estimated from measurement for three different electrodes.

Figure 99 shows the voltage profiles of three electrodes with compositions of NMC-811:carbon:PVDF of 96:2:2, 90:5:5, and 80:10:10, respectively. Included for comparison is the baseline when no porous cathode was present. The effective ionic conductivity is estimated from the difference in polarization. It is interesting to note that ion conductivity is higher for electrode with lower polymer and cathode content. This is consistent with the hypothesis that the high surface area carbon held together by polymer occupies the space between the large oxide particles and increases the tortuosity of the electrode, which results in a reduction in effective ionic conductivity through the electrode. This observation, combined with the importance of electronic conductivity shown previously, points to the need to develop highly efficient electronic conducting networks using as little conducting additive as possible.

In summary, the consortium continues to make advancements in both cathode and lithium-anode architectures. The team has refined the method of quantifying transport of lithium ions through the porous electrodes, which is essential in understanding performance limitations of thick cathodes. Electrochemical modeling work has been expanded to understand anode architecture effect on Li-metal cycling, which will support the search of new approaches of further increasing lithium cycling efficiency.

Highlights

- A 1D model is developed to describe Li-metal deposition process that correlates with experimental setup.
- Ion transport resistance through thick electrodes is quantified with a DC through membrane measurement technique.

Keystone Project 3: Cell Fabrication, Testing, and Diagnosis

This quarter, distinct progress was made in combined experimental and modeling efforts to understand design and performance limitations for high specific energy Li-metal batteries. At the end of the quarter, the Battery500 team had developed a 2.5 Ah Li/NMC cell that had achieved 100 cycles with only 2.5% capacity fade (Figure 100). The cell, which fulfilled the annual milestone for the program, had an energy of 350 Wh/kg at the beginning of life and was still cycling at the end of the quarter. The cell displayed a 40 Wh/kg improvement over the end of FY 2017. To achieve high performance, the team capitalized on improvements in electrolyte, mechanical cell management, and use of thick NMC cathodes. Key to the cell design is use of low volumes of electrolyte and thin lithium foil.

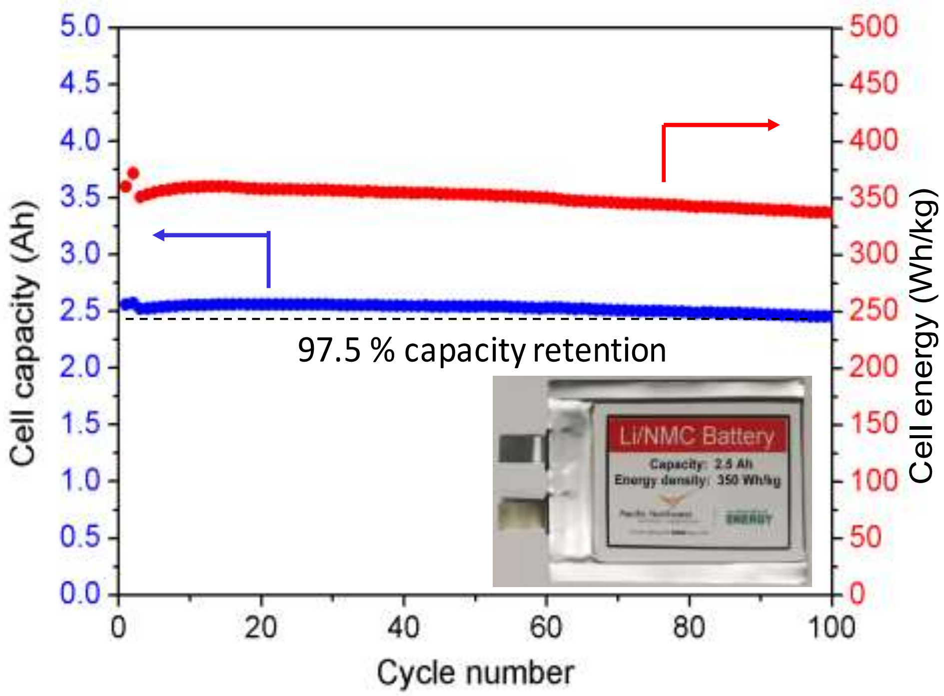

Figure 100. Final deliverable cell for FY 2018. The Li/NMC cell was still cycling at the end of the quarter.

On the modeling front, multiple advances were also made. Specific efforts during the quarter were focused on understanding transport in symmetric cells to align with experimental results, understanding the initial nucleation formation of Li-metal deposits, and the initial development of a kinetic model to better describe lithium electrodeposition and stripping. The root of these investigations was a specific focus on providing valuable information to improve electrodeposition characteristics of lithium. Dendritic protrusions formed during lithium electrodeposition are a core driver of nonuniform, porous lithium deposits and are key to the consumption of electrolyte that shortens the cycle life of Li-metal cells. The suppression of dendrites is thus an important goal for the consortium, and the modeling research is aligned to complement experimental research.

On the diagnostics and characterization front, the team has been focusing on better understanding the full set of influences on the cell. This includes characterizing the quantity of metallic lithium that is unable to be cycled and the pressure evolution during cycling. Post-testing analysis was used to look at lithium following the completion of testing of a 1.1 Ah Li/NMC pouch cell with a FY 2017 cell design that had over 200 cycles. The cell had experienced rapid failure during cycling, and differential capacity analysis indicated that the vast majority of the fade was due to loss of lithium inventory. This analysis was confirmed using a new method developed during Battery500 activities that is focused at identifying the quantity of lithium metal that cannot be cycled. The analysis (Figure 101) found that in over four different locations, the cell averaged 50 μm of dead lithium. This aligns directly with the total amount of lithium that was present in the lithium foil at the beginning of life for the cell. In addition to showing that nearly all the original lithium from the foil had been consumed, the analysis indicates that the extent of lithium that could not be cycled varied across different locations within the cell, with close to 10% variation between samples. Efforts are under way to compare the post-test method with *in operando* efforts.

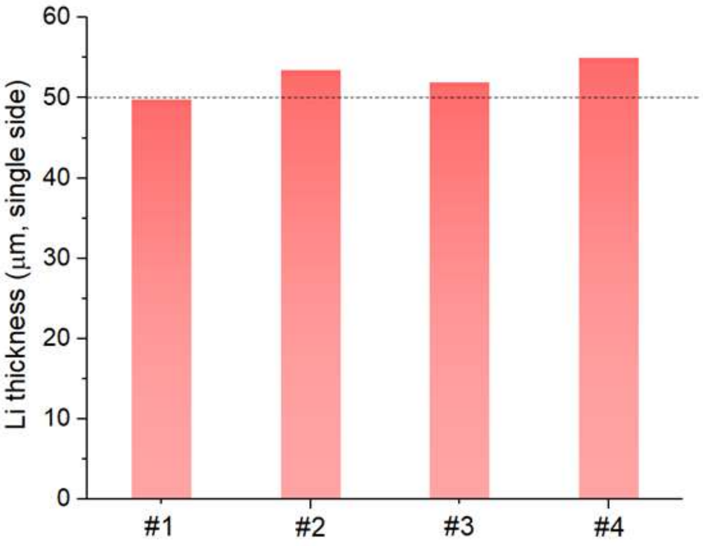

Figure 101. Quantified, non-cycling lithium metal following the completion of testing for a 1.1 Ah Li/NMC cell.

Using the combined advances from activities from the three Keystones, it was possible to significantly advance performance of rechargeable Li-metal cells. Quantification of Li-metal losses and understanding the Li-ion electrolyte concentration near electrodes will aid the Battery500 Consortium moving into FY 2019 to achieve extended cycle life and specific energy.

Highlights:

- Demonstrated full cells with greater than 350 Wh/kg energy density and over 100 cycles (and still cycling).
- The amount of inactive lithium in high-energy cells was quantified at the end of life.

Patents/Publications/Presentations

Patents

- Invention Disclosure
  - Cao, X., J-G. Zhang, and W. Xu. “Electrolytes for Stable Cycling of Rechargeable Li Metal and Li Ion Batteries.” IPID 31452-E (September 4, 2018).
  - Fang, C., X. Wang, and Y. S. Meng. “TGC Method and System for Metal Quantification.” UD00000763 (May 2018).
- U. S. Nonprovisional Patent Application
  - Zhang, J-G., S. Chen, and W. Xu. “Low Flammability Electrolytes for Stable Operation of Electrochemical Devices.” IPID 31111-E CIP. Application No. 15/788,188, filed date: 10/2017. (U. S. Patent Application 20180251681; publication date: 9/6/2018)

- U.S. Provisional Patent Application
    - Wang, S., J. Yang, H. Pan, J. Xiao, and J. Liu. "Battery Separator with Lithium Ion Conductor Coating." 62/687,125 (June 19, 2018).
- Foreign Patent Application
    - Zhang, J-G., S. Chen, W. Xu, X. Cao, and X. Ren. "Low Flammability Electrolytes for Stable Operation of Electrochemical Devices." IPID 31111-E CIP PCT. PCT Application No. PCT/US2018/049141, filed date: 8/2018.

Publications

- Li, Y., H. Xu, P. Chien, N. Wu, S. Xin, L. Xue, K. Park, Y. Hu, and J. B. Goodenough. "A Perovskite Electrolyte That Is Stable in Moist Air for Li-ion Batteries." *Angewandte Chemie (International Edition)* 57, no. 28 (2018): 8587–8591. Publication Date (Web): July 9, 2018.
- Xue, L., W. Zhou, S. Xin, H. Gao, Y. Li, A. Zhou, and J. B. Goodenough. "Room-Temperature Liquid Na-K Anode Membranes." *Angewandte Chemie (International Edition)* 130, no. 43 (2018): 14380–14383. Publication Date (Web): September 7, 2018.
- Yu, L., S. Chen, H. Lee, L. Zhang, M. H. Engelhard, Q. Li, S. Jiao, J. Liu, W. Xu*, and J.-G. Zhang.* "A Localized High-Concentration Electrolyte with Optimized Solvents and Lithium Difluoro(oxalate)borate Additive for Stable Lithium Metal Batteries." *ACS Energy Letters* 3, no. 9 (2018): 2059–2067. doi:10.1021/acsenergylett.8b00935, Publication Date (Web): July 31, 2018.
- Ren, X., S. Chen, H. Lee, D. Mei, M. H. Engelhard, S. D. Burton, W. Zhao, J. Zheng, Q. Li, M. S. Ding, M. Schroeder, J. Alvarado, K. Xu, Y. S. Meng, J. Liu, J.-G. Zhang,* and W. Xu.* "Localized High-Concentration Sulfone Electrolytes for High-Efficiency Lithium-Metal Batteries." *Chem* 4, no. 8 (August 9, 2018): 1877–1892. doi:10.1016/j.chempr.2018.05.002.
- Bak, S-M., Z. Shadike, R. Lin, X. Yu, and X-Q. Yang. "*In Situ/Operando* Synchrotron-Based X-Ray Techniques for Lithium-Ion Battery Research." *NPG Asia Materials* (2018): doi: 10.1038/s41427-018-0056-z, Publication Date (Web): July 3, 2018.
- Hu, E., X. Yu, R. Lin, X. Bi, J. Lu, S-M. Bak, K-W. Nam, H. L. Xin, C. Jaye, D. A. Fischer, K. Amine, and X-Q. Yang. "Evolution of Redox Couples in Li- and Mn-Rich Cathode Materials and Mitigation of Voltage Fade by Reducing Oxygen Release." *Nature Energy* 3 (2018): 690–698. doi: 10.1038/s41560-018-0207-z, Publication Date (Web): July 30, 2018.
- Piao, J-Y., Y-G. Sun, S-Y. Duan, A-M. Cao, X-L. Wang, R-J. Xiao, X-Q. Yu, Y. Gong, L. Gu, Y. Li, Z-J. Liu, Z-Q. Peng, R-M. Qiao, W-L. Yang, X-Q. Yang, J. B. Goodenough, and L-J. Wan. "Stabilizing Cathode Materials of Lithium-Ion Batteries by Controlling Interstitial Sites on the Surface." *Chem* 4, no. 7 (July 12, 2018): 1685–1695. doi: 10.1016/j.chempr.2018.04.020.
- Yue, X-Y., W-W. Wang, Q-C. Wang, J-K. Meng, Z-Q. Zhang, X-J. Wu, X-Q. Yang, and Y-N. Zhou. "CoO Nanofiber Decorated Nickel Foams as Lithium Dendrite Suppressing Host Skeletons for High Energy Lithium Metal Batteries." *Energy Storage Materials* 14 (2018): 335–344. doi: 10.1016/j.ensm.2018.05.017, Publication Date (Web): September 2018.
- Yin, L., G. Mattei, Z. Li, J. Zheng, W. Zhao, F. Omenya, C. Fang, W. Li, J. Li, Q. Xie, J.-G. Zhang, M. S. Whittingham, Y. S. Meng, A. Manthiram, and P. Khalifah. "Extending the Limits of Powder Diffraction Analysis: Diffraction Parameter Space, Occupancy Defects, and Atomic Form Factors." *Review of Scientific Instruments* 89 (2018): 093002. Publication Date (Web): September 26, 2018.
- Lopez, J., A. Pei, J. Y. Oh, G.-J. N. Wang, Y. Cui, and Z. Bao. "Effects of Polymer Coatings on Electrodeposited Lithium Metal." *Journal of the American Chemical Society* 140, no. 37 (2018): 11735–11744. Publication Date (Web): August 28, 2018.

- Mackanic, D. G., W. Michaels, M. Lee, D. Feng, J. Lopez, J. Qin, Y. Cui, and Z. Bao. "Crosslinked Poly(tetrahydrofuran) as a Loosely Coordinating Polymer Electrolyte." *Advanced Energy Materials* 8, no. 25 (2018): 1800703. Publication Date (Web): September 5, 2018.
- Shi, F., A. Pei, D. T. Boyle, J. Xie, X. Yu, X. Zhang, and Y. Cui. "Lithium Metal Stripping Beneath the Solid Electrolyte Interphase." *Proceedings of the National Academy of Sciences of the U. S. A.* 115, no. 34, (2018): 8529–8534. Publication Date (Web): August 6, 2018.
- Liu, Y., D. Lin, Y. Li, G. Chen, A. Pei, O. Nix, Y. Li, and Y. Cui. "Solubility-Mediated Sustained Release Enabling Nitrate Additive in Carbonate Electrolytes for Stable Lithium Metal Anode." *Nature Communications* 9, no. 3656. Publication Date (Web): September 7, 2018.
- Xie, J., J. Wang, H. R. Lee, K. Yan, Y. Li, F. Shi, W. Huang, A. Pei, G. Chen, R. Subbaraman, J. Christensen, and Y. Cui. "Engineering Stable Interfaces for Three-Dimensional Lithium Metal Anodes." *Science Advances* 4 (2018): eaat5168. Publication Date (Web): July 27, 2018.
- Chen, S., J. Zheng, L. Yu, X. Ren, M. H. Engelhard, C. Niu, H. Lee, et al. "High-Efficiency Lithium Metal Batteries with Fire-Retardant Electrolytes." *Joule* 2, no. 8 (2018): 1548–1558. PNNL-SA-131864. doi:10.1016/j, *Joule*.2018.05.002, Publication Date (Web): August 15, 2018.
- Yu, L., S. Chen, H. Lee, L. Zhang, M. H. Engelhard, Q. Li, S. Jiao, et al. "A Localized High-Concentration Electrolyte with Optimized Solvents and Lithium Difluoro(oxalate)borate Additive for Stable Lithium Metal Batteries." *ACS Energy Letters* 3, no. 9 (2018): 2059-2067. doi:10.1021/acsenergylett.8b00935, Publication Date (Web): September 14, 2018.
- Jiao, S., X. Ren, R. Cao, M. H. Engelhard, Y. Liu, D. Hu, D. Mei, et al. "Stable Cycling of High-Voltage Lithium Metal Batteries in Ether Electrolytes." *Nature Energy* 3, no. 9 (2018): 739–746. doi:10.1038/s41560-018-0199-8, Publication Date (Web): September 10, 2018.
- Wang, S., M. Yan, Y. Li, C. Vinado, and J. Yang. "Separating Electronic and Ionic Conductivity in Mix-Conducting Layered Lithium Transition Metal Oxides." *Journal of Power Sources* 393 (2018): 75–82.
- Wood, S. M., C. Fang, E. J. Dufek*, S. C. Nagpure, S. V. Sazhin, B. Liaw, and Y. S. Meng. "Predicting Calendar Aging in Lithium Metal Secondary Batteries: The Impacts of Solid Electrolyte Interphase Composition and Stability." *Advanced Energy Materials*. doi: 10.1002/aenm.201801427, Publication Date (Web): August 6, 2018.

Presentations

- EEST, Niagara Falls, Canada (August 14, 2018): "Can Multi-Electron Intercalation Reaction Batteries Replace Today's Li-ion Batteries?"; M. S. Whittingham. Invited.
- Columbia University, New York (September 14, 2018): "What are the Materials Limitations to Advancing Li-Batteries to the Next Level?"; M. S. Whittingham. Invited.
- 2nd Energy Harvesting Conference, Penn State Navy Yard, Philadelphia, Pennsylvania (September 5, 2018): "Energy Storage for Energy Harvesting Applications"; M. S. Whittingham. Invited.
- NYBEST Annual Technical Meeting, Binghamton, New York (September 27, 2018): "Battery Technologies: the Past, Present, and Future"; M. S. Whittingham. Invited.
- North East Center for Energy Materials Summer School on X-Ray Science, Newcastle, UK (September 6, 2018): "Structural and Chemical Insight into Energy Conversion and Storage with X-Ray Scattering and Spectroscopy"; M. Toney. Invited.
- Spring ACS Meeting, Boston, Massachusetts (August 20, 2018): "Electrode-Electrolyte Interfaces in Energy Conversion and Storage"; M. Toney. Invited.
- 2018 US-China Green Energy Summit (2018UCGES), San Francisco, California (August 3–4, 2018): "New Battery Technology for Electrical Vehicles and Grid Scale Energy Storage"; Y. Cui. Invited.

- EEST, Niagara Falls, Canada (August 13–17, 2018): "Nanomaterials Design and Interphases for Batteries"; Y. Cui. Invited plenary talk.
- 69th Annual ISE Meeting, Bologna, Italy (September 2–7, 2018): "Nanoscale Materials Design and Interphases for Next Generation of Batteries"; Y. Cui. Invited keynote talk.
- 3rd Fellow of the Royal Society of Chemistry (FRSC) Forum on Global Challenges and Chemistry Solutions: Energy, University of Science and Technology of China, Hefei, China (September 16, 2018): "Nanotechnology for Energy and Environment"; Y. Cui. Invited plenary talk.
- 4th International Conference on Energy and Biological Materials (4th ICEBM), University of Science and Technology of China (USTC), Hefei, China (September 17–18, 2018): "Nanomaterials Design and Interphases for Batteries"; Y. Cui. Invited keynote talk.
- Fourth China Energy Storage Engineering Conference & China-Japan Battery Seminar, Hefei, China (July 16, 2018): "Long-Life, High-Energy-Density Lithium-ion Batteries with High-Nickel Layered Oxide Cathodes"; A. Manthiram. Invited.
- Hefei University, Hefei, China (July 14–15, 2018): "Next-Generation Rechargeable Battery Chemistries"; A. Manthiram. Invited.
- 3rd International Symposium on Renewable Energy Technologies, Gold Coast, Australia (July 19–22, 2018): "Materials Challenges and Prospects of Electrical Energy Storage"; A. Manthiram. Invited plenary talk.
- 12th International Conference on Ceramic Materials and Components for Energy and Environmental Applications (CMCEE), Singapore (July 22–27, 2018): "Complexities of the Bulk and Surface Chemistry of High-Nickel Layered Oxide Cathodes for Energy Storage"; A. Manthiram. Invited keynote talk.
- Battery500 Consortium Meeting, Berkeley, California (August 1–3, 2018): "Progress on High-Nickel Layered Oxide Cathodes"; A. Manthiram. Invited.
- 16th Asian Conference on Solid-State Ionics, Shanghai, China (August 5–9, 2018): "Where is Electrical Energy Storage Headed?"; A. Manthiram. Invited plenary talk.
- EEST, Niagara Falls, Canada (August 13–17, 2018): "High-Nickel Oxide Cathodes for Lithium-Ion Batteries: Delineating the Complexities of Bulk and Surface Chemistries"; A. Manthiram. Invited plenary talk.
- 256th ACS Meeting, Electrochemical Interfaces Symposium, Boston, Massachusetts (August 19–23, 2018): "Interfacial Chemistry of High-Nickel Layered Oxide Cathodes for Lithium-Ion Batteries"; A. Manthiram. Invited.
- 256th ACS Meeting, Boston, Massachusetts (August 19–23, 2018): "Assessing Critical Pathways to Next Generation High Energy Safe Lithium Batteries"; Y. S. Meng. Invited.
- 256th ACS Meeting, Boston, Massachusetts (August 19–23, 2018): "Using Synchrotron X-ray and Neutron Based Scattering and TXM Imaging Techniques to Study the New Cathode Materials for Batteries"; E. Hu and X-Q. Yang.* Invited.
- Bruker TOPAS Users Meeting, Edinburgh, United Kingdom (June 29–July 1, 2018): "Refinements En Masse: Probing Batteries *In Operando* with High Spatial and Temporal Resolution"; P. Khalifah. Invited.
- Bruker TOPAS Users Meeting, Edinburgh, United Kingdom (June 29–July 1, 2018): "Systematic Studies of Four Key Defects in Layered Battery Systems – Insights from Average and Local Structure Studies"; P. Khalifah. Invited.
- University of Waterloo, Canada, (July 20, 2018): New Approaches for Powder Diffraction that Extend the Spatial Resolution, Temporal Resolution, and Sensitivity to Defects in Studies of Battery Materials"; P. Khalifah. Invited.

- 256th ACS Meeting, Electrochemical Interfaces Symposium, Boston, Massachusetts (August 19–23, 2018): "Synthetic Chemistry Approaches to Electrode/Electrolyte Interface Design"; P. Liu. Invited.
- Battery500 Consortium Meeting, Berkeley, California (August 1–3, 2018): "Effect of Design Parameters and Architectures: Models and Codes"; V. R. Subramanian. Invited.
- 2018 Critical Materials Institute Annual Meeting, Ames, Iowa (September 5–6, 2018): "Application of Critical Materials in Battery Research"; B. Liaw. Invited.
- Energy in Idaho, Idaho Business Review, Breakfast Series, Boise, Idaho (August 16, 2018): "INL's Energy Storage Research Activities"; B. Liaw. Invited.
- Battery Safety Council Technical Workshop (Forum 6) on Hazard Analysis and Risk Assessment, Washington, D. C. (July 24–25, 2018): "From Failure Mode & Effect Analysis (FMEA) to Battery Safety and Risk Assessments"; B. Liaw. Invited.
- Royal Society Materials Challenges for Sustainable Energy Technologies, London, United Kingdom (September 19, 2018): "Participation of Bonding and Non-Bonding Oxygen Redox States for Energy Storage and Conversion"; W. C. Chueh. Invited keynote talk.
- Hoover Institution, Washington, D. C. (September 18, 2018): "Game Changers – Energy Storage"; W. C. Chueh. Invited keynote talk.
- 5th Solid-State Chemistry & Ionics (SCI) Workshop, Fukuoka, Japan (September 11, 2018): "New Approaches for Investigating Ionic & Chemical Transport Across Interfaces"; W. C. Chueh. Invited keynote talk.
- 256th ACS Meeting, Boston, Massachusetts (August 20, 2018): "Materials Integration and Optimization for High-Energy-Density Rechargeable Lithium Metal Batteries"; Jun Liu. Invited talk.
- 256th ACS Meeting, Boston, Massachusetts (August 21, 2018): "Interfacial Chemistry in Lithium Metal and Lithium Sulfur Batteries"; Jun Liu. Invited keynote talk.
- International Conference on Advanced Cathodes, Seoul, South Korea (September 9–12, 2018): "Development and Optimization of Electrode/Electrolyte Materials"; Jun Liu. Invited keynote talk.